Understanding Complex Systems

Springer COMPLEXITY

Rafael Martínez-Guerra
Claudia A. Pérez-Pinacho
Gian Carlo Gómez-Cortés

Synchronization of Integral and Fractional Order Chaotic Systems

A Differential Algebraic and Differential Geometric Approach With Selected Applications in Real-Time

Springer

Springer Complexity

Springer Complexity is an interdisciplinary program publishing the best research and academic-level teaching on both fundamental and applied aspects of complex systems – cutting across all traditional disciplines of the natural and life sciences, engineering, economics, medicine, neuroscience, social and computer science.

Complex Systems are systems that comprise many interacting parts with the ability to generate a new quality of macroscopic collective behavior the manifestations of which are the spontaneous formation of distinctive temporal, spatial or functional structures. Models of such systems can be successfully mapped onto quite diverse "real-life" situations like the climate, the coherent emission of light from lasers, chemical reaction-diffusion systems, biological cellular networks, the dynamics of stock markets and of the internet, earthquake statistics and prediction, freeway traffic, the human brain, or the formation of opinions in social systems, to name just some of the popular applications.

Although their scope and methodologies overlap somewhat, one can distinguish the following main concepts and tools: self-organization, nonlinear dynamics, synergetics, turbulence, dynamical systems, catastrophes, instabilities, stochastic processes, chaos, graphs and networks, cellular automata, adaptive systems, genetic algorithms and computational intelligence.

The three major book publication platforms of the Springer Complexity program are the monograph series "Understanding Complex Systems" focusing on the various applications of complexity, the "Springer Series in Synergetics", which is devoted to the quantitative theoretical and methodological foundations, and the "SpringerBriefs in Complexity" which are concise and topical working reports, case-studies, surveys, essays and lecture notes of relevance to the field. In addition to the books in these two core series, the program also incorporates individual titles ranging from textbooks to major reference works.

Understanding Complex Systems

Founding Editor: S. Kelso

Future scientific and technological developments in many fields will necessarily depend upon coming to grips with complex systems. Such systems are complex in both their composition – typically many different kinds of components interacting simultaneously and nonlinearly with each other and their environments on multiple levels – and in the rich diversity of behavior of which they are capable.

The Springer Series in Understanding Complex Systems series (UCS) promotes new strategies and paradigms for understanding and realizing applications of complex systems research in a wide variety of fields and endeavors. UCS is explicitly transdisciplinary. It has three main goals: First, to elaborate the concepts, methods and tools of complex systems at all levels of description and in all scientific fields, especially newly emerging areas within the life, social, behavioral, economic, neuro- and cognitive sciences (and derivatives thereof); second, to encourage novel applications of these ideas in various fields of engineering and computation such as robotics, nano-technology and informatics; third, to provide a single forum within which commonalities and differences in the workings of complex systems may be discerned, hence leading to deeper insight and understanding.

UCS will publish monographs, lecture notes and selected edited contributions aimed at communicating new findings to a large multidisciplinary audience.

More information about this series at
http://www.springer.com/series/5394

Rafael Martínez-Guerra •
Claudia A. Pérez-Pinacho •
Gian Carlo Gómez-Cortés

Synchronization of Integral and Fractional Order Chaotic Systems

A Differential Algebraic and Differential Geometric Approach With Selected Applications in Real-Time

Springer

Rafael Martínez-Guerra
Departamento de Control Automatico
CINVESTAV-IPN
Mexico, D.F.
Mexico

Claudia A. Pérez-Pinacho
Departamento de Control Automatico
CINVESTAV-IPN
Mexico, D.F.
Mexico

Gian Carlo Gómez-Cortés
Departamento de Control Automatico
CINVESTAV-IPN
Mexico, D.F.
Mexico

ISSN 1860-0832 ISSN 1860-0840 (electronic)
Understanding Complex Systems
ISBN 978-3-319-15283-7 ISBN 978-3-319-15284-4 (eBook)
DOI 10.1007/978-3-319-15284-4

Library of Congress Control Number: 2015935188

Springer Cham Heidelberg New York Dordrecht London

Printed on acid-free paper

Springer International Publishing Switzerland is part of Springer Science+Business Media (www.springer.com)

To my wife and sons,
Marilen, Rafael, and Juan Carlos

To my parents and brothers,
Carlos, Virginia, Victor, Arturo, Carlos,
Javier, and Marisela

Rafael Martínez-Guerra

To my family
Miguel, Graciela and Miguel Jr.

Claudia Alejandra Pérez-Pinacho

To my parents

Gian Carlo Gómez-Cortés

Preface

In this book, several topics of Control theory are presented as a means to solving the synchronization and secure communication problems. Some analytic, algebraic, geometric, and asymptotic concepts are assembled as design tools for a wide variety of chaotic systems. Concepts from differential geometry and differential algebra reveal important structural properties of chaotic systems. The control community has attacked the synchronization concept as an observation problem. In this book, however, we have conceived synchronization theory as a tracking control problem under the master–slave configuration.

The presentation is organized as follows. The basic differential-algebraic and differential-geometric concepts are presented in Chaps. 1–3 in a novel way as design tools. In addition, some experimental results are presented. Most of the more recent results appear in Chaps. 4–14. The first three chapters present the basic concepts of differential algebra and differential geometry. Chapter 1 is introductory. It presents several concepts and examples in nonlinear control theory and synchronization. In Chap. 2, we deal with the synchronization problem using a proportional reduced-order observer. Chapter 3 is concerned with a sliding-mode observer, which is proposed for the synchronization problem. Chapter 4 shows the experimental synchronization of a Colpitts oscillator in real time. Chapter 5 is devoted to the synchronization and parameter estimations of an uncertain Rikitake system. Chapter 6 treats an aspect of chaotic communications and synchronization via a sliding-mode observer. Chap. 7 introduces synchronization and antisynchronization problems in chaotic systems by means of an observer. Chapter 8 expands our investigation to the synchronization of chaotic oscillators with Liouvillian properties and offers some experimental results. Chapter 9 extends the property called the algebraic observability condition (AOC) to the property known as fractional algebraic observability (FAO) to treat the synchronization problem of fractional-order systems. In Chapter 10, we expand our results to generalized synchronization by means of a differential primitive element, which is a linear combination of the known states and the inputs of the system. Chapter 11 studies generalized synchronization for a class of nondifferentially flat and Liouvillian chaotic system. Chapter 12 extends our results to generalized multisynchronization through a family of dynamical

feedbacks. Chapter 13 introduces fractional generalized synchronization via dynamical feedback. The book concludes with Chapter 14, which treats synchronization theory for a certain class of incommensurate fractional-order systems in which a new incommensurate fractional algebraic observability property has been introduced.

The book is written for an audience of graduate students, control engineers, and applied mathematicians interested in synchronization of chaotic systems that are by nature commensurate or incommensurate and in secure communications. It is self-contained and accessible to those with a basic knowledge of integer- and fractional-order differential equations for synchronization theory. For clarity, most of the concepts are introduced and explained by means of examples. Design applications are illustrated on several physical models of practical interest. The book can be used for a first-level graduate course on synchronization theory or as collateral reading for an advanced or specialized course on synchronization theory. Chapters 4–14 can be incorporated into a more advanced course on dynamical nonlinear feedback design.

The authors have attempted to write in such a way that this book can be read not only by mathematicians and physicists, but also by students in engineering (control, systems, electrical, mechanical, aerospace, chemical) who need more background than is provided in the basic mathematics courses and Chap. 1 of this book. We hope that the material presented here will also be useful in the study of secure communications and incommensurate systems.

Finally, the authors wish to express their gratitude to the referees for their careful and helpful review of the manuscript.

México, Mexico Rafael Martínez-Guerra
México, Mexico Claudia Alejandra Pérez-Pinacho
México, Mexico Gian Carlo Gómez-Cortés
August, 2014

Contents

List of Figures

Symbols and Acronyms

$\triangleq$	By definition
$\approx$	Approximately equal
$:=$	Defined as
$\equiv$	Equivalent to
$\neq$	Not equal to
$<\ (>)$	Less (greater) than
$\leq\ (\geq)$	Less (greater) than or equal to
$\forall$	For all
$\in$	Belongs to
$\subset$	Subset of
$\cup$	Union of sets
$\{\cdot\}$	Set
$\rightarrow$	Tends to
$\Rightarrow$	Implies
$\Longleftrightarrow$	Equivalent to, if and only if
$\sum$	Summation
$\mathbb{R}$	The set of real numbers
$\mathbb{R}^+$	The set of positive real numbers
$\mathbb{R}^{m\times n}$	The set of all $m \times n$ matrices with elements in $\mathbb{R}$
$\mathbb{R}_+^{m\times n}$	The set of all $m \times n$ matrices with elements in $\mathbb{R}^+$
$det\ A$	The determinant of a square matrix $A \in \mathbb{R}^{n\times n}$
A^T	The transpose of a matrix obtained by interchanging the rows and columns of A
$(\cdot,\cdot)^T$	The transpose of a vector
$(\cdot,\cdot)'$	The transpose of a vector
$rank\ A$	The minimal number of linearly independent rows or columns of $A \in \mathbb{R}^{m\times n}$
A^{-1}	Inverse of A
max	Maximum
min	Minimum

sup	Supremum, the least upper bound
inf	Infimum, the greatest lower bound
B_r	The ball $\{x \in \mathbb{R}^n \mid \parallel x \parallel \leq R\}$
$f : S_1 \to S_2$	A function f mapping a set S_1 into a set S_2
$\lambda_{\max}(P)(\lambda_{\min}(P))$	The maximum (minimum) eigenvalue of a symmetric matrix P
$P > 0$	A positive definite matrix P
$\dot{y}$	The first derivative of y with respect to time
$\ddot{y}$	The second derivative of y with respect to time
$\dddot{y}$	The third derivative of y with respect to time
$y^{(i)}$	The ith derivative of y with respect to time
lim	Limit
$\lvert a \rvert$	Absolute value of a scalar a
$\lVert x \rVert$	The Euclidean norm of a vector
$\langle \cdot, \cdot \rangle$	Dot product
difftrd°	Differential transcendence degree
∞	Infinity
$\square$	Designation of the end of proofs
lim sup	Limit superior
$K\langle u \rangle$	Differential field generated by the field K, the input $u(t)$, and the time derivative of u
$K\langle u, y \rangle$	Differential field generated by the field K, the input $u(t)$, the output $y(t)$, and the time derivatives of u and y
$\hat{x}$	Estimated value of x
GS	Generalized synchronization
AOC	Algebraic observability condition
FAO	Fractional algebraic observability
PV	Picard Vessiot
GOCF	Generalized observability canonical form
FGOCF	Fractional generalized observability canonical form
$D^{(r\alpha)}x(t)$	Fractional derivative of Caputo
LMI	Linear matrix inequality
LHP	Left half-plane
SMO	Sliding-mode observer
$\frac{\partial \Psi(x)}{\partial x}$	Jacobian of $\Psi(x)$
$L_f h$	Lie derivative of h with respect to f
K/k	Differential field extension

Chapter 1
Control Theory and Synchronization

Abstract This chapter focuses on the main concepts necessary to a proper understanding of the topics developed in this book. In reading this chapter, the emphasis should be on definitions, and in addition, some examples will be given in order to clarify the concepts of control theory and synchronization. The most important issues are topics on differential algebra, differential geometry, and their applications.

1.1 The Differential-Algebraic Point of View

Differential algebra was introduced by the American mathematician Joseph F. Ritt [24] during the first half of the twentieth century. This theory was introduced as a generalization of systems of algebraic equations, i.e., systems of differential equations that can be described by algebraic equations dependent on unknowns and their derivatives. The appearance and application of concepts of differential algebra to analyze dynamical systems, particularly in control theory, is due to Michel Fliess [9]. The differential-algebraic point of view is an alternative to techniques based on differential geometry.

Since differential algebra is based on modern algebra, we begin giving definitions of such concepts as differential field and differential field extension. Afterward, we shall introduce concepts of control theory in terms of differential algebra.

Definition 1.1 A differential field K is a set with the properties of a field that is additionally endowed with a single derivation that obeys the usual rules

$$\forall\, a, b \in K \quad \frac{d}{dt}(a+b) = \dot{a} + \dot{b}$$

$$\forall\, a, b \in K \quad \frac{d}{dt}(a \cdot b) = \dot{a} \cdot b + a \cdot \dot{b}.$$

Definition 1.2 A differential field extension K/k is given by the differential fields K and k such that:

(i) k is a subfield of K.
(ii) The usual rules of derivation of k are the rules of derivation of K restricted to k.

R. Martínez-Guerra et al., *Synchronization of Integral and Fractional Order Chaotic Systems*, Understanding Complex Systems,
DOI 10.1007/978-3-319-15284-4_1

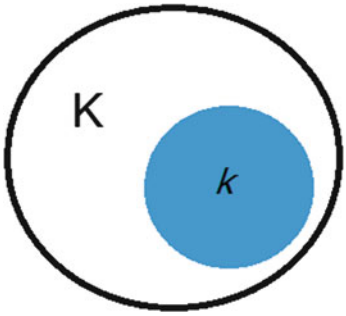

Fig. 1.1 A field extension

The following examples are trivial differential field extensions (Fig. 1.1):

Example 1.1 $\mathbb{R}$ is a field extension of $\mathbb{Q}$. $\mathbb{C}$ is a field extension of $\mathbb{R}$.

Definition 1.3 An element $\alpha \in K$ is said to be differentially algebraic over k if it satisfies a differential-algebraic equation defined by a polynomial $P(\alpha, \dot{\alpha}, \ldots, \alpha^{(n)}) = 0$ over k in α and its time derivatives.

Definition 1.4 An element $\alpha \in K$ is said to be differentially transcendental over k if it is not differentially algebraic over k.

Example 1.2 Given $k = \mathbb{Q}$, then $a = e^t \in L$ is differentially algebraic over $\mathbb{Q}$ because it satisfies $\dot{x} - x = 0$. In this case, a differentially transcendental element is given by $a = e^{\pi t}$.

The theorem of the differential primitive element [17, 24] states that there exists a single differential primitive element $\delta \in K$ such that $K = k\langle\delta\rangle$, i.e., K is differentially generated by k and δ. From the differential primitive element theorem, we establish the following definition.

Definition 1.5 A dynamics is defined as a finitely generated differential algebraic extension $K/k\langle u\rangle$ of the differential field $k\langle u\rangle$, where $k\langle u\rangle$ denotes the differential field generated by k and a finite set of differential quantities $u = (u_1, u_2, \ldots, u_m)$.

Example 1.3 Let us consider the following differential equation:

$$\dot{u}^2 y + 4\ddot{u} = 0.$$

In this case, y is algebraic over $K\langle u\rangle$, and therefore, it can be seen as a dynamics of the form $K\langle u, y\rangle / K\langle u\rangle$, where $K = \mathbb{R}$.

Definition 1.6 (Algebraic Observability Condition (AOC)) A state variable $x_i \in \mathbb{R}$ is said to be algebraically observable if it is algebraic over $\mathbb{R}\langle u, y\rangle$, that is, if x satisfies a differential algebraic polynomial in terms of $\{u, y\}$ (where $\mathbb{R}\langle u, y\rangle$

denotes the differential field generated by the field $\mathbb{R}$), the input u, the measurable output y, the time derivatives of u and y, and some of their time derivatives, i.e.,

$$P_i(x_i, u, \dot{u}, \ldots, y, \dot{y}, \ldots) = 0, \tag{1.1}$$

with coefficients in $\mathbb{R}\langle u, y\rangle$.

Example 1.4 Consider the following nonlinear system:

$$\begin{aligned} \dot{x}_1 &= -x_1 x_2, \\ \dot{x}_2 &= -x_2^2 + x_1 + u. \\ y &= x_2 \end{aligned} \tag{1.2}$$

It can easily be seen from Definition 1.6 that x_1 and x_2 are algebraically observable, because they satisfy

$$\begin{aligned} P(x_1, u, y, \dot{y}) &= x_1 - \dot{y} - y^2 + u = 0, \\ P(x_2, y) &= x_2 - y = 0, \end{aligned}$$

which are differential algebraic polynomials with coefficients over $\mathbb{R}\langle u, y\rangle$.

In control theory, we commonly talk about canonical forms for linear and nonlinear systems. Differential-algebraic tools give us methods to obtain controller and observability canonical forms. In this work, we will use the generalized observability canonical form [9], but we introduce it by means of the following definition.

Definition 1.7 A system is Picard–Vessiot (PV) if the $k\langle u\rangle$-vectorial space generated by derivatives of the set $\{y^{(\beta)}, \beta \geq 0\}$ has finite dimension.

Consider a system represented by $\bar{H}(\bar{y}, \bar{y}^{(1)}, \ldots, \bar{y}^{(n-1)}, \bar{y}^{(n)}, u, u^{(1)}, \ldots, u^{(\gamma)}) = 0$. It can be solved locally as follows:

$$\bar{y}^{(n)} = -\mathscr{L}(\bar{y}, \ldots, \bar{y}^{(n-1)}, u, u^{(1)}, \ldots, u^{(\gamma-1)}) + u^{(\gamma)}.$$

Recall that $\xi_i = \bar{y}^{(i-1)}$, $1 \leq i \leq n$. A local form is obtained, which can be seen as a generalized observability canonical form (GOCF),

$$\begin{aligned} \dot{\xi}_1 &= \xi_2, \\ \dot{\xi}_2 &= \xi_3, \\ &\vdots \\ \dot{\xi}_{n-1} &= \xi_n, \\ \dot{\xi}_n &= -\mathscr{L}(\xi_1, \ldots, \xi_n, u, u^{(1)}, \ldots, u^{(\gamma-1)}) + u^{(\gamma)}, \\ \bar{y} &= \xi_1. \end{aligned} \tag{1.3}$$

Next example clarifies the above definition. We consider a Rössler system [6]. The output is chosen as $y = x_2$. This system has the following dynamics:

$$\begin{aligned} \dot{x}_1 &= -x_2 - x_3, \\ \dot{x}_2 &= x_1, \\ \dot{x}_3 &= a(x_2 - x_2^2) - bx_3, \\ y &= x_2, \end{aligned} \tag{1.4}$$

where $a = 0.386$ and $b = 0.2$. Recalling that $y^{(i-1)} = \bar{y}^{(i-1)} = \xi_i$, we see that the following local form is achieved:

$$\begin{aligned} \dot{\xi}_1 &= \xi_2, \\ \dot{\xi}_2 &= \xi_3, \\ \dot{\xi}_3 &= -\xi_2 - a(\xi_1 - \xi_1^2) + b(-\xi_3 - \xi_1) \\ y &= \xi_1. \end{aligned} \tag{1.5}$$

The change of coordinates that allows us to achieve a local form is as follows:

$$\begin{aligned} \xi_1 &= x_2, \\ \xi_2 &= x_1, \\ \xi_3 &= -x_2 - x_3. \end{aligned} \tag{1.6}$$

Rössler's system is plotted in its original coordinates (1.4) and its local form (1.5) in Figs. 1.2 and 1.3.

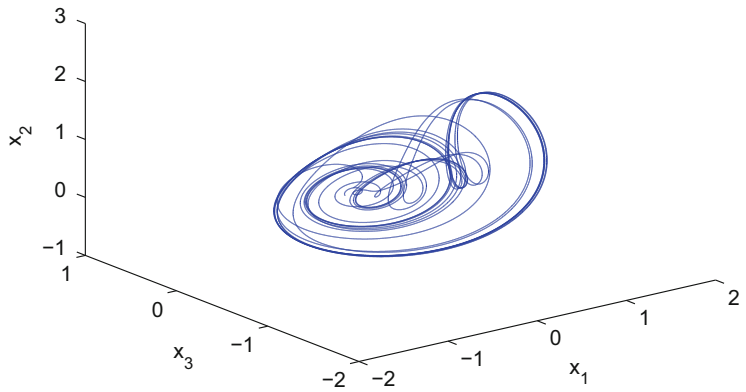

Fig. 1.2 Rössler system in original coordinates

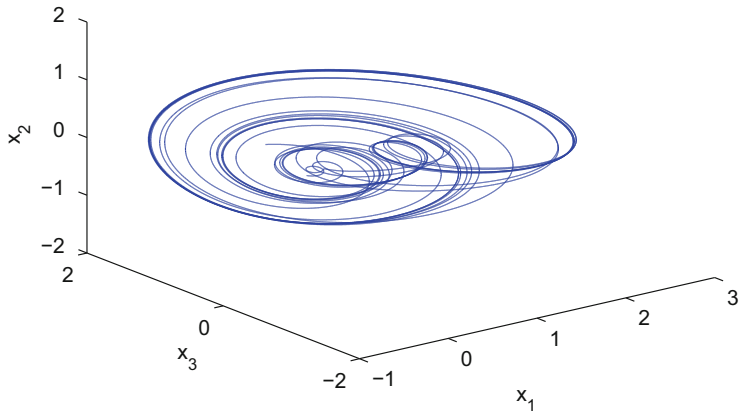

Fig. 1.3 Rössler system in local form

To end this section, we present an application of dynamical feedback control that can be constructed by means of differential-algebraic tools. The details regarding the development of this kind of control will be presented in subsequent chapters.

Given Rössler and Chua systems, we want to follow the trajectories of the Rössler system via the Chua system. This is a classical tracking control problem. Later, we will see that the synchronization problem can be seen as a tracking control problem, but for now, it is enough to present a single of dynamical feedback control to solve the tracking problem.

First, we consider the local form (1.5) of the Rössler system, and by choosing $\bar{y}_c = x_{s_3} + u_1$ as a primitive element for the Chua system, we achieve a local transformation defined as follows:

$$\begin{bmatrix} z_{c_1} \\ z_{c_2} \\ z_{c_3} \end{bmatrix} = \begin{bmatrix} x_{c_3} + u_1 \\ \dot{x}_{c_3} + u_2 \\ \ddot{x}_{c_3} + u_3 \end{bmatrix} = \begin{bmatrix} x_{c_3} + u_1 \\ -b_c x_{c_2} + u_2 \\ -b_c(x_{c_1} - x_{c_2} + x_{c_3}) + u_3 \end{bmatrix}, \tag{1.7}$$

where $u_1 = u_c$, $u_2 = \dot{u}_c$, and $u_3 = \ddot{u}_c$ are control signals. The Chua system with the control is given by the augmented controlled system

$$\begin{aligned} \dot{z}_{c_1} &= z_{c_2}, \\ \dot{z}_{c_2} &= z_{c_3}, \\ \dot{z}_{c_3} &= \Psi(x_c) + \bar{u}_c, \\ \dot{u}_1 &= u_2, \\ \dot{u}_2 &= u_3, \\ \dot{u}_3 &= \bar{u}_c, \end{aligned} \tag{1.8}$$

where $\Psi_c(x_c) = -b_m(\dot{x}_{c_1} - \dot{x}_{c_2} + \dot{x}_{c_3})$. We now have only to define $\bar{u}_c$ in such a way that the trajectories of the Chua system follow those of the Rössler system, i.e., $(z_{c_1}, z_{c_2}, z_{c_3}) \to (z_{r_1}, z_{r_2}, z_{r_3})$ as $t \to \infty$. To choose an appropriate control that satisfies the control objective, we first define the synchronization error in local coordinates as $e_z = z_r - z_c$. Then the error dynamics is given by

$$\begin{aligned} \dot{e}_1 &= e_2, \\ \dot{e}_2 &= e_3, \\ \dot{e}_3 &= \Psi_r(x_r) - \Psi_c(x_c) - \bar{u}_c(x_r, x_c, y_c), \end{aligned} \tag{1.9}$$

and the control signal is chosen as

$$\bar{u}_c(x_r, x_c, y_c) = \dot{u}_3 = \Psi_r(x_r) - \Psi_c(x_c) + \kappa e_z, \tag{1.10}$$

where $\kappa = [\kappa_1, \kappa_2, \kappa_3]$ is the vector of gains. With the selected control input, the closed-loop dynamics is given by $\dot{e}_z = Ae_z$, where $A \in \mathbb{R}^{3\times 3}$:

$$A = \begin{bmatrix} 0 & 1 & 0 \\ 0 & 0 & 1 \\ -\kappa_1 & -\kappa_2 & -\kappa_3 \end{bmatrix}. \tag{1.11}$$

We choose $(\kappa_1, \kappa_2, \kappa_3)$ such that A is a Hurwitz matrix. We then conclude that $\|e_z\| \to 0$ as $t \to \infty$.

Finally, some simulations were made to show the tracking in local coordinates. Figure 1.4 shows that the tracking control problem was solved, while Fig. 1.5 shows the tracking errors.

The set of definitions given in this section will be used frequently in this book, and some auxiliary definitions will be given in subsequent chapters.

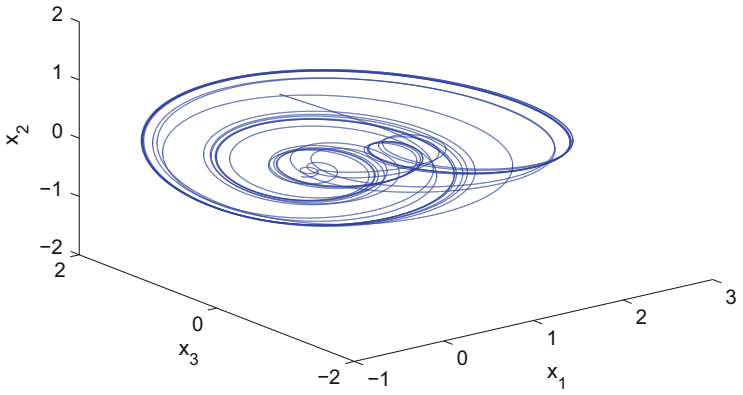

Fig. 1.4 Convergence of the Chua system trajectories to those of the Rössler system

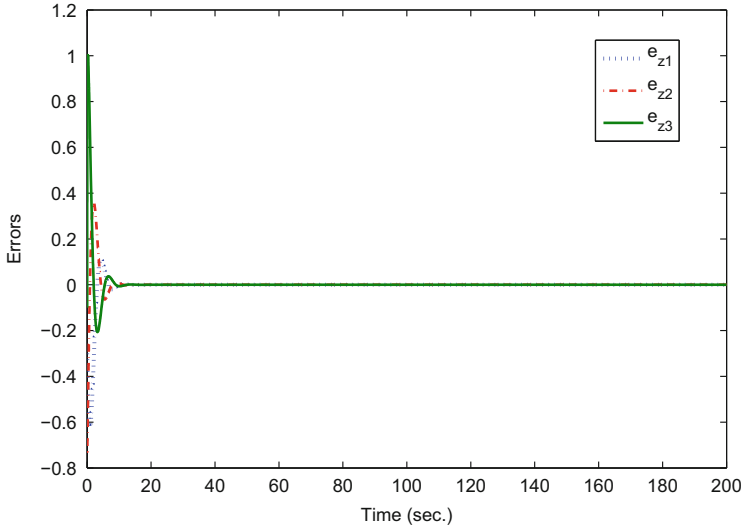

Fig. 1.5 Tracking errors

1.2 Differential-Geometric Point of View

Nonlinear geometric control theory has been studied since the 1980s [2, 13, 15, 21, 26]. It deals with concepts such as controllability and geometric properties of state spaces or subspaces and how those properties are preserved under coordinate changes, e.g., controlled invariant subspaces. Later, the linear geometric theory was extended to nonlinear systems [13]. However, the mathematical tools employed in nonlinear geometric theory are based mainly on differential geometry. In this section, we give a brief overview of nonlinear geometric control theory in order to introduce the necessary background to follow in Chaps. 3 and 6. Basically, we will use geometric control theory to develop sliding-mode observers.

Consider the vector-valued functions $f : \mathbb{R}^n \to \mathbb{R}^n$ and $g : \mathbb{R}^n \to \mathbb{R}^n$, where f, g are vector fields in C^∞. The Lie bracket is defined by

$$[f, g] \triangleq \frac{\partial f}{\partial x} g - \frac{\partial g}{\partial x} f,$$

where $\dfrac{\partial f}{\partial x}$ and $\dfrac{\partial g}{\partial x}$ are the Jacobian matrices of f and g. Using an alternative notation, it is possible to represent the Lie bracket as

$$[f, g] = (ad^1 f, g).$$

It is also defined as

$$(ad^k f, g) = [f, (ad^{k-1} f, g)], \quad 1 \leq k \leq n,$$

where by definition,

$$(ad^0 f, g) = g.$$

Let us now consider a C^∞ function $h : \mathbb{R}^n \to \mathbb{R}$. Let $\langle \cdot, \cdot \rangle$ denote the standard dot product on $\mathbb{R}^n$. Let dh denote the gradient of h ($dh = \nabla^T h$) with respect to x. Then the Lie derivative of h with respect to f is defined by

$$L_f h = L_f(h) = \langle dh, f \rangle = \nabla^T h \cdot f.$$

The following notation will be employed:

$$\begin{aligned} L_f^0 h &= h, \\ L_f^1 h &= L_f h, \\ &\vdots \\ L_f^k h &= L_f \left(L_f^{k-1} h \right). \end{aligned}$$

The Lie derivative of dh with respect to the vector field f is defined by

$$L_f(dh) = \left(\frac{\partial (dh)^T}{\partial x} f \right)^T + (dh) \frac{\partial f}{\partial x}.$$

One may easily verify that these Lie derivatives obey the following so-called Leibniz formula:

$$L_{[f,g]} h = \langle dh, [f, g] \rangle = L_g L_f h - L_f L_g h.$$

Furthermore, the following relation is valid:

$$dL_f h = L_f (dh).$$

We consider a nonlinear system described as follows:

$$\begin{cases} \dot{\xi} = f(\xi) + g(\xi) u, \\ y = h(\xi), \end{cases} \tag{1.12}$$

where $\xi \in \mathbb{R}^n$ is the state of the plant, $y \in \mathbb{R}$ is a measurable output, and f, g, h are smooth functions. If the system has uniform relative degree n, i.e.,

$$L_g h(\xi) = \cdots = L_g L_f^{n-2} h(\xi) = 0, \quad L_g L_f^{n-1} h(\xi) \neq 0,$$

then there exists a mapping

$$\eta = T(\xi) \tag{1.13}$$

that can transform the system (1.12) into the following observer canonical form:

$$\begin{aligned} \dot{\eta}_i &= \eta_{i+1}, \quad i = 1 \cdots n-1, \\ \dot{\eta}_n &= \Phi(\eta, u), \\ y &= \eta_1, \end{aligned} \tag{1.14}$$

where $\Phi(\eta, u)$ is a continuous nonlinear function.

Consider again the system (1.4), but now we look for a local transformation by means of geometric control techniques. If we put the system (1.4) in the form (1.14), we obtain $f(x) = (-x_2 - x_3, x_1, a(x_2 - x_2^2) - bx_3)^T$, $g(x) = (0, 0, -ax_2^2)$, and $h(x) = x_2$. Then we achieve the following change of coordinates:

$$\begin{aligned} \eta_1 &= h(x) = x_2, \\ \eta_2 &= L_f h(x) = x_1, \\ \eta_3 &= L_f^2 h(x) = -x_2 - x_3. \end{aligned} \tag{1.15}$$

Finally, in the new coordinates, the system (1.4) appears as

$$\begin{aligned} \dot{\eta}_1 &= \eta_2, \\ \dot{\eta}_2 &= \eta_3, \\ \dot{\eta}_3 &= -\eta_2 - a(\eta_1 - \eta_1^2) + b(-\eta_3 - \eta_1), \\ y_\eta &= \eta_1, \end{aligned} \tag{1.16}$$

which is in the same form as appeared in Sect. 1.1, but now it was obtained via geometric techniques. As we said at the beginning, we will use this procedure in Chaps. 3 and 6 to construct sliding-mode observers.

In the previous section, we used dynamical feedback control to solve the tracking control problem between Chua and Rössler systems. To end this section, we present an application of static feedback control to stabilize the system (1.4), which can be written as Eq. (1.12) so that we obtain

$$\begin{bmatrix} \dot{x}_1 \\ \dot{x}_2 \\ \dot{x}_3 \end{bmatrix} = \begin{bmatrix} -x_2 - x_3 \\ x_1 \\ ax_2 - bx_3 \end{bmatrix} + \begin{bmatrix} 0 \\ 0 \\ -ax_2^2 \end{bmatrix} u. \tag{1.17}$$

From (1.16), we have the Rössler system in new coordinates:

$$\begin{aligned}\dot{\eta}_1 &= \eta_2,\\ \dot{\eta}_2 &= \eta_3,\\ \dot{\eta}_3 &= -\eta_2 - a\eta_1 + b(-\eta_3 - \eta_1) + a\eta_1^2 u.\end{aligned} \tag{1.18}$$

Then the static feedback control that stabilizes (1.18) is given by

$$u = \frac{1}{a\eta_1^2}(b\eta_3 + \eta_2 + (1 + a + b)\eta_1). \tag{1.19}$$

Changing the control from the new coordinates to the original coordinates, we achieve the following equation, which stabilizes (1.17):

$$u = \frac{1}{ax_2^2}(-bx_3 + x_1 + (a + 1)x_2). \tag{1.20}$$

Note that it is possible to proceed in two ways: We can stabilize the system via Eq. (1.19) in the new coordinates and then change to original coordinates, or we can first change to original coordinates and then stabilize the system by means of Eq. (1.20) (Figs. 1.6 and 1.7).

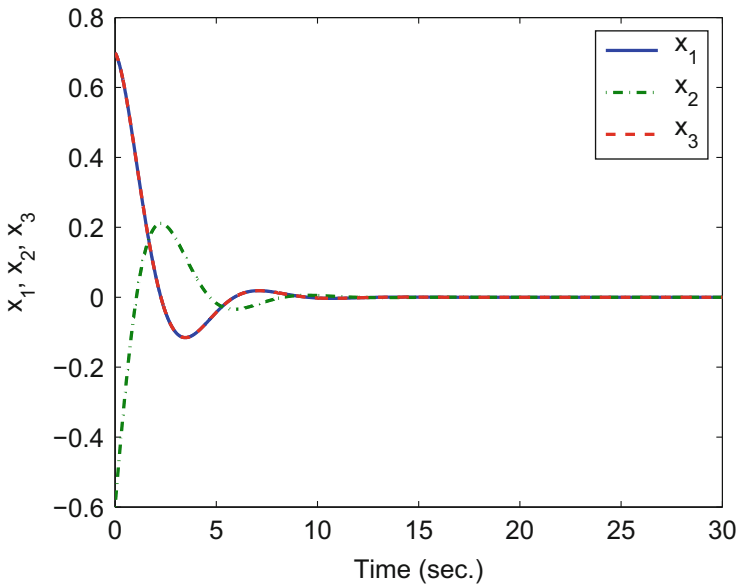

Fig. 1.6 Stabilization of the Rössler system in the original coordinates

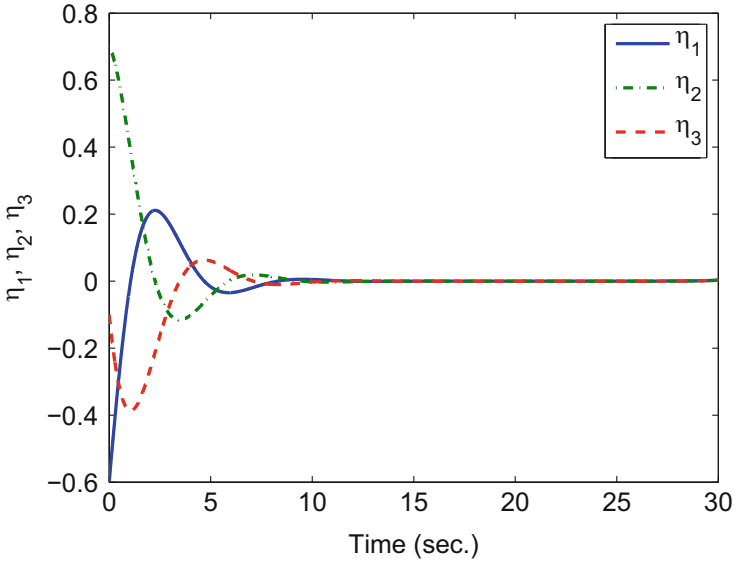

Fig. 1.7 Stabilization of the Rössler system in the new coordinates

1.3 Synchronization of Chaotic Systems

Consider now a type of nonlinear system whose steady-state behavior is more complicated and cannot be described simply as an equilibrium, periodic oscillation, or almost-periodic oscillation. This motion is usually referred to as chaos, and systems that exhibit this behavior are called chaotic systems. Some of these chaotic motions exhibit randomness, despite the deterministic nature of the system [15].

1.3.1 Attractors

A system whose behavior tends to evolve toward a set of numerical properties, this set is said an attractor. That is, when the trajectories of a system get close enough to the attractor, those values will remain close even if subjected to a slight perturbation.

Regular attractors act as limit cycles, in that the trajectories circle around a limiting trajectory that they asymptotically approach but never reach.

Strange attractors have two properties that describe their behavior: the trajectories on the attractor remain confined to a bounded region of phase space, and they separate exponentially fast from their neighbors. This raises the following question: how can trajectories diverge endlessly and yet stay bounded? The next example will answer this question intuitively.

Consider a nonuniform mass (set of initial conditions). A strange attractor typically arises when the flow contracts the mass in some directions (reflecting the dissipation in the system) and stretches it in others (leading to a sensitive dependence on initial conditions). The mass cannot stretch forever, and the distorted mass must therefore be folded back on itself to remain within the bounded region [27].

Strange attractors were thus called because they are often fractal sets. Nowadays, the dynamical property of sensitive dependence on initial conditions is considered more important than the geometric property of fractality.

As a example of a strange attractor, we can think of Chua's circuit. Chua introduced the concept of a "double scroll" as a way to describe the "anatomy" of the attractor of his circuit. The structure of Chua's attractor is described as two sheetlike objects curled together into a spiral form with infinitely many rotations while maintaining some space between the two scrolls that gradually decreases, thus causing them to meet eventually at some limit point. Thus Chua's attractor provides a definition of a double-scroll attractor [16].

1.3.2 Synchronization

Synchronization of chaos occurs in a process wherein two (or many) chaotic systems (either equivalent or inequivalent) have a common behavior due to coupling or forcing (periodic or noisy) of some property of their motion. The idea underlying the phenomenon of synchronization of chaos is that two chaotic systems may evolve on different attractors, but when coupled, they initially start on different attractors and then somehow eventually follow a common trajectory. Such synchronization between two systems is achieved when the trajectories of the systems are equal, which is the case when one of the two systems changes its trajectory to follow that of the other system or when both systems follow a new common trajectory [1, 10, 11].

A very important aspect in chaos theory is the synchronization of chaotic systems. After Pecora and Carroll [22] demonstrated that two apparently random and unpredictable chaotic behaviors can merge into a single trajectory, new expectations arose for chaos theory regarding the control of electrical and mechanical systems, as in the understanding and prediction in geophysical systems such as the atmosphere and ocean.

The phenomenon of synchronization of chaotic systems was at first thought impossible, because the solutions of such systems with nearby initial conditions diverge rapidly and moreover, are uncorrelated. However, in the work of Pecora and Carroll, it was shown that synchronization is possible.

One motivation for synchronization is the ability to send messages using chaotic secure communication systems. Such synchronized systems usually consist of two parts: a generator of chaotic signals (master) and a receiver (slave). A well-known example is the frequency synchronization of oscillating or rotating bodies. This process is known as natural synchronization. In other cases, to achieve synchronization,

it is necessary to introduce special actions or impose some restrictions. We then speak of forced or controlled synchronization.

Since chaotic systems are extremely sensitive to initial conditions, one might conclude that synchronization is infeasible, since in real systems, it is impossible to reproduce identical initial conditions for two similar systems. However, since 1990, with the experimental verification obtained by Pecora and Carroll, it became clear such that a situation was indeed feasible. Usually, synchronization of two or more chaotic systems is determined by the analysis of the error synchronization dynamics [19].

1.3.3 Some Examples of Synchronization

As a simple example, consider two identical Lorenz chaotic systems:

$$\begin{aligned} \dot{x}_1 &= -\sigma(x_2 - x_1), \\ \dot{x}_2 &= -\rho x_1 - x_2 - x_1 x_3, \\ \dot{x}_3 &= x_1 x_2 - \beta x_3, \end{aligned} \tag{1.21}$$

and

$$\begin{aligned} \dot{y}_1 &= -\sigma(y_2 - y_1), \\ \dot{y}_2 &= -\rho y_1 - y_2 - y_1 y_3, \\ \dot{y}_3 &= y_1 y_2 - \beta y_3, \end{aligned} \tag{1.22}$$

coupled as follows (see Fig. 1.8): Suppose a driving Lorenz system transmits a signal to a second Lorenz system (response system), and let that signal be the x-component of the first system. Wherever there is an x-component in the second system, we replace it with the signal from the first system:

$$\begin{aligned} \dot{y}_1 &= -\sigma(y_2 - x_1), \\ \dot{y}_2 &= -\rho x_1 - y_2 - x_1 y_3, \\ \dot{y}_3 &= x_1 y_2 - \beta y_3. \end{aligned} \tag{1.23}$$

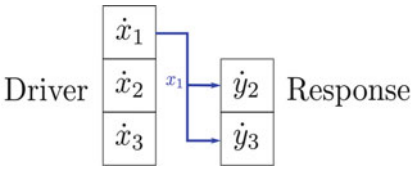

Fig. 1.8 Synchronization scheme

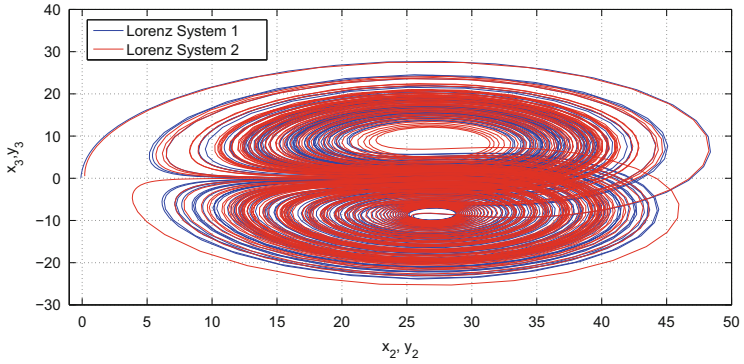

Fig. 1.9 No synchronization

This construction is called complete replacement. Note that we have replaced y_1 by x_1 in the above dynamics. This procedure gives the following augmented system, where the dynamics of $\dot{y}_1$ are omitted:

$$\begin{aligned}
\dot{x}_1 &= -\sigma(x_2 - x_1), \\
\dot{x}_2 &= -\rho x_1 - x_2 - x_1 x_3, \\
\dot{x}_3 &= x_1 x_2 - \beta x_3, \\
\dot{y}_2 &= -\rho y_1 - y_2 - y_1 y_3, \\
\dot{y}_3 &= y_1 y_2 - \beta y_3.
\end{aligned} \tag{1.24}$$

We can view x_1 as a driving signal for the second system. From arbitrary initial conditions, we will see that y_2 converges to x_2, and y_3 converges to x_3, as the system evolves. As time increases, the two equalities $x_2 = y_2$ and $x_3 = y_3$ arise, which means that both systems remain equal to each other as the system evolves. This situation is referred to as identical synchronization.

Figure 1.9 shows a phase plot with two different attractors for the states x_2, x_3, y_2, y_3 for the two identical Lorenz systems described in Eqs. (1.21) and (1.22). The trajectories of both systems unfold on different attractors, because the initial conditions are different (sensitivity to initial conditions), and there is no coupling between them, so they evolve differently. In Fig. 1.9, the systems are not synchronized. When the two Lorenz systems are coupled as described by Eq. (1.24), the two systems with different initial conditions will eventually become synchronized, as shown in Fig. 1.10.

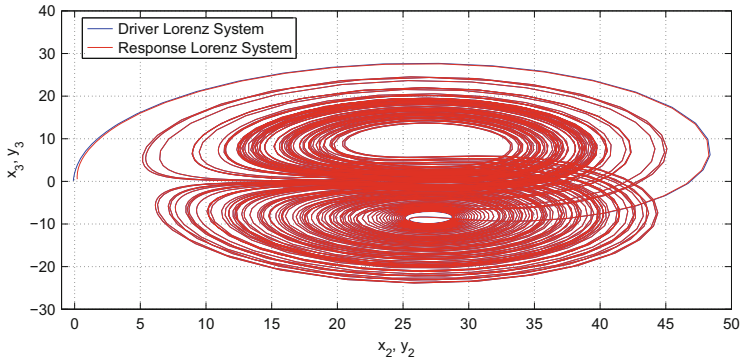

Fig. 1.10 Synchronization

1.3.4 Types of Synchronization

The coupling types are as follows:

1. *Unidirectional coupling,* whereby a system is subdivided into two subsystems, one of which leads while the other follows. The response of the slave system is forced to follow the dynamics of the driver system. In other words, the coupling does not alter the behavior of one of the two systems, so the resulting configuration becomes a unidirectional link. This type of configuration is known as "master–slave." An example of this configuration occurs in application to secure communications.
2. *Bidirectional coupling,* whereby both subsystems are coupled with another in some way so that their trajectories are mutually influenced by each other's behavior. A typical example occurs in lasers with feedback [25].

The most important type of synchronizations are as follows [23]:

- Complete synchronization.
- Generalized synchronization.
- Phase synchronization.
- Lag synchronization.

1.4 Complete Synchronization

We have said that two identical chaotic system are in a state of complete synchronization if the states of both systems coincide and vary chaotically in time. This is achieved by coupling both systems with the differences of the states in the corresponding dynamics. When this occurs, the coupling tends to make the corresponding state values equal. As a consequence, if the state values are equal,

then neither system will feel the coupling of the other. When there is a set of initial conditions such that the systems eventually evolve identically in time, the systems are said to be completely synchronized. Other names are given in the literature, such as conventional synchronization and identical synchronization.

As an example, consider the simplest case of chaos synchronization, whereby the coupling between the systems is unidirectional. However, in realistic situations, oscillators will often be coupled reciprocally when the dynamics of each system affects the oscillations in the other system through coupling. Consider the two mutually coupled Rössler systems

$$\begin{aligned} \dot{x_1} &= -\omega_1 y_1 - z_1 + C(x_2 - x_1), \\ \dot{y_1} &= \omega_1 x_1 + \alpha y_1, \qquad (1.25) \\ \dot{z_1} &= \beta + z_1(x_1 - \mu), \\ \dot{x_2} &= -\omega_2 y_2 - z_2 + C(x_1 - x_2), \\ \dot{y_2} &= \omega_2 x_2 + \alpha y_2, \qquad (1.26) \\ \dot{z_2} &= \beta + z_2(x_2 - \mu). \end{aligned}$$

Here $x_1, x_2, y_1, y_2, z_1, z_2$ are the states of the first and the second oscillators; α, β, and μ are the parameters governing the individual dynamics of the systems; C defines the strength of coupling between the oscillators; and ω_1, ω_2 determine the main frequencies of oscillations in the respective subsystems. Note that the systems are coupled only in the dynamics corresponding to the states x_1 and x_2, but this action of coupling $\pm(x_2 - x_1)$ is sufficient to synchronize both systems. We choose the parameter values of α, β, and μ such that at $C = 0$, both systems demonstrate chaotic oscillations, namely $\alpha = 0.165$, $\beta = 0.2$, $\mu = 10$.

1.5 Phase Synchronization

A periodic oscillator can be simply characterized by its maximum amplitude A and its frequency ω. The phase for every time t is simply ωt. Synchronization of the phase of a periodically driven chaotic system means that in some way, the phase of the oscillator becomes modified to follow the phase of a force. The general way to see this is the following. Assume the dynamics

$$\dot{x} = f(x) + p(t),$$

where $f(x)$ contains the dynamics of the chaotic oscillator, and $p(t)$ is a periodic oscillator. The idea is that the complete system remains chaotic, but its dynamics become modified in such a way that the phase of the chaotic attractor meets that of the applied force (periodic oscillator). It is worth mentioning that the concept of

the phase of a chaotic oscillator is not as simple as that of the phase of a periodic oscillator.

The concept of phase of oscillations is easy to understand if one considers harmonic oscillations $p(t) = A\cos(\Omega t + \varphi_0)$. These oscillations are characterized by the amplitude A and have period $T = \dfrac{2\pi}{\Omega}$. The argument $\phi(t) = \Omega t + \varphi_0$ is called the phase.

1.6 Lag Synchronization

It has been shown that when nonidentical chaotic oscillators are weakly coupled, the phases can be locked while the amplitudes remain highly uncorrelated [23]. But what happens when the coupling strength becomes larger? One would expect that with stronger coupling, a relationship between amplitudes might be established. Indeed, it has been demonstrated that there exists a regime of lag synchronization whereby the states of two oscillators are nearly identical, but one system lags in time behind the other. For intermediate coupling strengths, an interesting state can be observed: the states of two interacting systems nearly coincide if one is shifted in time $x_1(t) \approx x_2(t-\tau)$. Finally, with a further increase of coupling, the time shift decreases, and the regime tends to complete synchronization.

1.7 Generalized Synchronization

When an essential difference between the coupled systems exists, there is then no hope of having a trivial manifold in the phase space attracting the system trajectories, and therefore it is unclear whether nonidentical chaotic systems can synchronize. Two central issues are "milestones" of the subject. The first is that one should generalize the concept of synchronization to include nonidentity between the coupled systems. The second is that one should design some tests to detect it. This phenomenon is called generalized synchronization.

Generalized synchronization (GS) can be interpreted as the suppression of the dynamics of the driven system by the driving one, so that the "slave" system follows its "master." We discuss the GS of nonlinear systems that are completely triangularizable. For this class of systems, we use a dynamic feedback control that stabilizes the synchronization error dynamics.

In order to define the generalized synchronization (GS) of a coupled system, the GS problem is stated as follows: Consider two nonlinear system in a master–slave configuration whereby the master system is given by

$$\begin{aligned} \dot{x}_m &= F_m(x_m, u_m), \\ \dot{y}_m &= h_m(x_m), \end{aligned} \tag{1.27}$$

and the slave by

$$\begin{aligned} \dot{x}_s &= F_s(x_s, u_s(x_s, y_m)), \\ \dot{y}_s &= h_s(x_s), \end{aligned} \tag{1.28}$$

where $x_s = (x_{1_s}, \ldots, x_{n_s}) \in \mathbb{R}^{n_s}$, $x_m = (x_{1_m}, \ldots, x_{n_m}) \in \mathbb{R}^{n_m}$, $h_s : \mathbb{R}^{n_s} \to \mathbb{R}$, $h_m : \mathbb{R}^{n_m} \to \mathbb{R}$, $u_m = (u_{1_m}, \ldots, u_{m_m}) \in \mathbb{R}^{m_m}$, $u_s : \mathbb{R}^{n_s} \times \mathbb{R} \to \mathbb{R}$, y_m , $y_s \in \mathbb{R}$, F_s, F_m, h_s, h_m are assumed to be polynomial in their arguments.

This is a more general case, because systems (1.27) and (1.28) are not necessarily affine nonlinear systems. Indeed, the dynamics of the slave system does not need to be expressed as a linear part and a nonlinear part as in [22], where the nonlinear vector function is required to satisfy a Lipschitz condition.

Definition 1.8 (Generalized Synchronization) Slave and master systems are said to be in a state of GS if there exist a differential primitive element that generates a transformation $H_{m_s} : \mathbb{R}^{n_s} \to \mathbb{R}^{n_m}$ with $H_{m_s} = \Phi_m^{-1} \circ \Phi_s$ and an algebraic manifold $M = \{(x_s, x_m) | x_m = H_{m_s(x_s)}\}$ along with a compact set $B \subset \mathbb{R}^{n_m} \times \mathbb{R}^{n_s}$ with $M \subset B$ such that their trajectories with initial conditions in B approach M as $t \to \infty$.

The definition of GS leads us to the following criterion: $\lim_{t\to\infty} || H_{m_s}(x_s) - x_m || = 0$. It should be noted that identical or complete synchronization is a particular case of GS, that is, the transformation H_{m_s} is the identity.

In this chapter, we consider the master–slave configuration. Its main characteristic is that the link is unidirectional, i.e., the signal is transmitted from the master system to the slave system. Because of this, some authors use terminology from the theory of transceivers.

The synchronization of chaotic systems is a regime whereby after a time of transmission, two coupled chaotic systems exhibit identical chaotic oscillations. The synchronization can be solved from the point of view of control theory, by designing a slave system using a state observer that is able to estimate the variables of the master system.

We now briefly introduce the chaotic systems that will appear in this book.

1.8 Some Classical Chaotic Systems

1.8.1 Lorenz System

The set of differential equations called a Lorenz system derives from the work of the meteorologist/mathematician Edward N. Lorenz in his study of thermal variations in an air cell. The dynamics of a Lorenz system is represented as follows [5, 19]:

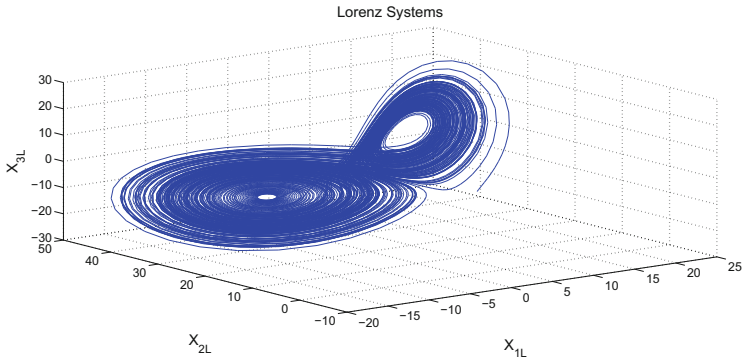

Fig. 1.11 Lorenz system

The system of differential equations Lorenz used was

$$\begin{aligned} \dot{x}_1 &= -\sigma(x_2 - x_1), \\ \dot{x}_2 &= \rho x_1 - x_2 - x_1 x_3, \\ \dot{x}_3 &= x_1 x_2 - \beta x_3, \end{aligned} \tag{1.29}$$

where σ, ρ, and β are positive parameters that denote physical characteristics of air flow. The variable x_1 corresponds to the amplitude of convective currents in the air cell, x_2 to the temperature difference between rising and falling currents, and x_3 to the deviation of the temperature from the normal temperature in the cell. A Lorenz system exhibits sensitivity to initial conditions and the presence of limit cycles that repeatedly double their period as ρ is varied in one direction until the orbits begin to behave chaotically. The plot of the trajectories of the Lorenz chaotic attractor resembles a butterfly or figure-eight. This is shown in Fig. 1.11.

1.8.2 Rössler System

The Rössler's attractor was designed by Otto Rössler [12] in 1976. His equations were later found useful in modeling equilibria in chemical reactions. This attractor has only one manifold. Figure 1.12 shows a Rössler chaotic system.

$$\begin{aligned} \dot{x}_1 &= -(x_2 + x_3), \\ \dot{y}_{x_2} &= x_1 + a x_2, \\ \dot{z} x_3 &= b + x_3(x_1 - c), \end{aligned} \tag{1.30}$$

where $a = b = 0.2$ and $c = 0.5$.

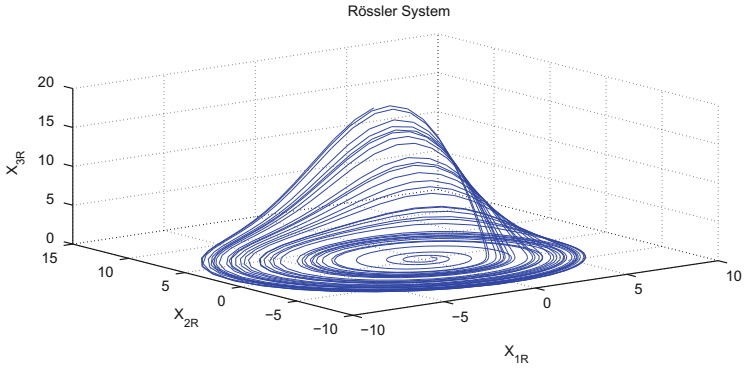

Fig. 1.12 A Rössler system

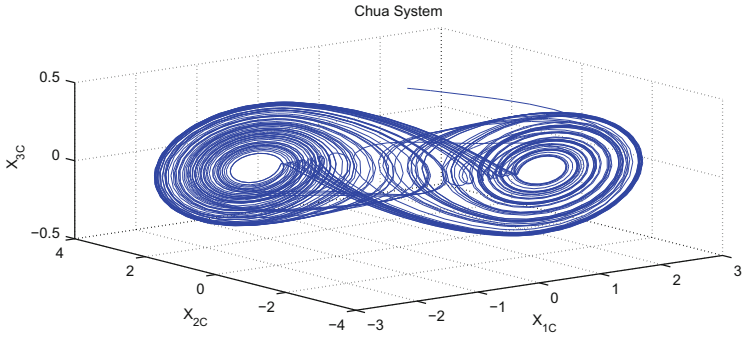

Fig. 1.13 Chua's system

1.8.3 Chua System

Chua's system was the first chaotic system observed in the laboratory [16, 20], confirmed by computer simulations, and rigorously mathematically proven. This system was created as an electric circuit with the following dynamical equations:

$$\begin{aligned} \dot{x}_1 &= \alpha(x_2 - h(x_1)), \\ \dot{x}_2 &= x_1 - x_2 + x_3, \\ \dot{x}_3 &= -\beta x_2, \end{aligned} \tag{1.31}$$

where h is a piecewise-linear function. In Fig. 1.13, we can observe the behavior of Chua's system

$$h(x) = \begin{cases} m_1(x+1) - m_0, & x < -1, \\ m_0 x \qquad\qquad\quad , & -1 \le x \le 1, \\ m_1(x-1) + m_0, & x > 1, \end{cases} \tag{1.32}$$

and α and β are bifurcation parameters. Note that Chua's equations contain only one scalar nonlinearity, which in this sense makes this system simpler than the Lorenz attractor, since the Lorenz equations contain three nonlinear terms consisting of products of two variables.

1.8.4 Colpitts System

The Colpitts oscillator [18], named after its inventor Edwin Colpitts, is another type of LC oscillator design. The basic configuration of the Colpitts oscillator uses a capacitor voltage divider as its feedback source. The two capacitors, C_1 and C_2, are placed across a common inductor L, as shown, so that C_1, C_2, and L form a tuned tank circuit. The advantage of this type of tank-circuit configuration is that with less self and mutual inductance in the tank circuit, frequency stability is improved along with the simpler design:

$$\begin{aligned} \dot{x}_1 &= x_2 - F(x_3), \\ \dot{x}_2 &= u + x_1 - bx_2 - x_3, \\ \dot{x}_3 &= \frac{(x_2 - d)}{\varepsilon}, \end{aligned} \tag{1.33}$$

where $u = \dfrac{v}{v^*}$ is the input of the system, $a = \dfrac{\sqrt{\frac{L}{C_1}}}{r}$, $b = \dfrac{R}{\sqrt{\frac{L}{C_1}}}$, $d = \dfrac{\sqrt{\frac{L}{C_1}} I_0}{v^*}$, $\varepsilon = \dfrac{C_2}{C_1}$, and the nonlinear equation is given by

$$F(x_3) = \begin{cases} -a(x_3 + 1), & x_3 \le -1 \\ 0 \qquad\quad , & x_3 \ge -1. \end{cases} \tag{1.34}$$

The circuit parameters are $L = 100\,\mu\text{H}$, $C_1 = C_2 = 47\,\text{nF}$, $R = 45\,\Omega$, $I_0 = 5\,\text{mA}$. We can observe the Colppits system in Fig. 1.14.

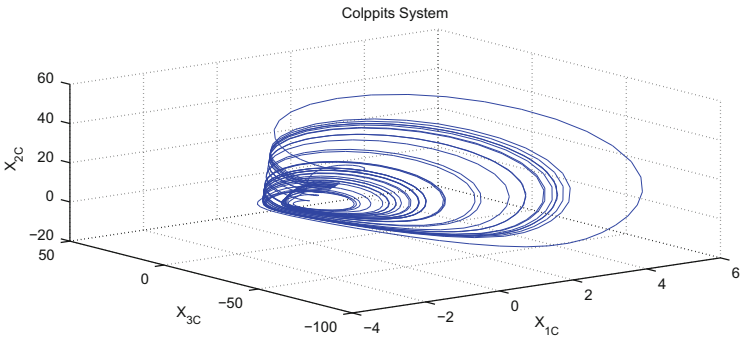

Fig. 1.14 Colppits system

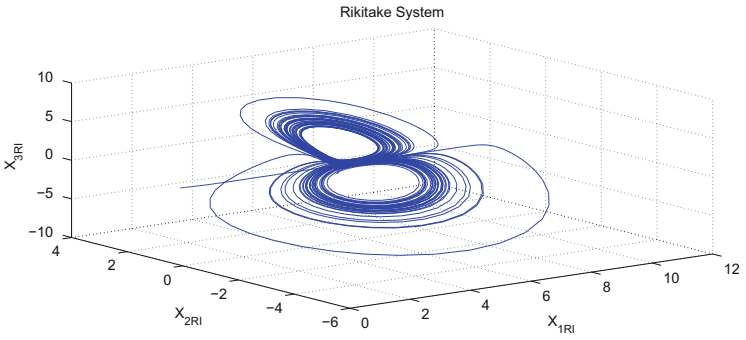

Fig. 1.15 Rikitake system

1.8.5 Rikitake System

The Rikitake system is a three-dimensional vector field obtained experimentally from a two-disk dynamo apparatus, which models the Earth's geomagnetic field and is used to explain the known irregular switch in its polarity. The system has a three-dimensional Lorenz-type chaotic attractor around its two singular points [14]. However, this attractor is not bounded by any ellipsoidal surface as in the Lorenz attractor:

$$\begin{aligned} \dot{x}_1 &= -\mu x_1 + x_2 x_3, \\ \dot{x}_2 &= -\mu x_2 + (x_3 - a) x_1, \\ \dot{x}_3 &= 1 - x_1 x_2, \end{aligned} \tag{1.35}$$

where a and μ are parameters that we will assume to be nonnegative. The Rikitake chaotic system is a simple three-dimensional quadratic autonomous chaotic system, which can generate complex two-scroll chaotic attractors simultaneously. We can observe the Rikitake system in Fig. 1.15.

1.8.6 Duffing System

Duffing's oscillator was introduced in 1918 by G. Duffing. In practice, one would like to understand the route to chaos in systems described by partial differential equations, such as flow in a randomly stirred fluid. This is, however, very complicated and difficult to treat either analytically or numerically. Here we consider an intermediate situation whereby the dynamics is described by a single ordinary differential equation, called the Duffing equation [8]. The Duffing equation describes the motion of a classical particle in a double-well potential.

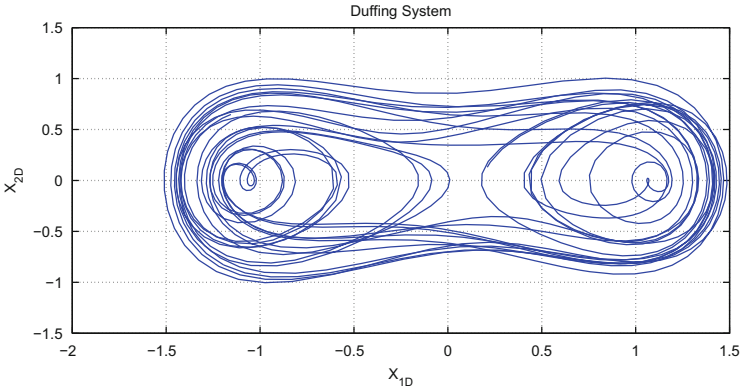

Fig. 1.16 Duffing system

The most general forced form of the Duffing equation is

$$\ddot{x} + \delta\dot{x} + (\beta x^3 \pm \omega_0^2 x) = \gamma\cos(\omega t + \phi), \tag{1.36}$$

where δ controls the size of the damping, γ controls the amplitude of the periodic driving force, ω controls the frequency of the periodic driving force. For $\beta > 0$, the equation represents a "hard spring," and for $\beta < 0$, it represents a "soft spring." If we take $\beta = 1$, $\omega_0 = 1$, reset the clock so that $\phi = 0$, and introduce a minus sign, it can be written as a system of first-order ordinary differential equations as

$$\begin{aligned} \dot{x}_1 &= x_2, \\ \dot{x}_2 &= x_1 - x_1^3 - \delta x_2 + \gamma\cos(\omega t). \end{aligned} \tag{1.37}$$

Figure 1.16 shows the trajectories of a Duffing chaotic system.

1.8.7 Van der Pol System

The Van der Pol oscillator is a nonconservative oscillator with nonlinear damping. Energy is dissipated at high amplitudes and generated at low amplitudes. As a result, there exist oscillations around a state at which energy generation and dissipation balance. It has been used in the study and design of many models, including such biological phenomena as the heartbeat and neurons, acoustic models, and radiation of mobile phones, and as a model of an electrical oscillator [4].

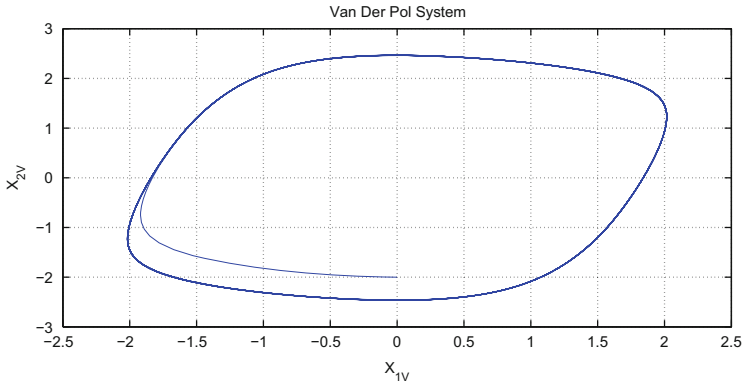

Fig. 1.17 Van der Pol system

The Van der Pol oscillator is described by the autonomous system

$$\begin{aligned} \dot{x}_1 &= x_2 - \epsilon \left(\frac{x_1^3}{3} - x_1 \right), \\ \dot{x}_2 &= -x_1. \end{aligned} \tag{1.38}$$

That is, it is not volume-preserving except when $\epsilon = 0$. If $\epsilon = 0$, the equation becomes $\ddot{x} + \dot{x} = 0$, the simple harmonic oscillator, which is conservative.

Figure 1.17 shows the behavior of the Van der Pol system.

1.9 Fractional-Order Systems

Fractional calculus is a mathematical topic whose history goes back more than 300 years. Its application to physics and engineering, however, has been reported on only in recent years. It has been found that such in interdisciplinary fields, many systems can be described by fractional differential equations. For instance, fractional derivatives have been widely used in the mathematical modeling of viscoelastic materials. Some electromagnetic problems are described using fractional integrodifferential operators. The anomalous diffusion phenomena in inhomogeneous media can be explained by a noninteger-derivative-based equation of diffusion. Study of fractional-order systems has attracted increasing attention in recent years, and it has been found that some such systems can demonstrate chaotic behavior.

The fractional calculus can be considered a generalization of the conventional calculus. That is, fractional calculus is a generalization of integration and differentiation to noninteger orders, which can be expressed by means of the fundamental

operator ${}_a D_t^r$, where a and t are the limits of the operation, and $r \in \mathbb{R}$. It is important to mention that the meaning of the operator depends on whether r is positive or negative, which correspond respectively to the operations of derivation and integration [3]:

$$ {}_a D_t^r = \begin{cases} \dfrac{d^r}{dt^r} & r > 0, \\ 1 & r = 0, \\ \int_a^t (d\tau)^{-r} & r < 0. \end{cases} \tag{1.39} $$

1.9.1 Fractional-Order Operator Block in Simulink

For numerical simulation of fractional-order systems, we used a toolbox in Matlab/Simulink called Ninteger. It uses an approximation in the frequency domain (rational transfer function) of a fractional-order derivative:

$$ C(s) = ks^q, \quad q \in \mathbb{R}. $$

The method for polynomial approximation is done using Matlab's CRONE toolbox, which uses a recursive distribution of N poles and N zeros:

$$ C(s) = k' \prod_{n=1}^{N} \frac{1 + s/\omega_{zn}}{1 + s/\omega_{pn}}, $$

where k' is a gain setting such that if $k = 1$, then $| C(s) | = 0\,\text{dB}$ in 1 rad/s. The poles and zeros are found in the range $[\omega_l ; \omega_h]$ and are given for a positive value of q:

$$ \begin{aligned} \alpha &= (\omega_h/\omega_l)^{\frac{q}{N}}, \quad \eta = (\omega_h/\omega_l)^{\frac{1-q}{N}}, \\ \omega_{z1} &= \omega\sqrt{\eta}, \quad \omega_{zn} = \omega_{p,n-1}\eta, \quad n = 2, \ldots, N, \\ \omega_{pn} &= \omega_{z,n-1}\alpha, \quad n = 1, \ldots, N. \end{aligned} $$

For a negative q, the roles of the zeros and poles are exchanged.

The Ninteger operation in the Matlab toolbox can be seen in Fig. 1.18.

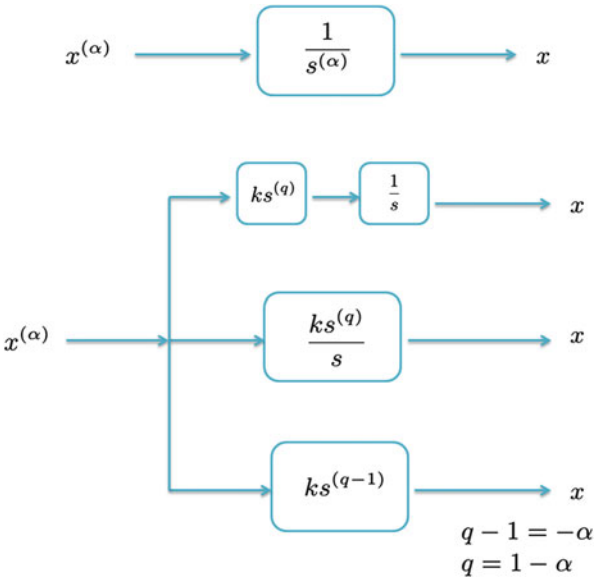

Fig. 1.18 Basic function of block Ninteger

1.10 Why Fractional Order?

The question then is this: can we give a deterministic natural assumption in some known cases to justify the use of fractional systems? The answer to this question is yes. Let us consider the following population dynamics, which is a classical model for competition between two species with population densities x and y:

$$\frac{dx}{dt} = x(k_1 - \rho_1 x - \alpha_1 y), \tag{1.40}$$

$$\frac{dy}{dt} = y(k_2 - \rho_2 y - \alpha_2 x), \tag{1.41}$$

where $k_1, k_2, \rho_1, \rho_2, \alpha_1$ y α_2 are positives constants.

In this model, we assume the following two hypotheses:

1. Two towns x and y each grow in proportion to their size, which in standard notation is given by $\frac{dx}{dt} = k_1 x(t)$, $\frac{dy}{dt} = k_2 y(t)$, or equivalently, $x(t) = C_1 e^{k_1 t}$, $y(t) = C_2 e^{k_2 t}$. Then the evolution of the populations over time follows a classical exponential law.
2. When one population grows beyond a certain point, then the other decreases, and conversely, which justifies the nonlinear terms of type x. Furthermore, the average of the two populations is limited by nature, so that those populations cannot grow indefinitely large, which explains the nonlinear terms of type x^2 and y^2.

When one understands these assumptions, it is clear that growth can be of an exponential nature but not necessarily classical. For example, the populations x and y could grow as a generalized exponential: $x(t) = C_1 E_\alpha(k_1 t^\alpha)$, $y(t) = C_2 E_\beta(k_2 t^\beta)$, where C_1, C_2, k_1, and k_2 are real constants, and $0 < \alpha, \beta \leq 1$. There are other classic exponential generalizations that may be used in real models.

Thus, we could replace the first instance of the hypothesis by $x(t) = C_1 E_\alpha(k_1 t^\alpha)$, $y(t) = C_2 E_\alpha(k_2 t^\alpha)$, which is equivalent to introducing a Caputo fractional derivative: $({}_a D_t^\alpha x)(t) = k_1 x(t)$, $({}_a D_t^\alpha y)(t) = k_2 y(t)$.

We thus arrive at the following generalized fractional mode:

$$ {}_a D_t^\alpha x = x(k_1 - \rho_1 x - \alpha_1 y), \tag{1.42} $$

$$ {}_a D_t^\alpha y = y(k_1 - \rho_1 y - \alpha_1 x), \tag{1.43} $$

where k_1, k_2, ρ_1, ρ_2, α_1, and α_2 are positive real constants.

It is possible to find examples in which the regular model is not accurate enough and the fractional model might provide a better approximation. Examples include the uncontrolled growth of cancer cells and the slow growth of human populations in unfavorable environments such a war and epidemic.

1.11 Fractional Circuit

In this section, we show a physical circuit for a fractional chaotic Rössler system. Its dynamics is defined as follows:

$$ \begin{aligned} x_{1R}^{(\alpha)} &= -(x_{2R} + x_{3R}), \\ x_{2R}^{(\alpha)} &= x_{1R} + a_R x_{2R}, \\ x_{3R}^{(\alpha)} &= 0.2 + x_{3R}(x_{1R} - 10), \end{aligned} \tag{1.44} $$

where $a_r = 0.63$ and $\alpha = 0.90$.

We can see in Fig. 1.19 the trajectories of the Rössler system.

Fig. 1.20 represents Eq. (1.44), $\frac{1}{s^{(\alpha)}}$ was made on the fractional Rössler as a representative example of the circuit implementation of a fractional.

Using the method of A. Charef [7], we can obtain an approximation of $\frac{1}{s^{(0.9)}}$ with an error of about 2 dB:

$$ H(s) = \frac{2.2675(s + 1.292)(s + 215.4)}{(s + 0.01292)(s + 2.154)(s + 359.4)}. \tag{1.45} $$

The F block in the feedback of the integrator in Fig. 1.20 represents the fractional integrator (1.45) shown in Fig. 1.21.

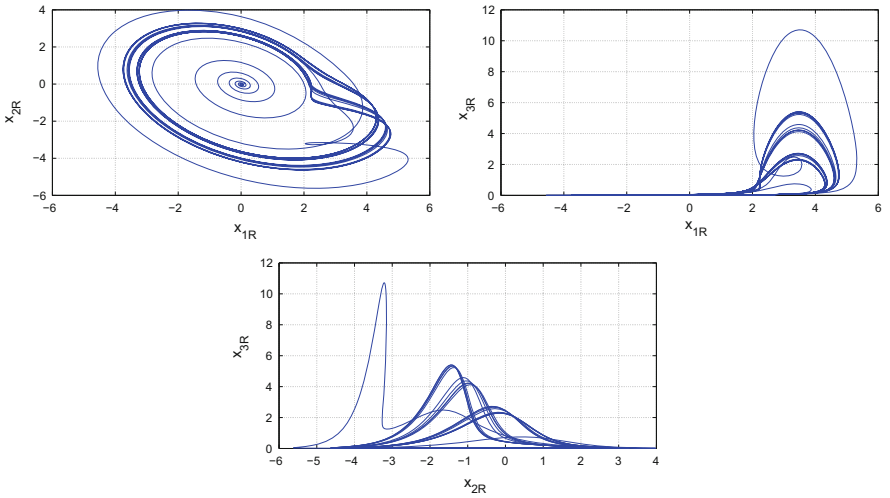

Fig. 1.19 Simulation of Rössler fractional system in Simulink: (**a**) $x_{1R} - x_{2R}$, (**b**) $x_{1R} - x_{3R}$, (**c**) $x_{2R} - x_{3R}$

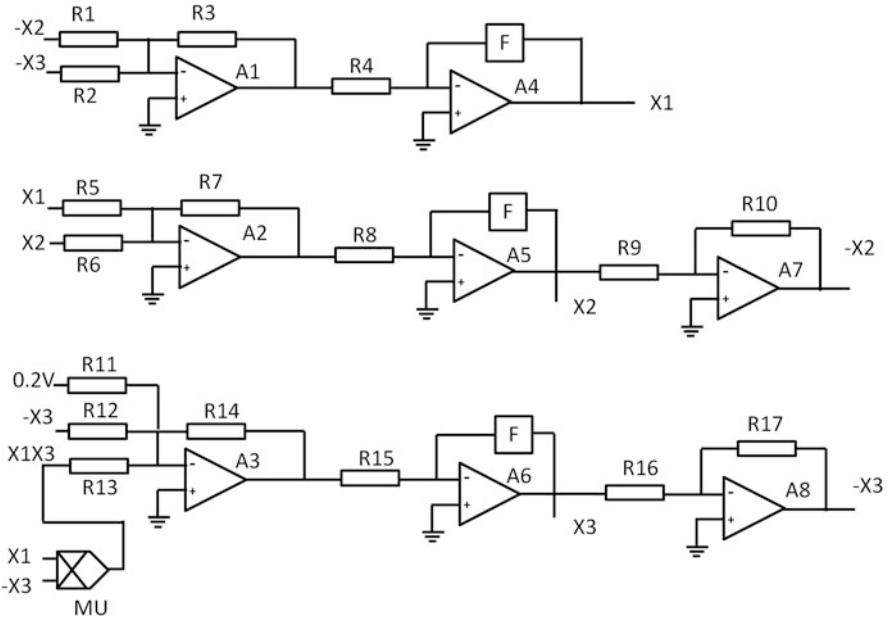

Fig. 1.20 Rössler's fractional circuit system

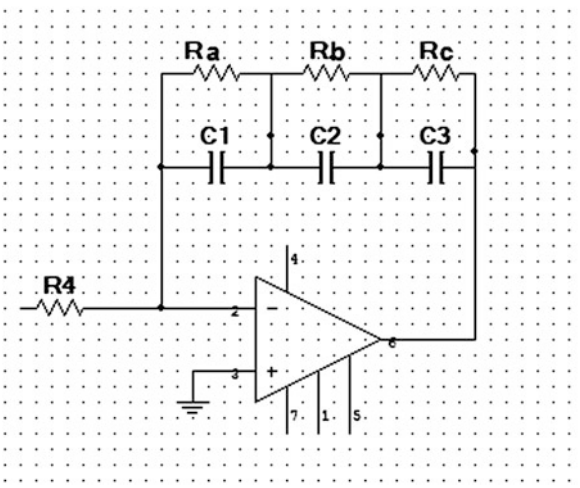

Fig. 1.21 Circuit of a fractional integrator $\frac{1}{s^{0.9}}$

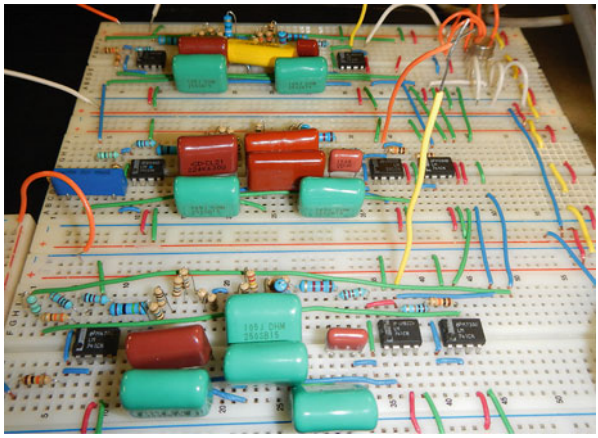

Fig. 1.22 Rössler fractional circuit

The circuit is designed to show a Rössler fractional-order system, where AD633 is a multiplier with a coefficient output of 0.1, and the LM741 circuit is an operational amplifier. We can obtain the equations of a fractional Rössler system in the Laplace domain as follows:

$$\frac{x_1(s)}{F(s)} = \frac{R_3}{C_0 R_4}\left[-\frac{R_{10}}{R_9 R_1}x_2(s) - \frac{R_{17}}{R_{16}R_2}x_3(s)\right], \tag{1.46}$$

$$\frac{x_2(s)}{F(s)} = \frac{R_7}{C_0 R_8}\left[\frac{x_1(s)}{R_5} + \frac{x_2(s)}{R_6}\right], \tag{1.47}$$

$$\frac{x_3(s)}{F(s)} = \frac{R_{14}}{C_0 R_{15}}\left[\frac{0.2}{R_{11}}x_2(s) - \frac{R_{17}}{R_{16}R_{12}}x_3(s) + \frac{k x_3(s)x_1(s)}{R_{13}}\right], \tag{1.48}$$

where k is the output constant of the AD633 multiplier (Fig. 1.22). The simulation was performed on the Workbench / Multisim 11.0. As can be seen, the physical

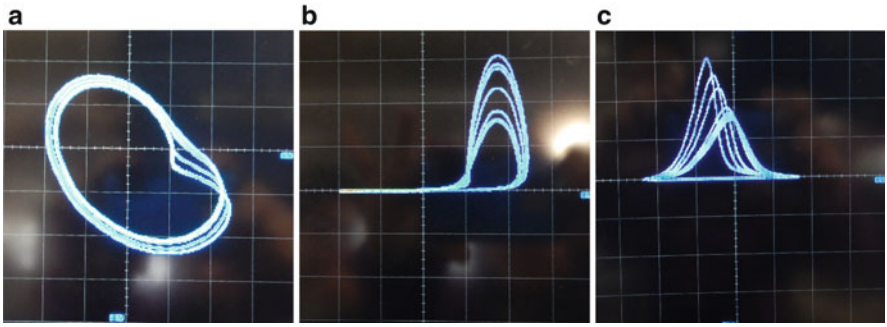

Fig. 1.23 Phase plane (**a**) $x_{1R} - x_{2R}$, (**b**) $x_{1R} - x_{3R}$ and (**c**) $x_{2R} - x_{3R}$

trajectories in Fig. 1.23 are similar to those obtained by numerical simulations in Fig. 1.19.

References

1. A. Balanov, N. Janson, D. Postnov, O. Sosnovtseva, *Synchronization: From Simple to Complex* (Springer, New York, 1965)
2. R.W. Brockett, Nonlinear control theory and differential geometry, in *Proceedings of ICM*, Warszawa, 1983, pp. 1357–1368
3. R. Caponetto, G. Dongola, L. Fortuna, I. Petrás, *Fractional Order Systems: Modeling and Control Applications*. World Scientific Series on Nonlinear Science Series A, vol. 72 (World Scientific Publishing, Singapore, 2010), pp. 1–4
4. R. Caponetto, G. Dongola, L. Fortuna, I. Petrás, *Fractional Order Systems: Modeling and Control Applications*. World Scientific Series on Nonlinear Science Series A, vol. 72 (World Scientific Publishing, Singapore, 2010), pp. 59–60
5. R. Caponetto, G. Dongola, L. Fortuna, I. Petrás, *Fractional Order Systems: Modeling and Control Applications*. World Scientific Series on Nonlinear Science Series A, vol. 72 (World Scientific Publishing, Singapore, 2010), pp. 62–65
6. J.-F. Chang, M.-L. Hung, Y.-S. Yang, T.-L. Liao, J.-J. Yan, Controlling chaos of the family of Rössler systems using sliding mode control. Chaos Solitons Fractals **37**(2), 609–622 (2008)
7. A. Charef, H.H. Sun, Y.Y. Tsao, B. Onaral, Fractal system as represented by singularity function. IEEE Trans. Autom. Control **37**(9), 1465–1470 (1992)
8. G. Duffing, *Erzwungene Schwingung bei veränderlicher Eigenfrequenz und ihre technische Bedeutung* (Vieweg, Braunschweig, 1918)
9. M. Fliess, Generalized controller canonical forms for linear and nonlinear dynamics. IEEE Trans. Autom. Control **35**(9), 994–1001 (1990)
10. A.L. Fradkov, *Cybernetical Physics: From Control of Chaos to Quantum Control* (Springer, Berlin, 2007), p. 213
11. A.L. Fradkov, B. Andrievsky, R.J. Evans, Adaptive observer-based synchronization of chaotic system with first-order coder in the presence of information constraints. IEEE Trans. Circ. Syst. I Reg. Pap. **55**(6), 1685–1694 (2008)
12. P. Gaspard, in *Encyclopedia of Nonlinear Science*, ed. by A. Scott (Routledge, New York, 2005), pp. 808–811

13. A. Isidori, *Nonlinear Control Systems*, 3rd edn. Communications and Control Engineering (Springer, New York, 1995)
14. M. Javidi, N. Nyamoradi, Numerical chaotic behaviour of the fractional Rikitake system. World Acad. Union **9**, 120–129 (2013)
15. H.K. Khalil, *Nonlinear Systems* (Prentice Hall, Upper Saddle River, 2002), pp. 4803–4811
16. L.M. Kocié, S. Gegovska-Zajkova, S. Kostadinova, *On Chua Dynamical System*, vol. 2 (Scientific Publications of the State University of Novi Pazar, Novi Pazar, 2010), pp. 53–60
17. E.R. Kolchin, *Differential Algebra and Algebraic Groups* (Academic, New York, 1973)
18. R. Martínez Guerra, J.L. Mata-Machuca, Generalized synchronization via the differential primitive element. Appl. Math. Comput. **232**, 848–857 (2014)
19. J.L. Mata Machuca, R. Martínez Guerra, R. López Aguilar, *Observadores para Sincronización de Sistemas Caóticos: Un Enfoque Diferencial y Algebraico* (Editorial Académica Española, Saarbrücken, 2013)
20. T. Matsumoto, L.O. Chua, M. Komuro, The double scroll. IEEE Trans. Circ. Syst. **Cas-32**(8), 798–818 (1985)
21. H. Nijmeijer, A. Van der Schaft, *Nonlinear Dynamical Control Systems* (Springer, New York, 1990)
22. L.M. Pecora, T.L. Caroll, Synchronization in chaotic systems. Phys. Rev. Lett. **64**(8), 821–824 (1990)
23. A. Pikovsky, M. Rosenblum, J. Kurths, *Synchronization: A Universal Concept in Nonlinear Sciences* (Cambridge University Press, Cambridge, 2002)
24. J.F. Ritt, *Differential Algebra* (Dover, New York, 1966)
25. A.E. Siegman, *Lasers* (University Science Books, Mill Valley, 1986)
26. D.E. Sontag, *Mathematical Control Theory: Deterministic Finite Dimensional Systems*, 2nd edn. (Springer, New York, 1998)
27. S.H. Strogatz, *Nonlinear Dynamics and Chaos* (Perseus Books, Cambridge, 1994), pp. 423–448

Chapter 2
A Model-Free-Based Proportional Reduced-Order Observer Design for the Synchronization of Lorenz Systems

Abstract In this chapter, we deal with the synchronization problem of a Lorenz system using a proportional reduced-order observer design in the algebraic and differential settings. We prove the asymptotic stability of the resulting error system, and by means of algebraic manipulations, we obtain estimates of the current states (master system). In this chapter, the construction of a proportional reduced-order observer is the main ingredient in our approach. Finally, we present simulations to illustrate the effectiveness of the suggested approach.

2.1 Introduction

In recent years, synchronization of chaotic systems has received a great deal of attention among scientists in many fields [1–5]. As is well known, the study of the synchronization problem for nonlinear systems has been very important from the nonlinear sciences point of view, in particular the applications to biology, medicine, cryptography, secure data transmission, and so on. In general, synchronization research has been focused onto two areas. The first is related to the employment of state observers, whereby the main application lies in the synchronization of nonlinear oscillators. On the other hand, the use of control laws makes it possible to achieve synchronization between nonlinear oscillators with different structures and orders [6]. Of particular interest is the connection between the observers for nonlinear systems and synchronization, which is also known as a master–slave configuration. Thus, the chaos synchronization problem can be posed as a one-observer design in which the coupling signal is viewed as the output, and the slave system as the (reduced-order) observer. In other words, basically, the chaos synchronization problem can be formulated as follows. Given a chaotic system that is considered the master (or driving) system, and another identical system, given as the slave (or response) system, the aim is to force the response of the slave system to synchronize with the master system [1, 2]. The idea is to use the output of the master system to control the slave system so that the states of the slave system follow the states of the master system asymptotically.

In this procedure, the construction of a full-order observer is unnecessary; that is, we construct a reduced-order observer (so-called model-free based observer) using

R. Martínez-Guerra et al., *Synchronization of Integral and Fractional Order Chaotic Systems*, Understanding Complex Systems,
DOI 10.1007/978-3-319-15284-4_2

the algebraic observability condition (AOC) applied to the estimation problem. The methodology proposed consists in the following. Define first a function as an additional state of the original system; this function is given in terms of the states. The dynamics of this new state is not known. The original system is then converted to an extended system in which the dynamics of the additional state is not known and supposed to be bounded. The original problem is then an observation problem, where the aim is to observe this additional state of the system. Since the dynamics of this new state is not known, a reduced-order observer for the unknown part of the system is proposed. In particular for its simplicity, a model-free-based proportional reduced-order observer is presented. Finally, we illustrate the effectiveness of the suggested approach with a Lorenz system.

The main contribution in this chapter is to present a technique for the synchronization problem. We propose a proportional reduced-order observer structure to synchronize with a Lorenz system. As far as we know, this class of observers has not been used in the literature. We introduce the algebraic observability concept in the differential-algebraic setting to construct a reduced-order observer for the synchronization problem. The methodology proposed is very simple and flexible. In our procedure, the new proposed reduced-order observer employs neither the well-known Kalman filter nor the Luenberger observer. Both require a copy of the system and a proportional correction given by the measurement of the error (the difference between the actual observed signal and its estimate). This reduced-order proportional observer does not require an accurate model of the system, since its structure just contains a proportional correction of the measurement of the error and a so-called derivator of adjustable gain. It should be noted that the reduced-order observer proposed is an alternative technique to the "observers" structure given in the literature. In addition, some algebraic manipulations are required with this technique. We note that some authors propose estimators without observer's gain, but we think it more natural to define an observer with a gain that attenuates the observation error (the difference between the actual observed signal and its estimate), and this observer must be able to be tuned through the observer's gain.

Our intention in choosing as an example the Lorenz system is to clarify the proposed methodology. However, it is worth mentioning that this method is applicable not only to the Lorenz system. It can be applied to a class of systems that satisfy the state representation described in Sect. 2.2. Additionally, it is clear that this class of systems should satisfy Definition 2.1 and some hypotheses given in Sects. 2.2.1 and 2.2.2. Among this class of systems we can mention some examples such as the Duffing system, Chen's chaotic system, Chua's chaotic circuit, Rössler's chaotic system, and the Colpitts chaotic circuit.

The remainder of this chapter is organized as follows: In Sect. 2.2, we describe the Lorenz system and introduce a basic definition on algebraic observability in a differential-algebraic framework. A reduced-order observer structure to synchronize with a Lorenz system is given as well. Section 2.3 presents some numerical results applied to the Lorenz system. Finally, in Sect. 2.4, we will close the chapter with some concluding remarks.

2.2 Synchronization of Lorenz System

Consider the Lorenz chaotic system described by the following set of differential equations:

$$\begin{aligned} \dot{x}_1 &= \sigma(x_2 - x_1), \\ \dot{x}_2 &= \rho x_1 - x_2 - x_1 x_3, \\ \dot{x}_3 &= x_1 x_2 - \beta x_3, \\ y &= x_1. \end{aligned} \tag{2.1}$$

With the positive parameters σ, ρ, $\beta > 0$, the system (2.1) exhibits chaotic behavior. In the classical synchronization scheme, we assume that the system (2.1) runs at the transmitter end and the state x_1 (output system) is sent to the receiver via the communication channel as the synchronization signal [1]. Furthermore, it is assumed that the receiver has exact knowledge of the parameters σ, ρ, $\beta > 0$ (i.e., there is no parametric uncertainty). The receiver's task is to construct a dynamical system to estimate or reconstruct the unknown signals x_2 and x_3 using the available signal x_1 and the known parameters. The basic practical question whether it is possible to construct the signals x_2 and x_3. In what follows, we give an answer to this question by introducing a basic definition related to the construction of the states.

2.2.1 Algebraic Observability Condition

Before proposing the reduced-order observer, a definition concerning on AOC is given. Consider the nonlinear system described by the following dynamic equations:

$$\begin{aligned} \dot{x}(t) &= f(x), \\ y(t) &= h(x), \end{aligned} \tag{2.2}$$

where $f \in \mathbb{R}^n$ is continuously differentiable and satisfies $f(0) = 0$, $x = (x_1, \ldots, x_n)^T \in \mathbb{R}^n$ is a state vector, and $y \in \mathbb{R}$ is a smooth nonsingular output.

Definition 2.1 The system (2.2) is said to be algebraically observable if the valued vector

$$x(t) = \phi(y, \dot{y}, \ddot{y}, \ldots, y^{(\mu)})(t). \tag{2.3}$$

is defined on $\mathbb{R}^{\mu+1} \to \mathbb{R}^n$ for a positive integer μ (ϕ is a polynomial with unknown $y, \dot{y}, \ddot{y}, \ldots, y^{(\mu)}$). The above condition will be called the algebraic observability condition (AOC).

In subsequent chapters, we shall generalize this condition to cases such as fractional and Liouvillian systems. The unknown state of the system can be included in a new variable $\eta(x)$. Then the augmented system (nonlinear systems immersion [7, 8]) can be considered instead of the original one, because we want to work on the dynamics η, which is unknown. The immersion can be realized as follows:

$$\begin{aligned} \dot{x}(t) &= f(x, \eta(x)), \\ \dot{\eta}(x) &= \Delta(x), \\ y &= h(x), \end{aligned} \tag{2.4}$$

where $\Delta(x)$ is a function of the states. The problem now is to construct the variable $\eta(x)$ and, once it is known, determine the value of the desired state.

Remark 2.1 In practice, identification of the variable depends on the variable choice to be estimated.

We obviously need to impose certain conditions on $\eta(x)$ and $\Delta(x)$. We propose a procedure to solve the problem stated above. We will assume that the following hypotheses are satisfied:

H1: $\eta(x)$ satisfies AOC property.
H2: the auxiliary variable γ is a C^1 real-valued function.
H3: $\Delta(x)$ is bounded, i.e., $\exists\ M \in \mathbb{R}^+$ such that $\|\Delta(x)\| \leq M, \forall x \in \Omega \subset \mathbb{R}^n$.

The following equation represents the dynamics of the unknown state:

$$\dot{\eta}(x) = \Delta(x). \tag{2.5}$$

Remark 2.2 In our case, $\eta(x)$ can be chosen as x_2 or x_3.

The hypothesis H1 is satisfied, since the Lorenz system satisfies the AOC, that is,

$$\dot{x}_1 = \sigma(x_2 - x_1) \Rightarrow x_2 = \phi(y, \dot{y}) = (1/\sigma)(\sigma y + \dot{y}), \tag{2.6}$$

where $\mu = 1, \sigma > 0$, and $y = x_1$. In the same manner, for x_3, we have

$$x_3 = -(1/x_1)(x_2 + \dot{x}_2) + \rho. \tag{2.7}$$

It is worth noting that x_3 loses the algebraic observability property when $x_1 = 0$. In other words, we do not have the synchronization signal x_1. We suppose, therefore, that $x_1 \neq 0$. Then

$$x_3 = \phi(y, \dot{y}, \ddot{y}) = (-\ddot{y} - \dot{y}(\sigma + 1))/\sigma y + \rho - 1,\ \mu = 2, \sigma > 0, y = x_1. \tag{2.8}$$

Remark 2.3 From (2.6) and (2.7), it is clear that x_2 and x_3 satisfy the AOC, and thus x_2 and x_3 are algebraically observable. Since the time derivatives $\dot{y}$ and $\ddot{y}$ are

not available, we will design, with the help of some auxiliary variables (γ satisfying H2), a reduced-order observer.

We propose a proportional reduced-order observer in order to estimate the variable $\eta(x)$ and determine the value of the desired state.

2.2.2 Observer Synthesis

We are now in a position to establish the following lemma, which describes the construction of a proportional reduced-order observer for the system (2.5), which is algebraically observable (see Definition 2.1).

Lemma 2.1 *The system*

$$\dot{\hat{\eta}} = k(\eta - \hat{\eta}) \tag{2.9}$$

is an asymptotic model-free-based proportional reduced-order observer for system (2.5), where $\hat{\eta}$ denotes the estimate of η, $k \in R^+$ determines the desired convergence rate of the observer if the following hypothesis is satisfied (in general, k can be chosen as a time-varying function, for instance in a Hardy field [9]):

H4: $\lim_{t\to t_0} e^{-\int k dt} = 0$ *with t_0 sufficiently large and* $\lim_{t\to t_0} \sup(M/|k|)) = 0$.

Proof Let us define the estimation error as follows:

$$e(t) = \eta(x) - \hat{\eta}(x). \tag{2.10}$$

This yields the nonlinear dynamics of the estimation error given by

$$\dot{e}(t) + ke(t) = \Delta(x). \tag{2.11}$$

Solving the above equation, we have

$$e(t) = e^{-\int k dt}\left[e_0 + \int_0^t e^{\int k dt}\Delta(s)ds\right], \tag{2.12}$$

where e_0 is an initial condition. Then with the assumptions H1–H4 and using the triangle and Cauchy–Schwarz inequalities from expression (2.12), we obtain

$$0 \le |e(t)| \le e^{-\int k dt}|e_0| + e^{-\int k dt}\int_0^t |e^{\int k dt}\Delta(s)|ds. \tag{2.13}$$

Thus, as $t \to t_0$ with t_0 sufficiently large,

$$0 \le \lim_{t\to t_0}\sup|e_0| \le |e_0| \lim_{t\to t_0}\sup[e^{-\int k dt}] + \lim_{t\to t_0}\sup\frac{[\int_0^t |e^{\int k dt}\Delta(s)|ds]}{|e^{\int k dt}|}. \tag{2.14}$$

From H1 and H4, we obtain

$$0 \leq \lim_{t \to t_0} \sup |e_0| \leq \lim_{t \to t_0} \sup \frac{[M \int_0^t |e^{\int k dt}| ds]}{|e^{\int k dt}|}. \tag{2.15}$$

This means that we can apply L'Hôpital's rule for the case $\frac{\infty}{\infty}$ as follows:

$$0 \leq \lim_{t \to t_0} \sup |e_0| \leq \lim_{t \to t_0} \sup \frac{[M \int_0^t |e^{\int k dt}| ds]}{|e^{\int k dt}|} = \lim_{t \to t_0} \sup \frac{M}{|k|}. \tag{2.16}$$

From H4, we obtain

$$0 \leq \lim_{t \to t_0} \sup |e(t)| \leq \lim_{t \to t_0} \sup \frac{M}{|k|} = 0. \tag{2.17}$$

Then

$$\lim_{t \to t_0} |e(t)| = 0. \tag{2.18}$$

Therefore, the reduced-order observer given by (2.9) exhibits asymptotic behavior. □

Corollary 2.1 *The dynamical system (2.9) along with*

$$\dot{\gamma} = \zeta(\gamma, x), \gamma_0 = \gamma(0) \tag{2.19}$$

constitutes a proportional asymptotic reduced-order observer for the system (2.5), where γ is a change of variable that depends on the estimated and state variables.

Remark 2.4 In practice, since γ is a variable that depends on x and η, its complexity depends on the form selected for η.

Remark 2.5 It should be noted that an integral action can be added in the proportional asymptotic reduced-order observer to achieve robustness in the observation process.

Using Lemma 2.1, we have the following proportional reduced-order observer:

$$\dot{\hat{x}}_2 = k_{x_2}(x_2 - \hat{x}_2), k_{x_2} > 0, \tag{2.20}$$

where $\hat{x}_2$ denotes the estimate of x_2, and $k_{x_2} \in R^+$ determines the desired convergence rate of the observer.

Replacing (2.6) in (2.20) leads to

$$\dot{\hat{x}}_2 = k_{x_2}\left(\frac{\dot{y}}{\sigma} + y\right) - k_{x_2}\hat{x}_2, \sigma > 0. \tag{2.21}$$

Since the time derivative $\dot{y}$ is not available, observer (2.21) cannot be implemented. In order to overcome this problem, let us consider the following auxiliary variable γ_{x_2}:

$$\gamma_{x_2} = -\frac{k_{x_2}}{\sigma} y + \hat{x}_2, \sigma > 0. \tag{2.22}$$

Then

$$\hat{x}_2 = \gamma_{x_2} + \frac{k_{x_2}}{\sigma} y, \sigma > 0. \tag{2.23}$$

The time derivative of (2.23) is

$$\dot{\hat{x}}_2 = \dot{\gamma}_{x_2} + \frac{k_{x_2}}{\sigma} \dot{y}, \sigma > 0. \tag{2.24}$$

Then from (2.21), (2.23), and (2.24), it can be easily shown that the time derivative $\dot{\gamma}_{x_2}$ is given by

$$\dot{\gamma}_{x_2} = -k_{x_2}\gamma_{x_2} + \left(1 - \frac{k_{x_2}}{\sigma} k_{x_2}\right) y, \gamma_{x_2}(0) = \gamma_{x_{2_0}}, \sigma, k_{x_2} > 0. \tag{2.25}$$

Then the reduced-order observer is given by Eqs. (2.23) and (2.25).

Remark 2.6 It is clear that the solution of the dynamics of the auxiliary variable is exponentially stable.

On the other hand, using the above technique, we estimate the variable x_3. From (2.1) and (2.6), we obtain

$$\dot{x}_3 = y\left(\frac{\dot{y} + \sigma y}{\sigma}\right) - \beta x_3. \tag{2.26}$$

Or in other words,

$$x_3 = \frac{-1}{\beta}\left(\dot{x}_3 - y\left(\frac{\dot{y} + \sigma y}{\sigma}\right)\right). \tag{2.27}$$

Then the following observer is suggested:

$$\dot{\hat{x}}_3 = k_{x_3}(x_3 - \hat{x}_3), k_{x_3} > 0. \tag{2.28}$$

Replacing (2.27) in (2.28), we obtain

$$\dot{\hat{x}}_3 = k_{x_3}\left[\frac{-1}{\beta}\left(\dot{x}_3 - y\left(\frac{\dot{y} + \sigma y}{\sigma}\right)\right) - \hat{x}_3\right]. \tag{2.29}$$

It should be noted that $\dot{x}_3$ is unknown and can be approximated by its estimate $\dot{\hat{x}}_3$, which is valid only in a region where $\|\dot{x}_3 - \dot{\hat{x}}_3\| < \epsilon, \epsilon > 0$. This yields the following relationship:

$$\dot{\hat{x}}_3 = k_{x_3}\left[\frac{-1}{\beta}\left(\dot{\hat{x}}_3 - y\left(\frac{\dot{y} + \sigma y}{\sigma}\right)\right) - \hat{x}_3\right]. \tag{2.30}$$

Or in other words,

$$\dot{\hat{x}}_3\left(1 + \frac{k_{x_3}}{\beta}\right) - \frac{k_{x_3}}{\beta\sigma} y\dot{y} = k_{x_3}\left[\frac{1}{\beta}y^2 - \hat{x}_3\right]. \tag{2.31}$$

By making some algebraic manipulations, we obtain

$$\begin{aligned}\dot{\hat{x}}_3 - \frac{k_{x_3}}{(\beta + k_{x_3})\sigma} y\dot{y} = \frac{k_{x_3}\beta}{\beta + k_{x_3}}\left[\left(\frac{1}{\beta} - \frac{k_{x_3}}{2(\beta + k_{x_3})\sigma}\right) y^2\right. \\ \left. - \left(\hat{x}_3 - \frac{k_{x_3}}{2(\beta + k_{x_3})\sigma} y^2\right)\right].\end{aligned} \tag{2.32}$$

Then from (2.32) and the following change of variable follows

$$\gamma_{x_3} = \hat{x}_3 - \frac{k_{x_3}}{2(\beta + k_{x_3})\sigma} y^2, \tag{2.33}$$

$$\dot{\gamma}_{x_3} = \frac{k_{x_3}\beta}{\beta + k_{x_3}}\left[\left(\frac{1}{\beta} - \frac{k_{x_3}}{2(\beta + k_{x_3})\sigma}\right) y^2 - \gamma_{x_3}\right]. \tag{2.34}$$

That is, the reduced-order observer to calculate $\hat{x}_3$ is given by the following relationship:

$$\hat{x}_3 = \gamma_{x_3} + \frac{k_{x_3}}{2(\beta + k_{x_3})\sigma} y^2; \beta, k_{x_3}, \sigma > 0, \tag{2.35}$$

$$\dot{\gamma}_{x_3} = \frac{k_{x_3}\beta}{\beta + k_{x_3}}\left[\left(\frac{1}{\beta} - \frac{k_{x_3}}{2(\beta + k_{x_3})\sigma}\right) y^2 - \gamma_{x_3}\right]; \gamma_{x_3}(0) = \gamma_{x_{3,0}}. \tag{2.36}$$

Remark 2.7 The proposed model-free-based proportional reduced-order observer employs neither the well-known Kalman filter nor the Luenberger observer. Both require a copy of the system and a proportional correction given by the measurement of the error (the difference between the actual observed signal and its estimate). This reduced-order proportional observer does not require an accurate model of the system, since its structure just contains a proportional correction of the measurement of the error and a so-called derivator of adjustable gain.

In what follows, we illustrate the performance of the reduced-order proportional observer by means of numerical simulations.

2.3 Numerical Results

In order to verify the effectiveness of the proposed methodology, we show the convergence of the estimates to the current signals. We have considered the initial conditions to the master system $x_1 = 1$, $x_2 = 0$, $x_3 = -5$, and the initial conditions to the slave system $\hat{x}_2 = -5$, $\hat{x}_3 = 8$. The parameters of the system are $\sigma = 10$, $\rho = 28$, $\beta = 8/3$; the initial conditions of the auxiliary functions of the reduced-order observer are $\gamma_{x_2} = -20$, $\gamma_{x_3} = 8$; and finally, the gain parameters in the proportional reduced-order observer are fixed as $k_{x_2} = 150$, $k_{x_3} = 250$. The convergence of the estimates to the true signals is shown in Fig. 2.1, and the error synchronization is shown in Fig. 2.2.

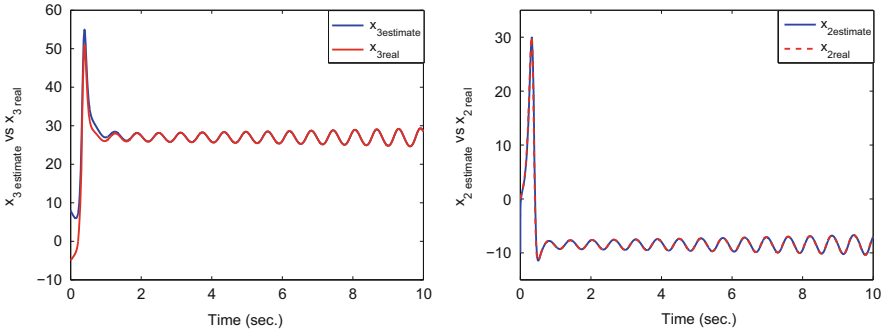

Fig. 2.1 Convergence of the estimates by means of a model-free-based proportional reduced-order observer

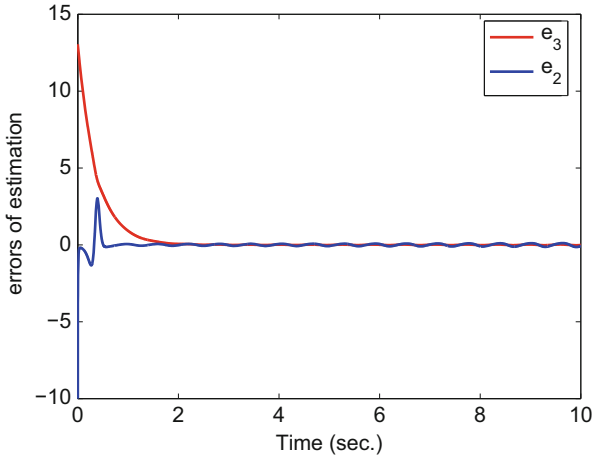

Fig. 2.2 Synchronization errors

2.4 Concluding Remarks

In this chapter, we have presented a model-free-based proportional reduced-order observer to address the synchronization problem of the Lorenz system. A model-free observer has the advantage of not requiring a copy of the system. In the next chapter, a model-free sliding-mode observer is developed. In order to achieve robustness against perturbations to the system and noisy measurements, we have proven the asymptotic stability of the resulting error system, and by means of simple algebraic manipulations, we construct the estimates of the slave system, which asymptotically converge to the current states of the master system. Finally, we have presented a simulation to illustrate the effectiveness of the suggested approach.

References

1. L.M. Pecora, T.L. Caroll, Synchronization in chaotic systems. Phys. Rev. Lett. **64**(8), 821–824 (1990)
2. O. Mörgul, E. Solak, Observed based synchronization of chaotic systems. Phys. Rev. E **54**(5), 4803–4811 (1996)
3. L. Liu, X. Wu, H. Hu, Estimating system parameters of Chua's circuit from synchronizing signal. Phys. Lett. A **324**, 36–41 (2004)
4. S. Chen, J. Hua, C. Wang, J. Lü, Adaptive synchronization of uncertain Rössler hyperchaotic system based on parameter identification. Phys. Lett. A **321**, 50–55 (2004)
5. M. Feki, Observer-based exact synchronization of ideal and mismatched chaotic systems. Phys. Lett. A **309**, 53–60 (2003)
6. S. Bowong, Stability analysis for the synchronization of chaotic systems with different order: application to secure communications. Phys. Lett. A **326**, 102–113 (2004)
7. D. Claude, M. Fliess, A. Isidori, Immersion directe et par bouclage, d'un systeme non linéaire dans un linéaire. Automatique Théorique, C. R. Acad. Sci. Paris **296**(Serie I), 237–240 (1983)
8. R. Martínez Guerra, Inmersion de un sistema no lineal y construcción de un observador para un sistema TPA, V Congreso Latinoamericano de Control Automático (Informática 92), Aut 141, Cuba, pp. 251–255 (1992)
9. R. Martínez-Guerra, R. González-Galán, A. Luviano-Juárez, J. Cruz-Victoria, Diagnosis for a class of non-differentially flat and Liouvillian systems. IMA J. Math. Control Inf. **24**, 117–195 (2007)

Chapter 3
A Model-Free Sliding Observer to the Synchronization Problem Using Geometric Techniques

Abstract In this chapter, a sliding-mode observer is proposed for the synchronization problem. This observer presents a simple structure that contains a pure sliding-mode term that turns out to be robust against output noises as well as sustained disturbances, while the slave system is a pure sliding-mode observer. Comparisons with two other model-based observers, the Thau observer and Bestle–Zeitz observer, are proposed. In this chapter, we use differential-geometric techniques. The performance of these observers is shown by the examples of the Lorenz system and Chua's circuit.

3.1 Introduction

The main approaches related to the construction of asymptotic observers for nonlinear processes use differential-geometric methods. The idea is to find a state transformation to represent the system as a linear equation plus a nonlinear term, which is a function of the system output. However, finding a nonlinear transformation that places a system of order n into so-called observer canonical form requires the integration of n coupled partial differential equations. Furthermore, this approach needs accurate knowledge of the nonlinear dynamics of the system. Here, in this chapter, we will present two observers based on geometric techniques: the Thau observer [12] and Bestle–Zeitz observer [2]. Additionally, a sliding-mode observer (SMO) is proposed for the synchronization problem, which presents a simple structure that contains a sliding-mode term that turns out to be robust against output noise as well as sustained disturbances, i.e., the slave system is a pure sliding-mode observer. This observer does not require an accurate model of the system, since its structure just contains a proportional correction of the sign function of the measurement of the synchronization error. The main advantage of the observer is that the sliding contribution of measurement error provides robustness against perturbations to the system and noisy measurements with a high-gain-like condition.

Early works dealing with SMOs that consider measurement noise were by Utkin and Drakunov [3]. They discussed the state estimation using sliding-mode techniques. Anulova [1] treated an analysis of systems with a sliding mode in the presence of noise. Slotine et al. [11] successfully designed the sliding-mode

R. Martínez-Guerra et al., *Synchronization of Integral and Fractional Order Chaotic Systems*, Understanding Complex Systems,
DOI 10.1007/978-3-319-15284-4_3

approach to construct observers that are highly robust with respect to noise in the input of the system. But it turns out that the corresponding stability analysis cannot be directly applied in situations with output noise (or mixed uncertainty). So it is still a challenge to suggest a workable technique to analyze the stability of identification error generated by sliding-mode-type (discontinuous nonlinearity) observers [4–10, 13–15].

In this chapter, we propose a model-free observer, an SMO for the synchronization problem, and compare our observer with the other two model-based observers. The intention of choosing as two examples the Lorenz system and Chua's circuit (see Chap. 1) is to clarify the proposed methodology. However, it is worth mentioning that this technique can be applied to many chaotic synchronization problems.

The remainder of this chapter is organized as follows: in Sect. 3.2, we give some definitions in a differential-geometric setting. In Sect. 3.3, we introduce the SMO structure to solve the synchronization problem and compare it with the other two observers. Section 3.4 presents some numerical results. Finally, in Sect. 3.5, we will close the chapter with some concluding remarks.

3.2 Observer Canonical Form of a Nonlinear System

We consider a nonlinear system described as follows:

$$\begin{cases} \dot{\xi} = f(\xi) + g(\xi)u, \\ y = h(\xi), \end{cases} \tag{3.1}$$

where $\xi \in \mathbb{R}^n$ is the state of the plant, $y \in \mathbb{R}$ is a measurable output, and f, g, h are smooth functions. If the system has uniform relative degree n, i.e.,

$$L_g h(\xi) = \cdots = L_g L_f^{n-2} h(\xi) = 0, \quad L_g L_f^{n-1} h(\xi) \neq 0,$$

then there exists a mapping

$$\eta = T(\xi) \tag{3.2}$$

that can transform the system (3.1) into the following observer canonical form (see Chap. 1):

$$\begin{aligned} \dot{\eta}_i &= \eta_{i+1}, \quad i = 1 \cdots n-1, \\ \dot{\eta}_n &= \Phi(\eta, u), \\ y &= \eta_1, \end{aligned} \tag{3.3}$$

where $\Phi(\eta, u)$ is a continuous nonlinear function. Here we consider the output $y = \eta_1 + \delta$, with δ an additive bounded noise.

3.3 Sliding-Mode Observer to the Synchronization Problem

Synchronization of chaotic systems can be classified into two types, called mutual synchronization and master–slave synchronization according to the coupling configuration. The former is a system with bidirectional coupling, and the latter has unidirectional coupling (see Chap. 1). In this chapter, we consider the master–slave configuration. It is also known as drive–response (see Fig. 1.8).

First consider a system described as follows:

$$\Sigma : \begin{cases} \dot{x} = f(x), \\ y = h(x), \end{cases} \tag{3.4}$$

where $x \in \mathbb{R}^n$ and $y \in \mathbb{R}$. Then consider any kind of observer for the system (3.4) with state $\hat{x}$. The system (3.4) will be the master, and the observer will be the slave.

Definition 3.1 The slave system *synchronizes* with the master system if

$$\| x(t) - \hat{x}(t) \| \underset{t \to \infty}{\longrightarrow} 0$$

for almost all (with respect to Lebesgue measure) combinations of initial states of the master and slave systems.

The SMO, to design the slave system, has the following form:

$$\begin{cases} \dot{\hat{\eta}}_i = \hat{\eta}_{i+1} + m_i \tau^{-i} \text{sign}(y - \hat{y}), \quad i = 1 \cdots n-1 \\ \dot{\hat{\eta}}_n = m_n \tau^{-n} \text{sign}(y - \hat{y}) \\ \hat{y} = \hat{\eta}_1, \end{cases} \tag{3.5}$$

where $1 > \tau > 0$, and the constants m_i are chosen such that the polynomial $m_n \gamma^n + m_{n-1}\gamma^{n-1} + \cdots + m_1 = 0$ has all its roots in the left half-plane. The function $\text{sign}(y - \hat{y})$ is defined as follows:

$$\text{sign}(y - \hat{y}) = \begin{cases} 1 & \text{if } (y - \hat{y}) > 0, \\ -1 & \text{if } (y - \hat{y}) < 0, \\ 0 & \text{if } (y - \hat{y}) = 0. \end{cases}$$

First, we consider a simple case in two dimensions. The slave is

$$\begin{aligned} \dot{\hat{\eta}}_1 &= \hat{\eta}_2 + m\tau^{-1}\text{sign}(y - \hat{y}), \ m > 0 \\ \dot{\hat{\eta}}_2 &= m^2\tau^{-2}\text{sign}(y - \hat{y}), \end{aligned} \tag{3.6}$$

where $\hat{\eta}_1, \hat{\eta}_2$ are the states in the slave system, and $\hat{y}$ is the estimate of the output y, and $m_1 = m, m_2 = m^2$, and τ are small positive parameters.

Since the output of the master system is $y = \eta_1 + \delta$, let us define the synchronization error as

$$\begin{aligned} e_1 &= \eta_1 - \hat{\eta}_1 \\ e_2 &= \tfrac{1}{m}\left(\eta_2 - \hat{\eta}_2\right). \end{aligned} \tag{3.7}$$

The recovered noise at the slave is

$$\hat{\delta} = y - \hat{y} = e_1 + \delta.$$

From (3.6) and (3.7), the synchronization dynamical error can be represented as

$$\dot{e} = A_\mu e - K\,\mathrm{sign}(Ce + \delta) + \Delta f,$$

with

$$\begin{aligned} A_\mu &= \begin{pmatrix} -\mu & m \\ 0 & -\mu \end{pmatrix}, \quad K = m\tau^{-1}\begin{pmatrix} 1 \\ m\tau^{-1} \end{pmatrix}, \\ \mu > 0, \quad \Delta f &= \begin{pmatrix} \mu e_1 \\ \frac{\Phi}{m} + \mu e_2 \end{pmatrix}, \quad C = \begin{pmatrix} 1 & 0 \end{pmatrix} \end{aligned} \tag{3.8}$$

where μ is a regularizing parameter and Δf is an uncertainty term (or unmodeled dynamic term).

The following assumptions are used for our theoretical results:

A1. There exist nonnegative constants L_{0f}, L_{1f} such that for every vector e, the following generalized quasi-Lipschitz conditions holds:

$$\|\Delta f\| \le L_{0f} + \left(L_{1f} + \|A_\mu\|\right)\|e\|. \tag{3.9}$$

A2. Information noise is assumed to be bounded as $\|\delta\|_\Lambda^2 = \delta^T \Lambda\, \delta \le \delta^+ < \infty$, where Λ is a symmetric positive definite matrix.

A3. There exists a positive definite matrix $Q_0 = Q_0^T > 0$ such that the following matrix Riccati equations hold:

$$PA_\mu + A_\mu^T P + PRP + Q = 0, \tag{3.10}$$

where

$$\begin{aligned} &R = \Lambda_f^{-1} + 2\|\Lambda_f\| L_{1f} I,\ 0 < \Lambda_f = \Lambda_f^T, \\ &Q = Q_0 + 2\left(L_{1f} + \|A_\mu\|\right)^2 I,\ I = \text{identity matrix} \end{aligned} \tag{3.11}$$

has a positive definite solution $P = P^T > 0$. Since $P > 0$, there exists $k > 0$ such that $K = kP^{-1}C^T$.

Remark 3.1 Notice that the dynamic $\Phi(\eta_1, \eta_2)$ in (3.3) is Lipschitz with respect to η_1 and η_2, so assumption A1 is satisfied for chaotic systems. The measurement is corrupted by a noise δ that is bounded, which is assumption A2. To calculate the solution to the Riccati equation (3.10), the following parameters have been selected:

$$\Lambda_f = \lambda_f I,\ L_{1f} = \mu,\ R = \left(\lambda_f^{-1} + 2\lambda_f \mu\right) I,$$
$$Q_0 = q_0 I,\ Q = \left(q_0 + 8\mu^2\right) I.$$

With $\lambda_f = 20$, $\mu = 0.0001$, $q_0 = \mu^2$, we obtain

$$P = 10^{-3}\begin{bmatrix} 3.16099 & -0.22096 \\ -0.22096 & 3.16099 \end{bmatrix} > 0,$$

which satisfies assumption A3.

The main result in this chapter is the following theorem.

Theorem 3.1 *The sliding-mode observer (3.6) can realize synchronization, and it converges to the following residual set:*

$$D_\varepsilon = \{e \mid \|e\|_P \leq \bar{\mu}(k)\}, \tag{3.12}$$

where P is a solution of the Riccati equations (3.10),

$$\bar{\mu}(k) = \left(\frac{\rho(k)}{\sqrt{\left(k\alpha_p\right)^2 + \rho(k)\alpha_Q} + k\alpha_p}\right)^2, \tag{3.13}$$

where

$$\rho(k) = 2\left\|\Lambda_f\right\| L_{0f}^2 + 4k\left(\sqrt{n\Lambda_f^{-1}}\right)\delta^+$$
$$k\alpha_p = k\left(\lambda_{\min}\left(P^{-1/2}C^T C P^{-1/2}\right)\right)$$
$$\alpha_Q = \lambda_{\min}\left(P^{-1/2}Q^T Q P^{-1/2}\right) > 0,$$

where n is the dimension of the chaotic system.

Proof We select the Lyapunov function candidate $V(e)$ as

$$V(e) = \|e\|_P^2 = e^T P\, e,\ 0 < P = P^T, \tag{3.14}$$

and using the matrix inequality

$$X^T Y + Y^T X \leq X^T \Lambda_f X + Y^T \Lambda_f^{-1} Y, \tag{3.15}$$

valid for every $X, Y \in \mathbb{R}^{n\times m}$, $0 < \Lambda_f = \Lambda_f^T$, it follows that

$$\begin{aligned}
\dot{V}(e) &= 2e^T P\, \dot{e} = 2e^T P \left(A_\mu e - K\,\text{sign}(Ce+\delta) + \Delta f\right) \\
&\leq 2e^T PA_\mu e - 2ke^T C^T \text{sign}(Ce+\delta) + 2e^T P\Delta f \\
&\leq e^T \left(PA_\mu + A_\mu^T P\right) e - 2ke^T C^T \text{sign}(Ce+\delta) \\
&\quad + e^T P\Lambda^{-1} Pe + \Delta^T f \Lambda_f \Delta f \\
&\leq e^T \left(PA_\mu + A_\mu^T P + PRP + Q\right) e - e^T Qe \\
&\quad + \left(L_{0f}^2 + \left(L_{1f} + \|A_\mu\|\right)^2 \|e\|^2\right) 2\,\|\Lambda_f\| \\
&\quad - 2ke^T C^T \text{sign}(Ce+\delta) \\
&= e^T \left(PA_\mu + A_\mu^T P + PRP + Q\right) e \\
&\quad - e^T Qe + 2\,\|\Lambda_f\|\, L_{0f}^2 - 2k\,(Ce)^T\,\text{sign}(Ce+\delta)
\end{aligned} \tag{3.16}$$

using

$$x^T \text{sign}\,[x+z] \geq \sum_{i=1}^{n} |x_i| - 2\sqrt{n}\,\|z_i\|\,.$$

Then

$$\begin{aligned}
\dot{V}(e) &\leq -e^T Qe + 2\,\|\Lambda_f\|\, L_{0f}^2 - 2k\left(\sum_{i=1}^{n} |(Ce)_i| - 2\sqrt{n}\,\|\delta\|\right) \\
&\leq -e^T Qe - 2k\sum_{i=1}^{n} |(Ce)_i| + \rho(k),
\end{aligned}$$

where

$$\rho(k) = 2\,\|\Lambda_f\|\, L_{0f}^2 + 4k\left(\sqrt{n\Lambda^{-1}}\right)\delta^+.$$

Thus

$$\dot{V}(e) \leq -\|e\|_Q - 2k\alpha_P\,\|e\|_P + \rho(k), \tag{3.17}$$

where

$$\begin{aligned}
\left(\sum_{i=1}^{n} |(Ce)_i|\right)^2 &\geq \sum_{i=1}^{n} (|(Ce)_i|)^2 = \|Ce\|^2 \\
&= \left\|CP^{-1/2}P^{-1/2}e\right\|^2 \geq \alpha_p e^T Qe
\end{aligned} \tag{3.18}$$

with

$$\alpha_P = \lambda_{\min}\left(P^{-1/2}C^T C P^{-1/2}\right) \geq 0, \tag{3.19}$$

so that from (3.17), we obtain

$$\dot{V}(e) = -\alpha_Q V(e) - \vartheta\sqrt{V(e)} + \beta, \tag{3.20}$$

where

$$\begin{aligned} \alpha_Q &= \lambda_{\min}\left(P^{-1/2}Q^T Q P^{-1/2}\right) > 0, \\ \vartheta &= 2k\alpha_p,\ \beta = \rho(k). \end{aligned} \tag{3.21}$$

If the assumptions A1–A3 are fulfilled, then

$$\left[1 - \frac{\bar{\mu}}{V}\right]_+ \to 0, \tag{3.22}$$

where the function $[\cdot]_+$ is defined as

$$[z]_+ = \begin{cases} z \text{ if } z \geq 0 \\ 0 \text{ if } z < 0. \end{cases} \tag{3.23}$$

The proof of this result is given in the appendix. The theorem actually states that the weighted estimation error $V(e) = e^T P\ e$ converges to the zone $\bar{\mu}(k)$ asymptotically. That is, it is ultimately bounded:

$$\bar{\mu}(k) \geq e^T P e \geq e_1^T P e_1.$$

□

Remark 3.2 Because

$$\bar{\mu}(k) = \left(\frac{\frac{2\|\Lambda_f\|L_{0f}^2}{k} + 4\left(\sqrt{n\Lambda_f^{-1}}\right)\delta^+}{\sqrt{\alpha_p^2 + \left[\frac{2\|\Lambda_f\|L_{0f}^2}{k^2} + \frac{4\left(\sqrt{n\Lambda_f^{-1}}\right)\delta^+}{k}\right]\alpha_Q} + \alpha_p} \right)^2, \tag{3.24}$$

and since P is bounded, we can select τ arbitrarily small (the gain of the slave (3.8) becomes larger) in order to make k very large (since $K = kP^{-1}C^T = m\tau^{-1}\begin{pmatrix} 1 \\ m\tau^{-1} \end{pmatrix}$), so the first term of (3.24) goes to zero. Here Λ_f^{-1} in A3 is any positive matrix, which we can choose small enough that the second term of (3.24) goes to zero.

Remark 3.3 Although we have restricted ours attention to the case of second-order chaotic systems, the observer construction and convergence analysis can be extended to the n-dimensional case. The master system is

$$\begin{aligned}\dot{\eta}_j &= \eta_{j+1} \quad j = 1, \ldots, n-1\\ \dot{\eta}_n &= H(\eta)\\ y &= \eta_1\end{aligned}$$

and the sliding-mode observer-based slave is constructed as

$$\begin{aligned}\dot{\hat{\eta}}_j &= \hat{\eta}_{j+1} + m_j \tau^{-j} \text{sign}(y - \hat{y}) \quad j = 1, \ldots, n-1\\ \dot{\hat{\eta}}_n &= m_n \tau^{-n} \text{sign}(y - \hat{y}),\end{aligned} \tag{3.25}$$

where the constants m_j are chosen such that the polynomial $m_n \gamma^n + m_{n-1}\gamma^{n-1} + \cdots + m_1 = 0$ has all its roots in the open left complex half-plane. As in the second-order case, it can be proved that the synchronization error converges to any accuracy by selecting sufficiently small values of the observer's gain.

3.4 Model-Based Observers to the Synchronization Problem

Now we compare our model-free observer with other model-based observers for the synchronization problem. The role of Lie derivatives in nonlinear state observation problems will be considered.

3.4.1 Bestle–Zeitz Observer for the Synchronization Problem

We consider the class of time-invariant nonlinear systems described by (3.4). It will be assumed that f is a C^∞ vector field in $\mathbb{R}^n$ and h is a C^∞ function. It is desirable to find a bijective C^∞ nonlinear transformation $T : \mathbb{R}^n \to \mathbb{R}^n$, where

$$x = T(z) \tag{3.26}$$

such that system (3.4) may be transformed into the *canonical form* defined by

$$\begin{cases} \dot{z} = \begin{bmatrix} 0 & \ldots & 0 \\ 1 & & \\ & \ddots & \vdots \\ & 1 & 0 \end{bmatrix} z - \begin{bmatrix} f_0^*(z) \\ f_1^*(z) \\ \vdots \\ f_{n-1}^*(z) \end{bmatrix} \triangleq f^*(z) \\ y = \begin{bmatrix} 0 \ldots 0 \ 1 \end{bmatrix} z \end{cases}. \tag{3.27}$$

Taking the derivative of (3.26) with respect to time yields

$$\dot{x} = \frac{\partial T}{\partial z} f^*(z), \tag{3.28}$$

where

$$\frac{\partial T}{\partial z} = \left[\frac{\partial T}{\partial z_1} \cdots \frac{\partial T}{\partial z_n} \right].$$

Making some algebraic manipulations and using the Lie derivative notation, it is possible to obtain the following:

$$\frac{\partial T}{\partial z_k} = \left(ad^{k-1} f, \frac{\partial T}{\partial z_1} \right) \quad (k = 1, \ldots, n).$$

Thus it is now possible to express all the columns of $\frac{\partial T}{\partial z}$ in terms of a single *starting vector* $\frac{\partial T}{\partial z_1}$ [2]:

$$\frac{\partial T}{\partial z} = \left[\left(ad^0 f, \tfrac{\partial T}{\partial z_1} \right) \left(ad^1 f, \tfrac{\partial T}{\partial z_1} \right) \ldots \left(ad^{n-1} f, \tfrac{\partial T}{\partial z_1} \right) \right]. \tag{3.29}$$

Now the following equation must be employed to obtain an expression for the starting vector $\frac{\partial T}{\partial z_1}$:

$$y = h(x) = z_n. \tag{3.30}$$

Taking the partial derivative of (3.30) with respect to z yields

$$\frac{\partial h(x)}{\partial x} \frac{\partial T}{\partial z} = \left[0 \ldots 0 \ 1 \right]. \tag{3.31}$$

Note that the first component of (3.31) may be written as

$$\frac{\partial h}{\partial x} \frac{\partial T}{\partial z_1} = \left\langle dh, \frac{\partial T}{\partial z_1} \right\rangle = L_f^0(dh) \frac{\partial T}{\partial z_1} = 0. \tag{3.32}$$

Similarly, Leibniz's formula may be used to simplify the second element of (3.31). By repeated application of Leibniz's formula and use of (3.29), the following matrix involving the starting vector may be obtained:

$$\begin{bmatrix} L_f^0(dh)(x) \\ L_f^1(dh)(x) \\ \vdots \\ L_f^{n-1}(dh)(x) \end{bmatrix} \frac{\partial T}{\partial z_1} = \begin{bmatrix} 0 \\ \vdots \\ 0 \\ 1 \end{bmatrix}.$$

The matrix

$$\mathscr{O}(x) = \begin{bmatrix} L_f^0(dh)(x) \\ L_f^1(dh)(x) \\ \vdots \\ L_f^{n-1}(dh)(x) \end{bmatrix}$$

is called the observability matrix of the system defined by (3.4). Thus the starting vector $\dfrac{\partial T}{\partial z_1}$ is equal to the last column of $\mathscr{O}^{-1}$.

The observer in the new coordinate system is given by

$$\begin{cases} \dot{\hat{z}} = \begin{bmatrix} 0 & \dots & 0 \\ 1 & & \\ & \ddots & \vdots \\ & & 1 \quad 0 \end{bmatrix} \hat{z} - \begin{bmatrix} f_0^*(z) \\ f_1^*(z) \\ \vdots \\ f_{n-1}^*(z) \end{bmatrix} - K(\hat{y} - y) \\ \\ \hat{y} = \begin{bmatrix} 0 \dots 0 \ 1 \end{bmatrix} \hat{z} \end{cases}, \tag{3.33}$$

where $\hat{y}$ and $K = \begin{bmatrix} k_0 \dots k_{n-1} \end{bmatrix}^T$. Define the error as

$$e_z = \hat{z} - z.$$

Hence the error satisfies the homogeneous differential equation

$$\dot{e}_z = \begin{bmatrix} 0 & \dots & 0 & -k_0 \\ 1 & & & -k_1 \\ & \ddots & \vdots & \\ & & 1 \ 0 & -k_{n-1} \end{bmatrix} e_z. \tag{3.34}$$

The characteristic polynomial of (3.34) is given by

$$p(s) = k_0 + k_1 s + \cdots + k_{n-1} s^{n-1} + s^n. \tag{3.35}$$

Thus we may easily assign the spectrum of (3.35) via an appropriate selection of K.

3.4.2 *Thau Observer for Synchronization*

Consider the nonlinear system described by

$$\begin{cases} \dot{x} = Ax + f(x) + Bu, \\ y = Cx, \end{cases} \tag{3.36}$$

where $f(\cdot) : \mathbb{R}^n \to \mathbb{R}^n$ is continuous; $A \in \mathbb{R}^{n\times n}$, $B \in \mathbb{R}^{n\times m}$, and $C \in \mathbb{R}^{p\times n}$. The nonlinear function $f(\cdot)$ may contain linear terms in x. It is assumed that the pair (A, C) is completely observable. Therefore, it is possible to find $K \in \mathbb{R}^{n\times p}$ such that the eigenvalues of $A_0 = A - KC$ are in the open left half-plane. Let $\hat{x}$ denote the estimate of the true state. Then $\hat{x}$ satisfies the equation

$$\begin{cases} \dot{\hat{x}} = A_0 \hat{x} + f(\hat{x}) + Ky + Bu \\ \hat{y} = C\hat{x}. \end{cases} \tag{3.37}$$

Let e be defined by

$$e = \hat{x} - x.$$

Thus e satisfies the differential equation

$$\dot{e} = A_0 e + f(\hat{x}) - f(x) = A_0 e + f(x + e) - f(x). \tag{3.38}$$

Since the spectrum of A_0 is contained in the left half-plane, there exists for every positive definite $Q \in \mathbb{R}^{n\times n}$ a unique positive definite $P \in \mathbb{R}^{n\times n}$ such that

$$A_0^T P + PA = -2Q.$$

Next consider the Lyapunov-function candidate

$$V(e) = e^T Pe.$$

The derivative of $V(e)$ evaluated along the solution of the error differential equation (3.38) is given by

$$\dot{V}(e) = \dot{e}^T Pe + e^T = 2e^T Qe + 2e^T P[f(x + e) - f(x)].$$

It is necessary to impose an additional constraint to ensure that the function $f(\cdot)$ is locally Lipschitz about the origin, that is, that there exists a positive constant L such that

$$\|f(x_1) - f(x_2)\| \leq L\|x_1 - x_2\|$$

for all x_1, x_2 in some open region R containing the origin. Therefore, if e is contained in R, then the following inequalities hold:

$$\dot{V}(e) \leq -2e^T Qe + 2L\|Pe\|\|e\| \leq (-2a + 2L\|P\|)\|e\|,$$

where a is the minimum eigenvalue of Q, and $\|P\|$ is the maximum eigenvalue of P. Hence if

$$\frac{a}{\|P\|} > L, \tag{3.39}$$

then $e = 0$ is an asymptotically stable equilibrium point of (3.38)

Remark 3.4 Model-based observers (Thau observer and Bestle–Zeitz observer) require complete information about the master system. A Bestle–Zeitz observer needs a complex transformation; the synchronization error can converge to zero. The gain of a Thau observer is not difficult to obtain. The synchronization error converges to a bounded zone. The model-free observer proposed in this chapter does not require any information about the master system. It is robust to bounded noise, but there is more chattering than with the model-based observers. We will demonstrate these results in the following examples.

3.5 Two Synchronization Problems

3.5.1 Lorenz System

The Lorenz system is a nonlinear system with the following dynamics:

$$\Sigma_L : \begin{cases} \dot{x}_1 = \sigma(x_2 - x_1), \\ \dot{x}_2 = \rho x_1 + x_2 - x_1 x_3, \\ \dot{x}_3 = x_1 x_2 - \beta x_3, \\ y = x_1, \end{cases} \tag{3.40}$$

and it is well known that with $\sigma = 10$, $\rho = 28$, and $\beta = \frac{8}{3}$, the Lorenz system exhibits chaos.

3.5.1.1 Sliding-Mode Observer to the Synchronization of the Lorenz System

The sliding-mode observer (SMO) cannot be applied directly to the Lorenz system. Thus when we apply the transformation (3.2), the Lorenz system is represented in the following observer canonical form:

$$\bar{\Sigma}_{L_C}: \begin{cases} \dot{z}_1 = z_2 \\ \dot{z}_2 = z_3 \\ \dot{z}_3 = f(z) \\ y = z_1, \end{cases}$$

where $f(z) = \sigma\{\rho(z_2 - z_1) + f_1(z) + z_1 f_2(z) - z_2 f_2(z) - z_1[z_1 f_1(z) - \beta f_2(z)] - z_3\}$ and $f_1(z) = \frac{z_2+z_1}{\sigma}$, $f_2(z) = \rho - 1 - \frac{z_2(\sigma+1)+z_3}{z_1}$.

Now the SMO can be applied to the Lorenz system, and its dynamics can be described as follows:

$$\begin{cases} \dot{\hat{z}}_1 = \hat{z}_2 + k_1 \text{sign}(y - \hat{y}) \\ \dot{\hat{z}}_2 = \hat{z}_3 + k_2 \text{sign}(y - \hat{y}) \\ \dot{\hat{z}}_3 = k_3 \text{sign}(y - \hat{y}) \\ \hat{y} = \hat{z}_1. \end{cases} \tag{3.41}$$

We choose $k_1 = 100, k_2 = 70, k_3 = 100$. The synchronization results are shown in Figs. 3.1 and 3.2. The synchronization states in Fig. 3.2 show that the SMO can be successfully applied to the synchronization problem, although there is some chattering in the synchronization error (Fig. 3.1).

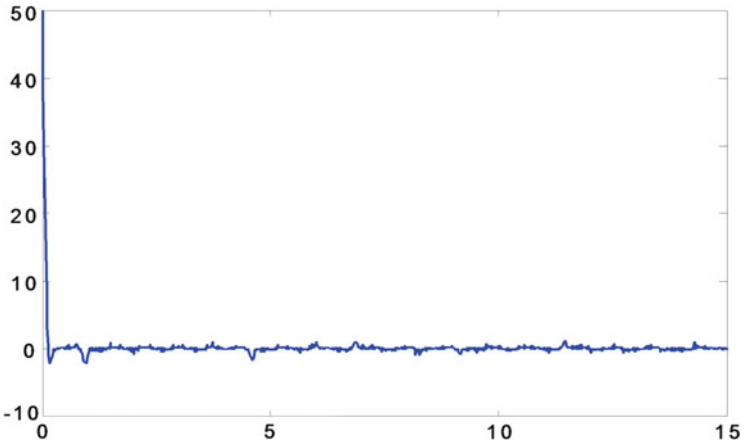

Fig. 3.1 Synchronization error of Lorenz system via SMO (sliding-mode observer)

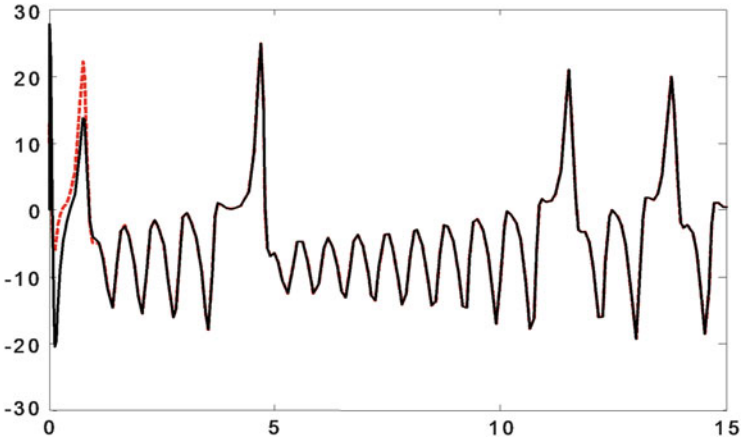

Fig. 3.2 Synchronization states of Lorenz system via SMO

3.5.1.2 Bestle–Zeitz Observer to Synchronization of Lorenz System

By applying the method described above, we have obtained the Jacobian of the desired transformation for the Lorenz system:

$$\frac{\partial T}{\partial z} = \begin{bmatrix} 0 & 0 & 1 \\ 0 & \frac{1}{\sigma} & -\frac{1}{\sigma} - x_1\left(\frac{\beta}{\sigma x_1} + \frac{x_2 - x_1}{{x_1}^2}\right) \\ -\frac{1}{\sigma x_1} & \frac{\beta}{\sigma x_1} + \frac{x_2 - x_1}{{x_1}^2} & \nu(x) \end{bmatrix},$$

where

$$\nu(x) = \frac{x_1}{\sigma} - \beta\left(\frac{\beta}{\sigma x_1} + \frac{x_2 - x_1}{{x_1}^2}\right) + \frac{\rho\, x_1 - x_2 - x_1 x_3}{{x_1}^2} + \left(-\frac{\beta}{\sigma\, {x_1}^2} - 2\frac{x_2 - x_1}{{x_1}^3} - {x_1}^{-2}\right)\sigma\,(x_2 - x_1)\,.$$

We now have only to integrate, with $T(0) = 0$, to obtain the desired transformation. Then, applying this transformation to the coordinate system yields the observer canonical form of the Lorenz system:

$$\begin{cases} \dot{z} = \begin{bmatrix} 0\,0\,0 \\ 1\,0\,0 \\ 0\,1\,0 \end{bmatrix} z - \begin{bmatrix} f_0^*(z) \\ f_1^*(z) \\ f_2^*(z) \end{bmatrix}, \\ \\ y = \begin{bmatrix} 0\,0\,1 \end{bmatrix} z \end{cases}$$

where

$$
\begin{aligned}
&f_0^*(z) \\
&\quad = -\left(1/2\,\frac{z_2(t)}{z_3(t)} - 1/2 - \beta - 1/2\,\sigma\right) z_1(t) \\
&\qquad + 1/4\,\frac{\beta\,(z_2(t))^2}{z_3(t)} - 3/4\,\beta^2 z_2(t) - (1/2\,\beta - 2\,\sigma)\,(z_3(t))^3 \\
&\qquad - (-\beta\,\sigma + 1/4\,\beta\,\sigma^2 + 1/4\,\beta^2\sigma - 1/2\,\beta^3 + 3/2\,\beta\,\sigma\,\rho + 1/4\,\beta + 1/4\,\beta^2) z_3(t) \\
&\qquad f_1^*(z) = (1/2 + 1/2\,\sigma)\,z_2(t) + (z_3(t))^3 \\
&\qquad\qquad - \left(\sigma\,\rho - 1/2\,\beta\,\sigma + 1/2 - 1/2\,\beta + 1/2\,\sigma^2\right) z_3(t) \\
&\qquad f_2^*(z) = 1/2\,z_2(t) - (-1/2 - 1/2\,\beta - 1/2\,\sigma)\,z_3(t)\,.
\end{aligned}
$$

Thus the Bestle–Zeitz observer is given by

$$
\begin{cases}
\dot{\hat{z}} = \begin{bmatrix} 0 & 0 & 0 \\ 1 & 0 & 0 \\ 0 & 1 & 0 \end{bmatrix} \hat{z} - \begin{bmatrix} f_0^*(\hat{z}) \\ f_1^*(\hat{z}) \\ f_2^*(\hat{z}) \end{bmatrix} - K(\hat{y} - y) \\
\hat{y} = \begin{bmatrix} 0 & 0 & 1 \end{bmatrix} \hat{z}
\end{cases}.
$$

We choose $K = \begin{bmatrix} 30 & 30 & 30 \end{bmatrix}^T$, and the synchronization results are shown in Fig. 3.3. The synchronization error in Fig. 3.3 is very small, but it is from a model-based observer, namely the Bestle–Zeitz observer. It requires complete information about the Lorenz system.

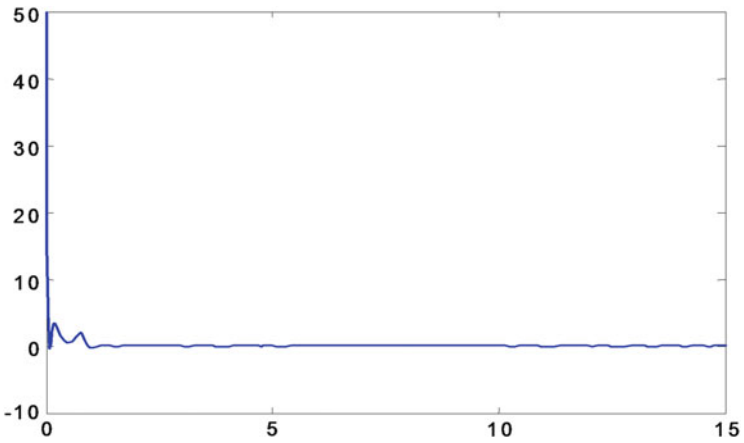

Fig. 3.3 Synchronization error of Lorenz system via Bestle–Zeitz observer

3.5.1.3 Thau Observer to Synchronization of Lorenz System

First, it is necessary to rewrite the system equations in the form required by the method described above. Thus, the Lorenz system can be expressed as in (3.36) using the following values:

$$A = \begin{pmatrix} -\sigma & \sigma & 1 \\ \rho & -1 & 0 \\ 0 & 0 & -\beta \end{pmatrix}, \qquad f(x) = \begin{pmatrix} -x_3 \\ -x_1 x_3 \\ x_1 x_2 \end{pmatrix}.$$
$$B = \begin{pmatrix} 0 \\ 0 \\ 0 \end{pmatrix} \qquad C = \begin{pmatrix} 1 & 0 & 0 \end{pmatrix}$$

Thus the system is written as follows:

$$\begin{cases} \dot{x} = \begin{bmatrix} -\sigma & \sigma & 1 \\ \rho & -1 & 0 \\ 0 & 0 & -\beta \end{bmatrix} x + \begin{bmatrix} -x_3 \\ -x_1 x_3 \\ x_1 x_2 \end{bmatrix} \\ y = \begin{bmatrix} 1 & 0 & 0 \end{bmatrix} x \end{cases}.$$

Therefore, the observer becomes

$$\begin{cases} \dot{\hat{x}} = \begin{bmatrix} -\sigma & \sigma & 1 \\ \rho & -1 & 0 \\ 0 & 0 & -\beta \end{bmatrix} \hat{x} + \begin{bmatrix} -\hat{x}_3 \\ -\hat{x}_1 \hat{x}_3 \\ \hat{x}_1 \hat{x}_2 \end{bmatrix} - K(\hat{y} - y) \\ \hat{y} = \begin{bmatrix} 1 & 0 & 0 \end{bmatrix} \hat{x} \end{cases}.$$

We select $K = \begin{bmatrix} 13 & 13 & 13 \end{bmatrix}^T$. The synchronization results are shown in Fig. 3.4. The synchronization error in Fig. 3.4 is greater than that for the Bestle–Zeitz observer

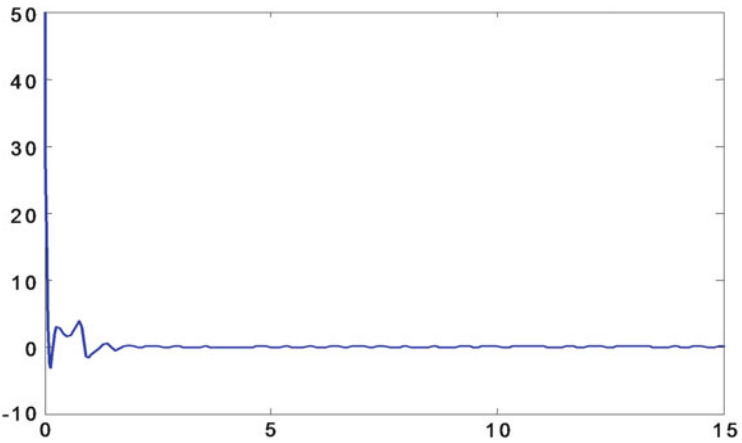

Fig. 3.4 Synchronization error of Lorenz system via Thau observer

in Fig. 3.3. Although it is from a model-based observer, the Thau observer requires less information than the Bestle–Zeitz observer.

3.5.2 *Chua's Circuit*

Some chaotic systems do not have the normal form (3.3), and we cannot apply a sliding-mode observer directly to the slave. Such an system is Chua's circuit

$$\begin{cases} C_1\dot{\xi}_1 = G\left(\xi_2 - \xi_1\right) - g(\xi_1) + u \\ C_2\dot{\xi}_2 = G\left(\xi_1 - \xi_2\right) + \xi_3 \\ L\dot{\xi}_3 = -\xi_2 \\ y = \xi_3 \end{cases}, \tag{3.42}$$

where $g(\xi_1) = m_0\eta_1 + \frac{1}{2}\left(m_1 - m_0\right)\left[\left|\xi_1 + B_p\right| + \left|\xi_1 - B_p\right|\right]$, ξ_1, ξ_2, and ξ_3 denote the voltages across C_1, C_2, and L. It is known that with $C_1 = \frac{1}{9}$, $C_2 = 1$, $L = \frac{1}{7}$, $G = 0.7$, $m_0 = -0.5$, $m_1 = -1.5$, $B_p = 1$, the circuit displays a double scroll. If we make the transformation $\eta = T(\xi)$ as

$$\begin{aligned} \eta_1 &= \xi_3, \\ \eta_2 &= -L\xi_2, \\ \eta_3 &= \tfrac{LG}{C_2}\left(\xi_2 - \xi_1\right) - \tfrac{L}{C_2}\xi_3, \end{aligned} \tag{3.43}$$

then Chua's circuit assumes the normal form

$$\begin{aligned} \dot{\eta}_1 &= \eta_2, \\ \dot{\eta}_2 &= \eta_3, \\ \dot{\eta}_3 &= f(\eta_1, \eta_2, \eta_3) + gu \\ y &= \eta_1, \end{aligned} \tag{3.44}$$

where $f(\eta_1, \eta_2, \eta_3) = -\frac{G}{C_2}\eta_3 - \frac{1}{C_2L}\eta_1 - \frac{G^2}{C_1C_2}\left[-2\eta_2 - \frac{1}{GL}\eta_1 - \frac{C_2}{G}\eta_3 - \frac{1}{C_1}g\left(-\eta_1 - \frac{1}{GL}\eta_1 - \frac{C_2}{G}\eta_3\right)\right]$, $g = \frac{G}{C_1C_2}$. Now the sliding-mode observer-based slave (3.25) can be applied. Chua's circuit (3.42) can be transformed into (3.44) from (3.43). So we design the sliding-mode slave as (3.41).

We choose $k_1 = 300$, $k_2 = 100$, $k_3 = 2$. The synchronization results of SMO are shown in Fig. 3.5. We can see that the synchronization error of Chua's circuit is a little larger than that of the Lorenz system. But synchronization is achieved.

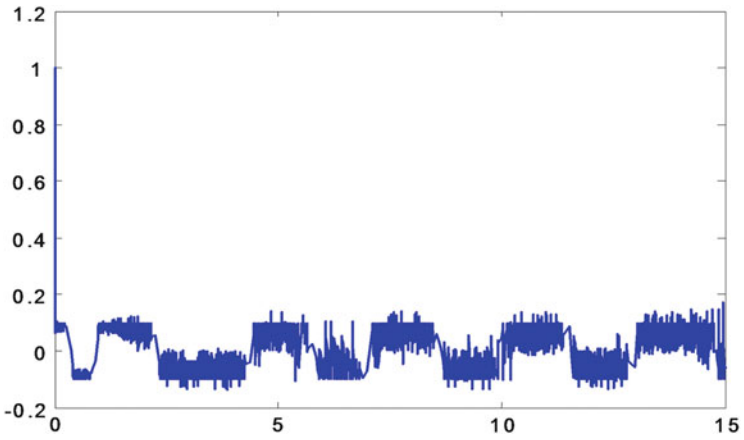

Fig. 3.5 Synchronization error of Chua's circuit via SMO

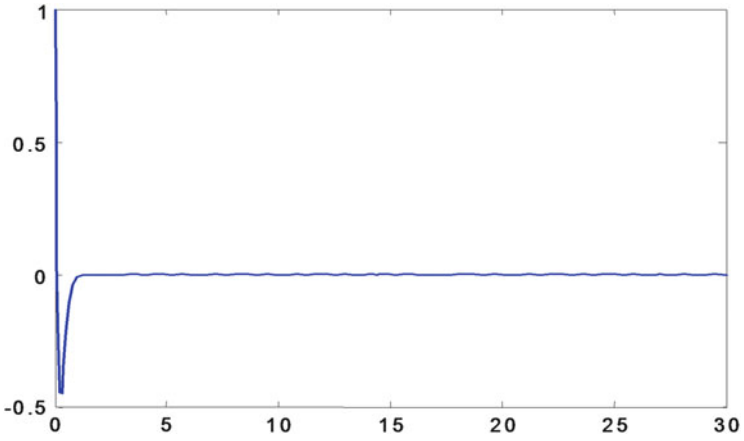

Fig. 3.6 Synchronization error of Chua's circuit via Bestle–Zeitz observer

We choose $K = \begin{bmatrix}13 & 13 & 13\end{bmatrix}^T$. The synchronization results via a Bestle–Zeitz observer are shown in Fig. 3.6. We choose $K = \begin{bmatrix}3 & 3 & 3\end{bmatrix}^T$. The synchronization results via the Thau observer are shown in Figs. 3.7 and 3.8. We can see that in both systems, the best performance is given by the model-based Bestle–Zeitz observer, but even the model-based Thau observer shows better performance than the model-free SMO, i.e., both Bestle–Zeitz and Thau require complete information about the system, but the SMO does not.

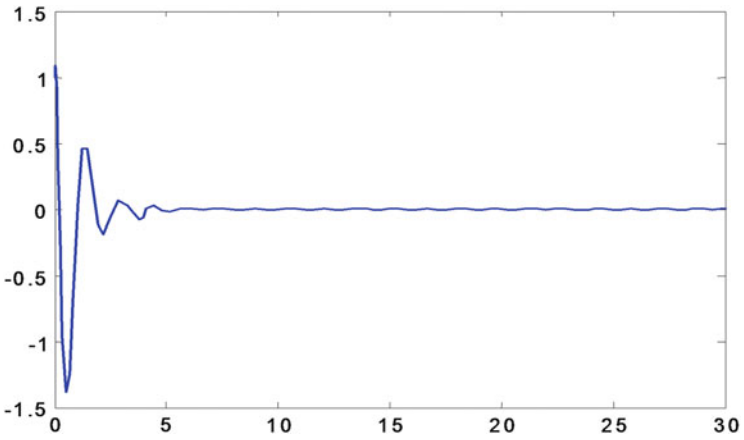

Fig. 3.7 Synchronization error of Chua's circuit via Thau observer

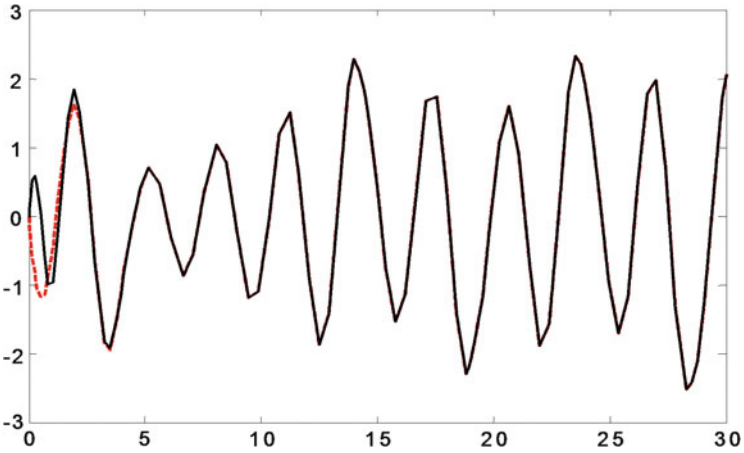

Fig. 3.8 Synchronization states of Chua's circuit via Thau observer

3.6 Concluding Remarks

In this chapter, we have proposed an SMO for the synchronization problem. This new observer presents a simple structure that contains a sliding-mode term that turns out to be robust against output noise as well as sustained disturbances. The slave system is a pure sliding-mode observer. The performance of the observer was shown using numerical simulation. The next chapter develops experimental synchronization by means of observers.

References

1. S.V. Anulova, Random disturbances of the operation of control systems in the sliding mode. Autom. Remote Control **47**(4, Part I), 474–479 (1986)
2. D. Bestle, M. Zeitz, Canonical form observer design for non-linear time-variable systems. Int. J. Control **38**(2), 419–432 (1983)
3. S.V. Drakunov, V. Utkin, Sliding mode observers tutorial, in *Proceedings of the 34th IEEE Conference on Decision and Control (CDC)*, New Orleans, LA, 13–15 Dec 1995, pp. 3376–3378
4. L. Fridman, Y. Shtessel, C. Edwards, X.-G. Yan, Higher-order Sliding-mode observer for state estimation and input reconstruction in nonlinear systems. Int. J. Robust Nonlinear Control **18**, 399–412 (2008)
5. A. Isidori, *Nonlinear Control System*, 3rd edn. (Springer, London, 1995)
6. R. Martínez-Guerra, J.C. Cruz-Victoria, R. Gonzalez-Galan, R. Aguilar-Lopez, A new reduced-order observer design for the synchronization of Lorenz system. Chaos Solitons Fractals **28**, 511–517 (2006)
7. O. Mörgul, E. Solak, Observer based synchronization of chaotic systems. Phys. Rev. E **54**, 4803–4811 (1996)
8. H. Nijmeijer, I.M. Mareels, An observer looks at synchronization. IEEE Trans. Circuits Syst. Part I **44**(10), 882–890 (1997)
9. U. Parlitz, L.O. Chua, L. Kocarev, K.S. Halle, A. Shang, Transmission of digital signals by chaotic synchronization. Int. J. Bifurcation Chaos **2**, 973–977 (1992)
10. L.M. Pecora, T.L. Carroll, Synchronization in chaotic systems. Phys. Rev. Lett. **64**, 821–824 (1990)
11. J. Slotine, J. Hedricks, E. Misawa, On sliding observers for nonlinear systems. J. Dyn. Meas. Control **109**, 245–252 (1987)
12. F.E. Thau, Observing the state of non-linear dynamic systems. Int. J. Control **17**, 471–479 (1973)
13. T. Ushio, Synthesis of synchronized chaotic systems based on observers. Int. J. Bifurcation Chaos **9**(3), 541–546 (1999)
14. B.L. Walcott, M.J. Corles, S.H. Zak, Comparative study of non-linear state-observation techniques. Int. J. Control **45**(6), 2109–2132 (1987)
15. W.C. Wu, L.O. Chua, A unified framework for synchronization and control of dynamical systems. Int. J. Bifurcation Chaos **4**, 979–998 (1994)

Chapter 4
Experimental Synchronization by Means of Observers

Abstract In this chapter, we deal with the experimental synchronization of the Colpitts oscillator in real time. Our approach is based on observer design theory in a master–slave configuration. Thus, the chaos synchronization problem can be posed as an observer design procedure, where the coupling signal is viewed as measurable output, and the slave system is regarded as an observer. A polynomial observer is used for synchronizing the Colpitts oscillator employing linear matrix inequalities. Moreover, comparison with a reduced-order observer and a high-gain observer is given to assess the performance of the proposed observer.

4.1 Introduction

In recent years, the synchronization of chaotic systems problem has received a great deal of attention among scientists in many fields [1, 5, 6, 26, 35]. Among the publications dedicated to chaos synchronization, many different approaches can be found. We cite the papers [1, 2, 15, 25, 31, 32], which propose the use of state observers to synchronize chaotic systems; feedback controllers are proposed in [7, 24, 34], while [14, 33] use a nonlinear backstepping control. The papers [11, 12] consider synchronization time-delayed systems; in [9, 18], directional and bidirectional linear coupling is considered; [3, 4] use nonlinear control, while [2, 7, 9, 11, 12, 14, 24, 33, 34] use active control and [22, 34] use adaptive control. Of particular interest is the connection between the observers for nonlinear systems and chaos synchronization, which is also known as the master–slave configuration [6, 8].

Thus, the chaos synchronization problem can be regarded as an observer design procedure, where the coupling signal is viewed as output and the slave system as an observer [1, 23, 35]. In this configuration, the two coupled systems are identical, and therefore identical synchronization occurs, which means that the difference of the master and slave state vectors converges to zero for $t \to \infty$.

In this chapter, a synchronization scheme is proposed for a class of Lipschitz nonlinear systems. Many problems in engineering and other applications are globally Lipschitz, such as the sinusoidal terms in robotics. Nonlinearities that are square or cubic in nature are not globally Lipschitz. However, they are locally so.

R. Martínez-Guerra et al., *Synchronization of Integral and Fractional Order Chaotic Systems*, Understanding Complex Systems,
DOI 10.1007/978-3-319-15284-4_4

Moreover, when such functions occur in physical systems, they frequently have a saturation in their growth rate, making them globally Lipschitz functions [16]. In this chapter, we have considered trajectories that are defined in the same invariant set, i.e., we consider an invariant set that contains the globally Lipschitz functions. Based on this fact, we state that trajectories remain in an invariant set. Thus, the class of systems covered in this chapter is fairly general.

The main contribution of this chapter consists in the solution of the synchronization problem via an exponential polynomial observer. In [10, 16, 19], existence conditions for the full-order observers for Lipschitz nonlinear systems are established. Also, the main purpose in this chapter is to extend those results by showing that the conditions given in [4, 8, 22] also guarantee the existence of a full-order observer with a high-order correction term. The reason is very simple: as is well known, an extended Luenberger observer [16, 19] can be seen as a first-order Taylor series around the observed state. Therefore, to improve the estimation, a high-order term is now included in the observer structure. The intention in choosing the examples of the Rössler and Rikitake systems is to clarify the proposed methodology. However, it is worth mentioning that this technique can be applied to almost any chaotic synchronization problem.

4.2 Exponential Polynomial Observer

4.2.1 Problem Statement

Consider the following nonlinear system:

$$\begin{aligned} \dot{x} &= f(x,u), \\ y &= Cx, \end{aligned} \tag{4.1}$$

where $x \in \mathbb{R}^n$ is the vector of state variable; $u \in \mathbb{R}^{m'}$ is the input vector $m' \leq n$; $f(\cdot) : \mathbb{R}^n \times \mathbb{R}^{m'} \longrightarrow \mathbb{R}^n$ is locally Lipschitz on x and uniformly bounded on u; $y \in \mathbb{R}$ is the output of the system.

To show the relationship between observers for nonlinear systems and synchronization, we give the following definition.

Definition 4.1 The dynamical system with state vector $\hat{x} \in \mathbb{R}^n$,

$$\begin{aligned} \dot{\hat{x}} &= \bar{f}(\hat{x}, y, u), \\ \hat{y} &= C\hat{x} \quad , \hat{x}_0 = \hat{x}(t_0), \end{aligned} \tag{4.2}$$

is in a state of exponential synchronization with system (4.1) if there exist positive constants $\bar{k}$ and $\bar{\xi}$ such that

$$||x - \hat{x}|| \leq \bar{k} \exp(-\bar{\xi} t).$$

In the master–slave synchronization scheme, x is viewed as the state variable of the master system, and $\hat{x}$ is considered the state variable of the slave system. Hence, the master–slave system synchronization problem between systems (4.1) and (4.2) can be solved by designing an observer for (4.1). In order to solve the synchronization problem as an observation problem, we introduce the algebraic observability condition (see Chap. 1).

The system (4.1) can be expressed in the following form:

$$\begin{aligned} \dot{x} &= Ax + \Psi(x, u), \\ y &= Cx \quad x_0 = x(t_0), \end{aligned} \tag{4.3}$$

where $\Psi(x, u)$ is a nonlinear vector that satisfies the Lipschitz condition

$$||\Psi(x, u) - \Psi(\hat{x}, u) \leq \varphi||x - \hat{x}||, \tag{4.4}$$

where φ is the Lipschitz constant.

The observer for system (4.3) has the form

$$\dot{\hat{x}} = A\hat{x} + \Psi(\hat{x}, u) + \sum_{i=1}^{m} K_i (y - C\hat{x})^{2i-1}, \tag{4.5}$$

where $\hat{x} \in \mathbb{R}^n$, and $K_i \in \mathbb{R}^n$ for $1 \leq i \leq m$.

Let us consider the following assumptions:

Assumption 4.1 For $\bar{A} := A - K_1 C$, there exists a unique symmetric positive definite matrix $P \in \mathbb{R}^{n \times n}$ that satisfies the following linear matrix inequality (LMI):

$$\begin{bmatrix} -\bar{A}^T P - P\bar{A} - I & \varphi P \\ \varphi P & I \end{bmatrix} > 0,$$

where φ is the Lipschitz constant.

Assumption 4.2 Let us define $M_i := PK_i C$. Then

$$\lambda_{\min}(M_i + M_i^T) \geq 0, \quad \text{for } 2 \leq i \leq m.$$

Remark 4.1 Using Schur complement (see[27]), the LMI in Assumption 4.1 can be represented as an algebraic Riccati equation,

$$\bar{A}^T P + P\bar{A} + \varphi^2 PP + I < 0,$$

or for some $\epsilon > 0$,

$$\bar{A}^T P + P\bar{A} + \varphi^2 PP + I + \epsilon I = 0. \tag{4.6}$$

Remark 4.2 Assumption 4.2 is used to improve the rate of convergence of the estimation error by injecting additional terms (from 2 to m) that depend on odd powers of the output error.

In order to prove the observer convergence, we analyze the observation error, which is defined as $e = x - \hat{x}$. From (4.3) and (4.5), the dynamics of the observer is given by

$$\dot{e} = \bar{A}e + F - \sum_{i=2}^{m} K_i (Ce)^{2i-1},$$

where $\bar{A} := A - K_1 C$ and $F := \Psi(x,u) - \Psi(\hat{x},u)$.

Now we present a lemma that will be useful in convergence analysis.

Lemma 4.1 ([28]) *Given the system (4.3) and its observer (4.5), with the error given by $e := x - \hat{x}$, if $P = P^T > 0$, then*

$$2e^T P[\Psi(x,u) - \Psi(\hat{x},u)] \leq \varphi^2 e^T PPe + e^T e.$$

□

The following proposition proves the observer convergence.

Proposition 4.1 *Let the system (4.3) be algebraically observable and suppose that Assumptions 4.1 and 4.2 hold. The nonlinear system (4.5) is an exponential polynomial observer of the system (4.3); that is, there exist constants $k > 0$ and $\xi > 0$ such that*

$$||e(t)|| \leq k||e(0)|| \exp(-\xi t),$$

where $k = \sqrt{\frac{\beta}{\alpha}}$, $\xi = \frac{\epsilon}{2\beta}$, $\alpha = \lambda_{\min}(P)$, and $\beta = \lambda_{\max}(P)$.

Proof we use the following Lyapunov function candidate $V = e^T Pe$:

$$\dot{V} = \dot{e}^T Pe + e^T P\dot{e} = e^T[\bar{A}^T P + P\bar{A}]e + 2e^T PF - 2e^T P \sum_{i=2}^{m} K_i (Ce)^{2i-1}.$$

Using Lemma 4.1, we obtain

$$\dot{V} \leq e^T[\bar{A}P + P\bar{A} + \varphi^2 PP + I]e - 2e^T P \sum_{i=2}^{m} K_i (Ce)^{2i-1}.$$

Performing some algebraic manipulations on the last term of the above inequality and taking into account that $Ce \in \mathbb{R}$, we obtain

$$\dot{V} \leq e^T[\bar{A}^T P + P\bar{A} + \varphi^2 PP + I]e - 2\sum_{i=2}^{m} (Ce)^{2i-2} e^T PK_i Ce.$$

For simplicity, we define $M_i = PK_iC, 2 \leq i \leq m$. Then we have

$$\dot{V} \leq e^T[\bar{A}^T P + P\bar{A} + \varphi^2 PP + I]e - \{(Ce)^2[e^T M_2 e + (e^T M_2 e)^T] + (Ce)^4[e^T M_3 e + (e^T M_3 e)^T] + \cdots + (Ce)^{2m-2}[e^T M_m e + (e^T M_m e)^T]\}. \tag{4.7}$$

The above expression can be rewritten in the simplified form

$$\dot{V} \leq e^T[\bar{A}^T P + P\bar{A} + \varphi^2 PP + I]e - \sum_{i=2}^{m}(Ce)^{2i-2}e^T(M_i + M_i^T)e.$$

From Assumption 4.2, the second term on the right-hand side of the above inequality will always be nonnegative. Therefore,

$$\dot{V} \leq e^T[\bar{A}^T P + P\bar{A} + \varphi^2 PP + I]e. \tag{4.8}$$

By Assumption 4.1 (and Remark 4.1), we have

$$\dot{V} \leq -\epsilon||e||^2. \tag{4.9}$$

We use the Lyapunov function $V = ||e||_P^2$. Then by the Rayleigh–Ritz inequality, we have that

$$\alpha||e||^2 \leq ||e||_P^2 \leq \beta||e||^2, \tag{4.10}$$

where $\alpha := \lambda_{\min}(P)$ and $\beta := \lambda_{\max}(P) \in \mathbb{R}^+$ (because P is positive definite).

Using (4.10), we obtain the following upper bound for (4.9):

$$\dot{V} \leq -\frac{\epsilon}{\beta}||e||_P^2. \tag{4.11}$$

Taking the time derivative of $V = ||e||_P^2$ and replacing it in inequality (4.11), we obtain

$$\frac{d}{dt}||e||_P \leq -\frac{\epsilon}{2\beta}||e||_P.$$

Finally, the result follows with

$$||e(t)|| \leq k||e(0)|| \exp(-\xi t), \tag{4.12}$$

where $k = \sqrt{\frac{\beta}{\alpha}}$ and $\xi = \frac{\epsilon}{2\beta}$ □

4.3 Asymptotic Reduced-Order Observer

Now let us consider the nonlinear system described by (4.1). The unknown states of the system can be included in a new variable $\eta(t)$, and the following new augmented system is considered:

$$\begin{aligned} \dot{x}(t) &= f(x, u, \eta), \\ \dot{\eta}(t) &= \triangle(x, u), \\ y(t) &= h(x), \end{aligned} \tag{4.13}$$

where $\triangle(x, u)$ is a bounded uncertain function. The problem is to reconstruct the variable $\eta(t)$. This problem is overcome by using a reduced-order observer. Before proposing the corresponding observer for reconstructing the variable $\eta(t)$, we introduce some hypotheses:

Assumption 4.3 $\eta(t)$ satisfies the AOC (see Chap. 1).

Assumption 4.4 γ is a C^1 real-valued function.

Assumption 4.5 $\triangle$ is bounded, i.e., $|\triangle| \leq M < \infty$.

Assumption 4.6 For t_0 sufficiently large, there exists $K > 0$ such that $\lim_{t \to t_0} \sup \frac{M}{K} = 0$.

The design of a proportional reduced-order observer for system (4.1) is given by the next lemma.

Lemma 4.2 *If Assumptions 4.3–4.6 are satisfied, then the system*

$$\dot{\hat{\eta}} = K(\eta - \hat{\eta}) \tag{4.14}$$

is an asymptotic reduced-order observer of free-model type for system (4.1), where $\hat{\eta}$ denotes the estimate of η, and $K \in \mathbb{R}^+$ determines the desired convergence rate of the observer. □

Remark 4.3 To reconstruct $\eta(t)$ using an auxiliary state $\hat{\eta}(t)$, we sometimes need to use the output time derivatives, but these may be unavailable. To overcome this problem, a completely artificial auxiliary function γ is defined in such away that it cancels out all unmeasurable terms. This action defines a differential equation for γ. This equation is solved, and then γ is substituted into the differential equation of the estimated state, and finally, the estimate of η is obtained.

We give the following immediate corollary.

Corollary 4.1 *The dynamic system (4.14) along with*

$$\dot{\gamma} = \psi(x, u, \gamma), \quad \textit{with } \psi_0 = \psi(0) \textit{ and } \gamma \in C^1$$

constitutes a proportional asymptotic reduced-order observer for system (4.1), where γ is a change of variable that depends on the estimated state $\hat{\eta}$ and the state variables. □

4.4 High-Gain Observer

We present a well-known estimation structure (high-gain observer) as a comparison with our proposed schemes.

Consider the class of nonlinear systems given by (4.1). In this case, to estimate the state-space vector x, we can suggest a nonlinear high-gain observer as follows:

$$\begin{aligned} \dot{\hat{x}} &= f(\hat{x}, u) + K(y - C\hat{x}), \\ \hat{x} &\in \mathbb{R}^n, \hat{x}_0 = \hat{x}(t_0), \end{aligned} \tag{4.15}$$

where the observer high-gain matrix is given by

$$K = S_\theta^{-1} C^T, \quad S_\theta = \left(\frac{1}{\theta^{i+j-1}} S_{ij} \right)_{ij=1,\ldots,n},$$

and the positive parameter θ determines the desired convergence velocity. Moreover, $S_\theta > 0$, $S_\theta = S_\theta^T$, should be a positive solution of the algebraic equation

$$\begin{aligned} S_\theta \left(E + \frac{\theta}{2} I \right) + \left(E^T + \frac{\theta}{2} I \right) S_\theta &= C^T C, \\ E &= \begin{bmatrix} 0 & I_{n-1,n-1} \\ 0 & 0 \end{bmatrix}. \end{aligned} \tag{4.16}$$

As is shown in [10], under certain technical assumptions (Lipschitz conditions in an invariant set for the nonlinear functions under consideration), this nonlinear observer has an arbitrary exponential decay for any initial conditions.

4.5 Synchronization by Means of Observers

4.5.1 Experimental Results

These proposals are applied to a Colpitts oscillator [6, 17]. The Colpitts oscillator has been widely considered for the synchronization problem; see, for instance, [6, 13].

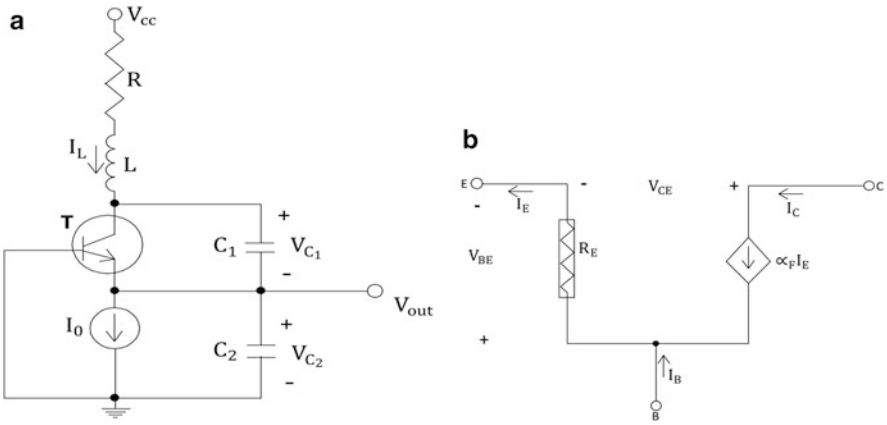

Fig. 4.1 Colpitts oscillator. (**a**) Circuit configuration. (**b**) Model of the bipolar junction transistor (BJT)

In this chapter, we consider the classical configuration of the Colpitts oscillator [20]. The circuit contains a bipolar junction transistor 2N2222A as the gain element (Fig. 4.1b) and a resonant network consisting of an inductor and two capacitors (Fig. 4.1a).

The Colpitts circuit is described by a system of three nonlinear differential equations as follows:

$$\begin{aligned} L\dot{I}_L &= -V_{C_1} - V_{C_2} - RI_L + V_{CC}, \\ C_2\dot{V}_{C_2} &= I_L - I_0, \\ C_1\dot{V}_{C_1} &= -f\left(V_{C_2}\right) + I_L, \end{aligned} \tag{4.17}$$

where $f(\cdot)$ is the driving-point characteristic of the nonlinear resistor. This can be expressed in the form $I_E = f\left(V_{C_2}\right) = f\left(V_{BE}\right)$. In particular, we have $f\left(V_{C_2}\right) = I_S \exp\left(-V_{C_2}/V_T\right)$.

We introduce the dimensionless state variables (x_1, x_2, x_3), and we choose the operation point of (4.19) to be the origin of the new coordinate system. In particular, we normalize voltages, currents, and time with respect to $V_{\text{ref}} = V_T$, $I_{\text{ref}} = I_0$, and $t_{\text{ref}} = 1/\omega_0$, respectively, where $\omega_0 = 1/\sqrt{LC_1C_2/\left(C_1 + C_2\right)}$ is the resonant frequency of the unloaded $L-C$ tank circuit. Then the state equation for the Colpitts oscillator can be rewritten as

$$\begin{aligned} \dot{x}_1 &= -cx_3 - cx_2 - dx_1, \\ \dot{x}_2 &= bx_1, \\ \dot{x}_3 &= -a\exp(-x_2) + ax_1 + a, \end{aligned} \tag{4.18}$$

where $a = b\dfrac{C_2}{C_1}$, $b = \dfrac{I_0}{\omega_0 C_2 V_T}$, $C = \dfrac{V_T}{\omega_0 L I_0}$, $d = \dfrac{R}{L\omega_0}$.

According to the definition given in Chap. 1, it is evident that system (4.18) is algebraically observable with respect to the output $y = x_2$, since the unknown states x_1 and x_3 can be rewritten as

$$x_1 = \frac{\dot{x}_2}{b} = \frac{\dot{y}}{b}, \tag{4.19}$$

$$x_3 = -\frac{1}{c}\left[\frac{1}{b}\ddot{y} + \frac{d}{b}\dot{y} + cy\right]. \tag{4.20}$$

Hence the Colpitts oscillator is algebraically observable with respect to the selected output $y = x_2$.

4.5.2 *Synchronization of the Colpitts Oscillator Employing an Exponential Polynomial Observer*

For the implementation of the observer, we first rewrite (4.18) in the form (4.3):

$$\dot{x} = \begin{bmatrix} -d & -c & -c \\ b & 0 & 0 \\ a & 0 & 0 \end{bmatrix} x + \begin{bmatrix} 0 \\ 0 \\ -a\exp(-\hat{x}_2) + a \end{bmatrix} \tag{4.21}$$

$$y = \begin{bmatrix} 0 & 1 & 0 \end{bmatrix} x. \tag{4.22}$$

Applying Proposition 4.1, we have

$$\dot{\hat{x}} = \begin{bmatrix} -d & -c & -c \\ b & 0 & 0 \\ a & 0 & 0 \end{bmatrix} \hat{x} + \begin{bmatrix} 0 \\ 0 \\ -a\exp(-\hat{x}_2) + a \end{bmatrix} + \sum_{i=1}^{m} \begin{bmatrix} k_{1,i} \\ k_{2,i} \\ k_{3,i} \end{bmatrix} \left(\begin{bmatrix} 0 & 1 & 0 \end{bmatrix} e\right)^{2i-1}.$$

Hence the state observer is rewritten as

$$\begin{aligned} \dot{\hat{x}}_1 &= -c\hat{x}_3 - c\hat{x}_2 - d\hat{x}_1 + k_{3,1}e_{1,2} + k_{3,2}(e_{1,2})^3 + \cdots + k_{3,m}(e_{1,2})^{2m-1}, \\ \dot{\hat{x}}_2 &= b\hat{x}_1 + k_{2,1}e_{1,2} + k_{2,2}(e_{1,2})^3 + \cdots + k_{2,m}(e_{1,2})^{2m-1}, \\ \dot{\hat{x}}_3 &= a\hat{x}_1 - a\exp(-\hat{x}_2) + a + k_{1,1}e_{1,2} + k_{1,2}(e_{1,2})^3 + \cdots + k_{1,m}(e_{1,2})^{2m-1}. \end{aligned} \tag{4.23}$$

We verified the real-time performance of the exponential observer using the WINCON platform. To achieve synchronization in real time, we implemented in WINCON the scheme (4.23) in the master–slave configuration. Figure 4.2 shows the real implementation of the Colpitts circuit. The circuit parameters are $L = 100\,\mu\text{H}$; $C_1 = C_2 = 47\,\text{nF}$, $R = 45\,\Omega$, $I_0 = 54\,\text{mA}$. Using the circuit parameters, we obtain $a = b = 6.2723$, $c = 0.0797$, and $d = 0.6898$.

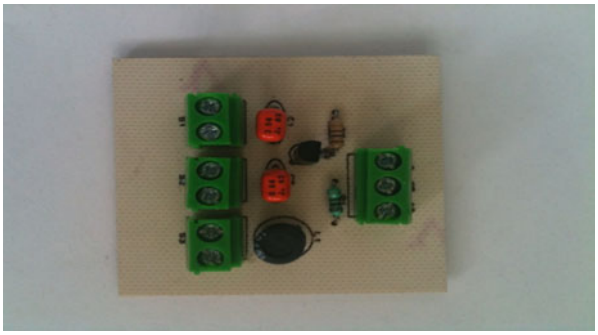

Fig. 4.2 Implementation of the Colpitts circuit (master system)

The nonlinear term $\Psi(x)$ in (4.21) satisfies the Lipschitz condition and is considered as follows:

$$\Psi(x) = \begin{bmatrix} 0 \\ 0 \\ -a\exp(-x_2) + a. \end{bmatrix}$$

It is necessary to calculate the Lipschitz constant φ introduced in (4.4) over the bounded set

$$\Omega = \left\{ x \in \mathbb{R}^3 | \quad |x_2| < M_2, \quad |x_3| < M_3 \right\}. \tag{4.24}$$

Considering the Jacobian of $\Psi(x)$ to be

$$\left[\frac{\partial \Psi(x)}{\partial x} \right] = \begin{bmatrix} 0 & 0 & 0 \\ 0 & 0 & 0 \\ 0 & a\exp(-x_2) & 0 \end{bmatrix}, \tag{4.25}$$

we conclude that[1]

$$\| \frac{\partial \Psi(x)}{\partial x} \|_\infty \leq 3\max\{0, \quad a\exp(-x_2)\} \quad , \quad a \in \mathbb{R}^+. \tag{4.26}$$

From (4.24), it is obvious that the following conditions hold for all points in the bounded set Ω:

$$a\exp(-x_2) < a\exp(M_2) = \max\{a\exp(-x_2)\} \quad a \in \mathbb{R}^+. \tag{4.27}$$

Hence

$$\| \frac{\partial \Psi(x)}{\partial x} \|_\infty \leq 3a\exp(M_2). \tag{4.28}$$

[1]Let us consider the matrix $\mathbb{A} = [a_{i,j}]_{1 \leq 1, j \leq n}$, then (see [27])

$$\| A \|_\infty := n \max_{1 \leq i,j \leq n} |a_{i,j}|$$

With (4.28), a Lipschitz constant that satisfies the Lipschitz condition (4.4) is defined as follows:

$$\varphi = 3a \exp(M_2).$$

In this case, $M_1 = 3$, $M_2 = 0.1$, $M_3 = 6$, and $a = 6.2723$, $\Rightarrow \varphi = 20.7959$.

Following the observer (4.23), for $m = 2$, and solving the LMI given by Assumption 4.1, the observer gains K_1 and K_2 and a positive definite matrix P are as follows:

$$K_1 = \begin{bmatrix} 10.2130 \\ 16.1211 \\ 10.1500 \end{bmatrix}, \quad K_2 = \begin{bmatrix} 3 \\ 2 \\ 3 \end{bmatrix}, \quad P = \begin{bmatrix} 38.8560 & -36.7794 & 19.4606 \\ -36.7794 & 37.9331 & -20,7898 \\ 19.4606 & -20.788 & 16.4869 \end{bmatrix} > 0,$$

with eigenvalues $\lambda_1(P) = 1.3151$, $\lambda_2(P) = 5.2514$, and $\lambda_3(P) = 86.7095$. The performance index (quadratic synchronization error) of the corresponding synchronization process is calculated as

$$J(t) = \frac{1}{t + 0.001} \int_0^t |e(t)|^2_{Q_0} \quad , \quad Q_0 = I.$$

Figure 4.3a–c shows the obtained results using the exponential polynomial observer (4.23). It is clear that the synchronization achieved is fairly acceptable

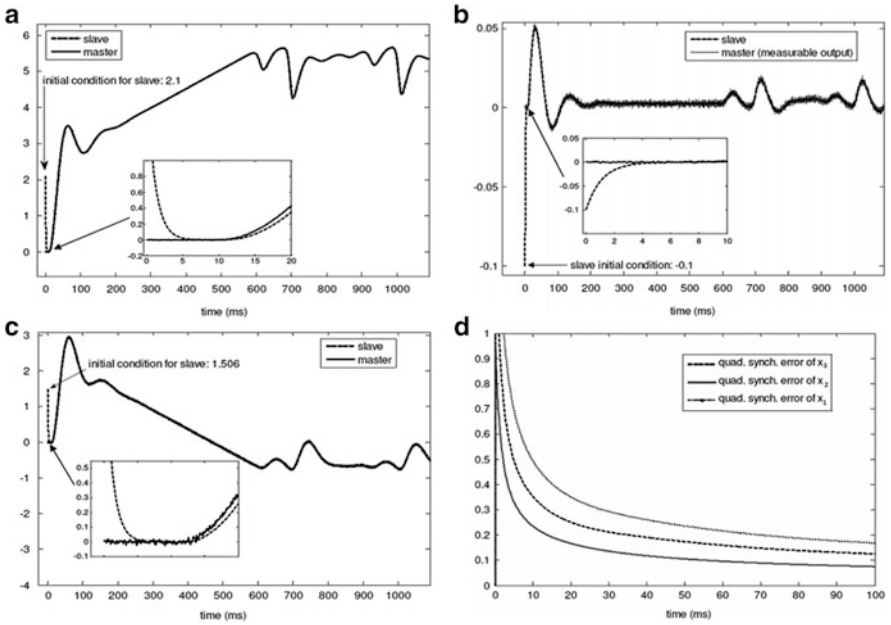

Fig. 4.3 Real-time synchronization of Colpitts oscillator employing observer: (**a**) variables x_1 and $\hat{x}_1$, (**b**) synchronization of variables x_2 and $\hat{x}_2$, (**c**) synchronization of variables x_3 and $\hat{x}_3$, and (**d**) performance index

even with noisy measurements. The Colpitts circuit starts at $x(0) = \begin{bmatrix}0 & 0 & 0\end{bmatrix}^T$, and the arbitrary initial conditions for the observer are $\hat{x}(0) = \begin{bmatrix}2.1 & -0.1 & 1.506\end{bmatrix}^T$. Figure 4.3d shows the performance index of the synchronization, which indicates exponential behavior.

4.6 Synchronization with a High-Gain Observer

The matrix $S_\theta > 0$, $S_\theta = S_\theta^T$, that satisfies the algebraic Riccati equation (4.16) for a third-order system ($n = 3$) is given by

$$S_\theta = \begin{bmatrix} \frac{1}{\theta} & -\frac{1}{\theta^2} & \frac{1}{\theta^3} \\ -\frac{1}{\theta^2} & -\frac{1}{\theta^3} & \frac{1}{\theta^4} \\ \frac{1}{\theta^3} & -\frac{1}{\theta^4} & \frac{1}{\theta^5} \end{bmatrix}, \tag{4.29}$$

and its corresponding inverse matrix is

$$S_\theta^{-1} = \begin{bmatrix} 3\theta & 3\theta^2 & \theta^3 \\ 3\theta^2 & 5\theta^3 & 2\theta^4 \\ \theta^3 & 2\theta^4 & \theta^5 \end{bmatrix}. \tag{4.30}$$

Then the high-gain observer for Colpitts system (4.30) is as follows:

$$\begin{aligned} \dot{\hat{x}}_1 &= -c\hat{x}_3 - c\hat{x}_2 - d\hat{x}_1 + \frac{5}{b}\theta^3(y - \hat{x}_2), \\ \dot{\hat{x}}_2 &= b\hat{x}_1 + 3\theta^2(y - \hat{x}_2), \\ \dot{\hat{x}}_3 &= a\hat{x}_1 - a\exp(-\hat{x}_2) + a + \left(3\theta^2 - \frac{5d}{bc}\right)\theta^3 - \frac{2}{bc}\theta^4\Big)(y - \hat{x}_2), \end{aligned} \tag{4.31}$$

Figure 4.5 depicts the synchronization between Colpitts oscillator given by (4.18) and its high-gain observer denoted by (4.31). In order to obtain exponential convergence, we have used $\theta = 100$. Note that the performance on the high-gain observer is not good in comparison with the exponential polynomial observer and with the proportional reduced-order observer. An important advantage of the proposed methodologies is that the magnitudes of the observer gains are smaller than those used in the high-gain observer.

4.6.1 Synchronization of the Colpitts Oscillator by Means of an Asymptotic Reduced-Order Observer

Let us consider the normalized system of the Colpitts oscillator. We assume that the output system is $y = x_2$. Therefore, the slave system consists of two estimation structures to achieve synchronization with the master system. Such structures are obtained as follows. First, verify that the master system (Colpitts oscillator) is algebraically observable, and then, using (4.14), construct the observer for the unknown states. Previously, we have verified that the master system (Colpitts oscillator) is algebraically observable (see Eqs. (4.31) and (4.20)). Then both unknown states of the master system are algebraically observable, and therefore, we can construct the observers based on Lemma 4.2 and Corollary 4.1.

For x_1, the observer is given by

$$\begin{aligned} \dot{\gamma}_3 &= -\frac{K_3^2}{b} y - K_3 \gamma_3, \\ \hat{x}_1 &= \frac{K_3}{b} y + \gamma_3, \end{aligned} \tag{4.32}$$

and for x_3, we have

$$\begin{aligned} \dot{\gamma}_4 &= -K_4[\gamma_4 + K_4 y], \\ \dot{\gamma}_5 &= [K_5 - d]\frac{K_5}{cb}[\gamma_4 + K_4 y] - K_5 y - K_5 \gamma_5, \\ \hat{x}_3 &= -\frac{K_5}{cb}[\gamma_4 + K_4 \gamma] + \gamma_5. \end{aligned} \tag{4.33}$$

Therefore, (4.32) and (4.33) constitute the slave system. We now present some experimental results for the synchronization of the Colpitts oscillator using the asymptotic reduced-order observer (4.32) and (4.33). Figure 4.4a, b shows the obtained results for the initial conditions $\hat{x}_1 = -2.498$ and $\hat{x}_3 = 1.506$ in the schemes (4.32) and (4.33), respectively. Note that the synchronization results achieved with the reduced-order observer are good. Figure 4.4c presents the phase portrait, where one may clearly observe the chaotic behavior of the Colpitts oscillator. Finally, Fig. 4.4d illustrates the performance index, which has a tendency to decrease.

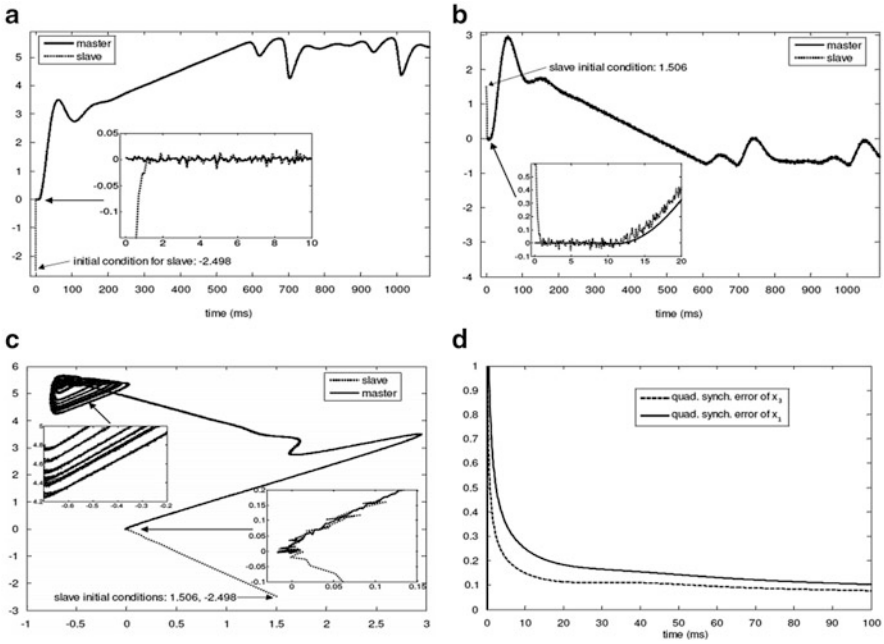

Fig. 4.4 Real-time synchronization of Colpitts oscillator using reduced-order observer: (**a**) synchronization of coordinates x_1 and $\hat{x}_1$, (**b**) synchronization between x_3 and $\hat{x}_3$, (**c**) phase portrait of the master system (x_3 (*horizontal*) versus x_1 (*vertical*)) and the slave system ($\hat{x}_3$ and $\hat{x}_1$), and (**d**) performance index

4.6.2 Rössler System

We consider the popular nonlinear Rössler's system [30], which is described by

$$\begin{aligned} \dot{x}_1 &= -(x_2 + x_3), \\ \dot{x}_2 &= x_1 + ax_2, \\ \dot{x}_3 &= b + x_3(x_1 - c), \\ y &= x_1. \end{aligned} \tag{4.34}$$

It is well known that in a large neighborhood of $(a = b = 0.2, c = 5)$, this system exhibits chaotic behavior.

Remark 4.4 It is not difficult to prove that system (4.34) is Lipschitz.

Before proposing the state observer, we prove the algebraic observability condition for system (4.34). Replacing y into the system (4.34), we obtain

$$\dot{y} = -x_2 - x_3, \tag{4.35}$$

$$\dot{x}_2 = y + ax_2, \tag{4.36}$$

$$\dot{x}_3 = b + x_3(y - c). \tag{4.37}$$

Taking the time derivative from (4.35) yields

$$\ddot{y} = -\dot{x}_2 - \dot{x}_3. \tag{4.38}$$

From (4.35), we get

$$x_3 = -y - x_2. \tag{4.39}$$

Replacing (4.36), (4.37), and (4.39) into (4.38) gives us

$$\dot{y} - y\dot{y} + c\dot{y} + y - x_2 y + (a + c)x_2 + b = 0. \tag{4.40}$$

In the same manner, for x_3, we have from (4.35) that

$$x_2 = -\dot{y} - x_3. \tag{4.41}$$

Substituting (4.36), (4.37), and (4.41) into Eq. (4.38) then yields

$$\dddot{y} - a\ddot{y} + \dot{y} + x_3 y - (a + c)x_3 + b = 0. \tag{4.42}$$

Remark 4.5 From (4.40) and (4.42), x_2 and x_3 are algebraically observable.

According to Proposition 4.1, we get the following system (slave system) for the observer (Fig. 4.5):

$$\begin{aligned}
\dot{\hat{x}}_1 &= -(\hat{x}_2 + \hat{x}_3) + k_{1,1}(x_1 - \hat{x}_1) + k_{1,2}(x_1 - \hat{x}_1)^m, \\
\dot{\hat{x}}_2 &= \hat{x}_1 + a\hat{x}_2 + k_{2,1}(x_1 - \hat{x}_1) + k_{2,2}(x_1 - \hat{x}_1)^m, \\
\dot{\hat{x}}_3 &= b + \hat{x}_3(\hat{x}_1 - c) + k_{3,1}(x_1 - \hat{x}_1) + k_{3,2}(x_1 - \hat{x}_1)^m.
\end{aligned} \tag{4.43}$$

We show some simulations for the Rössler system (4.34) and its observer given by system (4.43), where we have taken for the parameter values $a = b = 0.2$, $c = 5$, $K_1 = [k_{1,1}\ k_{2,1}\ k_{3,1}]^T = [5\ -5\ 5]^T$, $K_2 = [k_{1,2}\ k_{2,2}\ k_{3,2}] = [10\ 10\ 10]^T$, $m = 3$. The design of the exponential observer presented in this chapter is based on the solution of the Riccati equation, which can be obtained using the Matlab

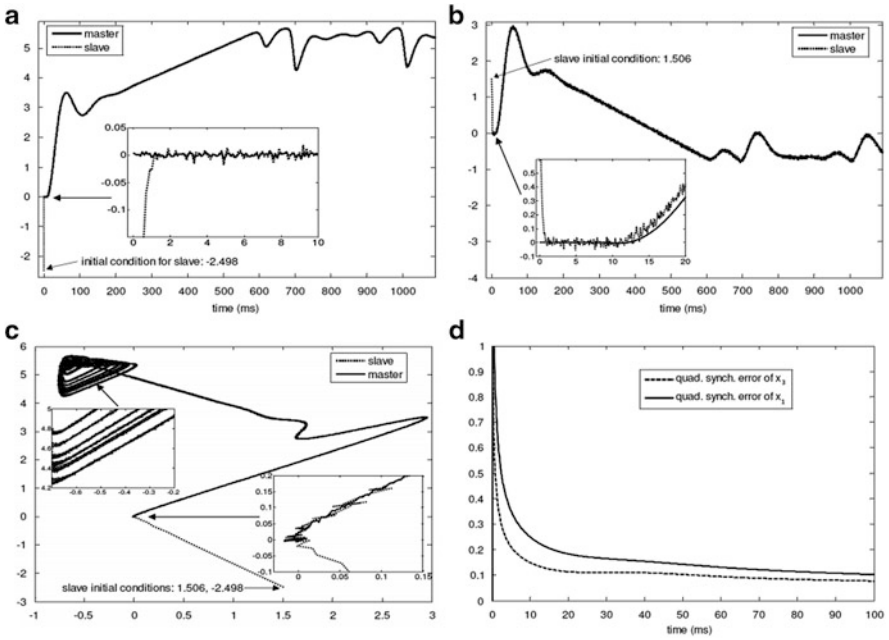

Fig. 4.5 Synchronization between Colpitts oscillator and its high-gain observer: (**a**) synchronization of coordinates x_1 and $\hat{x}_1$, (**b**) synchronization between x_3 and $\hat{x}_3$, (**c**) phase portrait of the master system (x_3 (*horizontal*) versus x_1 (*vertical*)) and the slave system ($\hat{x}_3$ versus $\hat{x}_1$), and (**d**) performance index

function ARE. The performance index of the corresponding synchronization process is calculated as [21]

$$J(t) = \frac{1}{t + 0.001} \int_0^1 \| e(t) \|_{Q_0}^2 \, d\tau \quad , Q_0 = I, \tag{4.44}$$

where $e(t)$ denotes the estimation error.

Figure 4.6a–c shows the convergence of the estimated states (slave system) to the real states (master system) without any noise in the system output. The initial conditions are $x_1 = -0.5$, $x_2 = 0.5$, $x_3 = 4$, $\hat{x}_1 = -4$, $\hat{x}_2 = 3$, $\hat{x}_3 = -4$.

Figure 4.7a, b shows the chaotic behavior of system (4.34) and the observer given by system (4.43). They also show the convergence of the state estimates to the real states, without any noise in the system output. Furthermore, in Fig. 4.8a–c is shown the effect of noise on the estimation process. A white noise is added in the measurement (around the current value of the measured output). We can see that the exponential polynomial observer is robust against noisy measurement. Finally, Fig. 4.9 illustrates the performance index for the corresponding estimation

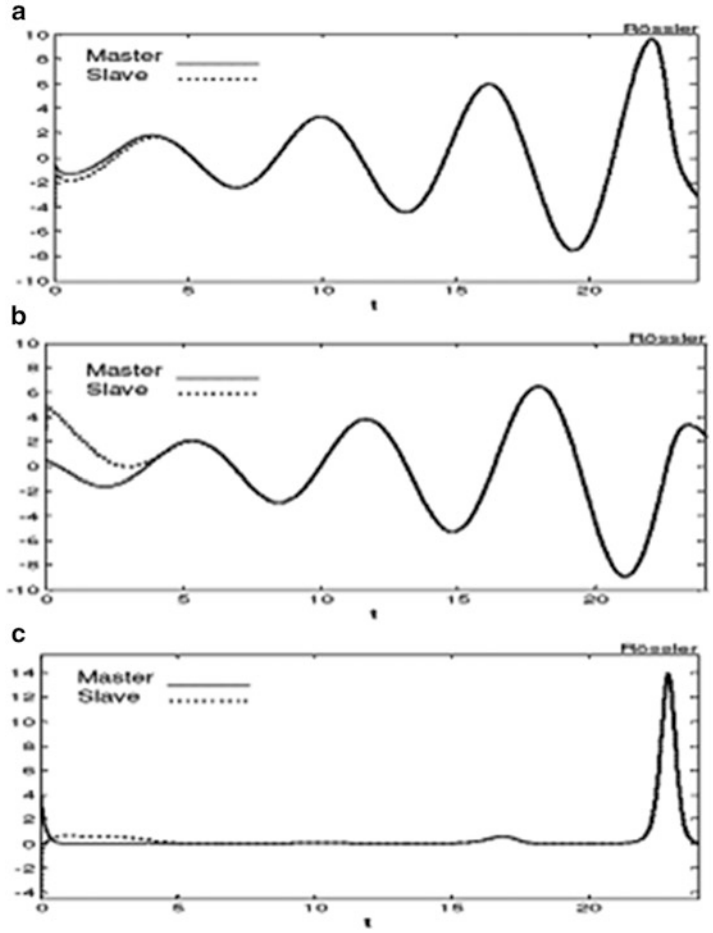

Fig. 4.6 Synchronization between drive system (4.34) and response system (4.43), without any noise in the system output, (**a**) signals x_1 and $\hat{x}_1$; (**b**) signals x_2 and $\hat{x}_2$; (**c**) signals x_3 and $\hat{x}_3$

processes. It should be noted that the quadratic estimation error (performance index) is bounded and has a tendency to decrease.

The corresponding high-gain observer is given by

$$\dot{\hat{x}}_1 = -(\hat{x}_2 + \hat{x}_3) - 3\theta(\hat{x}_1 - y),$$

$$\dot{\hat{x}}_2 = \hat{x}_2 + a\hat{x}_2 - \frac{1}{\hat{x}_1 - a}[3\theta(1 + \hat{x}_3) + 3\theta^2 a - \theta^3](\hat{x}_1 - y),$$

$$\dot{\hat{x}}_3 = b + \hat{x}_3(\hat{x}_1 - c) - \frac{1}{\hat{x}_1 - c - a}[-3\theta(1 + \hat{x}_3) + 3\theta^2 a - \theta^3](\hat{x}_1 - y.) \qquad (4.45)$$

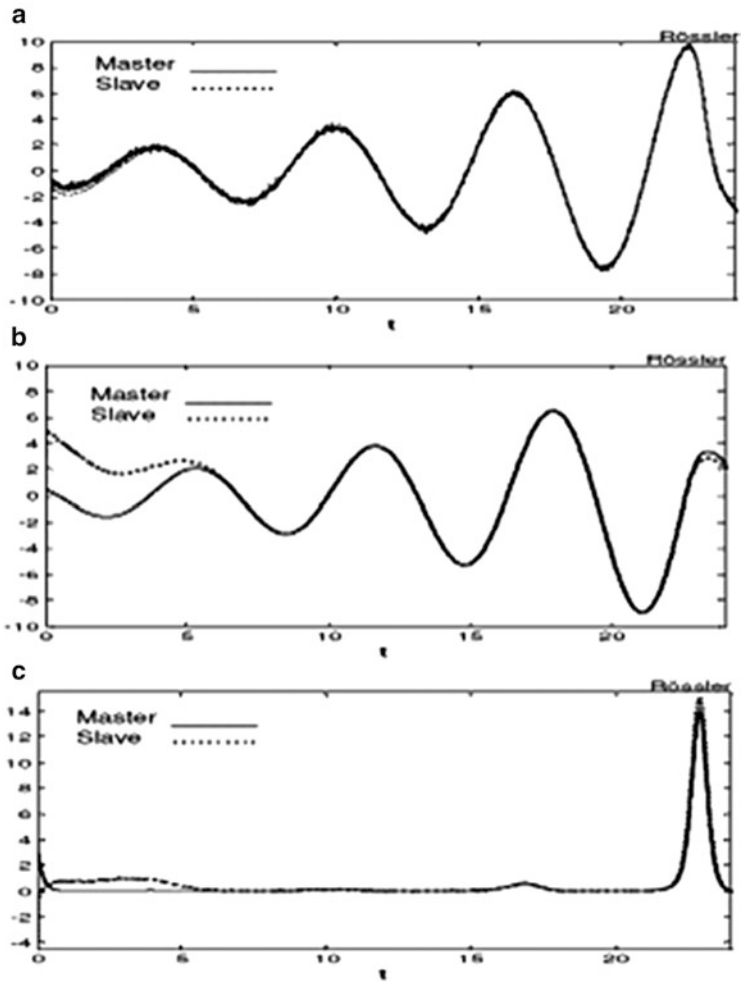

Fig. 4.7 Chaotic behaviour of drive system (4.34) and response system (4.43), with white noise in the system output ($\sigma = 0.1$), (**a**) signals x_1, x_3 and $\hat{x}_1$, $\hat{x}_3$; (**b**) signals x_1, x_2, x_3 and $\hat{x}_1$, $\hat{x}_2$, $\hat{x}_3$

We show a simulation for the Rössler system (4.35) and the observer given by systems (4.44) and (4.45), where we have taken for the parameter values $a = b = 0.2$, $c = 5$, $m = 3$, $K_1 = [k_{1,1}\ k_{2,1}\ k_{3,1}]^T = [5\ -5\ 5]^T$, $K_2 = [k_{1,2}\ k_{2,2}\ k_{3,2}]^T = [10\ 10\ 10]^T$, $\theta = 2$. All simulation results in this chapter were carried out with the help of Matlab 7.1 with Simulink 6.3 as the toolbox.

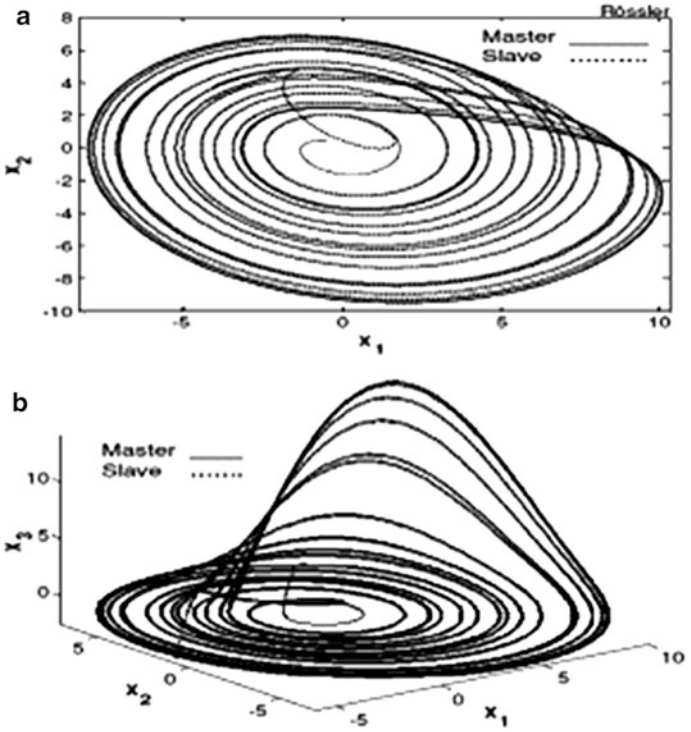

Fig. 4.8 Synchronization between drive system (4.34) and response system (4.43), without any noise in the system output, (**a**) signals x_1 and $\hat{x}_1$; (**b**) x_2 signals $\hat{x}_2$ and; (**c**) signals x_3 and $\hat{x}_3$

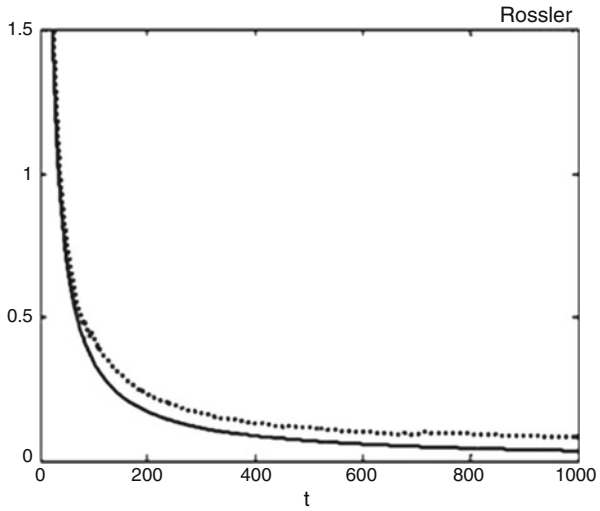

Fig. 4.9 Quadratic estimation error, (**a**) without any noise in the system output (*solid line*); (**b**) with white noise ($\sigma = 0.1$) in the system output (*dotted line*)

4.6.3 Rikitake Oscillator

A simple mechanical model used to study the reversals of the Earth's magnetic field, idealized by the Japanese geophysicist Rikitake [29], consists of two identical coupled single Faraday-disk dynamos of the Bullard type. The dynamics of this system is governed by the following three-dimensional system of nonlinear differential equations:

$$\begin{aligned} \dot{x}_1 &= -\mu x_1 + x_2 x_3, \\ \dot{x}_2 &= -\mu x_2 + (x_3 - a)x_1, \\ \dot{x}_3 &= 1 - x_2 x_1. \\ y &= x_1 \end{aligned} \tag{4.46}$$

Here a and μ are parameters, which we will assume to be nonnegative.

Remark 4.6 It is not hard to see that above system is Lipschitz.

Before proposing the exponential polynomial observer, we prove the algebraic observability condition for system (4.46) (see Chap. 1). Replacing $y = x_1$ in system (4.46), we obtain

$$\dot{y} = -\mu y + x_2 x_3, \tag{4.47}$$

$$\dot{x}_2 = -\mu x_2 + (x_3 - a)y, \tag{4.48}$$

$$\dot{x}_3 = 1 - x_2 y. \tag{4.49}$$

Taking the derivative with respect to time from (4.47), we have

$$\ddot{y} = -\mu \dot{y} + \dot{x}_2 x_3 + x_2 \dot{x}_3. \tag{4.50}$$

From (4.47), we get

$$x_3 = \frac{1}{x_2}\{\dot{y} + \mu y\}. \tag{4.51}$$

Substituting (4.48), (4.49) and (4.51) into (4.50), we obtain

$$\begin{aligned} 0 = x_2^4 - \frac{1}{y}x_2^3 + \left\{\frac{\ddot{y}}{y} + 2\mu\frac{\dot{y}}{y} + \mu^2\right\}x_2^2 \\ + a\{\dot{y} + \mu y\}x_2 - \{\dot{y} + \mu y\}^2 \end{aligned} \tag{4.52}$$

In the same manner for x_3, we have from (4.47)

$$x_2 = \frac{1}{x_3}\{\dot{y} + \mu y\} \tag{4.53}$$

substituting (4.48), (4.49) and (4.53) into (4.50)

$$0 = x_3^4 - ax_3^3 - \left\{ \frac{\ddot{y}}{y} + 2\mu\frac{\dot{y}}{y} + \mu^2 \right\} x_3^2 + \{\frac{\dot{y}}{y} + \mu\}x_3 - \{\dot{y} + \mu y\}^2 \tag{4.54}$$

Remark 4.7 From (4.52) and (4.54), x_2 and x_3 are algebraically observable.

Going back to the original coordinate system, we get the following system (slave system) for the observer

$$\begin{aligned} \dot{\hat{x}}_1 &= -\mu\hat{x}_1 + \hat{x}_2\hat{x}_3 + k_{1,1}(x_1 - \hat{x}_1) + k_{1,2}(x_1 - \hat{x}_1)^m \\ \dot{\hat{x}}_2 &= -\mu\hat{x}_2 + (\hat{x}_3 - a)\hat{x}_1 + k_{2,1}(x_1 - \hat{x}_1) + k_{2,2}(x_1 - \hat{x}_1)^m \\ \dot{\hat{x}}_3 &= 1 - \hat{x}_1\hat{x}_2 + k_{3,1}(x_1 - \hat{x}_1) + k_{3,2}(x_1 - \hat{x}_1)^m \end{aligned} \tag{4.55}$$

Now, some numerical results for Rikitake system (4.46) and its observer given by system (4.55) are presented. System (4.46) is chaotic with the set of parameter values $\mu = 1, a = 0.375$. We have chosen the parameter values for systems (4.46) and (4.55) as $\mu = 1, a = 0.375, m = 3, K_1 = [k_{1,1}, k_{2,1}, k_{3,1}]^T = [2 \quad 2 \quad 2]$, $K_2 = [k_{1,2} \quad k_{2,2} \quad k_{3,2}]^T = [3\ 3\ 3]^T$.

Figure 4.10a–c shows the convergence of the estimated states (slave system) to the real states (master system), without any noise in the system output. The initial conditions are $x_1 = -1, x_2 = 0.5, x_3 = 4, \hat{x}_1 = -4, \hat{x}_2 = -1, \hat{x}_3 = 2$.

Figure 4.11a–c shows the chaotic behaviour of the master system (4.46) and the slave system (4.55), and also show the convergence of the estimated states (slave system) to the real states (master system), without any noise in the system output.

In Fig. 4.12a–c, are shown the estimated states with the presence of noise in the system output (white noise with $\sigma = 0.1$, ± 10 around the current value of the system output). It should be noted that the proposed observer is robust against noisy measurements. In Fig. 4.13 is illustrated the performance index for the corresponding synchronization process without any noise in the system output and with noise in the system output (white noise with $\sigma = 0.1$, ± 10 around the current value of the system output). In both cases, the corresponding performance index has a tendency to decrease.

The high-gain observer for the system (4.46) is given by the next system

$$\begin{aligned} \dot{\hat{x}}_1 &= -\mu\hat{x}_1 + \hat{x}_2\hat{x}_3 - 3\theta(\hat{x}_1 - y) \\ \dot{\hat{x}}_2 &= -\mu\hat{x}_2 + (\hat{x}_3 - a)\hat{x}_1 \\ &\quad - \frac{1}{-2\hat{x}_1\hat{x}_3^2 + a\hat{x}_1\hat{x}_3 + \hat{x}_2 - 2\hat{x}_1\hat{x}_2^2}[3\theta z_1 + 3\theta^2 z_2 + \theta^3\hat{x}_2](\hat{x}_1 - y) \\ \dot{\hat{x}}_3 &= 1 - \hat{x}_2\hat{x}_1 + \frac{1}{-2\hat{x}_1\hat{x}_3^2 + a\hat{x}_1\hat{x}_3 + \hat{x}_2 - 2\hat{x}_1\hat{x}_2^2}[3\theta z_3 + 3\theta^2 z_4 + \theta^3\hat{x}_3](\hat{x}_1 - y) \end{aligned} \tag{4.56}$$

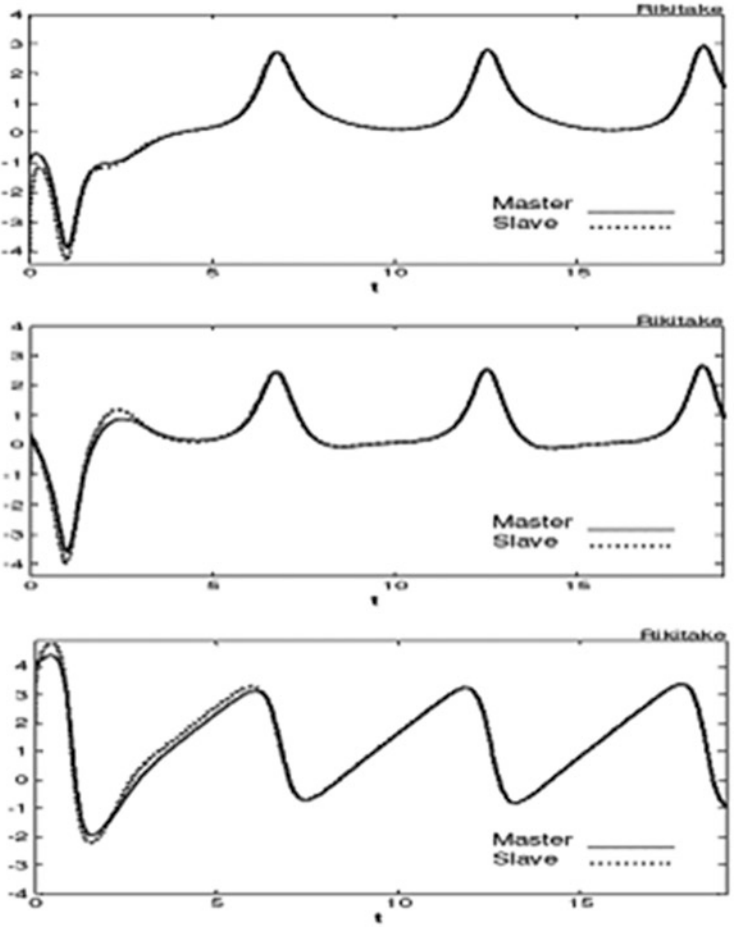

Fig. 4.10 Synchronization between drive system (4.46) and response system (4.55), without any noise in the system output, (**a**) signals x_1 and $\hat{x}_1$; (**b**) signals x_2 and $\hat{x}_2$; (**c**) signals x_3 and $\hat{x}_3$

where

$$
\begin{aligned}
z_1 &= \mu^2 \hat{x}_2 - 2\mu \hat{x}_1 \hat{x}_3 + a\mu \hat{x}_1 - \hat{x}_2 \hat{x}_3^2 + a\hat{x}_2 \hat{x}_3 + \hat{x}_2^3 \\
z_2 &= 2\mu \hat{x}_2 - 2\hat{x}_1 \hat{x}_3 + a\hat{x}_1 \\
z_3 &= \mu^2 \hat{x}_3 - \mu + 2\mu \hat{x}_1 \hat{x}_2 - \hat{x}_3^3 + a\hat{x}_3^2 + \hat{x}_2^2 \hat{x}_3 \\
z_4 &= 2\mu \hat{x}_3 - 1 + 2\hat{x}_1 \hat{x}_2
\end{aligned}
\tag{4.57}
$$

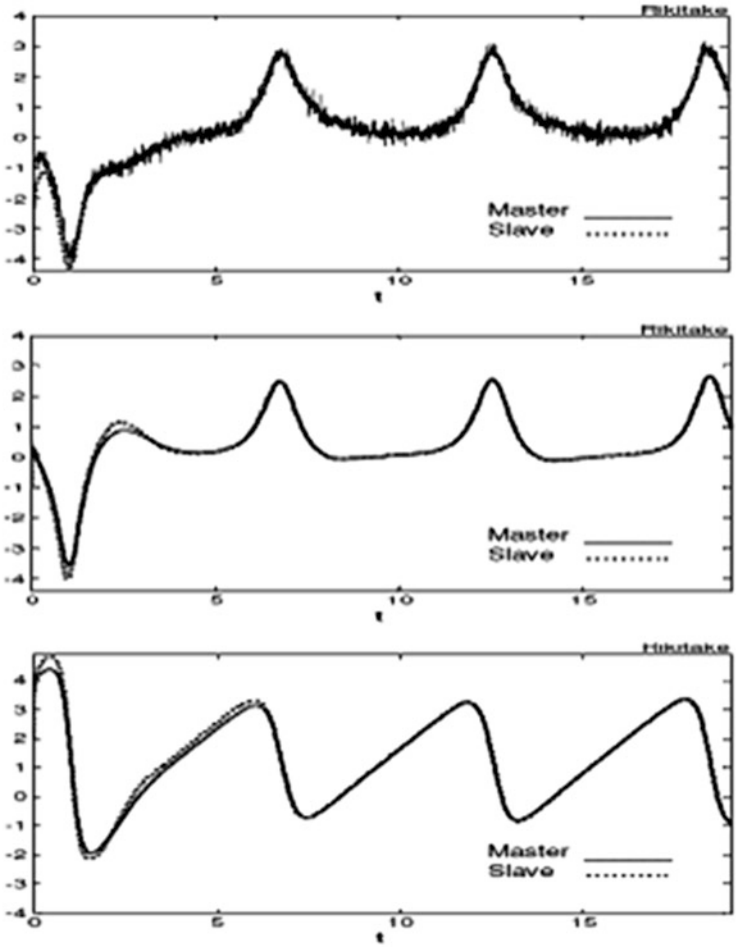

Fig. 4.11 Chaotic behaviour of drive system (4.46) and response system (4.55), with white noise in the system output ($\sigma = 0.1$), (**a**) signals x_1, x_3 and $\hat{x}_1$, $\hat{x}_3$; (**b**) signals x_2, x_3 and $\hat{x}_2$, $\hat{x}_3$; (**c**) signals x_1, x_2 and $\hat{x}_1$, $\hat{x}_2$

Now, some numerical results for Rikitake system (4.46) and its observer given by systems (4.57) are presented.

System (4.46) is chaotic with the set of parameter values $\mu = 1, a = 0.375$.

We have chosen the parameter values for systems (4.46), (4.67) as $\mu = 1$, $a = 0.375$, $m = 3$, $K_1 = [k_{1,1}\ k_{2,1}\ k_{3,1}]^T = [2\ 2\ 2]$, $K_2 = [k_{1,2}\ k_{2,2}\ k_{3,2}]^T = [3\ 3\ 3]$, $\theta = 2$. Figures 4.14a–c and 4.15a–c show the convergence of the estimated states (slave system) to the real states (master system), for different sets of initial conditions, without any noise in the system output.

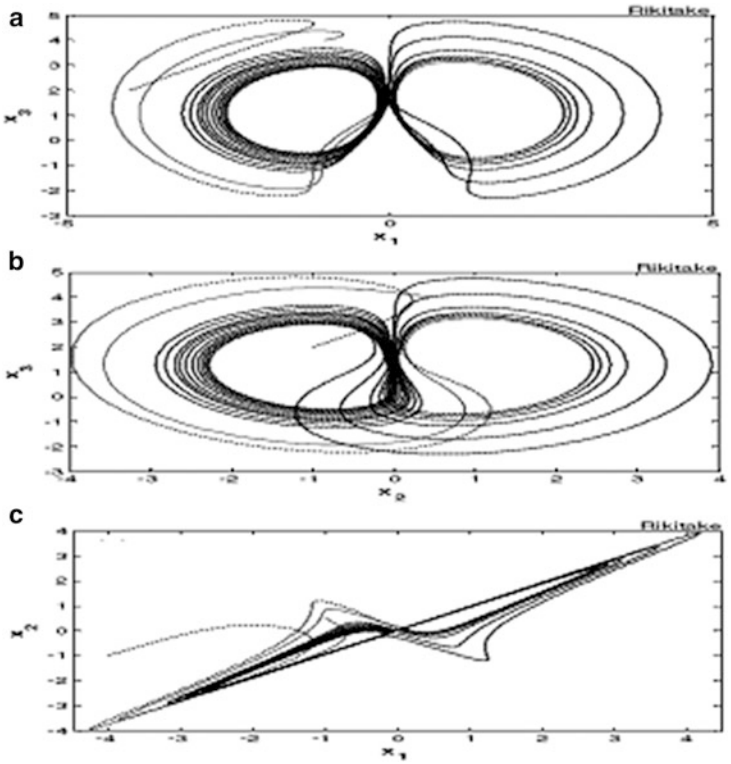

Fig. 4.12 Synchronization between drive system (4.46) and response system (4.55), with white noise in the system output ($\sigma = 0.1$) , (**a**) signals x_1 and $\hat{x}_1$; (**b**) signals x_2 and $\hat{x}_2$; (**c**) signals x_3 and $\hat{x}_3$

Figure 4.16a–c shows the chaotic behaviour of the master system (4.46) and the slave system (4.57), and also show the convergence of the estimated states (slave system) to the real states (master system), without any noise in the system output.

In Fig. 4.17a–c is shown the estimated states with the presence of noise in the system output (white noise with $\sigma = 0.1, \pm 10$ around the current value of the system output). It should be noted that the proposed observer is robust against noisy measurements.

In Fig. 4.18 is illustrated the performance index for the corresponding synchronization process without any noise in the system output and with noise in the system output (white noise with $\sigma = 0.1, \pm 10$ around the current value of the system output)

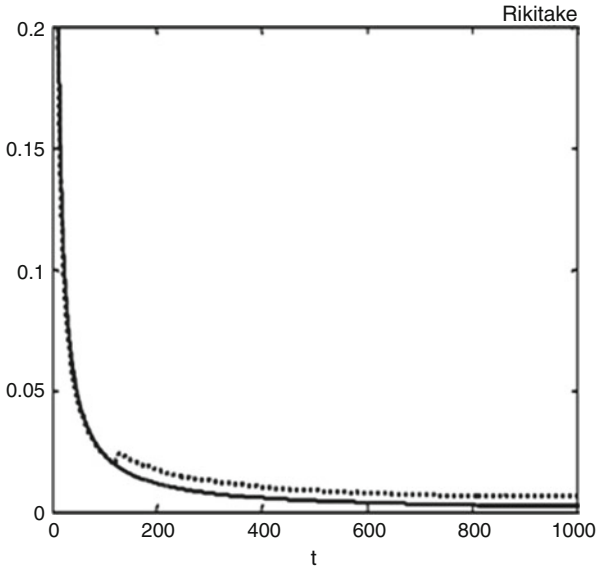

Fig. 4.13 Performance index, (**a**) without any noise in the system output (*solid line*); (**b**) with white noise ($\sigma = 0.1$) in the system output (*dotted line*)

Now, we consider the Lorenz chaotic system described by the following set of differential equations:

$$\begin{aligned} \dot{x}_1 &= \sigma(x_2 - x_1) \\ \dot{x}_2 &= \rho x_1 - x_2 - x_1 x_3 \\ \dot{x}_3 &= x_1 x_3 - \beta x_3 \\ y &= x_1 \end{aligned} \tag{4.58}$$

with positive parameters ($\sigma, \rho, \beta > 0$) the system (4.58) exhibits chaotic behaviour.

In the same form, we prove the algebraic observability condition for system (4.58). After algebraic manipulations we obtain:

$$\dot{y} + \sigma y + \sigma x_2 = 0 \tag{4.59}$$

$$-\ddot{y} + \dot{y}(\sigma + 1) + y\sigma(\rho + 1) + y\sigma x_3 = 0 \tag{4.60}$$

Remark 4.8 From (4.59) and (4.60), is clear that x_2 and x_3 satisfies the AOC (see Chap. 1), thus x_2 and x_3 are algebraically observable.

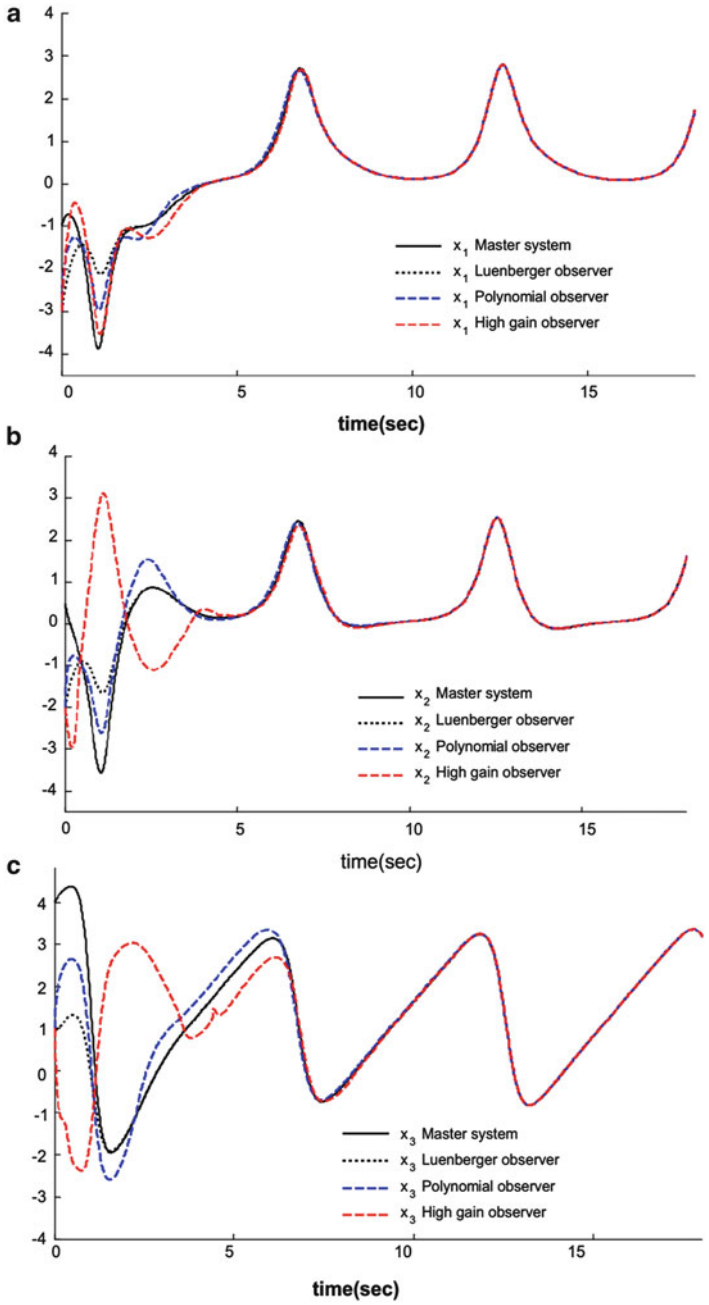

Fig. 4.14 Synchronization between master system (4.46) and its observers: exponential polynomial observer (4.56) and high-gain observer (4.57), without any noise in the system output: (**a**) signals x_1 and $\hat{x}_1$; (**b**) signals x_2 and $\hat{x}_2$; and (**c**) signals x_3 and $\hat{x}_3$. The initial conditions are $x_1 = -1$, $x_2 = 0.5$, $x_3 = 4$; $\hat{x}_1 = -3$; $\hat{x}_2 = -2$; $\hat{x}_3 = -1$

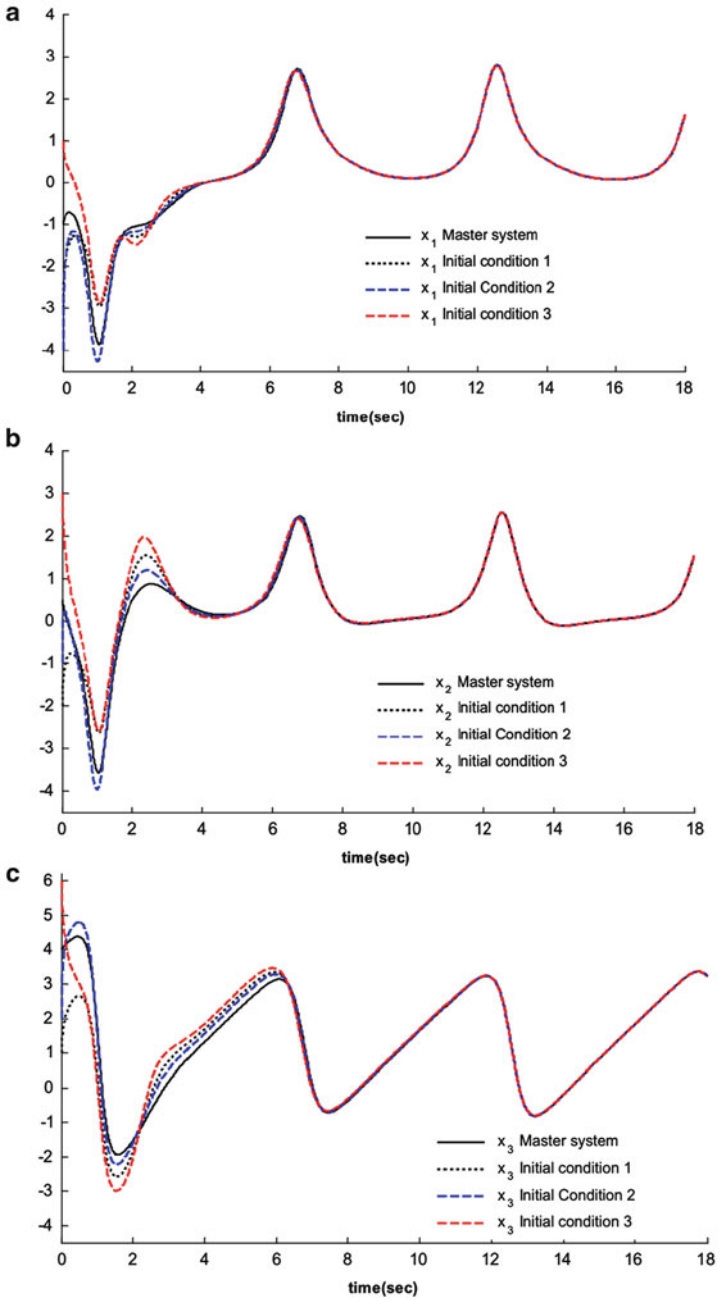

Fig. 4.15 Synchronization between master system (4.46) and the exponential polynomial observer (4.56), without any noise in the system output (**a**) signals x_1 and $\hat{x}_1$; (**b**) signals x_2 and $\hat{x}_2$; and (**c**) signals x_3 and $\hat{x}_3$. The initial conditions are $x_1 = -1$, $x_2 = 0.5$, $x_3 = 4$; initial condition 1: $\hat{x}_1 = -3$; $\hat{x}_2 = -2$; $\hat{x}_3 = 1$; initial condition 2: $\hat{x}_1 = -4$; $\hat{x}_2 = -1$; $\hat{x}_3 = 2$; and initial condition 3: $\hat{x}_1 = 1$; $\hat{x}_2 = 3$; $\hat{x}_3 = 6$

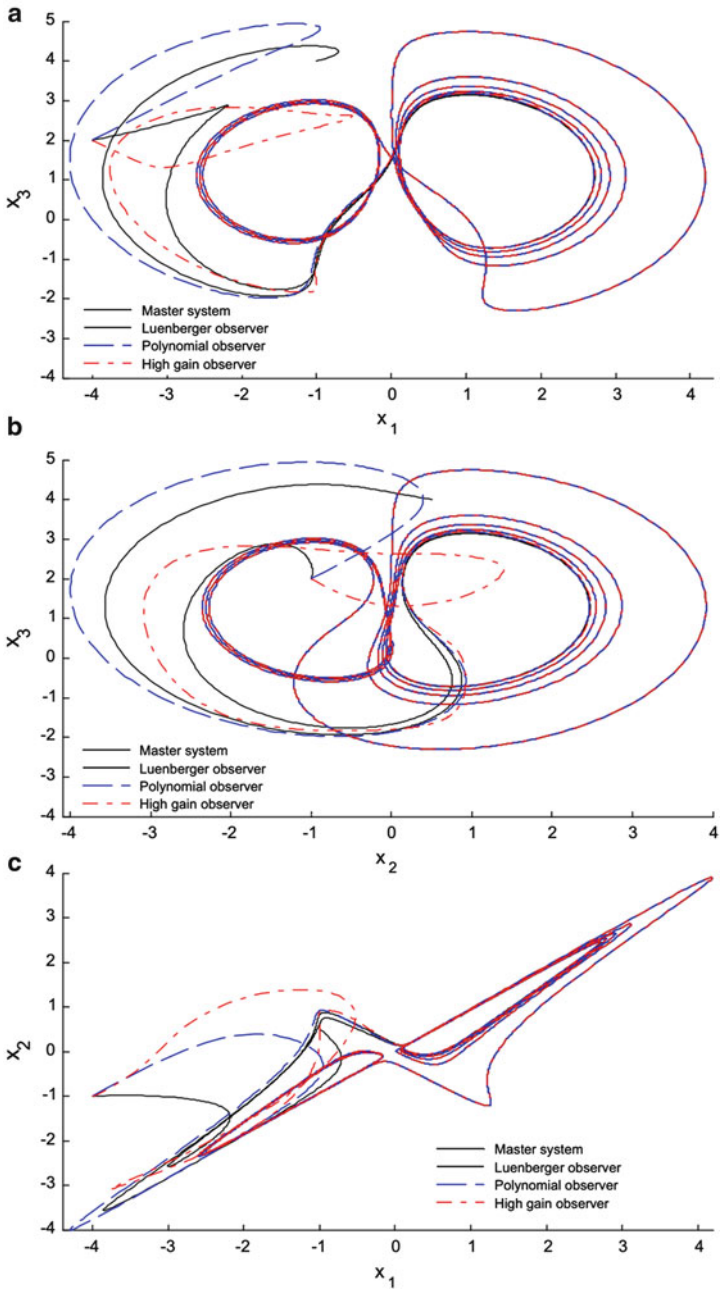

Fig. 4.16 Chaotic behavior of master system (4.46) and its observers: exponential polynomial observer (4.56) and high-gain observer (4.57), without any noise in the system output: (**a**) signals $x_1,\ x_3$ and $\hat{x}_1,\ \hat{x}_3$; (**b**) signals $x_2,\ x_3$ and $\hat{x}_2,\ \hat{x}_3$; and (**c**) signals $x_1,\ x_2$ and $\hat{x}_1,\ \hat{x}_2$. The initial conditions are $x_1 = -1,\ x_2 = 0.5,\ x_3 = 4,\ \hat{x}_1 = -4,\ \hat{x}_2 = -1,\ \hat{x}_3 = 2$

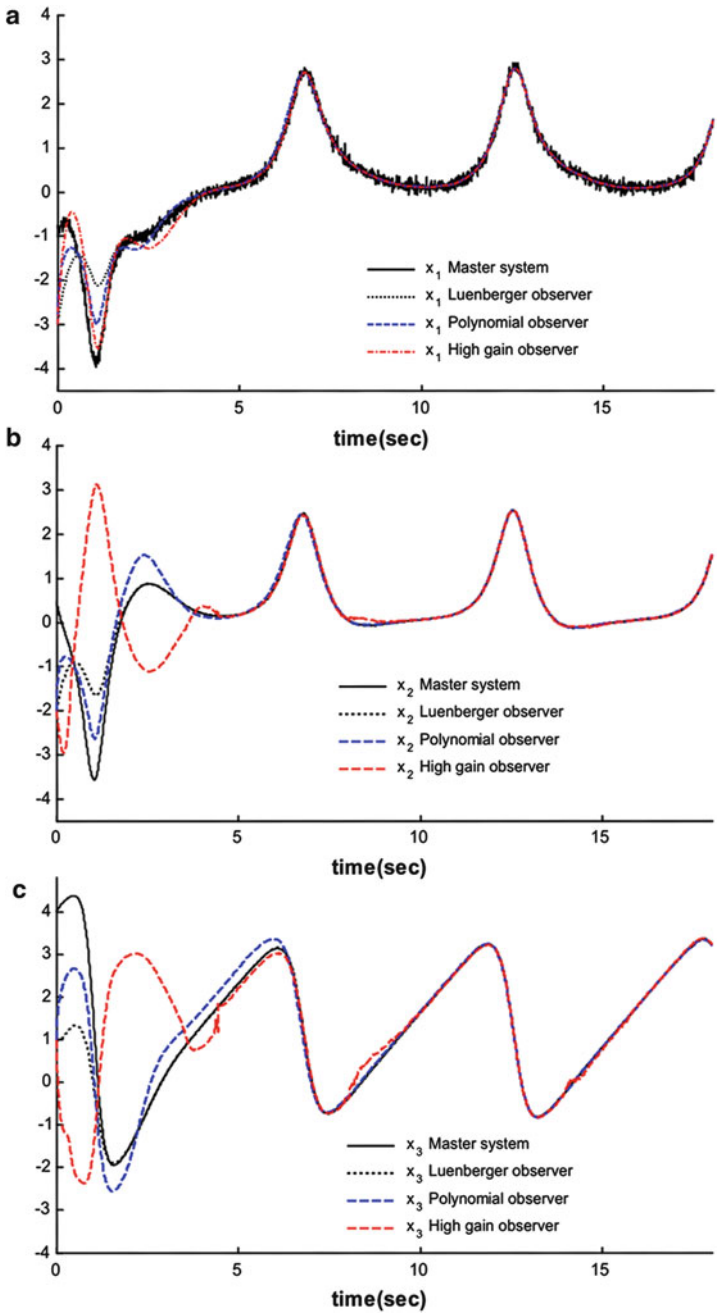

Fig. 4.17 Synchronization between master system (4.46) and its observers: exponential polynomial observer (4.56) and high-gain observer (4.57), with white noise in the system output ($\sigma = 0.1$): (**a**) signals x_1 and $\hat{x}_1$; (**b**) signals x_2 and $\hat{x}_2$; and (**c**) signals x_3 and $\hat{x}_3$. The initial conditions are $x_1 = -1$, $x_2 = 0.5$, $x_3 = 4$; $\hat{x}_1 = -3$; $\hat{x}_2 = -2$; $\hat{x}_3 = 1$

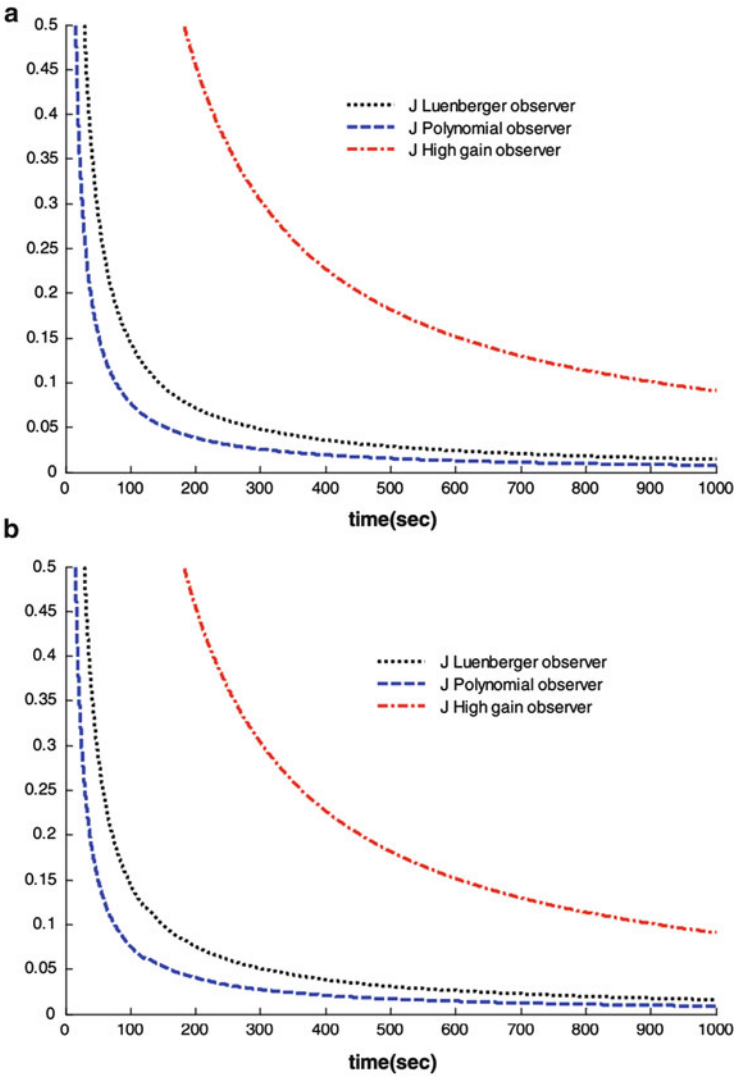

Fig. 4.18 Performance index: (**a**) without any noise in the system output; (**b**) with white noise in the system output ($\sigma = 0.1$). The intial conditions are $x_1 = -1,\ x_2 = 0.5,\ x_3 = 4,\ \hat{x}_1 = -3,\ \hat{x}_2 = -2,\ \hat{x}_3 = 1$

4.7 Bounded Error Observer Based Design of Synchronizing Chaotic Systems

In this section, we assume that the output system is measured exactly. Then we only reconstruct the remaining variables. We begin synchronizing the Rössler system via *bounded error observer*.

Consider the system (4.34) and make the change of variables

$$\begin{aligned} \hat{z}_2 &= \hat{x}_2 + ky \\ \hat{z}_3 &= \hat{x}_3 + ky \end{aligned} \tag{4.61}$$

where k is a fixed real constant. The dynamics of $\{\hat{z}_2, \hat{z}_3\}$ is given by

$$\dot{\hat{z}}_2 = -[k-a]\hat{z}_2 + \hat{\zeta}_2 \tag{4.62}$$

$$\dot{\hat{z}}_3 = -[c+k-y]\hat{z}_3 + \hat{\zeta}_3 \tag{4.63}$$

with $\hat{\zeta}_2 = y - k[ay + \hat{z}_3] + 2k^2 y$, $\hat{\zeta}_3 = b + k[-y^2 + cy - \hat{z}_2] + 2k^2 y$, $k \geq \max\{a, y-c\}$.

Corollary 4.2 *In accordance with Eqs. (4.62) and (4.63) the general differential equation is given by*

$$\dot{\hat{\xi}} = -h\hat{\xi} + \hat{\zeta} \tag{4.64}$$

which is uniformly bounded, with $h > 0$ *, if the following assumptions are considered:*

A1: $|\hat{\zeta} - \zeta| < N < \infty$

A2: For t_0 *sufficiently large,* $\lim_{t \to t_0} \sup \dfrac{N}{h} = 0$

Proof Let us define the estimation error (the difference between the actual observed signal and its estimate) as follows:

$$e := \hat{\xi} - \xi \tag{4.65}$$

applying the time derivative to (4.65), and taking $\Psi = \hat{\zeta} - \zeta$, we obtain

$$\dot{e} + he = \Psi \tag{4.66}$$

we obtain the solution from (4.65)

$$e = \exp(-ht)e_0 + \int_0^t \exp(h[\tau - t])\Psi d\,\tau \tag{4.67}$$

where e_0 is an initial condition.

Using Triangle and Cauchy–Schwarz inequalities from expression (4.63):

$$0 \leq |e| \leq |\exp(-ht)||e_0| + \int_0^t |\exp(h[\tau - t])\Psi d\,\tau| \tag{4.68}$$

from A1:

$$0 \leq |e| \leq |\exp(-ht)||e_0| + N\int_0^t |\exp(h[\tau - t])d\,\tau| \tag{4.69}$$

thus, as $t \to t_0$, t_0 sufficiently large

$$0 \leq \lim_{t\to t_0}\sup|e| \leq \lim_{t\to t_0}\sup N\int_0^t |\exp(h[\tau - t])d\,\tau| \tag{4.70}$$

$$0 \leq \lim_{t\to t_0}\sup|e| \leq \lim_{t\to t_0}\sup\frac{N}{h}|1 - \exp(-ht)| \tag{4.71}$$

$$0 \leq \lim_{t\to t_0}\sup|e| \leq \lim_{t\to t_0}\sup\frac{N}{h} \tag{4.72}$$

From A2 $\lim_{t\to t_0}|e| = 0$, for t_0 sufficiently large. □

Corollary 4.3 *The bounded error observer for Rössler system is given by*

$$\begin{aligned}
\dot{\hat{z}}_2 &= -[k - a]\hat{z}_2 + \hat{\zeta}_2 \\
\dot{\hat{z}}_3 &= -[c + k - y]\hat{z}_3 + \hat{\zeta}_3 \\
\hat{x}_1 &= y \\
\hat{x}_2 &= \hat{z}_2 - ky \\
\hat{x}_3 &= \hat{z}_3 - ky
\end{aligned}$$

with $\hat{\zeta}_2 = y - k[ay + \hat{z}_3] + 2k^2 y$, $\hat{\zeta}_3 = b + k[-y^2 + cy - \hat{z}_2] + 2k^2 y$, $k \geq \max\{a, y - c\}$. □

Now, the synchronization of Lorenz system via bounded error observer is given by the following corollary

Corollary 4.4 *In the same manner given above. The bounded error observer for Lorenz system (4.58) is as follows*

$$\begin{aligned}
\dot{\hat{z}}_2 &= -[1 - k\sigma]\hat{z}_2 + \hat{\eta}_2 \\
\dot{\hat{z}}_3 &= -\beta\hat{z}_3 + \hat{\eta}_3 \\
\hat{x}_1 &= y \\
\hat{x}_2 &= \hat{z}_2 - ky \\
\hat{x}_3 &= \hat{z}_3 - ky
\end{aligned}$$

with $\hat{\eta}_2 = \rho y - y\hat{z}_3 + ky[1 + y - \sigma] - k^2\sigma y$, $\hat{\eta}_3 = y\hat{z}_2 + k[-y^2 + \beta y + \sigma\hat{z}_2 - \sigma y] - k^2\sigma y$, $k \geq 1/\sigma$.

It is supposed that η_2, η_3 satisfies the assumption A1. □

Finally, the synchronization of Rikitake system via bounded error observer is given by the following corollary

Corollary 4.5 *In the same manner given above. The bounded error observer for Rikitake system (4.46) is as follows*

$$\begin{aligned}
\dot{\hat{z}}_2 &= -(\mu - k\hat{z}_3 + k^2 y)\hat{z}_2 + \hat{\theta}_2 \\
\dot{\hat{z}}_3 &= (k^2 y - k\hat{z}_2)\hat{z}_3 + \hat{\theta}_3 \\
\hat{x}_1 &= y \\
\hat{x}_2 &= \hat{z}_2 - ky \\
\hat{x}_3 &= \hat{z}_3 - ky
\end{aligned}$$

with $\hat{\theta}_2 = (\hat{z}_3 - a)y - ky^2 - k^2 y\hat{z}_2 + k^3 y^2$, $\hat{\theta}_3 = 1 - y\hat{z}_2 + k(y^2 - \mu y) - k^2 y\hat{z}_2 + k^3 y^2$. *Here the observer gain should satisfies the next relations,*

$$|k| \leq \frac{\max\{\hat{z}_2\}}{\max\{y\}}$$

and

$$k > \frac{-\text{sign}\{k\}\max\{\hat{z}_3\} \pm \sqrt{\max\{\hat{z}_3\} - 4\max\{y\}\mu}}{2\max\{y\}}$$

it is supposed that θ_2, θ_3 *satisfies the assumption A1.* □

4.8 Numerical Results

In order to verify the effectiveness of the proposed methodology, we show the convergence of the estimates to the current signals for the applications in Sect. 4.7.

We show some simulations for the Rössler's system. We have considered the following initial condition vector to the master system $x_{m0} = (0.5, -2.5, -4)$, and the initial conditions to the slave system (observer) $\hat{x}_2 = -2.5$, $\hat{x}_3 = -4$, the parameters of system are $a = b = 0.2$, $c = 5$ and observer gain is fixed as $k = 5$. Figure 4.19 shows the convergence of the state estimates (slave system) to the real states (master system).

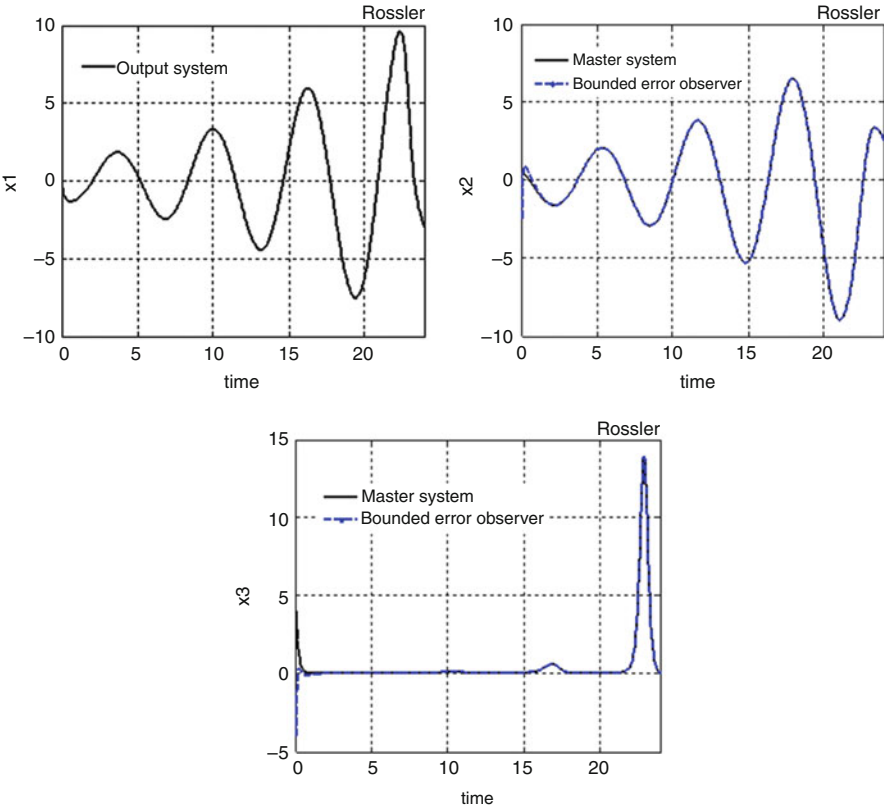

Fig. 4.19 Synchronization of Rössler system

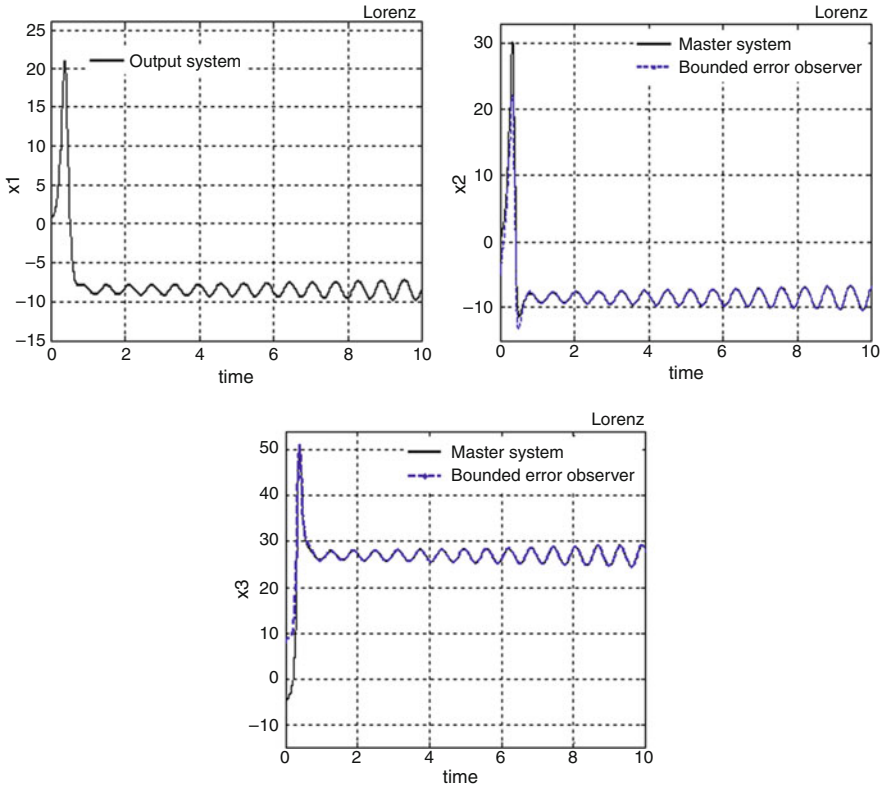

Fig. 4.20 Synchronization of Lorenz system

To simulate the Lorenz system the observer gain is fixed as $k = -1$. The initial condition vector to the master system is $x_{m0} = (1, 0, -5)$ and the initial conditions to the slave system (observer) $\hat{x}_2 = -5$, $\hat{x}_3 = 8$. Figure 4.20 shows the synchronization of Lorenz system.

Finally we have chosen the values for the Rikitake system and the observer as $\mu = 1$, $a = 0.375$, $k = -0.5$. Figure 4.21 shows the convergence of the state estimates (slave system) to the real states (master system). The initial condition vector is $x_{m0} = (-1, 0.5, 4)$ and the initial conditions for slave system are $\hat{x}_2 = -1$, $\hat{x}_3 = 2$.

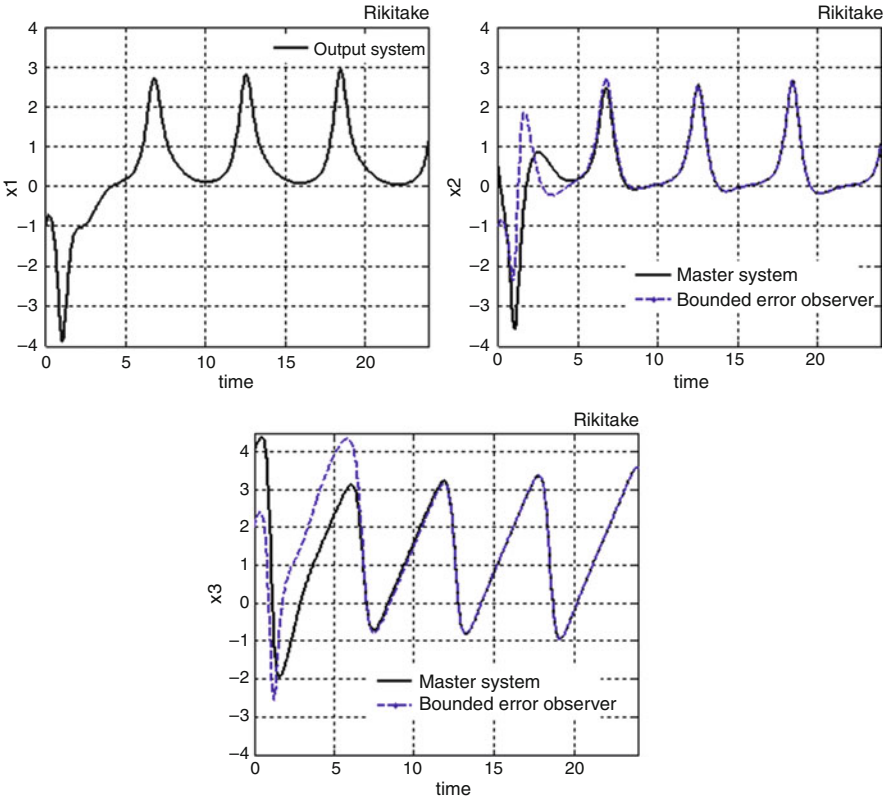

Fig. 4.21 Synchronization of Rikitake system

4.9 Conclusion

In this chapter we tackled the synchronization problem based upon observers theory. As well as, as main contributions, we show the real-time synchronization in the Colpitts oscillator by using two observer structures: an exponential polynomial observer and an asymptotic reduced-order observer, as well as, for comparison purposes we implemented a high gain observer and a bounded error observer. Some experimental results show the efectiveness of the proposed methodologies.

References

1. M. Chen, D. Zhou, Y. Shang, A sliding mode observer based secure communication scheme. Chaos Solitons Fractals **25**, 573–578 (2005)
2. E. Cherrier, M. Boutayeb, J. Ragot, Observers-based synchronization and input recovery for a class of nonlinear chaotic models. IEEE Trans. Circuits Syst. Regul. Pap. **53**(9), 1977–1988 (2006)

3. E. Elabbasy, H. Agiza, M. El-Dessoky, Global chaos synchronization for four scroll attractor by nonlinear control. Sci. Res. Essay **1**, 65–71 (2006)
4. A. Emadzadeh, M. Haeri, Global synchronization of two different chaotic systems via nonlinear control, in *Proceedings of ICCAS*, Gyeonggi-Do (2005)
5. M. Feki, Sliding mode control and synchronization of chaotic systems with parametrics uncertainties. Chaos Solitons Fractals A **41**, 1390–1400 (2009)
6. H.B. Fotsin, J. Daafouz, Adaptive synchronization of uncertain chaotic Colpitts oscillator based on parameter identification. Phys. Lett. A **339**, 304–315 (2005)
7. A.L. Fradkov, *Cybernetical Physics: From Control of Chaos to Quantum Control* (Springer, Berlin, 2007), p. 213
8. A.L. Fradkov, B. Andrievsky, R.J. Evans, Adaptive observer-based synchronization of chaotic system with first-order coder in the presence of information constraints. IEEE Trans. Circuit Syst. I Regul. Pap. **55**(6), 1685–1694 (2008)
9. S. Garfinkel, G. Spafford, *Practical Unix and Internet Security* (O' Reilly and Associates, Sebastopol, CA, 1996)
10. J. Gauthier, H. Hammouri, S. Othman, A simple observer for nonlinear systems. Applications to bioreactors. IEEE Trans. Autom. Control **37**, 875–880 (1992)
11. D. Ghosh, S. Banerjee, A. Chowdhury, Synchronization between variable time-delayed systems and cryptography. Europhys. Lett. **80**, 1–6 (2007)
12. D. Ghosh, A. Chowdhury, P. Saha, On the various kinds of synchronization in delayed duffing-van der pol system. Commun. Nonlinear Sci. Numer. Simul. **13**, 790–803 (2008)
13. L. Guo-Hui, Synchronization and anti-synchronization of Colpitts oscillators using active control. Chaos Solitons Fractals **26**, 87–93 (2005)
14. A. Harb, W. Ahmad, Chaotic systems synchronization in secure communication systems, in *Proceedings of World Congress Computer Science Computer Engineering, and Applied Computing*, Las Vegas (2006)
15. C. Hua, X. Guan, Synchronization of chaotic systems based on PI observer design. Phys. Lett. A **334**, 382–389 (2005)
16. R.E. Kalman, A new approach to linear filtering and prediction problems. Trans. ASME - J. Basic Eng. Ser. D **82**, 35–45 (1960)
17. M.P. Kennedy, Chaos in Colpitts oscillator. IEEE Trans. Circuits Syst. I **41**, 771–774 (1994)
18. D. Li, J. Lu, X. Wu, Linearly coupled synchronization of the unified chaotic systems and the lorenz systems. Chaos Solitons Fractals **23**, 79–85 (2005)
19. D. Luenberger, An introduction to observers. IEEE Trans. Autom. Control **16**, 596–602 (1971)
20. G.M. Maggio, O. De Feo, M.P. Kennedy, Nonlinear analysis of the Colpitts oscillator and applications to design. IEEE Trans. Circuits Syst. I **46**, 1118–1130 (1999)
21. R. Martinez-Guerra, J.L. Mata-Machuca, *Fault Detection and Diagnosis in Nonlinear Systems: A Differential and Algebraic Viewpoint Understanding Complex Systems* (Springer, New York, 2014)
22. L. Min, J. Jing, A new theorem to synchronization of unified chaotic systems via adaptive control. Chaos Solitons Fractals **24**, 1363–1371 (2004)
23. H. Nijmeijer, I.M.Y. Mareels, An observer looks at synchronization. IEEE Trans. Circuits Syst. I Fundam. Theory Appl. **44**, 882–890 (1997)
24. N. Noroozi, M. Roopaei, P. Karimaghaee, Adaptive control and synchronization in a class of partially unknown chaotic systems. Chaos **19**, 023121-1–023121-10 (2009)
25. R. Núñez Pérez, Measurement of Chua chaos and its applications. J. Appl. Res. Technol. **6**(1), 45–53 (2009)
26. L. Pecora, T. Carrol, Synchronization in chaotic systems. Phys. Rev. Lett. **64**, 821–824 (1990)
27. A. Poznyak, *Advanced Mathematical Tools for Automatic Control Engineers: Deterministic Techniques*, vol. 1 (Elsevier, Amsterdam, 2008), pp. 77–212
28. S. Raghavan, J. Hedrick, Observer design for a class of nonlinear systems. Int J. Control **59**, 515–528 (1994)
29. T. Rikitake, Oscillations of a system of disk dynamos. Proc. Camb. Philos. Soc. **54**, 89–105 (1958)

30. O. Rössler, An equation for continuous chaos. Phys. Lett. **57A**, 397–398 (1976)
31. H. Serrano-Guerrero, C. Cruz-Hernández, R.M. López-Gutiérrez, L. Cardoza-Avenda no, R.A. Chávez-Pérez, Chaotic synchronization in nearest-neighbor coupled networks of 3D CNNs. J. Appl. Res. Technol. **11**(1), 26–41 (2013)
32. R.J. Wai, Y.W. Lin, H.C. Yang, Experimental verification of total sliding-mode control Chua's chaotic circuit. IET Circuits Devices Syst. **5**, 451–461 (2011)
33. C. Wang, S. Ge, Adaptive backstepping control of uncertain lorenz system. Int. J. Bifurcat. Chaos **11**, 1115–1119 (2001)
34. F. Wang, C. Liu, A new criterion for chaos and hyperchaos synchronization using linear feedback control. Phys. Lett. A **360**, 274–278 (2006)
35. F. Zhu, Observer-based synchronization of uncertain chaotic systems and its application to secure communications. Chaos Solitons Fractals **40**(5), 2384–2391 (2009)

Chapter 5
Synchronization of an Uncertain Rikitake System with Parametric Estimation

Abstract In this chapter, we deal with the synchronization and parameter estimations of an uncertain Rikitake system. The strategy consists in proposing a slave system that has to follow asymptotically the unknown Rikitake system, referred to as the master system. The gains of the slave system are adjusted continually according to a convenient adaptation control law until the measurable output errors converge to zero. The convergence analysis is carried out using Barbalat's lemma.

5.1 Introduction

The goal is to synchronize the complete response of the slave system to the master system by driving the slave with a signal derived from the master. The problem can now be easily tackled when the parameters of the master system are known. Most of the methods require complete knowledge of the system's parameters [1–4]. However, to achieve synchronization between two chaotic systems is far from being straightforward. In fact, there are few publications on this challenging problem, because it consists in both identification of the unknown parameters and the design of a controller to achieve synchronization. In [5], an observer was applied to identify the unknown parameter of the Lorenz system. In [6], the authors studied the same problem for Chen's chaotic system with the same method. The interest in parameter identification rests in its potential applications in communications, essentially when parameter modulation is used for message transmission, since a certain number of drawbacks have been revealed in the practical implementation of most chaos-based secure communications algorithms. In particular, one of the basic issues of interest is the effect of uncertainty and parameter mismatch on the stability of the process of synchronization of chaotic oscillators.

In this chapter, an adaptation asymptotic method for the synchronization and identification of the Rikitake system with several unknown parameters is presented. This system resembles the reversal of polarity of the Earth's electromagnetic field, and it is well known that it has chaotic behavior for some set of initial conditions and

R. Martínez-Guerra et al., *Synchronization of Integral and Fractional Order Chaotic Systems*, Understanding Complex Systems,
DOI 10.1007/978-3-319-15284-4_5

some set of parameter values. By this method, we can achieve chaos synchronization and identify the unknown parameters simultaneously. Roughly speaking, the suggested approach consists in designing a controlled slave system whose controllers and adaptive parameters are adjusted according to a proposed adaptive algorithm. It is done in such a way that the synchronization errors between the outputs of both systems, the uncertain Rikitake and the slave, converge asymptotically to zero. The synchronization in this chapter is seen as a control problem consisting in the design of a controller for the receiver using the transmitted signal derived from the master to ensure that the controlled receiver synchronizes with the transmitter. Hence, the requirement for synchronized behavior is that given the transmitted signal, the slave be forced to follow the master system. Numerical results show the synchronization error (difference between master and slave states). This can help in analyzing the behavior of the synchronization procedure. The convergence analysis of the proposed scheme is carried out using the Lyapunov method in conjunction with the Barbalat's lemma. It is important to emphasize that the robustness of our control strategy allows us to detect effectively piecewise constant variations on the parameter values of the uncertain Rikitake system.

The remainder of this chapter is organized as follows. In Sect. 5.2, we introduce the problem statement. In Sect. 5.3, we develop our solution to synchronize and identify the constant unknown parameters of the Rikitake system by means of the Lyapunov method. To assess the effectiveness of our method, we present some numerical simulations in Sect. 5.4. Finally, we present our conclusions in Sect. 5.5.

5.2 Problem Statement

5.2.1 Rikitake Model System

Previously, in Chap. 4, the Rikitake system [7] was synchronized by means of observers, and we assumed complete knowledge of parameters. Now we will work with the same system with μ and a now considered unknown:

$$\begin{aligned} \dot{x}_1 &= -\mu x_1 + z_1 y_1, \\ \dot{y}_1 &= -\mu y_1 + (z_1 - a) x_1, \\ \dot{z}_1 &= 1 - x_1 y_1, \end{aligned} \tag{5.1}$$

where the parameters μ and a have some physical meaning when they are positive. For a physical meaning of the states x_1, y_1, and z_1 we recommend that the reader consult [7]. However, the states x_1 and y_1 are directly related to the currents through each disk of the dynamo system, and z_1 is related to the angular velocity of one of the disks. This system exhibits chaotic behavior for the parameter values in a neighborhood $\{\mu = 5, a = 2\}$ and for a large enough set of initial conditions.

5.2.2 Some Algebraic Properties and Problem Formulation

In this section, we present some algebraic properties that the Rikitake system satisfies. To this end, we introduce the following definitions.

Definition 5.1 Consider a smooth nonlinear system described by a state vector $X = \{x_i\}_{i=1}^n \in \mathbb{R}^n$ and by the output vector $G = \{g_i\}_{i=1}^m \in \mathbb{R}^m$ of the form

$$\dot{X} = f(X, P), G = h(X), \tag{5.2}$$

where $h(\cdot)$ is a smooth vector function and $P \in \mathbb{R}^l$ is a constant parameter vector, with $l < n$. Let $G^{(j)}$ denote the jth time derivative of the vector G. We say that the vector state X is algebraically observable if it can be uniquely expressed as

$$X = \Phi(G, G^{(1)}, \ldots, G^{(j)})$$

for some integer j and for some smooth function Φ.

Definition 5.2 Under the same conditions as in Definition 5.1, if the vector of parameters P satisfies the relation

$$\Omega_1(G, \ldots, G^{(j)}) = \Omega_2(Y, \ldots, Y^{(j)})P, \tag{5.3}$$

where $\Omega_1(\cdot)$ and $\Omega_2(\cdot)$ are respectively $n \times 1$ and $n \times n$ smooth matrices, then P is said to be algebraically linearly identifiable with respect to the output vector G [8].

According to the previous definitions, it is evident that system (5.1) is algebraically observable with respect to the outputs $g_1 = x_1$ and $g_2 = y_1$, since the state z_1 can be rewritten as

$$z_1 = \frac{\dot{g}_2 + \mu g_2}{g_1} + a. \tag{5.4}$$

Hence the Rikitake system is algebraically observable with respect to the selected outputs $g_1 = x_1$ and $g_2 = y_1$. Moreover, substituting the above expression into the first differential equation of (5.1), we have

$$\begin{aligned} \dot{g}_1 g_1 - \dot{g}_2 g_2 = -\mu(g_1^2 + g_2^2) + a g_1 g_2 = \\ = [-(g_1^2 + g_2^2) + g_1 g_2]p. \end{aligned} \tag{5.5}$$

Therefore, we conclude that system (5.1) with vector of parameters $p = (\mu, a)$ is algebraically identifiable with respect to the available outputs. That is, the unavailable state z_1 and the vector of parameters p can be simultaneously recovered from the knowledge of the outputs $g_1 = x_1$ and $g_2 = y_1$.

From the above definitions, it is possible to solve the synchronization problem of the uncertain Rikitake system, provided that the states x_1 and y_1 are always available. Moreover, it is also possible to recover the unknown parameters μ and a. Thus, we are ready to establish the main control problem of this chapter.

Lemma 5.1 *Consider the uncertain Rikitake system (5.1), referred to as the master system, with the available output states x_1 and y_1. Let us propose the following slave-controlled system:*

$$\begin{aligned} \dot{x}_2 &= -\hat{\mu} x_1 + z_2 y_1 - u_1, \\ \dot{y}_2 &= -\hat{\mu} y_2 + (z_2 - \hat{a}) x_1 - u_2, \\ \dot{z}_3 &= 1 - x_1 y_1 - u_3. \end{aligned} \tag{5.6}$$

Then the control objective is to find $u = (u_1, u_2, u_3)$ and $\hat{p} = (\hat{\mu}, \hat{a})$ such that the slave system (5.6) follows the unknown Rikitake system (5.1); with $\hat{p}$ converging to the actual values of (μ, a). In other words, we need to find u and $\hat{p}$ of system (5.6) such that $(w_1, \hat{p}) \to (w_2, p)$, as long as $t \to \infty$.[1] □

The proof is given in next section.

We finish this section by introducing the following errors:

$$e_x = x_1 - x_2;\ e_y = y_1 - y_2;\ e_z = z_1 - z_2;\ \tilde{\mu} = \mu - \hat{\mu};\ \tilde{a} = a - \hat{a}.$$

According to them, we define the following vectors:

$$e^T = (e_x, e_y, e_z)\ ;\ \tilde{p}^T = (\tilde{\mu}, \tilde{a}).$$

5.3 Lyapunov-Based Formulation

In this section we solve the synchronization and parameter identification of the constant unknown parameters of the Rikitake system by means of the Lyapunov method. To this end, we first calculate the dynamics of the synchronization errors between the master and the slave systems. Next, based on a simple quadratic Lyapunov function, we propose the needed controller and the needed estimator that ensure the synchronization of both systems.

[1] Here we denote the vector states related to the master and slave systems by w_1 and w_2, respectively. That is, $w_i^T = (x_i, y_i, z_i)$; for $i = \{1, 2\}$.

Before solving the control problem, we introduce the following assumptions related to the selected outputs of the master system:

(A1) The states $x = x_1$ and $y = y_1$ are available for measurement.
(A2) All the states of the master system are bounded, with the generic property that the steady solution x and y, continues oscillating around zero.

Remark 5.1 Assumption A2 is true because in most cases, all the states of the Rikitake system are bounded for a large set of initial conditions and for a large set of positive parameters μ and a. In fact, assumption A2 depends on the set of initial conditions and the values of the parameter vector q. To clarify the meaning of this property, we present a case in which assumption A2 does not hold. Selecting the parameter values as $\{\mu > 0; a > 0\}$, and the initial condition as $w_1(0) = (x_1(0) = 0, x_1(0) = 0, z_1(0) = \bar{z})$, we have that $x_1(t) = 0$, $y_1(t) = 0$, and $z_1(t) = t + \bar{z}$. Evidently, assumption A2 cannot be fulfilled, because the states x and y remain fixed at the origin, and the state z_1 is unbounded [9]. In fact, no identification method or scheme can be proposed if the master system has solutions that tend either to infinity or to a constant.

Remark 5.2 In this chapter, as a fundamental assumption, we suppose that all states of the master system are bounded with the property that the steady states x and y continue oscillating around zero, i.e., these steady solutions should not be fixed at zero. In this manner, the results are not affected when any additional terms are included. For bounded perturbations, if the trajectories remain or belong to the same manifold or an equivalent space state region of the unperturbed system, all the assumptions considered are adequate.

Proof of Lemma 5.1. From (5.1) and (5.6), we have

$$\dot{e} = \begin{bmatrix} \dot{e}_x \\ \dot{e}_y \\ \dot{e}_z \end{bmatrix} = \begin{bmatrix} -\tilde{\mu}x + e_z y + u_1 \\ -\tilde{\mu}y + (e_z - \tilde{a})x + u_2 \\ u_3 \end{bmatrix}. \tag{5.7}$$

For the sake of simplicity, we write $y = y_1$ and $x = x_1$. As we can see, the above system can be considered a control problem, where the vector inputs u and $\tilde{p}$ must be proposed such that the state e asymptotically converges to zero.

Consider a Lyapunov function

$$V = \frac{1}{2}e^T e + \frac{1}{2}\tilde{p}^T \tilde{p}. \tag{5.8}$$

The time derivative of V along the trajectories of (5.7) is then given by

$$\begin{aligned} \dot{V} = -\tilde{\mu}\dot{\hat{\mu}} - \tilde{a}\dot{\hat{a}} - \tilde{\mu}e_x^2 + e_x e_z y + e_x u_1 - \tilde{\mu} y e_y \\ + e_z x e_y - \tilde{a} x e_y + u_2 e_y + e_z u_3. \end{aligned} \tag{5.9}$$

In order to make V negative semidefinite, we propose $\dot{\hat{p}}$ and u as follows:

$$\dot{\hat{p}} = \begin{bmatrix} \dot{\hat{\mu}} \\ \dot{\hat{a}} \end{bmatrix} = \begin{bmatrix} -e_x x - e_y y \\ -x e_y \end{bmatrix} \tag{5.10}$$

and u, as

$$u = \begin{bmatrix} u_1 \\ u_2 \\ u_3 \end{bmatrix} = \begin{bmatrix} -k_1 e_x - k_{11} e_x^k \\ -k_2 e_y - k_{21} e_y^k \\ -e_y x \end{bmatrix}, \tag{5.11}$$

where k_1, k_2, k_{11}, and k_{21} are strictly positive constants and k is any odd integer.

Substituting expressions (5.11) into (5.7), we have that the closed-loop system can be read as

$$\begin{aligned} \dot{e}_x &= -\tilde{\mu} x + e_z y - k_1 e_x - k_{11} e_x^{2k+1} \\ \dot{e}_y &= -\tilde{\mu} y + (e_z - \tilde{a}) x - k_2 e_y - k_{21} e_y^{2k+1} \\ \dot{e}_z &= -e_x y, \end{aligned} \tag{5.12}$$

where the parameter dynamics are given by

$$\dot{\hat{\mu}} = -e_x x - y e_y \; ; \; \dot{\hat{a}} = -x e_y. \tag{5.13}$$

Substituting (5.12) and (5.13) into (5.9), we obtain

$$\dot{V} = -\left(k_1 e_x^2 + k_2 e_y^2 + k_{11} e_x^{k+1} + k_{22} e_y^{k+1} \right). \tag{5.14}$$

This implies that $\dot{V}$ is negative semidefinite, and so V converges. Hence the sets of signals $e_x, e_y, e_z, \tilde{\mu}, \tilde{a}$ are bounded. Let us proceed to show that $\mathbf{e}$ converges to zero as long as $t \to \infty$, by applying Barbalat's lemma [10].[2] Integrating both sides of (5.14), we obtain

$$\int_0^t \left(k_1 e_x^2(s) + k_2 e_y^2(s) + k_{11} e_x^{k+1}(s) + k_{22} e_y^{k+1}(s) \right) ds \leq V(0). \tag{5.15}$$

From the equations of (5.12) and A2, it follows that $\dot{e}$ is bounded, which implies that e is uniformly continuous. Using Barbalat's lemma, it follows that vector states e converge to as $t \to \infty$. Once again, differentiating (5.12), it is easily shown that $\ddot{\mathbf{e}}$ is bounded. Thus, $\dot{\mathbf{e}}$ is uniformly continuous, and also $\mathbf{e}$ has a finite limit as $t \to \infty$.

[2] Barbalat's lemma states that if the differential function $f(t)$ has a finite limit as $t \to \infty$, and if df/dt is uniformly continuous, then $df/dt \to 0$ as $t \to \infty$. A consequence of this lemma is that if $f \in L_2$ and df/dt is bounded, then $f \to 0$ as $t \to \infty$.

From Barbalat's lemma, we conclude that $\dot{\mathbf{e}} \to 0$ as $t \to \infty$. Since V converges as $t \to \infty$, we have that the two parameter errors $\tilde{\mu}$ and $\tilde{a}$ converge as $t \to \infty$. Besides, from (5.13), it follows that $\dot{\hat{\mu}}$ and $\dot{\hat{a}}$ converge to zero as $t \to \infty$. Roughly speaking, when t is large enough, $\hat{\mu}$ and $\hat{a}$ are almost constant, and the differential equations of (5.12) imply that

$$\begin{aligned} 0 &= (\mu - \hat{\mu})x, \\ 0 &= (a - \hat{a})y. \end{aligned} \tag{5.16}$$

However, once again from assumption A2, we have that the steady states x and y remain oscillating around zero. Therefore, we must have $\mu = \hat{\mu}$ and $a = \hat{a}$. That is, $\tilde{p}^T \to 0$ as $t \to \infty$. □

5.4 Numerical Results

Numerical simulations have been carried out in order to test the effectiveness of the proposed asymptotic control strategy for synchronization and recovery of the unknown parameters of the uncertain Rikitake system. The program uses the Runge–Kutta integration algorithm, with the integration step set to 0.001.

In the first simulation, we illustrate the qualitative property described in assumption A2. To this end, we fixed the master system parameter as $q = (\mu = 2, a = 5)$, while the initial conditions were selected as $w_1(0) = (x_1(0) = 1, y_1(0) = -1, z_1(0) = 0)$. Figure 5.1 shows the behavior of the whole state of the Rikitake system. We can see from this figure that the whole state solution of the master system is bounded, and the states x_1 and y_1 remain oscillating around zero; therefore, we can claim that assumption A2 is completely fulfilled.

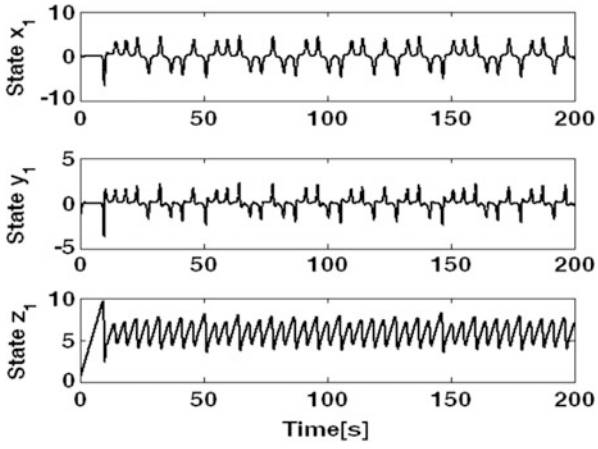

Fig. 5.1 This figure depicts the qualitative behavior of the Rikitake system when it is initialized to $w_1(0) = (1, -1, 0)$ and the parameter vector is fixed at $q = (2, 5)$

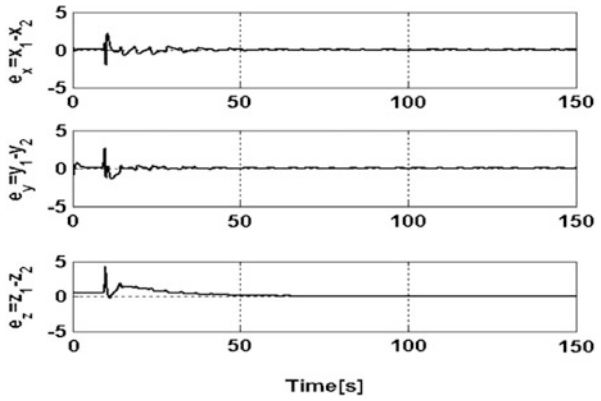

Fig. 5.2 This figure shows the convergence to zero of the master–slave synchronization error when the master system is initialized to $w_1(0) = (1, -1, 0)$ and its parameters vector is fixed at $q = (2, 5)$

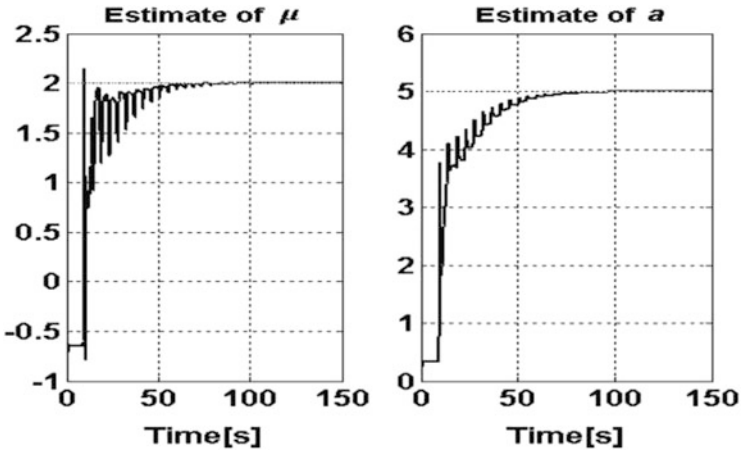

Fig. 5.3 This figure shows the parameter estimation when the master system is initialized to $w_1(0) = (1, -1,0)$ and the actual parameter vector is fixed at $q = (2, 5)$

To show the performance of the proposed control strategy, we carried out a second simulation using the same setup as above, fixing the slave system gains as $k_1 = k_2 = 0.8$ and $k_{12} = k_{22} = 0.266$ with the slave system initialized at zero, i.e., $w_2(0) = 0$ and $\hat{p}(0) = 0$. In Fig. 5.2, we can see that the synchronization errors converge asymptotically to zero. That is, the slave system follows the uncertain master system almost perfectly. The estimated parameters are shown in Fig. 5.3. As we expect, better performance can be obtained as long as the time is increased. From these simulations, we conclude that the proposed estimator reconstructs the parameters reasonably well after an elapsed time of 100 s.

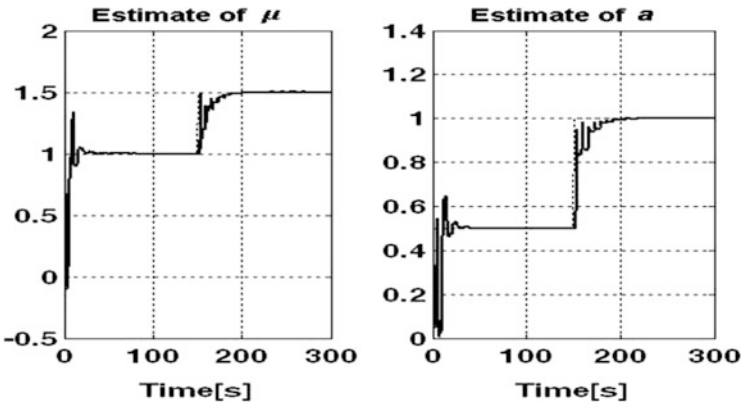

Fig. 5.4 Parameter estimates when abrupt parametric variations in μ and a are presented in the master system

Finally, to show the robustness of the proposed asymptotic parameter estimation method, we have subjected the parameter values of the master system to piecewise constant variations, as follows:

$$\text{if } t \leq 150 \text{ then } \{\mu = 1, a = 1.5\} \text{ else } \{\mu = 0.5, a = 1.0\}.$$

In this case, the initial conditions and the control gains of the slave system were set as before, while the master system was initialized at $\mathbf{w}_1(0) = (0.5, -0.3, 0.2)$. Figure 5.4 shows the numerical simulation of the corresponding parameter estimation process from $t = 0$ s to $t = 300$ s. From this simulation, we can see that even when the values of both parameters were abruptly changed at $t = 150$, the slave system was able to detect it and estimate once again the new unknown parameter values rather accurately, needing only 60 s.

5.5 Concluding Remarks

A Lyapunov-based approach for the synchronization and parameter identification of the constant unknown parameters of a Rikitake system was presented under the assumptions that the two output states x and y are available for measurement. To accomplish this task, we first show that the system is observable and linearly algebraically identifiable with respect to the available outputs. Then we propose a slave controlled system whose controllers were proposed such that the vector synchronization error and the vector parameter error among the master and slave systems converge asymptotically to zero. The convergence proof was carried out

using the traditional Lyapunov method in combination with Barbalat's lemma and assumption A2. Also, it is worth mentioning that our parameter identification algorithm does not require that the Rikitake system always exhibits chaotic behavior. Finally, numerical simulations were carried out to evaluate the performance of the proposed solution.

References

1. R. Martinez-Guerra, I.R. Ramirez-Palacios, E. Alvarado-Trejo, On parametric and state estimation: application to a simple academic example, in *Proceedings of the 37th IEEE CDC*, Tampa, FL, December, 1998, pp. 764–765
2. A. Fradkov, *Cybernetical Physics: From Control of Chaos to Quantum Control* (Springer, Berlin, 2007)
3. R. Martínez-Guerra, Y. Wen, Chaotic synchronization and secure communication via sliding-mode observer. Int. J. Bifurcat. Chaos **18**, 235–243 (2008)
4. R. Martínez-Guerra, J. Cruz, R. Gonzalez, R. Aguilar, A new reduced-order observer design for the synchronization of Lorenz systems. Chaos Solitons Fractals **28**, 511–517 (2006)
5. X. Guan, H. Peng, L. Li, Y. Wang, Parameter identification and control of Lorenz chaotic system. Acta Phys. Sin. **50**, 26–29 (2001)
6. J. Lu, S. Zhang, Controlling Chen's chaotic attractor using backstepping design based on parameters identification. Phys. Lett. A **286**, 148–152 (2001)
7. T. Rikitake, Oscillations of a system of disk dynamos. Proc. Camb. Philos. Soc. **54**, 89 (1958)
8. M. Fliess, H. Sira-Ramirez, An algebraic framework for linear identification. ESAIM **9**, 151–168 (2003)
9. T. McMillen, The shape and dynamics of the Rikitake attractor. Nonlinear J. **1**, 1–10 (1999)
10. K.J. Åström, B. Wittenmark, *Adaptive Control*, 2nd edn. (Addison-Wesley, Boston, 1995)

Chapter 6
Secure Communications and Synchronization via a Sliding-Mode Observer

Abstract An information signal embedded in a chaotic transmitter can be recovered by a receiver if it is a replica of the transmitter. In this chapter, an aspect of chaotic communication is introduced. A sliding-mode observer replaces the conventional chaotic system at the receiver side, which does not need information from the transmitter, so the uncertainties in the transmitter and the transmission line do not affect the synchronization. The proposed communication scheme is robust with respect to some disturbances and uncertainties. Three chaotic systems, the Duffing equation, Van der Pol oscillator, and Chua's circuit, are provided to illustrate the effectiveness of the chaotic communication.

6.1 Introduction

The general idea for transmitting information via chaotic systems is that an information signal is embedded in the transmitter system that produces a chaotic signal. The information signal is recovered when the transmitter and the receiver are identical. Since Pecora and Carroll's observation on the possibility of synchronizing two chaotic systems, several synchronization schemes have been developed [1].

There are many applications to chaotic communication [6] and chaotic network synchronization [7]. The techniques of chaotic communication can be divided into three categories: (a) chaos masking [8], whereby the information signal is added directly to the transmitter; (b) chaos modulation [4, 9], which is based on master–slave synchronization, where the information signal is injected into the transmitter as a nonlinear filter; (c) chaos shift keying [3], in which the information signal is supposed to be binary and is mapped to the transmitter and receiver. In these three cases, the information signal can be recovered by a receiver if transmitter and receiver are synchronized. In order to reach synchronization, the receiver should be a replica of the transmitter [5–8].

Linear and nonlinear observers in the control theory literature can be applied to the design of receivers. The receiver is regarded as a chaotic observer, which has two parts: a duplicated chaotic system of the transmitter and an adjustable observer gain [4]. Some modifications are made when it is difficult to obtain a replica of the synchronization. For example, if the transmitter and receiver are set to the same

R. Martínez-Guerra et al., *Synchronization of Integral and Fractional Order Chaotic Systems*, Understanding Complex Systems,
DOI 10.1007/978-3-319-15284-4_6

chaotic structures, then parameter identification methods can be used to construct the chaotic receiver [10]; when there are uncertainties in synchronization (e.g., the transmitter is not known exactly, there is noise in the transmission line), the transmitter and the receiver could be established in the same fuzzy models. A fuzzy-model-based design method has been applied to reach synchronization [11]; stability analysis of observer-based chaotic communication with respect to uncertainties can be found in [9, 12, 15].

Robust control techniques and many traditional schemes have been applied in robust synthesis for chaotic synchronization, e.g., a robust observer and the H_∞ technique are used in [13, 14]. Since a sliding-mode observer contains a sliding-mode term, it provides robustness against an inaccurate modeling of measurement and output noise [24]. Early work dealing with sliding-mode observers that consider measurement noise includes [15]. Those authors discussed state estimation using a sliding-mode technique. The authors of [16] discussed variable structure control as a high-speed switched feedback control resulting in a sliding mode. In [17], the authors analyzed systems with a sliding mode in the presence of noise. In [18], a sliding-mode approach to construct observers that are highly robust with respect to noise in the input of the system was successfully designed.

But it turns out that the corresponding stability analysis cannot be directly applied in situations with output noise (or mixed uncertainty). So it is still a challenge to suggest a workable technique to analyze the stability of the identification error generated by sliding-mode-type (discontinuous nonlinearity) observers [19, 20, 25].

In this chapter, we design a pure sliding-mode observer for chaotic communications. The main difference between this and the above methods is that the receiver is no longer a chaotic system. The uncertainty of the transmitter will not affect the synchronization. The proposed communication scheme can be more robust than both transmitter and receiver employed in chaotic systems, but the information may be recovered by an observer that does not have knowledge of the transmitter. It is a big challenge to secure communication by means of chaos. Numerical simulations using a prototype of chaotic oscillators are also provided.

6.2 Chaotic Communication Based on a Sliding-Mode Observer

In normal chaotic communication, the transmitter and receiver are chaotic systems. They can be described in the form of the following nonlinear system:

$$\begin{aligned} \dot{\xi} &= f(\xi) + g(\xi)u, \\ y &= h(\xi), \end{aligned} \tag{6.1}$$

where $\xi \in \mathbb{R}^n$ is the state of the plant, $u \in \mathbb{R}$ is a control input, $y \in \mathbb{R}$ is a measurable output, f, g, and h are smooth nonlinear functions. Most chaotic systems have uniform relative degree n, i.e.,

$$L_g h(\xi) = \cdots = L_g L_f^{n-2} h(\xi) = 0, \quad L_g L_f^{n-1} h(\xi) \neq 0.$$

So there exists a mapping

$$\eta = T(\xi) \tag{6.2}$$

that can transform the system (6.1) into the following normal form [21]:

$$\begin{aligned} \dot{\eta}_i &= \eta_{i+1}, \quad i = 1, \ldots, n-1, \\ \dot{\eta}_n &= \Phi(\eta, u), \\ y &= \eta_1, \end{aligned} \tag{6.3}$$

where $\Phi(\cdot)$ is a continuous nonlinear function.

First, we discuss a simple case, in which the transmitter and the receiver are second-order chaotic oscillators, for example the Duffing equation and Van der Pol oscillator. When $n = 2$, then (6.3) becomes

$$\begin{aligned} \dot{\eta}_1 &= \eta_2, \\ \dot{\eta}_2 &= \Phi(\eta_1, \eta_2, u), \\ y &= \eta_1. \end{aligned} \tag{6.4}$$

The Duffing equation describes a specific chaotic circuit [22]. It can be written as

$$\begin{aligned} \dot{\eta}_1 &= \eta_2, \\ \dot{\eta}_2 &= p_1 \eta_1 - p_2 \eta_1^3 - p\eta_2 + q\cos(\omega t) + u_t, \end{aligned} \tag{6.5}$$

where p, p_1, p_2, q, and ω are constants, and u_t is a control input. It is known that the solution of (6.5) exhibits almost periodic and chaotic behavior. In the uncontrolled case, if we select $p_1 = 1.1$, $p_2 = 1$, $p = 0.4$, $q = 2.1$, $\omega = 1.8$, the Duffing oscillator (6.5) has a chaotic response, as shown in Fig. 6.1.

The Van der Pol oscillator can be described as [23]

$$\begin{aligned} \dot{\eta}_1 &= \eta_2, \\ \dot{\eta}_2 &= a_1 \left[(1 - a_2 \eta_1^2)\eta_2 - a_3 \eta_1\right] + u_t. \end{aligned} \tag{6.6}$$

In the uncontrolled case, if we select $a_1 = 1.5$, $a_2 = 1$, $a_3 = 1$, the Van der Pol oscillator (6.6) has a chaotic response, as shown in Fig. 6.2.

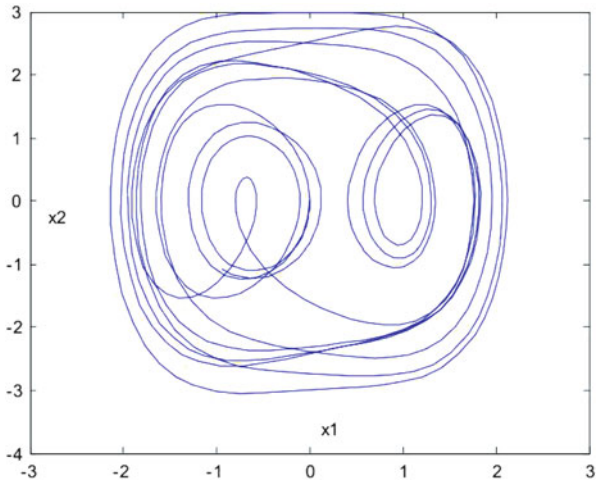

Fig. 6.1 Chaotic behavior of Duffing equation with $x(0) = [0, 0]^T$

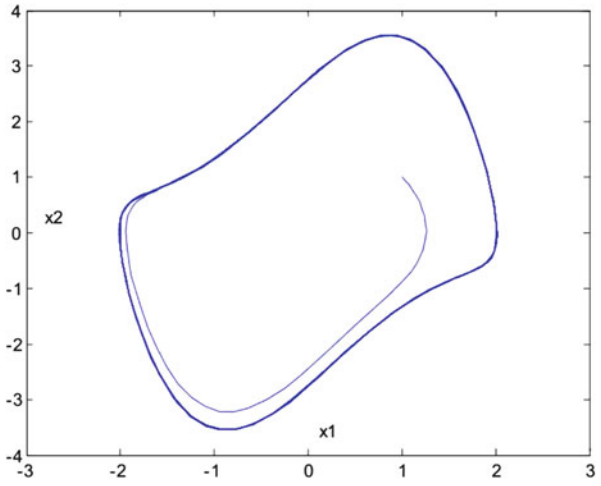

Fig. 6.2 Chaotic behavior of a Van der Pol oscillator with $x(0) = [1, 1]^T$

In this chapter, chaos modulation [2, 4, 9] is used for communication, whereby the information signal s is embedded in the output of the chaotic transmitter. The transmitter is a slight modification of the normal chaotic system (6.4) as follows:

$$\begin{aligned} \dot{\eta}_1 &= \eta_2, \\ \dot{\eta}_2 &= \Phi(\eta_1, \eta_2), \\ y &= \eta_1 + s, \end{aligned} \tag{6.7}$$

where the output $y = \eta_1 + s$ is chaotic masking.

In this chapter, we discuss an observer-based receiver, and we propose the following sliding-mode observer for the receiver:

$$\begin{aligned}\dot{\hat{\eta}}_1 &= \hat{\eta}_2 + m\tau^{-}1\text{sign}(y-\hat{y}), \quad m>0,\\ \dot{\hat{\eta}}_1 &= m^2\tau^{-}2\text{sign}(y-\hat{y}),\end{aligned} \tag{6.8}$$

where $\hat{\eta}_1$, $\hat{\eta}_2$ are the states on the receiver side; $\hat{y}$ is the estimate of the output y; m and τ are small positive parameters $m > 0$, $0 < \tau < 1$; and the sign function is defined as

$$\alpha(x) = \begin{cases} 1 & (y-\hat{y}) > 0,\\ -1 & (y-\hat{y}) < 0\\ 0 & (y-\hat{y}) = 0.\end{cases}$$

The schematic diagram of the chaotic communication based on a sliding-mode observer is shown in Fig. 6.3.

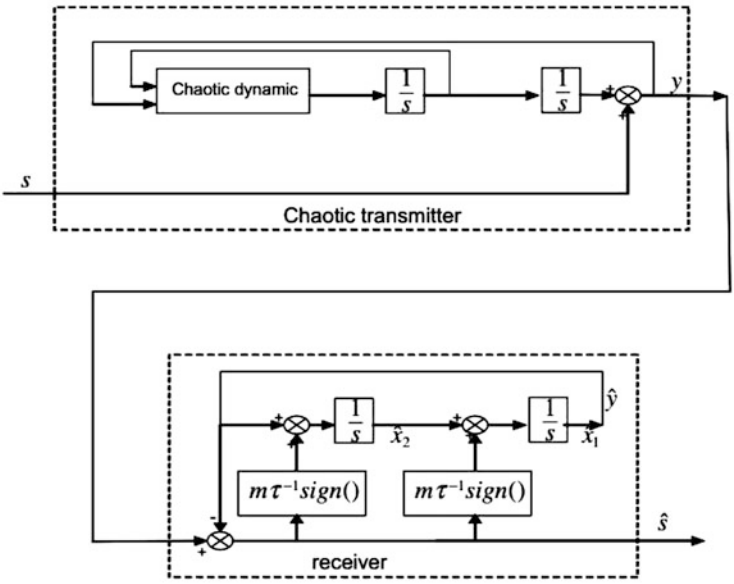

Fig. 6.3 Sliding-mode chaotic communication

The receiver (6.8) proposed in this chapter is very easy to apply and is robust with respect to uncertainty on the transmitter side. For example, in [4, 9], the receiver is

$$\begin{aligned}\dot{\hat{\eta}}_1 &= \eta_2 + l_1(y - \hat{y}),\\ \dot{\hat{\eta}}_2 &= a_1\left[(1 - a_2\hat{\eta}_1^2)\hat{\eta}_2 - a_3\hat{\eta}_1\right] + l_2(y - \hat{y}),\\ \hat{y} &= \hat{\eta}_1,\end{aligned} \tag{6.9}$$

where l_1 and l_2 are solutions of a Riccati inequality. Any uncertainty on the transmitter side, for example if the parameters a_1, a_2, and a_3 are not known exactly, will affect the accuracy of the recovery of the information signal.

Let us define the synchronization error as

$$\begin{aligned}e_1 &= \eta_1 - \hat{\eta}_1,\\ e_2 &= \frac{1}{m}(\eta_2 - \hat{\eta}_2).\end{aligned} \tag{6.10}$$

The recovered signal at the receiver is

$$\hat{s} = y - \hat{y} = e_1 + s.$$

By (6.7) and (6.8), the synchronization error can be represented as

$$\dot{e} = A_\mu e - K\text{sign}(Ce + s) + \Delta f, \tag{6.11}$$

as is given in Chap. 3 with $\delta = s$ and with

$$\begin{aligned}A_\mu &= \begin{pmatrix}-\mu & m\\ 0 & -\mu\end{pmatrix}, \quad \mu > 0,\\ K &= m\tau^{-}1\begin{pmatrix}1\\ m\tau^{-}1\end{pmatrix},\\ \Delta f &= \begin{pmatrix}\mu e_1\\ \dfrac{\Phi}{m} + \mu e_2\end{pmatrix},\\ C &= \begin{pmatrix}1\ 0\end{pmatrix}.\end{aligned}$$

We can then reformulate the following theorem for secure communications.

Theorem 6.2 *The sliding-mode observer-based receiver (6.8) can recover the information signal s embedded in the chaotic transmitter (6.7). The signal recovery error $\tilde{s} = s - \hat{s}$ converges to the following residual set:*

$$D_\varepsilon = \{\tilde{s} |\ \|\ \tilde{s}\ \|_P \leq \bar{\mu}(k)\},$$

and P is a solution of the Riccati equations

$$\bar{\mu} = \left(\frac{\rho(k)}{\sqrt{(k\alpha_p)^2 + \rho(k)\alpha_Q} + k\alpha_p} \right)^2,$$

where

$$\begin{aligned} \rho(k) &= 2 \parallel \Lambda_f \parallel L_{0f}^2 + 4k \left(\sqrt{n\Lambda_f^{-1}} \right) \bar{s}, \\ k\alpha_p &= k(\lambda_{\min}(P^{-1/2} C^T C P^{-1/2}), \\ \alpha_Q &= \lambda_{\min}(P^{-1/2} Q^T Q P^{-1/2}) > 0, \end{aligned}$$

where n is the dimension of the chaotic system.

Proof The proof is similar to that of Theorem 3.1 and is therefore omitted. □

Remark 6.1 The theorem actually states that the weighted estimation error $V(e) = e^T Pe$ converges to the zone $\bar{\mu}(k)$ asymptotically; that is, it is ultimately bounded:

$$\bar{\mu}(k) \geq e^T Pe \geq e_1^T Pe_1,$$

$$\bar{\mu}(k) = \left(\frac{\dfrac{2 \parallel \Lambda_f \parallel L_{0f}^2}{k} + 4(\sqrt{n\lambda_f^{-1}})\bar{s}}{\sqrt{\alpha_p^2 + [\dfrac{2 \parallel \lambda_f \parallel L_{0f}^2}{k^2} + \dfrac{4(\sqrt{n\lambda_f^{-1}})\bar{s}}{k}] + \alpha_Q} + \alpha_p} \right)^2. \tag{6.12}$$

Remark 6.2 Although we have restricted attention to the case of a second-order chaotic system, the observer construction and convergence analysis can be extended to the n-dimensional case. The chaotic transmitter is

$$\begin{aligned} \dot{\eta}_j &= \eta_{j+1}, \quad j = 1, \ldots, n-1, \\ \dot{\eta}_n &= H(\eta, s), \\ y &= \eta_1 + s, \end{aligned} \tag{6.13}$$

and the sliding-mode observer-based receiver is constructed as

$$\begin{aligned} \dot{\hat{\eta}}_j &= \hat{\eta}_{j+1} + m_j \tau^{-j} \operatorname{sign}(y - \hat{y}), \quad 1 \leq j \leq n-1, \\ \dot{\hat{\eta}}_n &= m_n \tau^{-n} \operatorname{sign}(y - \hat{y}), \end{aligned} \tag{6.14}$$

where the constants k_j are chosen such that the polynomial $\gamma^n + k_{n-1}\gamma^{n-1} + \cdots + k_1 = 0$ has all its roots in the open left-hand complex half-plane.

Remark 6.3 Some chaotic systems do not have the normal form (6.3), and we cannot apply a sliding-mode observer directly to the receiver, for example Chua's circuit

$$\begin{aligned} C_1\dot{\xi}_1 &= G(\xi_2 - \xi_1) - g(\xi_1) + u, \\ C_2\dot{\xi}_2 &= G(\xi_1 - \xi_2) + \xi_3, \\ L\dot{\xi}_3 &= -\xi_2, \\ y &= \xi_3, \end{aligned} \tag{6.15}$$

where $g(\xi_1) = m_0\eta_1 + 1/2(m_1 - m_0)[|\xi_1 + B_p|] + |\xi_1 - B_p|]$, ξ_1, ξ_2, ξ_3 denote the voltages across C_1, C_2, and L. It is known that with $C_1 = 1/9$, $C_2 = 1$, $L = 1/7$, $G = 0.7$, $m_0 = -0.5$, $m_1 = -1.5$, $B_p = 1$, the circuit displays a double scroll, as depicted in Fig. 6.4. But if we make the transformation $\eta = T(\xi)$ as

$$\begin{aligned} \eta_1 &= \xi_3, \\ \eta_2 &= -L\xi_2, \\ \eta_3 &= \frac{LG}{C_2}(\xi_2 - \xi_1) - \frac{L}{C_2}\xi_3, \end{aligned} \tag{6.16}$$

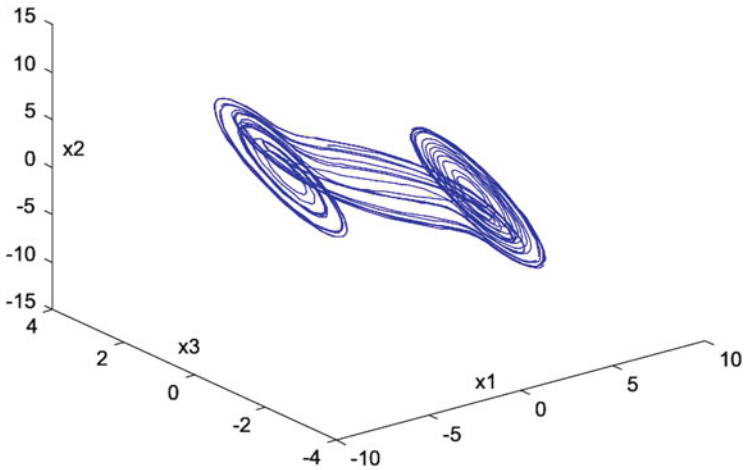

Fig. 6.4 Chaotic behavior of Chua's circuit with initial condition $[0, 0, 1]^T$

then Chua's circuit assumes the normal form

$$\begin{aligned}\dot{\eta}_1 &= \eta_2,\\ \dot{\eta}_2 &= \eta_3,\\ \dot{\eta}_3 &= f(\eta_1,\eta_2,\eta_3)+gu,\\ y &= \eta_1,\end{aligned} \tag{6.17}$$

where $f(\eta_1,\eta_2,\eta_3) = G/C_2\{-\eta_3 - (G/C_1)[-2\eta_2 - (1/GL)\eta_1 - (C_2/G)\eta_3 - (1/C_1)g(-\eta_1 - 1(1/GL)\eta_1 - (C_2/G)\eta_3)]\} - (1/C_2L)\eta_1$, $g = G/C_1C_2$. Now a sliding-mode observer-based receiver (6.14) can be applied.

6.3 Numerical Simulation

We use three types of chaotic systems as transmitters, whereby the information signal s is embedded in the output of the transmitter:

1. Duffing's equation is

$$\begin{aligned}\dot{\eta}_1 &= \eta_2 + \frac{1}{\tau}s,\\ \dot{\eta}_2 &= -1.1y - y^3 - 0.4\eta_2,\\ &\quad +2.1\cos(1.8t) + \frac{1}{\tau^2}s,\\ y &= \eta_1 + s,\quad \eta(0) = [0,0]^T.\end{aligned} \tag{6.18}$$

2. The Van der Pol oscillator is

$$\begin{aligned}\dot{\eta}_1 &= \eta_2 + \frac{1}{\tau}s,\\ \dot{\eta}_2 &= 1.5[(1-\eta_1^2)\eta_2 - \eta_1] + \frac{1}{\tau^2}s,\\ y &= \eta_1 + s,\quad \eta(0) = [2,-1]^T.\end{aligned} \tag{6.19}$$

3. For Chua's circuit, we use the following parameters: $C_1 = \frac{1}{9}$, $C_2 = 1$, $L = \frac{1}{7}$, $G = 0.7$, $m_0 = -0.5$, $m_1 = -1.5$, $B_p = 1$.

By the transformation (6.16), Chua's circuit (6.15) can be written as

$$\begin{aligned}
\dot{\eta}_1 &= \eta_2, \\
\dot{\eta}_2 &= \eta_3, \\
\dot{\eta}_3 &= \frac{31}{4.9}\eta_3 - \frac{310}{7}\eta_1 - \frac{22}{4.9}\eta_3 - \frac{22}{7}\eta_2 - \frac{220}{7}\eta_1, \\
&\quad -0.7\eta_2 - 7\eta_1 + 22g(\eta_1, \eta_2, \eta_3), \\
y &= \eta_2, \eta(0) = [1, 0, -7]^T,
\end{aligned} \tag{6.20}$$

where $g(\eta_1, \eta_2, \eta_3) = |-(1/4.9)\eta_3 - (1/7)\eta_2 - (10/7)\eta_1 + 1| - |-(1/4.9)\eta_3 - (1/7)\eta_2 - (10/7)\eta_1 - 1|$. We use η_2 and η_3 as the transmitter:

$$\begin{aligned}
\dot{\eta}_2 &= \eta_3 + \frac{1}{\tau}s, \\
\dot{\eta}_3 &= \frac{31}{4.9}\eta_3 - \frac{310}{7}\eta_1 - \frac{22}{4.9}\eta_3 - \frac{22}{7}y - \frac{220}{7}\eta_1, \\
&\quad -0.7y - 7\eta_1 + 22g(\eta_1, y, \eta_3) + \frac{1}{\tau^2}s, \\
y &= \eta_2 + s,
\end{aligned} \tag{6.21}$$

where η_1 satisfies $\dot{\eta}_1 = \eta_2$.

Now we design the sliding-mode receiver as (6.8). We choose $m = 0.1$, $\tau = 0.01$. The sliding-mode observer-based receiver is

$$\begin{aligned}
\dot{\hat{\eta}}_1 &= \hat{\eta}_2 + 10\text{sign}(y - \hat{y}), \\
\dot{\hat{\eta}}_2 &= 10^2\text{sign}(y - \hat{y}), \\
\hat{y} &= \hat{\eta}_1, \quad \hat{\eta}(0) = [1, 1]^T.
\end{aligned} \tag{6.22}$$

The information signal s is chosen as a sinusoidal signal with frequency of 100 Hz as in [4], i.e.,

$$s = 0.05\sin(200\pi t).$$

Figures 6.5, 6.6, 6.7 show the communication process with three different chaotic transmitters and one receiver. Here the waveform of the transmitted signal y is shown in subplot (a), and the convergence behavior of $s - \hat{s}$ is shown in subplots (b).

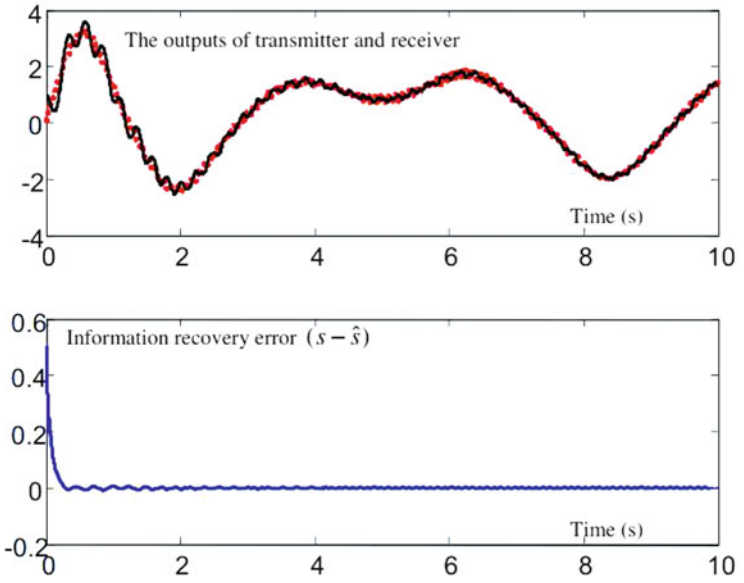

Fig. 6.5 Duffing equation for chaotic communication

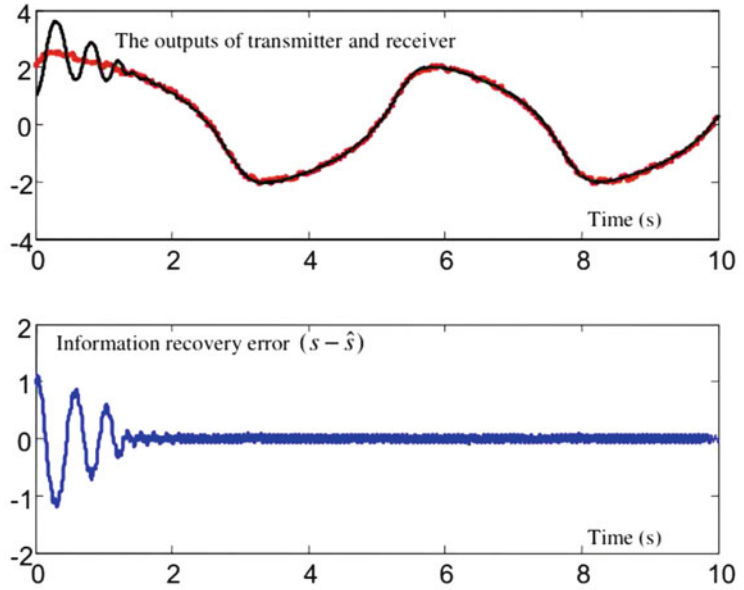

Fig. 6.6 Van der Pol oscillator for chaotic communication

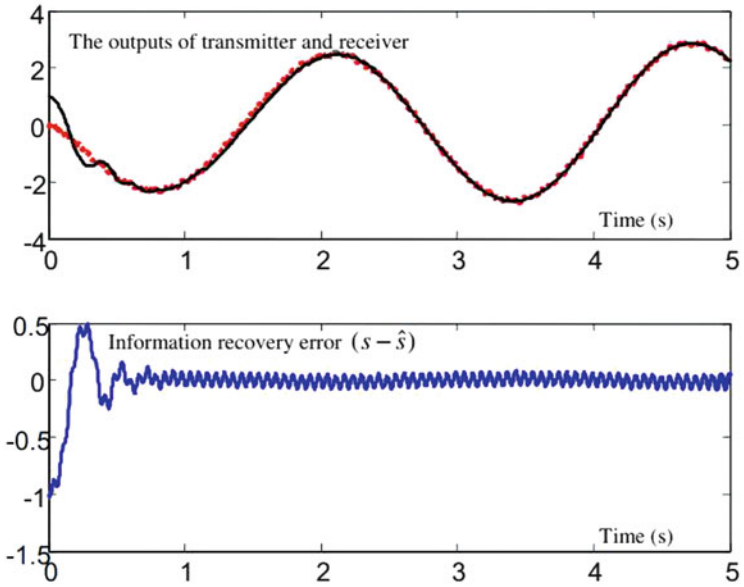

Fig. 6.7 Chua's circuit for chaotic communication

Following a transient process with $t > 0.1$ s, the maximum relative error is defined as

$$e_{\max} = \frac{\max(|s - \hat{s}|)}{\max(|s|)}.$$

For Duffing's oscillator, $e_{\max} \cong 1.5\,\%$. For the Van der Pol oscillator, $e_{\max} \cong 2\,\%$. For Chua's circuit, $e_{\max} \cong 1.915\,\%$. Although the relative errors are different, they are acceptable for signal communication. It is interesting to see that a single receiver (6.8) can recover the information signal from three different chaotic transmitters.

A model-based observer requires complete information for the transmitter. We use a linear observer [4] for comparison with our results; see Fig. 6.8. We find that the model-based observer gives the best performance, but if the transmitter is unknown or partially known, such a receiver does not work. Another advantage of a model-based receiver is that it can be applied to any chaotic transmitter as in (6.1), but a sliding-mode observer is suitable only for a chaotic system that has the normal form (6.3).

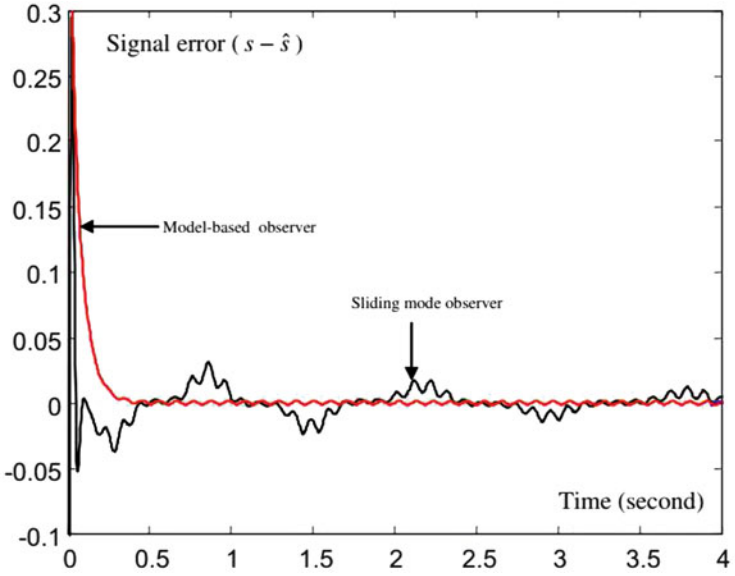

Fig. 6.8 Signal errors for different types of receivers

6.4 Conclusions

In this chapter, we have proposed a chaotic communication approach, whereby the receiver is a sliding-mode observer. The main difference between such an approach and normal chaos modulation in communication is that the receiver is no longer a chaotic system. The proposed scheme is robust with respect to uncertainty. Although the communication signal error can be made arbitrarily small by selecting a proper observer gain in the receiver. A large observer gain will also enlarge the transmission noise. A sliding-mode-based receiver cannot work as well as a normal receiver, and it may impose a security risk on the current secure communication system using chaotic communication techniques when the transmitter is in the form of (6.3), or it can be transformed into this form. To the best of our knowledge, this kind of receiver has not yet been implemented in a real-world application. But we hope that this chapter will encourage further research effort in the field of real chaotic communication.

References

1. L.M. Pecora, T.L. Carroll, Synchronization in chaotic systems. Phys. Rev. Lett. **64**, 821–824 (1990)
2. O. Morgul, E. Solak, Observer based synchronization of chaotic systems. Phys. Rev. E **54**, 4803–4811 (1996)

3. U. Parlitz, L.O. Chua, L. Kocarev, K.S. Halle, A. Shang, Transmission of digital signals by chaotic synchronization. Int. J. Bifurcat. Chaos **2**, 973–977 (1992)
4. T.L. Liao, N.S. Huang, An observer-based approach for chaotic synchronization with applications to secure communication. IEEE Trans. Circuits Syst. II **46**, 1144–1150 (1999)
5. W.C. Wu, L.O. Chua, A unified framework for synchronization and control of dynamical systems. Int. J. Bifurcat. Chaos **4**, 979–998 (1994)
6. M. Hasler, Synchronization of chaotic systems and transmission of information. Int. J. Bifurcat. Chaos **8**, 647–659 (1998)
7. T.W. Chow, J.C. Feng, K.T. Ng, Chaotic network synchronization with application to communications. Int. J. Commun. Syst. **14**, 217–230 (2001)
8. L. Kocarev, K.S. Halle, K. Eckert, L.O. Chua, U. Parlitz, Experimental demonstration of secure communication via chaotic synchronization. Int. J. Bifurcat. Chaos **2**, 709–713 (1992)
9. M. Boutayeb, M. Darouach, H. Rafaralahy, Generalized state-space observer for chaotic synchronization and secure communication. IEEE Trans. Circuits Syst. I **49**, 345–349 (2002)
10. H. Huijberts, H. Nijmeijer, R. Willems, System identification in communication with chaotic systems. IEEE Trans. Circuits Syst. I **47**, 800–808 (2000)
11. K.Y. Lian, T.S. Chiang, C.S. Chiu, P. Liu, Synthesis of fuzzy model-based designs to synchronization and secure communication for chaotic systems. IEEE Trans. Syst. Man Cybern. B **31**, 66–83 (2001)
12. R. Martinez-Guerra, J.C. Cruz-Victoria, R. Gonzalez-Galan, R. Aguilar-Lopez, A new reduced order observer design for the synchronization of Lorenz system. J. Chaos Soliton Fractals **28**, 511–517 (2006)
13. J.A.K. Suykens, P.F. Curran, L.O. Chua, Robust synthesis for master–slave synchronization of Lur'e systems. IEEE Trans. Circuits Syst. I **46**, 841–850 (1999)
14. J.A.K. Suykens, P.F. Curran, J. Vandewalle, L.O. Chua, Robust nonlinear H_∞ synchronization of chaotic Lur'e systems. IEEE Trans. Circuits Syst. I **44**, 891–940 (1999)
15. S.V. Drakunov, V. Utkin, Sliding mode observers: tutorial, in *Proceedings of 34th IEEE Conference on Decision and Control (CDC)* (1995), pp. 3376–3378
16. R. De Carlo, S. Zak, S. Drakunov, Variable structure and sliding mode control, in *Control Handbook*, ed. by W.S. Levine. Electrical Engineering Handbook Series (CRC Press, Boca Raton, 1996), pp. 941–950
17. S.V. Anulova, Random disturbances of the operation of control systems in the sliding mode. Autom. Remote Control **47**, 474–479 (1986)
18. J. Slotine, J. Hedricks, E. Misawa, On sliding observers for nonlinear systems. J. Dyn. Meas. Control **109**, 245–252 (1987)
19. R. Martinez-Guerra, R. Aguilar, A. Poznyak, A new robust sliding-mode observer design for monitoring in chemical reactors. Trans. ASME J. Dyn. Syst. Meas. Control **126**, 473–478 (2004)
20. W. Yu, M.A. Moreno, X. Li, Observer based neuro identifier. IEE Proc. Control Theory Appl. **147**, 145–152 (2000)
21. A. Isidori, *Nonlinear Control System* (Springer, London, 1995)
22. G. Chen, X. Dong, On feedback control of chaotic continuous-time systems. IEEE Trans. Circuits Syst **40**, 591–601 (1993)
23. V. Venkatasubramanian, Singularity induces bifurcation and the van der Pol oscillator. IEEE Trans. Circuits Syst. I **41**, 765–769 (1994)
24. A. Levant, Sliding order and sliding accuracy in sliding mode control. Int. J. Control **58**, 1247–1263 (1993)
25. L. Fridman, Y. Shtessel, C. Edwards, X.-G. Yan, Higher-order sliding-mode observer for state estimation and input reconstruction in nonlinear systems. Int. J. Robust Nonlinear Control **18**, 399–412 (2008)

Chapter 7
Synchronization and Antisynchronization of Chaotic Systems: A Differential and Algebraic Approach

Abstract In this chapter, chaotic systems synchronization and antisynchronization problems are tackled by means of differential and algebraic techniques for nonlinear systems. An observer is proposed for systems satisfying an algebraic observability property. This observer can be used as a slave system whose states are synchronized with the master (chaotic) system. This approach has the advantages of being independent of the chaotic nature of the master system. It uses a reduced set of measurable signals from the master system, and it also solves the antisynchronization problem as a straightforward extension of the synchronization problem. A Colpitts oscillator is given to illustrate the effectiveness of the suggested approach.

7.1 Introduction

In this chapter we have taken the classic Colpitts oscillator as a suitable chaotic system to illustrate the proposed methodology. As in previous chapters, where the synchronization of a Colpitts oscillator was carried out by means of observers, the synchronization of Colpitts oscillators using feedback techniques has been reported in [1–3]. In those works, the approach of a Luenberger-like observer is indirectly used with the disadvantage of assuming measurable the three state variables of the first Colpitts oscillator taken as the master system to synchronize the second one.

Antisynchronization is another phenomenon of interest in chaotic oscillators. With our approach, we show that once the synchronization problem is solved, antisynchronization is a straightforward modification of the designed observer for synchronization.

This chapter is organized as follows: In Sect. 7.2, we present some basic definitions and examples to introduce the differential-algebraic setting and the antisynchronization problem. In Sect. 7.3, the statement of the problem is presented in terms of the algebraic observability of an unknown variable and the construction of a reduced-order observer. In Sect. 7.4, these techniques are applied to solve the problem of synchronization and antisynchronization of a Colpitts oscillator. Furthermore, we show some numerical results that illustrate how synchronization and antisynchronization are achieved, and finally, in Sect. 7.5, some concluding remarks are presented.

R. Martínez-Guerra et al., *Synchronization of Integral and Fractional Order Chaotic Systems*, Understanding Complex Systems,
DOI 10.1007/978-3-319-15284-4_7

7.2 Statement of the Problem

As in previous chapters, let us consider the following system:

$$\begin{aligned} \dot{x}(t) &= f(x,u), \\ y(t) &= h(x,u), \end{aligned} \tag{7.1}$$

where $x = (x_1\ x_2 \ldots x_n)^T \in \mathbb{R}^n$ is the state vector, $u \in \mathbb{R}^m$ is the input vector, $y \in \mathbb{R}^p$ is the output vector, and h is assumed to be an analytic vector function.

System (7.1) can be seen as a dynamics given by $K\langle u, y\rangle / K\langle u\rangle$ with output y and where K is the differential field given by $\mathbb{R}$ [5].

Let $x_i, i \in \{1, \ldots, n\}$, be an unknown state variable of (7.1), and let us introduce the new variable $\eta(x_i)$ as a function of the unknown state x_i. Then (7.1) can be seen as the following extended dynamics:

$$\begin{aligned} \dot{x}(t) &= f(x,\eta,u), \\ \dot{\eta} &= \Delta(x,u), \\ y(t) &= h(x,u), \end{aligned} \tag{7.2}$$

where $\Delta(x,u)$ is an unknown function.

As can be seen, it is impossible to construct a classical Luenberger observer, because the dynamics (7.4) has an unknown part. Under these conditions, Lemma 2.1 describes the construction of a purely proportional reduced-order observer for (7.1), which is a model-free reduced-order observer.

7.2.1 Antisynchronization

The synchronization problem is solved in terms of the asymptotic convergence of the observed variables given by (2.17) (see Chap. 2). From this expression, we have

$$\limsup_{t\to\infty} |\eta - \hat{\eta}| = \bar{\varepsilon}, \tag{7.3}$$

where $\bar{\varepsilon} = \frac{M}{|K|}$. If we choose the change of variable $\hat{\xi} = -\hat{\eta}$, then (7.3) becomes

$$\limsup_{t\to\infty} \left|\eta + \hat{\xi}\right| = \bar{\varepsilon},$$

where $\hat{\xi}$ can be considered the estimated state of the antisynchronized system.

Remark 7.1 Note that antisynchronization error $\bar{\varepsilon}$ defines a ball with definite radius equal to $\frac{M}{|K|}$, which can be made small enough with an appropriate choice of the observer's gain K ($K \in \mathbb{R}^+$, the convergence rate of the observer).

7.3 Synchronization and Antisynchronization of a Colpitts Oscillator

The classic Colpitts oscillator is a single-transistor implementation of a sinusoidal oscillator that has been widely used in electronic devices and communication systems [6]. The fundamental frequency of this oscillator can be tuned from radio frequency to the microwave range [2]. It is well known that this circuit can exhibit chaotic behavior in different frequency ranges. The first experimental chaotic behavior at kilohertz frequencies was reported in [4]. Thereafter, many experiments have reported chaos in Colpitts oscillators in higher frequency ranges [3].

Let us consider the Colpitts oscillator whose circuit is shown in Fig. 7.1. It consists of a single bipolar transistor, which is biased in its active region by means of the constant voltage source V. It contains a feedback network consisting of

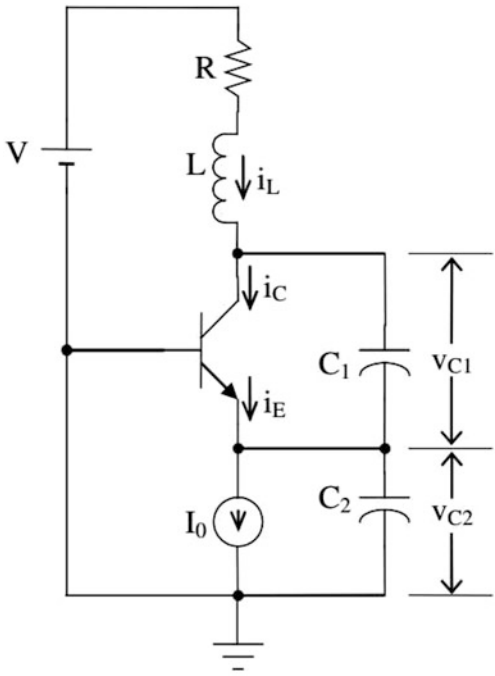

Fig. 7.1 Colpitts oscillator circuit

an inductor L with a series resistance R and a capacitive divider formed by C_1 and C_2. By applying Kirchhoff's laws on voltages and currents, we can get the corresponding equation for this circuit as follows (see Chap. 4):

$$\begin{aligned} C_1 \frac{dv_{C_1}}{dt} &= i_L - i_C, \\ L \frac{di_L}{dt} &= V - v_{C_1} - v_{C_2} - Ri_L, \\ C_2 \frac{dv_{C_2}}{dt} &= i_L - i_C + i_E(v_{C_2}) - I_0, \end{aligned} \tag{7.4}$$

where v_{C_1} and v_{C_2} are the respective capacitor voltages, and i_L is the inductor current, I_0 is the constant current source, and i_C, i_E are respectively the collector and emitter currents.

Here, a piecewise linear model is considered for the I–V curves of the emitter–base junction [2]:

$$i_E(v_{C_2}) = \begin{cases} \dfrac{-v_{C_2} - v^*}{r}, & v_{C_2} < -v^*, \\ 0 & v_{C_2} \geq -v^*, \end{cases} \tag{7.5}$$

where r is the small-signal ON resistance of the emitter–base junction, and v^* is the breakpoint voltage ($v^* \approx 0.7\,\mathrm{V}$).

After normalizing voltages, currents, and time by introducing the dimensionless quantities $v_{\mathrm{ref}} = v^*$, $i_{\mathrm{ref}} = \frac{v^*}{\sqrt{L/C_1}}$, $t_{\mathrm{ref}} = \sqrt{LC_1}$ and taking into account that $i_E \approx i_C$, then (7.6) takes the form

$$\begin{aligned} \dot{x}_1 &= x_2 - F(x_3), \\ \dot{x}_2 &= u - x_1 - bx_2 - x_3, \\ \dot{x}_3 &= (x_2 - d)/\varepsilon, \\ y &= x_3, \end{aligned} \tag{7.6}$$

where $u = \frac{V}{v^*}$ is the input of the system, $x = \left[\, v_{C_1}\ i_L\ v_{C_2} \,\right]^T = \left[\, v_{ce}\ i_L\ -v_{be} \,\right]^T$ is the state vector, $a = \frac{\sqrt{L/C_1}}{r}$, $b = \frac{R}{\sqrt{L/C_1}}$, $d = \frac{\sqrt{L/C_1}I_0}{v^*}$, $\varepsilon = \frac{C_2}{C1}$, and the nonlinear (7.5) is given by

$$F(x_3) = \begin{cases} -a(x_3 + 1), & x_3 < -1, \\ 0 & x_3 \geq -1. \end{cases} \tag{7.7}$$

As can be seen, system (7.6) has the form (7.1). Then it can be seen as a dynamics of the form $\mathbb{R}\langle u, y\rangle / \mathbb{R}\langle u\rangle$, since it can be expressed as

$$\varepsilon \dddot{y} + b\varepsilon \ddot{y} + (\varepsilon + 1)\dot{y} - F(y) - \dot{u} + d = 0.$$

In our approach, we need neither an exact copy of the Colpitts oscillator nor the complete information from the three states of the original oscillator. We consider only a measurable state variable or output $y = x_3$, and we analyze the algebraic observability for the other states. Therefore, the first step is to rewrite the system (7.6) in terms of its output:

$$\begin{aligned} \dot{x}_1 &= x_2 - F(y), \\ \dot{x}_2 &= u - x_1 - bx_2 - y, \\ \dot{y} &= (x_2 - d)/\varepsilon. \end{aligned} \tag{7.8}$$

Then from (7.8), we obtain

$$x_1 = u - b(\varepsilon\dot{y} + d) - \varepsilon\ddot{y} - y \tag{7.9}$$

and

$$x_2 = \varepsilon\dot{y} + d, \tag{7.10}$$

so it is possible to express the states x_1 and x_2 as differential algebraic polynomials of y, u, and their time derivatives with $b, \varepsilon, d \in \mathbb{R}^+$. Then we can conclude that the system (7.6) is algebraically observable over $\mathbb{R}\langle u, y\rangle$ (see Definition 1.6), and therefore it is possible to construct a new dynamical system (the observer) that will produce new state variables that are synchronized with the state variables of the actual system (7.6).

7.3.1 Observer Design

From Lemma 2.1 given in Chap. 2, we proceed by constructing a reduced-order observer for each state variable. In this way, for the variable x_2 we have

$$\dot{\hat{x}}_2 = K_2(x_2 - \hat{x}_2), \tag{7.11}$$

where $K_2 > 0$, and from (7.10),

$$\dot{\hat{x}}_2 = K_2(\varepsilon\dot{y} + d - \hat{x}_2), \tag{7.12}$$

but we do not know the time derivative $\dot{y}$. In order to avoid this difficulty, we introduce an auxiliary variable γ_2 as follows:

$$\gamma_2 \triangleq \hat{x}_2 - K_2\varepsilon y.$$

That is,

$$\hat{x}_2 = \gamma_2 + K_2 \varepsilon y. \tag{7.13}$$

Taking the time derivative from (7.13) and taking into account (7.12), we obtain

$$\dot{\gamma}_2 = K_2(d - \gamma_2 - K_2 \varepsilon y), \tag{7.14}$$

so that we have an observer for x_2 consisting of (7.13) and (7.14). Now for the variable x_1, we have

$$\dot{\hat{x}}_1 = K_1(x_1 - \hat{x}_1), \tag{7.15}$$

where $K_1 > 0$, and from (7.9),

$$\dot{\hat{x}}_1 = K_1(c - b\varepsilon \dot{y} - bd - \varepsilon \ddot{y} - y - \hat{x}_1). \tag{7.16}$$

In this case, we need a second-order time derivative of y. In the same manner as above, we introduce a new variable

$$x_4 \triangleq \dot{y}, \tag{7.17}$$

and we propose an observer for x_4,

$$\dot{\hat{x}}_4 = K_4(x_4 - \hat{x}_4),$$

that is,

$$\dot{\hat{x}}_4 = K_4(\dot{y} - \hat{x}_4), \tag{7.18}$$

and we define the auxiliary variable

$$\gamma_4 \triangleq \hat{x}_4 - K_4 y,$$

or

$$\hat{x}_4 = \gamma_4 + K_4 y. \tag{7.19}$$

Then by taking the time derivative from (7.19) and comparing with (7.18), we obtain

$$\dot{\gamma}_4 = K_4\gamma_4 - K_4^2 y. \tag{7.20}$$

On the other hand, by replacing (7.17) in (7.16), we can write

$$\dot{\hat{x}}_1 = K_1(c - b\varepsilon x_4 - bd - \varepsilon\dot{x}_4 - y - \hat{x}_1). \tag{7.21}$$

Finally, to avoid calculating x_4, we introduce an auxiliary variable

$$\gamma_5 \triangleq \hat{x}_1 + K_1\varepsilon x_4,$$

which yields

$$\hat{x}_1 = \gamma_5 - K_1\varepsilon x_4. \tag{7.22}$$

Taking the time derivative and comparing with (7.21), we obtain

$$\dot{\gamma}_5 = K_1\left[-\gamma_5 + c + (K_1 - b)\,\varepsilon x_4 - bd - y\right]. \tag{7.23}$$

Then we can construct the following asymptotic observer for x_1:

$$\begin{aligned}
\hat{x}_1 &= \gamma_5 - K_1\varepsilon\hat{x}_4 = \gamma_5 - K_1\varepsilon\left(\gamma_4 + K_4 y\right),\\
\dot{\gamma}_4 &= K_4\gamma_4 - K_4^2 y,\\
\dot{\gamma}_5 &= K_1\left[-\gamma_5 + c + (K_1 - b)\,\varepsilon\left(\gamma_4 + K_4 y\right) - bd - y\right].
\end{aligned} \tag{7.24}$$

7.4 Numerical Results

The parameter values considered in the numerical simulations correspond to chaotic behavior [2]; they are $a = 30, b = 0.8, d = 0.6, \varepsilon = 1$. The input u is maintained constant $u = 0.6$. The initial conditions are $x_1(0) = 2$, $x_2(0) = x_3(0) = 0.5$.

In Fig. 7.2, the synchronization of the three state variables is shown. As can be seen, this synchronization occurs immediately. In the phase space shown in Fig. 7.3, one can appreciate the antisynchronization achieved by simply changing signs in the observers (7.15) and (7.11) for reconstructing $-x_1$ and $-x_2$, instead of x_1 and x_2.

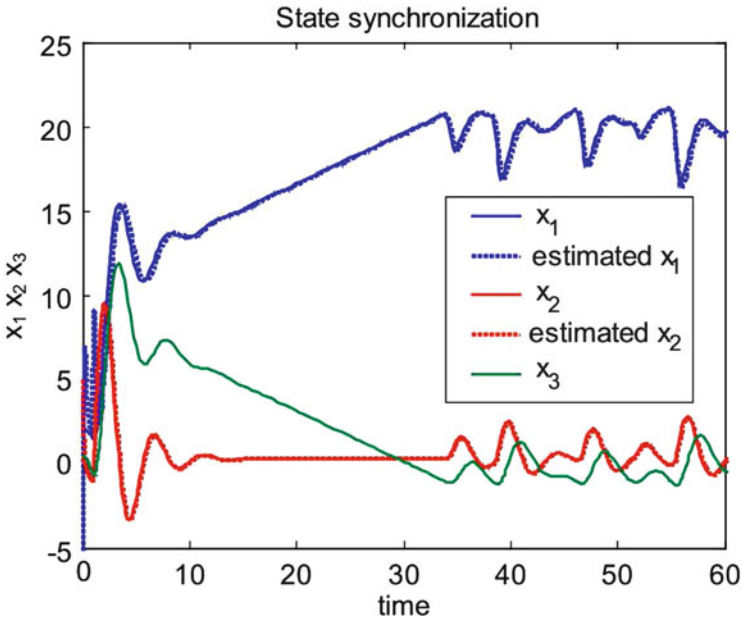

Fig. 7.2 Synchronization of the three state variables

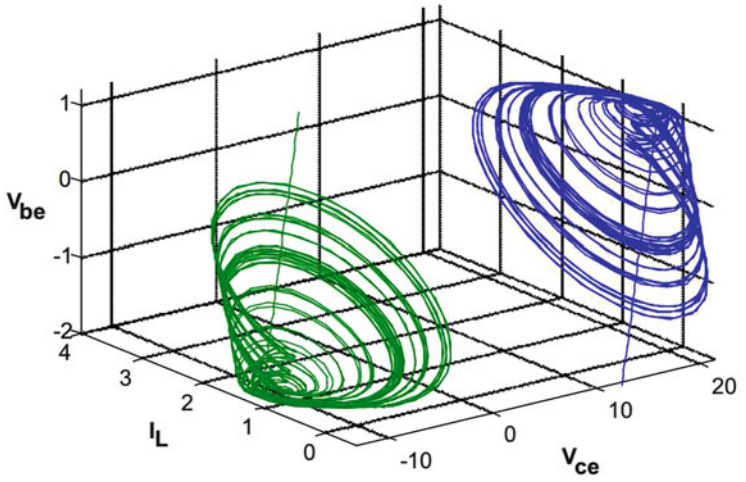

Fig. 7.3 Phase trajectories of the original and the antisynchronized systems

7.5 Concluding Remarks

In this chapter, the problems of synchronization and antisynchronization have been treated by means of differential and algebraic techniques. A reduced-order observer based on an algebraic observability condition was proposed. This observer has been used as a slave system whose states are synchronized with the chaotic system. A reduced set of measurable state variables was needed to achieve the synchronization with this approach. The antisynchronization problem was proved to be a straightforward extension of the synchronization problem. A Colpitts oscillator model was given as an illustrative case to show the effectiveness of the suggested approach, and some numerical simulations were presented to help the reader visualize the synchronization and antisynchronization results.

References

1. V. Rubezic, B. Lutovac, R. Ostojic, Linear generalized synchronization of two chaotic Colpitts oscillators, in *9th International Conference on Electronics Circuits and Systems*, vol. 1 (2002), pp. 223–225
2. G.H. Li, Synchronization and anti-synchronization of Colpitts oscillators using active control. Chaos Solitons Fractals **26**, 87–93 (2005)
3. G.H. Li, S.P. Zhou, K. Yang, Controlling chaos in Colpitts oscillator. Chaos Solitons Fractals **33**, 582–587 (2007)
4. M.P. Kennedy, Chaos in the Colpitts oscillator. IEEE Trans. Circuits Syst. I **41**(11), 771–774 (1994)
5. R. Martinez-Guerra, J.L. Mata-Machuca, *Fault Detection and Diagnosis in Nonlinear Systems: A Differential and Algebraic Viewpoint*, Understanding Complex Systems, DOI 10.1007/978-3-319-03047, Springer International Publishing Switzerland 2014
6. G.M. Maggio, O.D. Feo, M.P. Kennedy, Nonlinear analysis of the Colpitts oscillator and applications to design. IEEE Trans. Circuits Syst. I **46**(9), 1118–1130 (1999)

Chapter 8
Synchronization of Chaotic Liouvillian Systems: An Application to Chua's Oscillator

Abstract In this chapter, we deal with the synchronization of chaotic oscillators with Liouvillian properties (chaotic Liouvillian system) based on a nonlinear observer design. The strategy consists in proposing a polynomial observer (slave system) that tends to follow exponentially the chaotic oscillator (master system). The proposed technique is applied in the synchronization of Chua's circuit. Simulation and experimental results are used to visualize and illustrate the effectiveness of the proposed scheme in synchronization.

8.1 Introduction

Synchronization of chaotic systems has received attention from researchers in many fields. In general, synchronization research has been focused on the following areas: nonlinear observers [1–17], nonlinear control [18], feedback controllers [5], nonlinear backstepping control [19], time-delayed systems [12, 20], directional and bidirectional linear coupling [21], adaptive control [9], adaptive observers [22, 23], sliding-mode observers [13, 24], and active control [25], among others.

This chapter considers the master–slave synchronization problem via an exponential polynomial observer (EPO) based on differential and algebraic techniques [26–28]. In Chap. 1, differential and algebraic concepts allowed us to establish an algebraic observability condition, and therefore, they provide a first step to constructing an algebraic observer. An observable system in this sense can be regarded as a system whose state variables can be expressed in terms of the input and output variables and a finite number of their time derivatives. Thus, the chaos synchronization problem can be posed as an observer design procedure, whereby the coupling signal is viewed as output and the slave system is regarded as observer. The main characteristic is that the coupling signal is unidirectional, i.e., the signal is transmitted from the master system (Chua's circuit) to the slave system (EPO). The slave is tasked with recovering the unknown state trajectories of the master system. The strategy consists in proposing an EPO that exponentially reconstructs the unknown states of Chua's system.

R. Martínez-Guerra et al., *Synchronization of Integral and Fractional Order Chaotic Systems*, Understanding Complex Systems,
DOI 10.1007/978-3-319-15284-4_8

Chua's circuit is a nonlinear electronic chaotic oscillator. This circuit is easily constructed [29] and has been employed in a variety of applications [30], e.g., communication systems [31]. The chaotic associative memory architecture proposed in [32] uses a network of Chua's oscillators coupled via piecewise linear conductances.

In this chapter, Chua's oscillator is viewed as a chaotic system with some Liouvillian properties [26, 28], referred to as a chaotic Liouvillian oscillator. The Liouvillian character of the system (if a variable can be obtained by the adjunction of integrals or exponentials of integrals) is exploited as an observability criterion, that is, with this property we can determine whether a variable can be reconstructed with measurable output.

This chapter is organized as follows. In Sect. 8.2, we give some definitions regarding the differential-algebraic approach and Liouvillian systems. In Sect. 8.3, we treat the synchronization problem and its solution by means of an exponential polynomial observer. In Sect. 8.4, we present the synchronization of Chua's circuit [33], and we offer some numerical simulations and real-time experiments. Finally, in Sect. 8.5, we close the chapter with some concluding remarks.

8.2 Definitions

We begin with some basic definitions related to Liouvillian systems.

By way of motivation, let us consider the following examples.

Example 8.1 Consider the nonlinear system

$$\begin{aligned} \dot{x}_1 &= x_2 + x_3^2, \\ \dot{x}_2 &= x_3, \\ \dot{x}_3 &= u. \end{aligned} \tag{8.1}$$

If we define $y = x_2$, then

$$\begin{aligned} x_2 &= y, \\ x_3 &= \dot{y}, \\ \dot{x}_1 &= y + \dot{y}^2. \end{aligned} \tag{8.2}$$

The above system is not algebraically observable, since x_1 cannot be expressed as a differential algebraic polynomial in terms of $\{u, y\}$ (see Chap. 1).

Motivated by this fact, we present the following definition.

Definition 8.1 (Liouvillian System) A dynamical system is said to be Liouvillian if the elements (for example, state variables or parameters) can be obtained by an adjunction of integrals or exponentials of integrals of elements of $\mathbb{R}$.

Example 8.2 We consider a nonlinear system as in Example 8.1. From (8.2), we can observe that although x_1 does not satisfy the AOC (Chapter 2), we can obtain it by means of the integral

$$x_1 = \int (y + \dot{y}^2).$$

Therefore the nonlinear system (8.1) is Liouvillian.

Example 8.3 Consider the following nonlinear second-order system that models a predator–prey situation:

$$\begin{aligned} \dot{x}_1 &= x_1 x_2 - x_1 + k, \\ \dot{x}_2 &= -x_1 x_2 - x_2. \\ y &= x_1 \end{aligned} \tag{8.3}$$

We have, therefore,

$$\begin{aligned} \dot{y} &= y x_2 - y + k, \\ \dot{x}_2 &= -y x_2 - x_2, \end{aligned} \tag{8.4}$$

which we can solve directly to obtain

$$\begin{aligned} \dot{y} &= y x_2 - y + k, \\ x_2 &= \exp\left(- \int (y + 1)\, dt \right). \end{aligned}$$

We obtain the parameter k as

$$k = \dot{y} - \exp\left(- \int (y + 1)\, dt \right) + y,$$

and we say that system (8.3) is Liouvillian.

For further information, we recommend [26, 28].

8.3 Problem Formulation and Main Result

Let us consider the following chaotic Liouvillian system:

$$\begin{aligned} \dot{x} &= A\, x + \psi(x) + \varphi(x) + \zeta(u), \\ y &= C\, x, \end{aligned} \tag{8.5}$$

where $x \in \mathbb{R}^n$ is the state vector[1]; $u \in \mathbb{R}^l$ is the input vector, $l \leq n$; $y \in \mathbb{R}$ is the measured output; $\zeta(\cdot) : \mathbb{R}^l \to \mathbb{R}^n$ is an input-dependent vector function; $A \in \mathbb{R}^{n\times n}$ and $C \in \mathbb{R}^{1\times n}$ are constants; and $\psi(\cdot) : \mathbb{R}^n \to \mathbb{R}^n$, $\varphi(\cdot) : \mathbb{R}^n \to \mathbb{R}^n$ are state-dependent nonlinear vector functions.

We restrict each $\psi_i(\cdot)$ to be nondecreasing, that is, for all $a, b \in \mathbb{R}$, $a > b$, it satisfies the following monotone sector condition:

$$0 \leq \frac{\psi_i(a) - \psi_i(b)}{a - b}, \qquad i = 1, \ldots, n. \tag{8.6}$$

In the same manner, we restrict each $\varphi_i(\cdot)$ to be nondecreasing, that is, for all $a, b \in \mathbb{R}$, $a > b$, it satisfies

$$\frac{\varphi_i(a) - \varphi_i(b)}{a - b} \leq 0, \qquad i = 1, \ldots, n. \tag{8.7}$$

To show the relation between the observers for nonlinear systems and chaos synchronization, we give a definition of the observer.

Definition 8.2 (Exponential Observer) An exponential observer for (8.5) is a system with state $\hat{x}$ such that

$$\|x - \hat{x}\| \leq \kappa \exp(-\xi t),$$

where κ and ξ are positive constants.

In the context of master–slave synchronization, x can be considered the state variable of the master system, and $\hat{x}$ can be viewed as the state variable of the slave system. Hence, the master–slave synchronization problem can be solved by designing an observer for (8.5).

In what follows, we will solve the synchronization problem using an exponential polynomial observer based on the Lyapunov method [26]. To this end, we first compute the dynamics of the synchronization error (difference between the master and the slave systems). Next, by means of a simple quadratic Lyapunov function, we prove the exponential convergence.

System (8.5) is assumed to be a chaotic Liouvillian system. Then by Definition 8.1, all states of (8.5) can be reconstructed. In this sense, we will propose an observer scheme.

The observer structure. The observer for system (8.5) has the following form:

$$\dot{\hat{x}} = A\hat{x} + \psi(\hat{x}) + \varphi(\hat{x}) + \zeta(u) + \Sigma_{i=1}^{m} K_i \left(y - C\hat{x}\right)^{2i-1}, \tag{8.8}$$

where $\hat{x} \in \mathbb{R}^n$ and $K_i \in \mathbb{R}^n$ for $1 \leq i \leq m$.

[1]Mathematically, chaotic systems are characterized by local instability and *global boundedness of the trajectories*, i.e., $\|x(t)\|$ is bounded for all $t \geq 0$.

Remark 8.1 The meaning of m can be understood as follows. As is well known, an extended Luenberger observer can be seen as a first-order Taylor series around the observed state. Therefore, to improve the estimation performance, high-order terms are included in the observer structure. In other words, the rate of convergence can be increased by injecting additional terms with increasing powers of the output error.

8.3.1 Observer Convergence Analysis

In order to prove observer convergence, we analyze the observer error, which is defined as $e = x - \hat{x}$. From Eqs. (8.5) and (8.8), the dynamics of the state estimation error is given by

$$\dot{e} = (A - K_1 C)e + \phi(e) + \rho(e) - \Sigma_{i=2}^{m} K_i \, (Ce)^{2i-1}, \tag{8.9}$$

where $\phi(e) := \psi(x) - \psi(\hat{x})$ and $\rho(e) := \varphi(x) - \varphi(\hat{x})$.

It follows from (8.6) that each component of $\phi(e)$ satisfies

$$0 \leq \frac{\phi_i(e_i)}{e_i}, \qquad \forall \; e_i \neq 0, \tag{8.10}$$

which implies a relationship between $\phi(e)$ and e as follows:

$$e^T \phi(e) = \Sigma_{i=1}^{n} e_i \phi_i(e_i) = \Sigma_{i=1}^{n} e_i^2 \frac{\phi_i(e_i)}{e_i}.$$

Using (8.10), we have the following condition:

$$0 \leq e^T \phi(e). \tag{8.11}$$

By a similar analysis, from (8.7) we have

$$e^T \rho(e) \leq 0. \tag{8.12}$$

Properties (8.11) and (8.12) will allow us prove that the state estimation error $e(t)$ decays exponentially.

We now present our main result.

Theorem 8.1 *Consider the chaotic Liouvillian system (8.5) and the observer (8.8). If there exist a matrix $P = P^T > 0$ and scalars $\varepsilon > 0$, $\epsilon_1 > 0$, $\epsilon_2 > 0$ satisfying the linear matrix inequality (LMI)*

$$\begin{bmatrix} (A - K_1 C)^T P + P(A - K_1 C) + \varepsilon I & P + \epsilon_1 I & P - \epsilon_2 I \\ P + \epsilon_1 I & 0 & 0 \\ P - \epsilon_2 I & 0 & 0 \end{bmatrix} \leq 0 \tag{8.13}$$

and

$$\lambda_{\min}\left(M_i + M_i^T\right) \geq 0 \quad , \quad i = 2, \ldots, m, \tag{8.14}$$

with $M_i := PK_iC$, *then there exist positive constants* κ *and* ξ *such that for all* $t \geq 0$,

$$\|e(t)\| \leq \kappa \, \exp(-\xi t),$$

where $\kappa = \sqrt{\dfrac{\beta}{\alpha}}\,\|e(0)\|$, $\xi = \dfrac{\varepsilon}{2\beta}$, $\alpha = \lambda_{\min}(P)$, *and* $\beta = \lambda_{\max}(P)$.

Proof We use the following Lyapunov function candidate $V = e^T Pe$. From (8.9), the time derivative of V is

$$\begin{aligned}\dot{V} &= e^T\left[(A - K_1C)^T P + P(A - K_1C)\right]e \\ &\quad +2e^T P\phi(e) + 2e^T P\rho(e) - 2\Sigma_{i=2}^{m}(Ce)^{2i-2}e^T M_i e \\ &= e^T\left[(A - K_1C)^T P + P(A - K_1C)\right]e \\ &\quad +2e^T P\phi(e) + 2e^T P\rho(e) - \Sigma_{i=2}^{m}(Ce)^{2i-2}e^T(M_i + M_i^T)e,\end{aligned}$$

and in view of (8.13) and (8.14),

$$\dot{V} \leq -\varepsilon e^T e - 2\epsilon_1\, e^T\phi(e) + 2\epsilon_2\, e^T\rho(e).$$

By properties (8.11) and (8.12), we have

$$\dot{V} \leq -\varepsilon\|e\|^2. \tag{8.15}$$

We write the Lyapunov function as $V = \|e\|_P^2$. Then by the Rayleigh–Ritz inequality, we have that

$$\alpha\|e\|^2 \leq \|e\|_P^2 \leq \beta\|e\|^2, \tag{8.16}$$

where $\alpha := \lambda_{\min}(P)$ and $\beta := \lambda_{\max}(P) \in \mathbb{R}^+$ (because P is positive definite).

Using (8.16), we obtain the following upper bound for (8.15):

$$\dot{V} \leq -\frac{\varepsilon}{\beta}\|e\|_P^2. \tag{8.17}$$

Taking the time derivative of $V = \|e\|_P^2$ and replacing in inequality (8.17), we obtain

$$\frac{d}{dt}\|e\|_P \leq -\frac{\varepsilon}{2\beta}\|e\|_P.$$

Finally, the result follows with

$$\|e(t)\| \leq \kappa \exp(-\xi\, t), \tag{8.18}$$

where $\kappa = \sqrt{\frac{\beta}{\alpha}}\|e(0)\|$, and $\xi = \frac{\varepsilon}{2\beta}$. □

Corollary 8.1 *Let us consider $\psi(\cdot) \equiv 0$. Then system (8.8) is an exponential observer of system (8.5) if there exist a matrix $P = P^T > 0$ and scalars $\varepsilon > 0$, $\epsilon_2 > 0$ satisfying*

$$\begin{bmatrix} (A - K_1C)^T P + P(A - K_1C) + \varepsilon I & P - \epsilon_2 I \\ P - \epsilon_2 I & 0 \end{bmatrix} \leq 0 \tag{8.19}$$

and

$$\lambda_{\min}\left(M_i + M_i^T\right) \geq 0, \quad i = 2, \ldots, m, \tag{8.20}$$

with κ and ξ defined as in Theorem 8.1.

Proof The proof is similar to that of Theorem 8.1. □

Corollary 8.2 *Let us consider $\varphi(\cdot) \equiv 0$. Then system (8.8) is an exponential observer of system (8.5) if there exist a matrix $P = P^T > 0$ and scalars $\varepsilon > 0$, $\epsilon_1 > 0$ satisfying the LMI*

$$\begin{bmatrix} (A - K_1C)^T P + P(A - K_1C) + \varepsilon I & P + \epsilon_1 I \\ P + \epsilon_1 I & 0 \end{bmatrix} \leq 0 \tag{8.21}$$

and

$$\lambda_{\min}\left(M_i + M_i^T\right) \geq 0, \quad i = 2, \ldots, m, \tag{8.22}$$

With κ and ξ defined as in Theorem 8.1.

Proof The result follows directly from the procedure in Theorem 8.1. □

8.4 Numerical and Experimental Results

In this section, we consider the synchronization of a Chua system that is considered a chaotic Liouvillian oscillator.

8.4.1 Numerical Results

Chua's circuit [30] is shown in Fig. 8.1. It is a simple oscillator circuit that exhibits a variety of bifurcations and chaos. The circuit contains three linear energy-storage elements (an inductor and two capacitors), a linear resistor, and a single nonlinear resistor N_R.

The state equations for the Chua circuit are as follows:

$$\begin{aligned} C_1 \frac{dv_{C_1}}{dt} &= G(v_{C_2} - v_{C_1}) - g(v_{C_1}), \\ C_2 \frac{dv_{C_2}}{dt} &= G(v_{C_1} - v_{C_2}) + i_L, \\ L \frac{di_L}{dt} &= -v_{C_2}, \end{aligned} \tag{8.23}$$

where $G = \dfrac{1}{R}$, and $g(\cdot)$ is a nondecreasing function defined by

$$g(v_R) = m_0 v_R + \frac{1}{2}(m_1 - m_0)(|v_R + B_p| - |v_R - B_p|). \tag{8.24}$$

This relation is shown graphically in Fig. 8.2. The slopes in the inner and outer regions are m_0 and m_1 respectively, with $m_1 < m_0 < 0$, $\pm B_p$ denoting the

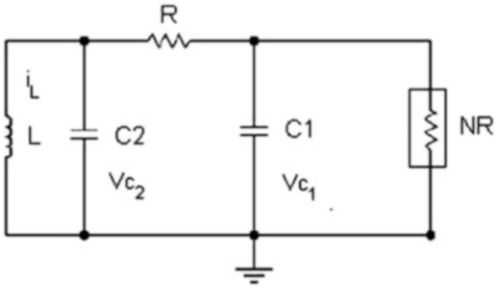

Fig. 8.1 Chua's circuit, with parameter values $C_1 = 10\,\text{nF}$, $C_2 = 100\,\text{nF}$, $R = 1.8\,\text{k}\Omega$, $L = 18\,\text{mH}$, $m_0 = -0.409\,\text{ms}$, $m_1 = -0.756\,\text{ms}$ and $B_p = 1.08\,\text{V}$

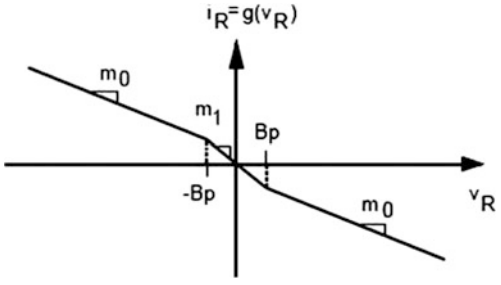

Fig. 8.2 Three segment piecewise-linear $v - i$ characteristic of the linear resistor in Chua's circuit. The outer regions have slopes m_0; the inner region has slope m_1. There are two breakpoints at $\pm B_p$

breakpoints. The nonlinear resistor N_R is said to be voltage-controlled because the current in the element is a function of the voltage across its terminals.

In the first reported study of this circuit, Chua and Matsumoto [30, 34] showed by computer simulation that the system possesses a strange attractor called the double scroll. Experimental confirmation of the presence of this attractor was given shortly afterward in [35]. Since then, the system has been studied extensively; a variety of bifurcation phenomena and chaotic attractors in the circuit have been discovered experimentally and confirmed mathematically [34].

In what follows, we consider the measured output $y = v_{c_2}$. From the equations of (8.23) we obtain

$$\begin{aligned} v_{c_1} &= \frac{C_2}{G}\dot{y} + y + \frac{1}{LG}\int y dt, \\ v_{c_2} &= y, \\ i_L &= -\frac{1}{L}\int y dt. \end{aligned} \tag{8.25}$$

Then Chua's system (8.23) is Liouvillian. This implies that unknown variables v_{C_1} and i_L can be reconstructed with the selected output $y = v_{C_2}$.

Chua's system (8.23) is of the form (8.5) with $\zeta(u) = 0$, $\varphi(\cdot) = 0$,

$$A = \begin{bmatrix} -\frac{G}{C_1} & \frac{G}{C_1} & 0 \\ \frac{G}{C_2} & -\frac{G}{C_2} & \frac{1}{C_2} \\ 0 & -\frac{1}{L} & 0 \end{bmatrix}, \quad \psi(x) = \begin{bmatrix} -\frac{g(x_1)}{C_1} \\ 0 \\ 0 \end{bmatrix},$$

$$C = \begin{bmatrix} 0 & 1 & 0 \end{bmatrix}, \qquad x = \begin{bmatrix} v_{C_1} & v_{C_2} & i_L \end{bmatrix}^T.$$

Since $g(x_1)$ is nonincreasing and C_1 is a positive constant, it follows that $\psi_1(x) = \psi_1(x_1) = -g(x_1)/C_1$ is nondecreasing as in (8.6). Indeed, $\psi_2(x) = \psi_3(x) = 0$ also satisfy property (8.6), and Chua's system (8.23) is Liouvillian, so that we may proceed with the observer design.

Taking into account that $\varphi(\cdot) = 0$, we will use conditions in Corollary 8.2 to obtain the observer gains. Using LMI software, observer gains are computed to drive the estimation error to zero.

Applying (8.8), we obtain the observer for Chua's system (8.23):

$$\dot{\hat{x}} = \begin{bmatrix} -\frac{G}{C_1} & \frac{G}{C_1} & 0 \\ \frac{G}{C_2} & -\frac{G}{C_2} & \frac{1}{C_2} \\ 0 & -\frac{1}{L} & 0 \end{bmatrix} \hat{x} + \begin{bmatrix} -\frac{g(\hat{x}_1)}{C_1} \\ 0 \\ 0 \end{bmatrix} + \sum_{i=1}^{m} \begin{bmatrix} k_{1,i} \\ k_{2,i} \\ k_{3,i} \end{bmatrix} \left(\begin{bmatrix} 0 & 1 & 0 \end{bmatrix} e \right)^{2i-1}.$$

Hence the state observer can be rewritten as

$$\begin{aligned}
\dot{\hat{x}}_1 &= -\tfrac{G}{C_1}\hat{x}_1 + \tfrac{G}{C_1}\hat{x}_2 - \tfrac{g(\hat{x}_1)}{C_1} + k_{1,1}e_{1,2} + k_{1,2}(e_{1,2})^3 + \cdots + k_{1,m}(e_{1,2})^{2m-1} \\
\dot{\hat{x}}_2 &= \tfrac{G}{C_2}\hat{x}_1 - \tfrac{G}{C_2}\hat{x}_2 + k_{2,1}e_{1,2} + k_{2,2}(e_{1,2})^3 + \cdots + k_{2,m}(e_{1,2})^{2m-1} \\
\dot{\hat{x}}_3 &= -\tfrac{1}{L}\hat{x}_3 + k_{3,1}e_{1,2} + k_{3,2}(e_{1,2})^3 + \cdots + k_{3,m}(e_{1,2})^{2m-1}.
\end{aligned} \tag{8.26}$$

Figure 8.2 shows the general diagram of the synchronization of Chua's circuit (8.23) and the exponential observer (8.26) in the master–slave configuration.

Numerical simulations for the synchronization of Chua's system are carried out in order to show the performance of the exponential observer; later, we present experimental results. The parameter values considered in the numerical simulations correspond to chaotic behavior [33], and these are $C_1 = 10\,\text{nF}$, $C_2 = 100\,\text{nF}$, $R = 1.8\,\text{k}\Omega$, $L = 18\,\text{mH}$, $m_0 = -0.409\,\text{ms}$, $m_1 = -0.756\,\text{ms}$, and $B_p = 1.08\,\text{V}$. The Matlab-Simulink® program uses the Dormand–Prince integration algorithm, with the integration step set to 1×10^{-5}.

We fix $m = 2$ in the observer (8.26). The LMI (8.21) is feasible with $\varepsilon = 0.001$ and $\epsilon_1 = 0.001$, and a solution is

$$P = \begin{bmatrix} 0.0008 & -0.0006 & 0.1021 \\ -0.0006 & 0.0005 & -0.0805 \\ 0.1021 & -0.0805 & 15.0959 \end{bmatrix}, \; K_1 = \begin{bmatrix} k_{1,1} \\ k_{2,1} \\ k_{3,1} \end{bmatrix} = \begin{bmatrix} 1.5 \\ 0.5 \\ 45 \end{bmatrix},$$

and K_2 is chosen such that (8.22) is satisfied. Then we obtain

$$K_2 = \begin{bmatrix} k_{1,2} \\ k_{2,2} \\ k_{3,2} \end{bmatrix} = \begin{bmatrix} 7.1573 \\ 14.1040 \\ 0.0268 \end{bmatrix}.$$

Figures 8.3, 8.4, 8.5, and 8.6 show the obtained results for the initial conditions $x_1 = x_2 = x_3 = 0$, $\hat{x}_1 = 1$, $\hat{x}_2 = 0.5$ and $\hat{x}_3 = 0.002$. The synchronization results were achieved with the polynomial observer.

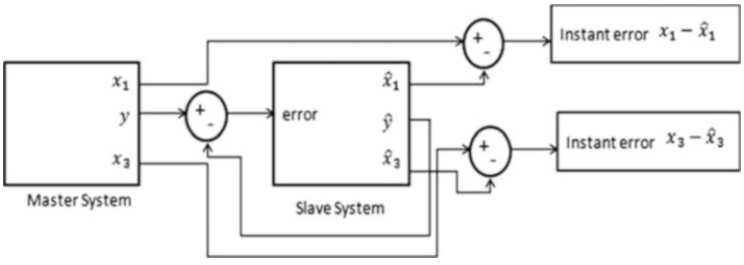

Fig. 8.3 Synchronization diagram

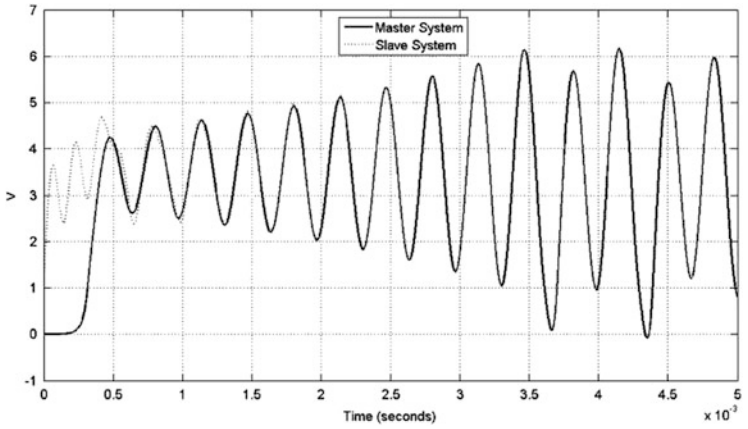

Fig. 8.4 Synchronization of v_{c1}

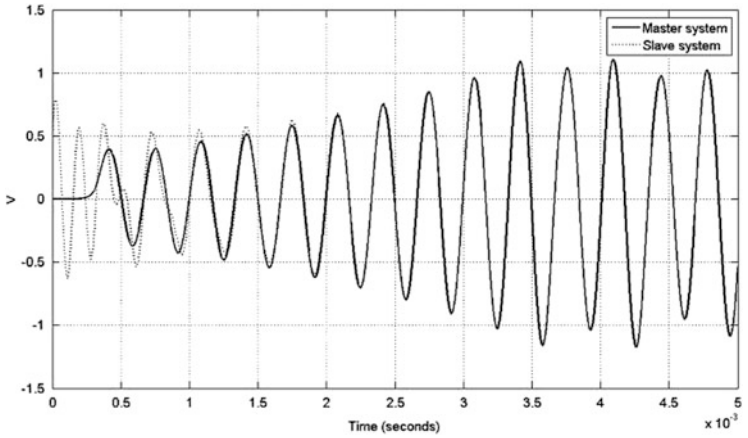

Fig. 8.5 Synchronization of v_{c2}

The performance index (quadratic synchronization error) of the corresponding synchronization process is calculated as [36]

$$J(t) = \frac{1}{t + 0.001} \int_0^t |e(t)|^2_{Q_0} \quad , \quad Q_0 = I.$$

Figures 8.7 and 8.8 illustrate the performance index, which has a tendency to decrease. Finally, Fig. 8.9 presents the synchronization in a phase diagram, where one clearly may observe the chaotic behavior of Chua's circuit.

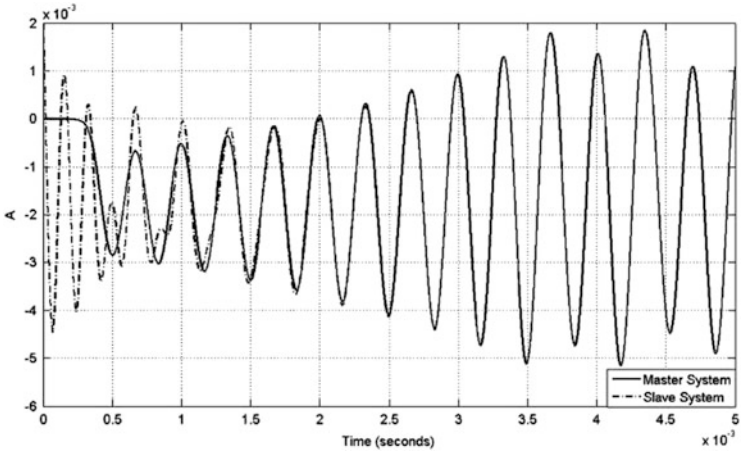

Fig. 8.6 Synchronization of i_L

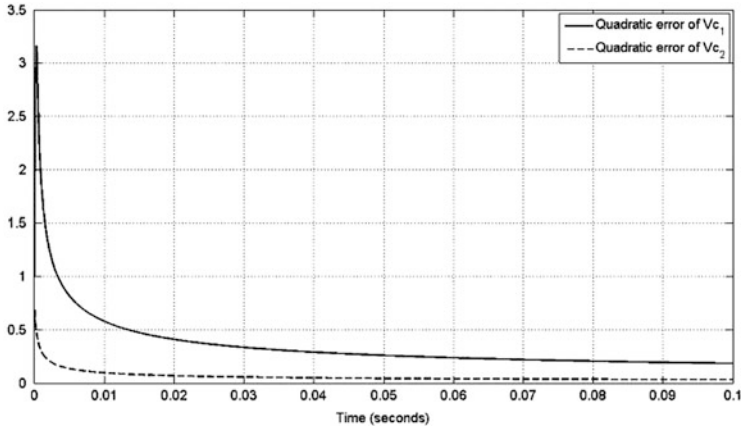

Fig. 8.7 Quadratic synchronization errors of v_{c1} and v_{c2}

8.4.2 Experimental Results

Some experiments were carried out for the synchronization of Chua's system in order to show the performance of the exponential observer. The parameter values are the same as in numerical simulations, but in this case, they were physically implemented. The implementation of Chua's circuit is shown in Figs. 8.10 and 8.11.

The measured output was obtained by means of the oscilloscope LeCroy Wave Runner ® 104MXi. This device supports the Matlab-Simulink® platform, and hence the implementation of the observer was also possible. The initial conditions

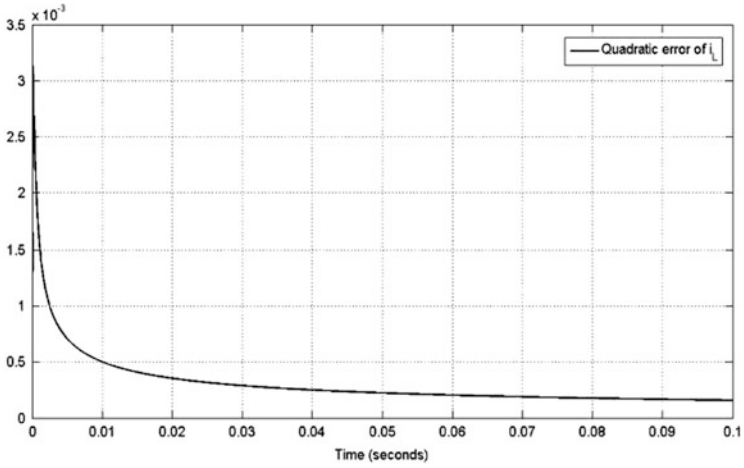

Fig. 8.8 Quadratic synchronization error of i_L

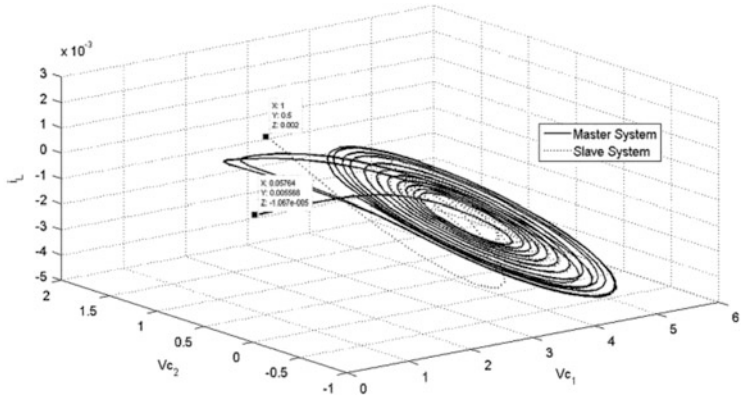

Fig. 8.9 Phase diagram

of the observer were chosen as $\hat{x}_1(0) = 0.5$, $\hat{x}_2(0) = 0.25$, and $\hat{x}_3(0) = 0.001$. Figure 8.12 shows the behavior of the Chua oscillator.

The performance of the proposed observer is evaluated by means of the relative error, which in this case, is defined as

$$\bar{e}_i = \frac{|x_i - \hat{x}_i|}{|x_i|}, \quad i = 1, 3. \tag{8.27}$$

Figures 8.13 and 8.14 illustrate the corresponding relative errors, where it should be noted that $\bar{e}_1 = 0$ and $\bar{e}_3 = 0$ for $t > 0.006$ s, as was expected.

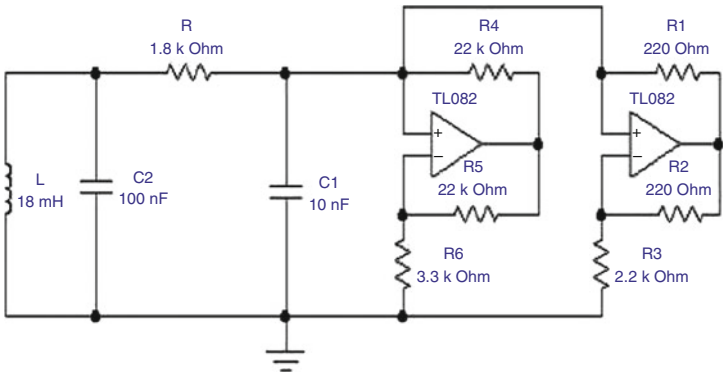

Fig. 8.10 Chua's circuit

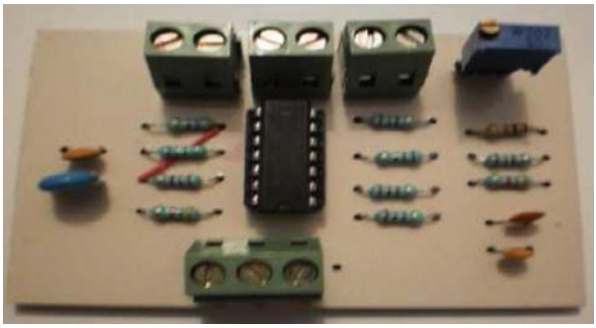

Fig. 8.11 Implementation of Chua's circuit

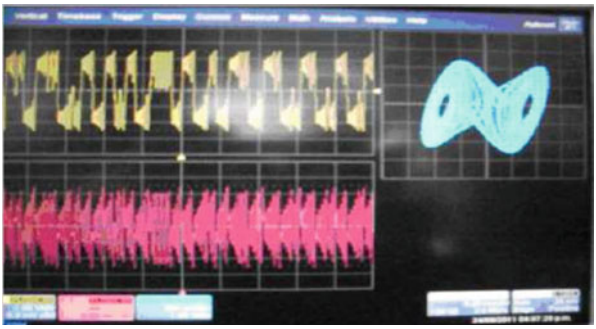

Fig. 8.12 Chaotic behavior of the Chua oscillator

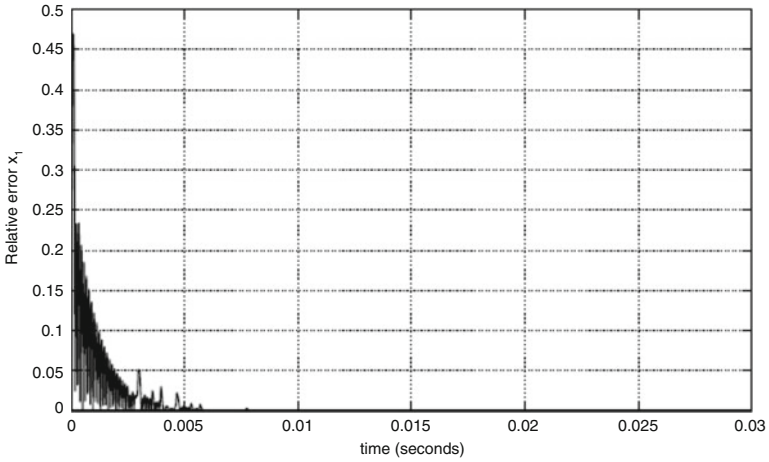

Fig. 8.13 Relative error $\bar{e}_1$

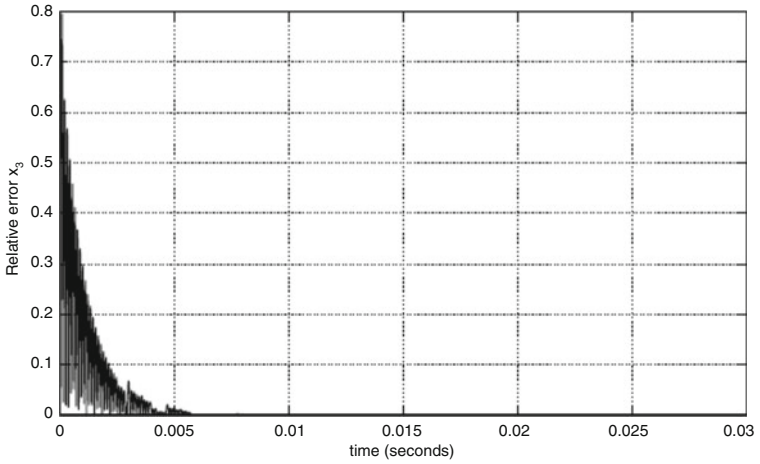

Fig. 8.14 Relative error $\bar{e}_3$

8.5 Concluding Remarks

The synchronization problem of chaotic Liouvillian systems has been treated using differential and algebraic techniques. We proposed a polynomial observer and proved that the estimation error exponentially converges to zero by means of properties of nondecreasing and nonincreasing, linear matrix inequalities, and the Lyapunov method. This observer has been used as a slave system whose states are exponentially synchronized with the chaotic system (Chua's circuit). A reduced set of measurable state variables was needed to achieve the synchronization with this approach. The effectiveness of the suggested methodology was established by means of numerical simulations and real-time implementation.

References

1. L.M. Pecora, T.L. Carroll, Synchronization in chaotic systems. Phys. Rev. Lett. **64**, 821–824 (1990)
2. H. Nijmeijer, I.M.Y. Mareels, An observer looks at synchronization. IEEE Trans. Circuits Syst. I **44**, 882–890 (1997)
3. M. Feki, Observer-based exact synchronization of ideal and mismatched chaotic systems. Phys. Lett. A **309**, 53–60 (2003)
4. O. Morgül, M. Feki, A chaotic masking scheme by using synchronized chaotic systems. Phys. Lett. A **251**, 169–176 (1999)
5. A. Fradkov, *Cybernetical Physics: From Control of Chaos to Quantum Control* (Springer, Berlin, 2007)
6. Y. Ushio, Synthesis of synchronized chaotic systems based on observers. Int. J. Bifurcat. Chaos **9**, 541–546 (1999)
7. T.L. Carroll, L.M. Pecora, Synchronizing chaotic circuits. IEEE Trans. Circuits Syst. I **38**, 453–456 (1991)
8. O. Morgül, E. Solak, Observer based synchronization of chaotic systems. Phys. Rev. E **54**, 4803–4811 (1996)
9. C. Aguilar-Ibañez, R. Martínez-Guerra, R. Aguilar-López, J.L. Mata-Machuca, Synchronization and parameter estimations of an uncertain Rikitake system. Phys. Lett. A **374**, 3625–3628 (2010)
10. X. Zhao, Z. Li, S. Li, Synchronization of a chaotic finance system. Appl. Math. Comput. **217**, 6031–6039 (2011)
11. M. Boutayeb, M. Darouach, H. Rafaralahy, Generalized state observers for chaotic synchronization and secure communication. IEEE Trans. Circuits Syst. I **49**, 345–349 (2002)
12. R. Martínez-Guerra, J.L. Mata-Machuca, R. Aguilar-López, A. Rodríguez-Bollain, Chaotic synchronization and its applications in secure communications (Chapter 8), in *Applications Chaos and Nonlinear Dynamics in Engineering*, ed. by S. Banerjee, M. Mitra, L. Rondoni. Understanding Complex Systems, vol. 1 (Springer, Berlin, 2011), pp. 231–272
13. R. Martínez-Guerra, W. Yu, Chaotic communication and secure communication via sliding-mode observer. Int. J. Bifurcat. Chaos **18**, 235–243 (2008)
14. J. Mata-Machuca, R. Martínez-Guerra, R. Aguilar-López, An exponential polynomial observer for synchronization of chaotic systems. Commun. Nonlinear Sci. Numer. Simulat. **15**, 4114–4130 (2010)
15. R. Martínez-Martínez, J.L. Mata-Machuca, R. Martínez-Guerra, J.A. León, G. Fernández-Anaya, Synchronization of nonlinear fractional order systems. Appl. Math. Comput. **218**, 3338–3347 (2011)
16. J.L. Mata-Machuca, R. Martínez-Guerra, Asymptotic synchronization of the Colpitts oscillator. Comput. Math. Appl. **63**, 1072–1078 (2012)
17. Z. Zhang, H. Shao, Z. Wang, H. Shen, Reduced-order observer design for the synchronization of the generalized Lorenz chaotic systems. Appl. Math. Comput. **218**, 7614–7621 (2012)
18. E. Elabbasy, H. Agiza, M. El-Dessoky, Global chaos synchronization for four scroll attractor by nonlinear control. Sci. Res. Essay **1**, 65–71 (2006)
19. C. Wang, S. Ge, Adaptive backstepping control of uncertain Lorenz system. Int. J. Bifurcat. Chaos **11**, 1115–1119 (2001)
20. D. Ghosh, A. Chowdhury, P. Saha, On the various kinds of synchronization in delayed Duffing–Van der Pol system. Commun. Nonlinear Sci. Numer. Simulat. **13**, 790–803 (2008)
21. G. Grassi, D.A. Miller, Synchronizing chaotic systems up to an arbitrary scaling matrix via a single signal. Appl. Math. Comput. **218**, 6118–6124 (2012)
22. H.B. Fotsin, J. Daafouz, Adaptive synchronization of uncertain chaotic Colpitts oscillator based on parameter identification. Phys. Lett. A **339**, 304–315 (2005)

23. J.L. Mata-Machuca, R. Martínez-Guerra, Ricardo Aguilar-López, C. Aguilar-Ibañez, A chaotic system in synchronization and secure communications. Commun. Nonlinear Sci. Numer. Simulat. **17**, 1706–1713 (2012)
24. M. Ayati, H. Khaloozadeh, Stable chaos synchronisation scheme for nonlinear uncertain systems. IET Control Theory Appl. **4**, 437–447 (2010)
25. Y. Lan, Q. Li, Chaos synchronization of a new hyperchaotic system. Appl. Math. Comput. **217**, 2125–2132 (2010)
26. R. Aguilar-López, J.L. Mata-Machuca, R. Martínez-Guerra, *Observability and Observers for Nonlinear Dynamical Systems: Nonlinear Systems Analysis* (Lambert Academic Publishing (LAP), Germany, 2011). ISBN: 978-3-8454-3171-0
27. R. Martínez-Guerra, J.J. Rincón-Pasaye, Synchronization and anti-synchronization of chaotic systems: a differential and algebraic approach. Chaos Solitons Fractals **28**, 511–517 (2009)
28. R. Martínez-Guerra, J. Mendoza-Camargo, Observers for a class of Liouvillian and, non-differentially flat systems. IMA J. Math. Control Inf. **21**, 493–509 (2004)
29. T. Matsumoto, A chaotic attractor from Chua's circuit. IEEE Trans. Circuit Syst. **31**(12), 1055–1058 (1984)
30. L.O. Chua, Chua's circuit: ten years later. IEICE Trans. Fundam. **E77-A**, 1811–1822 (1994)
31. G. Kolumban, G. Kis, Performance evaluation of FM-DCSK modulation scheme, in *Proceedings of the 1998 International Symposium on Nonlinear Theory and Its Applications (NOLTA'98)*, vol. 1 (Crans-Montana, Switzerland 1998), pp. 81–84
32. S. Jankowski, A. Londei, C. Mazur, A. Lozowski, Synchronization and association in a large network of coupled Chua circuits. Int. J. Electronics **79**, 823–828 (1995)
33. M.P. Kennedy, Robust opamp realization of Chua's circuit. Frequenz **46**(34), 66–68 (1992)
34. L.O. Chua, M. Komuro, T. Matsumoto, The double scroll family, parts I and II. IEEE Trans. Circuits Syst. **33**(11), 1073–1118 (1986)
35. G.Q. Zhong, F. Ayron, Experimental confirmation of chaos Chua's circuit. Int. J. Circuit Theory Appl. **13**(11), 93–98 (1985)
36. R. Martínez-Guerra, A. Poznyak, V. Díaz, Robustness of high-gain observers for closed-loop nonlinear systems: theoretical study and robotics control application. Int. J. Syst. Sci. **31**, 1519–1529 (2000)

Chapter 9
Synchronization of Partially Unknown Nonlinear Fractional-Order Systems

Abstract In this chapter, a synchronization scheme for partially known nonlinear fractional order systems is proposed. In this approach, the unknown dynamics is considered as the master system, and the slave system estimates the unknown variables. For solving this problem, we introduce a fractional algebraic observability property, which is used as the main tool in the design of the master system. As a numerical example, we consider a fractional-order Lorenz chaotic system, and by means of some simulations, we demonstrate the effectiveness of the suggested approach.

9.1 Introduction

We begin by mentioning some works related to synchronization in fractional systems. For example, [6] and [5] proposed a feedback controller that allows one to achieve synchronization between two identical fractional-order chaotic systems. The theoretical analysis utilized is the stability criterion of linear fractional systems; [10] studied the synchronization of fractional-order chaotic systems with unidirectional linear error feedback coupling; [7] presented a classical Luenberger observer design for the synchronization of fractional-order chaotic systems, i.e., the observer structure needs a copy of the system and a linear output error feedback. The application is restricted to scalar coupling signals; [2] and [5] gave sufficient conditions for synchronization between two identical fractional systems using Laplace transform theory.

The main contribution in this chapter is to present a technique for the synchronization problem in partially known nonlinear fractional-order systems. We propose a new procedure using the master–slave synchronization scheme for estimating the unknown state variables based on a fractional algebraic observability (FAO) property (is not required a copy of the system). The rest of this chapter is organized as follows: in Sect. 9.2, we give some basic definitions on fractional derivatives. The main result is given in Sect. 9.3. In Sect. 9.4, we show some numerical simulations, and finally, we give conclusions in Sect. 9.5.

R. Martínez-Guerra et al., *Synchronization of Integral and Fractional Order Chaotic Systems*, Understanding Complex Systems,
DOI 10.1007/978-3-319-15284-4_9

9.2 On Fractional Derivatives

There are several definitions of a fractional derivative of order α; see, for example, [8, 11, 12]. We will use the Caputo fractional operator in the definition of fractional-order systems, because the meaning of the initial conditions for systems described using this operator is the same as for integer-order systems.

Definition 9.1 (Caputo Fractional Derivative) The Caputo fractional derivative of order $\alpha \in \mathbb{R}^+$ of a function x is defined as (see [11])

$$x^{(\alpha)} = {}_{t_0}D_t^{\alpha} x(t) = \frac{1}{\Gamma(m-\alpha)} \int_{t_0}^{t} \frac{d^m x(\tau)}{d\tau^m} (t-\tau)^{m-\alpha-1} \, d\tau, \tag{9.1}$$

where $m-1 \leq \alpha < m$, $\frac{d^m x(\tau)}{d\tau^m}$ is the mth derivative of x in the usual sense, $m \in \mathbb{N}$, and Γ is the gamma function.[1]

Now we define a sequential operator, see [8], as follows:

$$\mathscr{D}^{(r\alpha)} x(t) = \underbrace{{}_{t_0}D_t^{\alpha} \, {}_{t_0}D_t^{\alpha} \ldots {}_{t_0}D_t^{\alpha} \, {}_{t_0}D_t^{\alpha}}_{r\text{-times}} \, x(t), \tag{9.2}$$

i.e., it is the Caputo fractional derivative of order α applied $r \in \mathbb{N}$ times sequentially, with $\mathscr{D}^{(0)} x(t) = x(t)$. We note that if $r = 1$, then $\mathscr{D}^{(\alpha)} x(t) = x^{(\alpha)}$.

9.2.1 Mittag-Leffler-Type Function

The Mittag-Leffler function with two parameters is defined as in [4]:

$$E_{\alpha,\beta}(z) = \Sigma_{i=0}^{\infty} \frac{z^i}{\Gamma(\alpha i + \beta)}, \quad z, \, \beta \in \mathbb{C}, \; \mathbb{R}e(\alpha) > 0. \tag{9.3}$$

This function is used to solve fractional differential equations in analogy to the exponential function in integer-order systems. In the particular case $\alpha = \beta = 1$, we have that $E_{1,1}(z) = e^z$. Now if we have particular values of α, the function (9.3) has asymptotic behavior at infinity.

[1] To simplify the notation, we have omitted the time-dependence on $x^{(\alpha)}$. In what follows, we take $t_0 = 0$.

Theorem 9.1 ([11]) *If $\alpha \in (0,2)$, β is an arbitrary complex number, and μ is an arbitrary real number such that*

$$\frac{\pi\alpha}{2} < \mu < \min\{\pi, \pi\alpha\}, \tag{9.4}$$

then for an arbitrary integer $\kappa \geq 1$ the following expansion holds:

$$E_{\alpha,\beta}(z) = -\Sigma_{i=1}^{\kappa} \frac{1}{\Gamma(\beta - \alpha i) z^i} + O\left(\frac{1}{|z|^{\kappa+1}}\right) \tag{9.5}$$

with $|z| \to \infty$, $\mu \leq |\arg(z)| \leq \pi$. □

The Mittag-Leffler function has the following properties:

Property 1. $\int_0^t \tau^{\beta-1} E_{\alpha,\beta}(-k\tau^\alpha)\, d\tau = t^\beta E_{\alpha,\beta+1}(-kt^\alpha)$, $\beta > 0$ (see [11]).

Property 2. $E_{\alpha,\beta}(-x)$, is completely monotonic, i.e., $(-1)^n E_{\alpha,\beta}^{(n)}(-x) \geq 0$ for $0 < \alpha \leq 1$ and $\beta \geq \alpha$, for all $x \in (0,\infty)$ and $n \in \mathbb{N} \cup \{0\}$ (see [9]).

We will use these facts in the following problem.

9.3 Main Result

We take the initial condition problem for an autonomous fractional-order nonlinear system with $0 < \alpha < 1$:

$$\begin{aligned} x^{(\alpha)} &= f(x), \quad x(0) = x_0, \\ y &= h(\bar{x}), \end{aligned} \tag{9.6}$$

where $x \in \Omega \subset \mathbb{R}^n$, $f : \Omega \to \mathbb{R}^n$ is a Lipschitz continuous function,[2] with $x_0 \in \Omega \subset \mathbb{R}^n$. In this case, y denotes the output of the system (the measure that we can obtain), $\bar{x} \in \mathbb{R}^p$ represents the states that we can observe (known states), $h : \mathbb{R}^p \to \mathbb{R}^q$ is a continuous function, and $1 \leq p < n$.

Consider the system given by (9.6). We will separate it into two dynamical systems with states $\bar{x} \in \mathbb{R}^p$ and $\eta \in \mathbb{R}^{n-p}$ respectively. The whole state is grouped

[2] This ensures a unique solution; see [4].

as $x^T = (\bar{x}^T, \eta^T)$. The first system describes the known states, and the second represents unknown states. Then the system (9.6) can be written as

$$\begin{aligned} \bar{x}^{(\alpha)} &= \bar{f}(\bar{x}, \eta), \\ \eta^{(\alpha)} &= \Delta(\bar{x}, \eta), \\ y &= h(\bar{x}), \end{aligned} \tag{9.7}$$

where $f^T(x) = \left(\bar{f}^T(\bar{x}, \eta), \Delta^T(\bar{x}, \eta)\right)$, $\bar{f} \in \mathbb{R}^p$, and $\Delta \in \mathbb{R}^{n-p}$. Now the problem is this: how can we estimate the η' states? This question arises because if we know the η' states, we can use these signals to generate measurements depending on them. In order to solve this observation problem, let us introduce the following observability property (similar to the property used in nonlinear integer-order systems; see [1]):

Definition 9.2 (FAO) A state variable $\eta_i \in \mathbb{R}$ satisfies the fractional algebraic observability (FAO) criterion if it is a function of the first $r \in \mathbb{N}$ sequential derivatives of the available output $y_{\bar{x}}$, i.e.,

$$\eta_i = \phi_i \left(y_{\bar{x}}, y_{\bar{x}}^{(\alpha)}, \mathscr{D}^{(2\alpha)} y_{\bar{x}}, \ldots, \mathscr{D}^{(r\alpha)} y_{\bar{x}} \right), \tag{9.8}$$

where $\phi_i : \mathbb{R}^{(r+1)p} \to \mathbb{R}$.

If we assume that the components of the unknown state vector η satisfy FAO, then we can describe our problem in terms of the master–slave synchronization scheme, which is defined in the following way.

Consider the master system

$$\eta_i^{(\alpha)} = \Delta_i(\bar{x}, \eta), \tag{9.9}$$

$$y_{\eta_i} = \eta_i = \phi_i \left(y_{\bar{x}}, y_{\bar{x}}^{(\alpha)}, \mathscr{D}^{(2\alpha)} y_{\bar{x}}, \ldots, \mathscr{D}^{(r\alpha)} y_{\bar{x}} \right), \tag{9.10}$$

for $p + 1 \leq i \leq n$, where η_i is a component of the state vector η, and y_{η_i} denotes the output of the ith master system.

Now let us propose a fractional dynamical system with the same order α, which will be the slave system:

$$\hat{\eta}_i^{(\alpha)} = k_{\hat{\eta}_i}(y_{\eta_i} - \hat{\eta}_i), \tag{9.11}$$

$$y_{\hat{\eta}_i} = \hat{\eta}_i, \tag{9.12}$$

for $p + 1 \leq i \leq n$, where $\hat{\eta}_i$ is the state, $y_{\hat{\eta}_i}$ denotes the output of the slave system, and $k_{\hat{\eta}_i}$ is a positive constant.

In the master–slave synchronization scheme, the output of the master system (9.10) describes the target signal, while (9.12) represents the response signal.

Therefore, the synchronization problem can be established as follows: given the master system (9.9) and slave system (9.11), determine some conditions such that the output of the slave system (9.12) synchronizes with the output of the master system (9.10).

Let us define the synchronization error as

$$e_i = y_{\eta_i} - y_{\hat{\eta}_i} = \eta_i - \hat{\eta}_i. \tag{9.13}$$

We now establish a convergence analysis of the synchronization error.

Proposition 9.1 *Let the system (9.6) be expressed in the form (9.7), where the following conditions are satisfied:*

H1: η_i *satisfies the FAO property for* $p+1 \leq i \leq n$.
H2: Δ_i *is bounded, i.e.,* $\exists\, M \in \mathbb{R}^+$ *such that* $\|\Delta(x)\| \leq M$, $\forall\, x \in \Omega$.
H3: $k_{\hat{\eta}_i} \in \mathbb{R}^+$.

Then synchronization of the master output (9.10) with the slave output (9.12) is achieved for a global initial condition of the states.

Proof From H1, we can write Eqs. (9.9)–(9.13). Taking the fractional derivative of Eq. (9.13), we have

$$e_i^{(\alpha)} = \eta_i^{(\alpha)} - \hat{\eta}_i^{(\alpha)}. \tag{9.14}$$

Substituting the fractional dynamics (9.9) and (9.11) into (9.14), we obtain

$$e_i^{(\alpha)} + k_{\hat{\eta}_i} e_i = \Delta_i(x). \tag{9.15}$$

There exists a unique solution for the system (9.15), due to the fact that $\Delta_i(x(t)) - k_{\hat{\eta}_i} e_i(t)$ is a Lipschitz continuous function on e.[3]

The solution of (9.15) is taken from [4]. Then we have

$$\begin{aligned} e_i(t) = {} & e_0 E_{\alpha,1}(-k_{\hat{\eta}_i} t^\alpha) \\ & + \int_0^t (t-\tau)^{\alpha-1} E_{\alpha,\alpha}(k_{\hat{\eta}_i}(t-\tau)^\alpha)\Delta_i(\tau) d\tau, \end{aligned} \tag{9.16}$$

where $e_i(0) = e_{i0}$.

Using the triangle and Cauchy–Schwarz inequalities and H2, we obtain

$$\begin{aligned} |e_i(t)| \leq {} & |e_{i0} E_{\alpha,1}(-k_{\hat{\eta}_i} t^\alpha)|, \\ & + M \int_0^t |(t-\tau)^{\alpha-1} E_{\alpha,\alpha}(-k_{\hat{\eta}_i}(t-\tau)^\alpha)| d\tau. \end{aligned}$$

[3] Equation (9.15) is nonautonomous, but the Lipschitz condition ensures a unique solution [4].

The functions $(t-\tau)^{\alpha-1}E_{\alpha,\alpha}(-k_{\hat{\eta}_i}(t-\tau)^{\alpha})$ and $E_{\alpha}(-k_{\hat{\eta}_i}t^{\alpha})$ are nonnegative due to Property 2 of the Mittag-Leffler function and H3:

$$|e_i(t)| \leq |e_{i0}|E_{\alpha,1}(-k_{\hat{\eta}_i}t^{\alpha}) + M\int_0^t (t-\tau)^{\alpha-1}E_{\alpha,\alpha}(-k_{\hat{\eta}_i}(t-\tau)^{\alpha})d\tau.$$

Using Property 1 of the Mittag-Leffler function gives us

$$|e_i(t)| \leq |e_{i0}|E_{\alpha,1}(-k_{\hat{\eta}_i}t^{\alpha}) + Mt^{\alpha}E_{\alpha,\alpha+1}(-k_{\hat{\eta}_i}t^{\alpha}).$$

If $t \to \infty$, we use Eq. (9.5) with $\mu = 3\pi\alpha/4$ due to H3:

$$\lim_{t\to\infty}|e_i(t)| \leq |e_{i0}|\lim_{t\to\infty}E_{\alpha,1}(-k_{\hat{\eta}_i}t^{\alpha}) + M\lim_{t\to\infty}t^{\alpha}E_{\alpha,\alpha+1}(-k_{\hat{\eta}_i}t^{\alpha}) = \frac{M}{k_{\hat{\eta}_i}}.$$

□

Remark 9.1 If the FAO of a state variable is expressed in terms of the fractional sequential derivatives of the output y, which are unknown, then is necessary to introduce an artificial variable (if it is possible) in order to avoid the use of these unknown derivatives.

9.4 Numerical Example

In this section, we study the synchronization of nonlinear fractional-order systems by numerical simulation.

Remark 9.2 Chaotic systems are characterized by global boundedness of the trajectories (see [3]). By this fact, H2 is always satisfied.

We consider the fractional-order Lorenz system described by a set of three fractional differential equations, as follows:

$$\begin{aligned} x^{(\alpha)} &= \begin{pmatrix} ax_2 - ax_1 \\ bx_1 - cx_2 - x_1x_3 \\ x_1x_2 - dx_3 \end{pmatrix} \\ y &= x_1 \end{aligned} \tag{9.17}$$

with parameters $a = 10$, $b = 28$, $c = -8$, $d = 8/3$, and $\alpha = 0.8$. The system (9.17) exhibits chaotic behavior [13].

Now we will apply the proposed methodology. First, we rewrite system (9.17) in the form (9.7):

$$\begin{aligned} \bar{x}^{(\alpha)} &= a(\eta_2 - \bar{x}_1), \\ \eta^{(\alpha)} &= \begin{pmatrix} b\bar{x}_1 - c\eta_2 - \bar{x}_1\eta_3 \\ \bar{x}_1\eta_2 - d\eta_3 \end{pmatrix}, \\ y_{\bar{x}} &= \bar{x}_1, \end{aligned} \tag{9.18}$$

where $\bar{x}_1 = x_1$, $\eta_2 = x_2$, and $\eta_3 = x_3$.

Before proposing a master system in the form (9.9) and (9.10), we need to determine whether $\eta_2 = x_2$ and $\eta_3 = x_3$ satisfy the FAO property.

For η_2, we have

$$y_{\bar{x}}^{(\alpha)} = a(\eta_2 - y_{\bar{x}}) \quad \Rightarrow \quad \eta_2 = \phi_2\left(y_{\bar{x}}, y_{\bar{x}}^{(\alpha)}\right) = \frac{1}{a}y_{\bar{x}}^{(\alpha)} + y_{\bar{x}}. \tag{9.19}$$

In the same manner for η_3, we obtain

$$\eta_3 = -\frac{1}{y_{\bar{x}}}\left(\eta_2^{(\alpha)} + c\eta_2 - by_{\bar{x}}\right). \tag{9.20}$$

Substituting (9.19) into (9.20), we have

$$\begin{aligned} \eta_3 &= \phi_3\left(y_{\bar{x}}, y_{\bar{x}}^{(\alpha)}, \mathscr{D}^{(2\alpha)}y_{\bar{x}}\right) \\ &= -\frac{1}{ay_{\bar{x}}}\left[\mathscr{D}^{(2\alpha)}y_{\bar{x}} + (a+c)y_{\bar{x}}^{(\alpha)} + a(c-b)y_{\bar{x}}\right]. \end{aligned} \tag{9.21}$$

Note that $\eta_3 = x_3$ loses the FAO property when $y_{\bar{x}} = x_1 = 0$, whence only Eq. (9.19) satisfies FAO with respect to the selected output $y_{\bar{x}} = x_1 \neq 0$.

Then from (9.19), we obtain the following master system in the form (9.9) and (9.10), for $\eta_2 = x_2$:

$$\begin{cases} \eta_2^{(\alpha)} = b\bar{x}_1 - c\eta_2 - \bar{x}_1\eta_3, \\ \\ y_{\eta_2} = \eta_2 = \dfrac{1}{a}y_{\bar{x}}^{(\alpha)} + y_{\bar{x}}. \end{cases} \tag{9.22}$$

The next step is the design of the slave system that synchronizes with (9.22). Using Eq. (9.11), we obtain

$$\hat{\eta}_2^{(\alpha)} = k_{\hat{\eta}_2}(\eta_2 - \hat{\eta}_2). \tag{9.23}$$

Substituting (9.19) into (9.23) leads to

$$\hat{\eta}_2^{(\alpha)} = k_{\hat{\eta}_2}\left(\frac{1}{a}y_{\bar{x}}^{(\alpha)} + y_{\bar{x}}\right) - k_{\hat{\eta}_2}\hat{\eta}_2. \tag{9.24}$$

Since $y_{\bar{x}}^{(\alpha)}$ is not available, the slave (9.24) cannot be implemented. In order to overcome this problem, let us consider the following auxiliary variable $\gamma_{\hat{\eta}_2}$:

$$\gamma_{\hat{\eta}_2} = -\frac{k_{\hat{\eta}_2}}{a}y_{\bar{x}} + \hat{\eta}_2. \tag{9.25}$$

Then

$$\hat{\eta}_2 = \gamma_{\hat{\eta}_2} + \frac{k_{\hat{\eta}_2}}{a}y_{\bar{x}}. \tag{9.26}$$

The fractional derivative of order α of (9.26) is

$$\hat{\eta}_2^{(\alpha)} = \gamma_{\hat{\eta}_2}^{(\alpha)} + \frac{k_{\hat{\eta}_2}}{a}y_{\bar{x}}^{(\alpha)}. \tag{9.27}$$

Substituting (9.26) and (9.27) into (9.24), we obtain

$$\gamma_{\hat{\eta}_2}^{(\alpha)} = -k_{\hat{\eta}_2}\gamma_{\hat{\eta}_2} + \left(1 - \frac{k_{\hat{\eta}_2}}{a}\right)k_{\hat{\eta}_2}y_{\bar{x}}, \qquad \gamma_{\hat{\eta}_2}(0) = \gamma_{\hat{\eta}_{2_0}}. \tag{9.28}$$

Then the slave system for $\eta_2 = x_2$ is given by

$$\begin{cases} \hat{\eta}_2 = \gamma_{\hat{\eta}_2} + \dfrac{k_{\hat{\eta}_2}}{a}y_{\bar{x}} \\ y_{\hat{\eta}_2} = \hat{\eta}_2. \end{cases} \tag{9.29}$$

Now, since the discontinuity of Eq. (9.21) for $y_{\bar{x}} = x_1$ is equal to zero, we cannot construct a slave system for η_3 in the proposed form. To overcome this problem, we propose the following slave system:

$$\begin{cases} \hat{\eta}_3^{(\alpha)} = \bar{x}_1\hat{\eta}_2 - d\,\hat{\eta}_3, \\ y_{\hat{\eta}_3} = \hat{\eta}_3. \end{cases} \tag{9.30}$$

Due to Eq. (9.13) and $\eta_3^{(\alpha)}$ from (9.18),[4] we have

$$e_3^{(\alpha)} + de_3 = \bar{x}_1 e_2. \tag{9.31}$$

It should be noted that Eq. (9.31) has the same form as (9.15). Thus in this case, using Proposition 9.1, we obtain

$$|e_3| \leq \frac{mM}{dk_{\hat{\eta}_2}}, \tag{9.32}$$

where m is the bound of $\bar{x}_1$.

We now present the corresponding simulation. We consider the following initial conditions to the master system: $\bar{x}_1(0) = 1$, $\eta_2(0) = 0$, $\eta_3(0) = -5$. The initial conditions to the slave system are $\hat{\eta}_2(0) = -5$, $\hat{\eta}_3(0) = 20$, and the parameters are $a = 10$, $b = 28$, $c = -8$, $d = 8/3$, $\alpha = 0.8$. The initial conditions of the auxiliary functions are $\gamma_{\hat{\eta}_2}(0) = -20$, and finally, the gain parameter is $k_{\hat{\eta}_2} = 150$. The convergence of the estimates to the true signals is shown in Fig. 9.1.

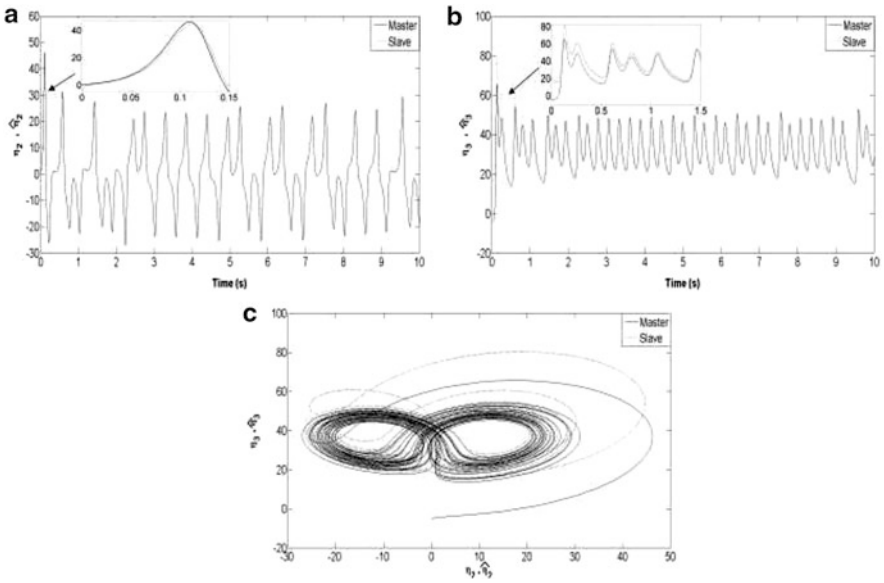

Fig. 9.1 Synchronization of the fractional-order Lorenz system with $a = 10$, $b = 28$, $c = -8$, $d = 8/3$, $\alpha = 0.8$, and initial conditions for master $\bar{x}_1(0) = 1$, $\eta_2(0) = 0$, $\eta_3(0) = -5$ and for slave $\hat{\eta}_2(0) = -5$, $\hat{\eta}_3(0) = 20$: (**a**) and (**b**) shows the estimates convergence, and (**c**) shows the trajectories of master and slave systems

[4]This equation is used instead of FAO.

9.5 Conclusions

We have designed a fractional observer for partially known nonlinear fractional-order systems. We introduced a new concept called fractional algebraic observability, which is of fundamental importance in determining the unknown dynamics of fractional-order nonlinear systems by means of the master–slave synchronization scheme. In particular, we applied the results to chaotic fractional-order systems. However, this technique can be applied to other classes of systems that satisfy the properties of Proposition 9.1.

References

1. R. Aguilar-López, J. Mata-Machuca, R. Martínez-Guerra, *Observability and Observers for Nonlinear Dynamical Systems: Nonlinear Systems Analysis* (Lambert Academic Publishing GmbH & Co. KG, Dudweiler Landstr. 99, 66123 Saarbrücken, Germany 2011)
2. W. Deng, C. Li, Chaos synchronization of the fractional lu system. Physics A **353**, 61–72 (2005)
3. A. Fradkov, *Cybernetical Physics: From Control of Chaos to Quantum Control* (Springer, Berlin, 2007)
4. A. Kilbas, H. Srivastava, J. Trujillo, *Theory and Applications of Fractional Differential Equations* (Elsevier B.V., Amsterdam, 2006)
5. W. Li, W. Deng, Chaos synchronization of fractional-order differential systems. Int. J. Mod. Phys. B **20**, 791–803 (2006)
6. C. Li, X. Liao, J. Yu, Synchronization of fractional order chaotic systems. Phys. Rev. E **68**, 067203-1–067203-3 (2003)
7. J. Lu, Synchronization of a class of fractional-order chaotic systems via a scalar transmitted signal. Chaos Solitons Fractals **27**, 519–525 (2006)
8. K. Miller, B. Ross, *An Introduction to the Fractional Calculus and Fractional Differential Equations* (Wiley, New York, 1993)
9. K. Miller, S. Samko, Completely monotonic functions. Integral Transforms Spec. Funct. **12**, 389–402 (2001)
10. G. Peng, Synchronization of fractional order chaotic systems. Phys. Lett. A **363**, 426–432 (2007)
11. I. Podlubny, *Fractional Differential Equations* (Academic, San Diego, 1999)
12. I. Podlubny, Geometric and physical interpretation of fractional integration and fractional differentiation. Fract. Calc. Appl. Anal. **5**, 367–386 (2002)
13. X. Wen, Z. Mu, J. Lu, Stability analysis of a class of nonlinear fractional-order systems. Trans. Circuits Syst. II IEEE **55**, 1178–1182 (2008)

Chapter 10
Generalized Synchronization via the Differential Primitive Element

Abstract Generalized synchronization (GS) in nonlinear systems appears when the states of one system are equal through a functional mapping to the states of another. This mapping can be obtained if there exists a differential primitive element that generates a differential transcendence basis. We introduce a new definition of GS in nonlinear systems using the concept of differential primitive element. In this chapter, we investigate the GS problem when we have strictly different nonlinear systems, and we consider that for both the slave and master systems, only some states are available from measurements. The first component of the mapping is called a differential primitive element, which in general, is defined by means of a linear combination of the known states and the inputs of the system. Furthermore, we design a new dynamical feedback controller able to achieve complete synchronization in the coordinate transformation systems and GS in the original coordinates. These particular forms of GS are illustrated with numerical results of well-known chaotic benchmark systems.

10.1 Introduction

One of the current challenges is to achieve and explain synchronization of strictly different chaotic systems. The generalized synchronization (GS) concept was introduced in [1], and a new definition is given in this chapter to describe the onset of synchronization in directionally coupled chaotic systems. Generalized synchronization is one of the fundamental phenomena, widely studied recently, having both theoretical and applied significance [2–9]. It occurs when the trajectories of one system are equal through a functional mapping to the trajectories of another. In an equivalent form, GS appears if there exists a differential primitive element that generates a mapping H_{ms} from the trajectories $x_m(t)$ of the attractor in the master algebraic manifold M to the trajectories $x_s(t)$ in the slave space R^{n_s}, i.e., $H_{ms}(x_s(t)) = x_m(t)$ (see Definition 10.2). For identical systems, the functional mapping corresponds to the identity [10].

Two problems in GS can be mentioned: determining whether there exists a functional mapping relating the slave with the master, and determining the form of that function. Some methods require that the form of the functional mapping

R. Martínez-Guerra et al., *Synchronization of Integral and Fractional Order Chaotic Systems*, Understanding Complex Systems,
DOI 10.1007/978-3-319-15284-4_10

be known beforehand to establish the presence of GS, while other methods do not require such knowledge.

In this chapter, we propose a method for GS in nonlinear systems, where it is sufficient to know the output[1] of the system to generate this transformation, which is represented by means of a differential transcendence basis, that is, there exists an element $\bar{y}$, and let $n \geq 0$ be the minimum integer such that $\bar{y}^{(n)}$ is analytically dependent on $\bar{y}, \bar{y}^{(1)}, \ldots, \bar{y}^{(n-1)}$ such that

$$\bar{H}(\bar{y}, \bar{y}^{(1)}, \ldots, \bar{y}^{(n-1)}, \bar{y}^{(n)}, u, u^{(1)}, \ldots, u^{(\gamma)}) = 0. \tag{10.1}$$

The main idea is to find a dynamical control signal such that it is possible to synchronize the coordinate transformation system, that is, the original system is converted to a triangular form through an adequate choice of the differential primitive element given normally as a linear combination of the known states and the inputs of the system, where the coefficients belong to the differential field generated by the field K and the control input u. As far as we know, the GS problem has been tackled with a static feedback using differential geometry. The remainder of this chapter proceeds as follows. In Sect. 10.2, we mention some basic definitions and important results. In Sect. 10.3, we present some numerical simulations, and Sect. 10.4 closes the chapter with some concluding remarks.

10.2 Statement of the Problem and Main Results

Let us consider the following basic definition, along with the definitions given in the introductory chapter (see [11, 12]).

Definition 10.1 A system is Picard–Vessiot (PV) if the $k\langle u\rangle$-vector space generated by the derivatives of the set $\{y^{(\mu)}, \mu \geq 0\}$, has finite dimension.

System (10.1) can be solved locally as

$$\bar{y}^{(n)} = -\mathscr{L}(\bar{y}, \ldots, \bar{y}^{(n-1)}, u, u^{(1)}, \ldots, u^{(\gamma-1)}), +u^{(\gamma)}$$

where we recall that $\xi_i = \bar{y}^{(i-1)}$, $1 \leq i \leq n$. Then a local form is obtained that can be viewed as a generalized observability canonical form (GOCF),

$$\begin{aligned} \dot{\xi}_1 &= \xi_2, \\ \dot{\xi}_2 &= \xi_3, \\ &\vdots \end{aligned}$$

[1] We consider the synchronization when only some states are available from measurements.

$$\begin{aligned}\dot{\xi}_{n-1} &= \xi_n,\\ \dot{\xi}_n &= -\mathscr{L}(\xi_1,\ldots,\xi_n,u,u^{(1)},\ldots,u^{(\gamma-1)}) + u^{(\gamma)},\\ \bar{y} &= \xi_1.\end{aligned} \tag{10.2}$$

Let us now consider the following nonlinear class of systems:

$$\begin{aligned}\dot{x} &= F(x,u),\\ y &= Cx,\end{aligned} \tag{10.3}$$

where $x \in \mathbb{R}^n$ is the state vector, $F(\cdot)$ is a nonlinear vectorial function, u is the input, y is the output, and C is a real matrix of appropriate size.

The next lemma is an important technical result.

Lemma 10.1 *A nonlinear system (10.3) is transformable to a GOCF if and only if it is PV.*

Proof Let the set $\{\epsilon, \epsilon^{(1)},\ldots,\epsilon^{(n-1)}\}$ be a finite differential transcendence basis with $\epsilon^{(i-1)} = y^{(i-1)}$, $1 \le i \le n$, where $n \ge 0$ is the minimum integer such that $y^{(n)}$ is dependent on $y, y^{(1)},\ldots,y^{(n-1)},u,\ldots$. Redefining $\xi_i = \epsilon^{(i-1)}$, $1 \le i \le n$, this yields

$$\begin{aligned}\dot{\xi}_j &= \xi_{j+1} \quad 1 \le j \le n-1,\\ \dot{\xi}_n &= -\mathscr{L}(\xi_1,\ldots,\xi_n,u,\dot{u},\ldots,u^{(\gamma-1)}) + u^{(\gamma)},\\ y &= \xi_1.\end{aligned} \tag{10.4}$$

□

We discuss the GS of nonlinear systems that are completely triangularizable (GOCF). For this class of systems, the GS problem is solvable in the sense of [1, 13] using a dynamic feedback that stabilizes the synchronization error dynamics. The GS problem is stated as follows: consider two nonlinear systems in a master–slave configuration, where the master system is given by

$$\begin{aligned}\dot{x}_m &= F_m(x_m,u_m),\\ y_m &= h_m(x_m),\end{aligned} \tag{10.5}$$

and the slave by

$$\begin{aligned}\dot{x}_s &= F_s(x_s,u_s(x_s,y_m)),\\ y_s &= h_s(x_s),\end{aligned} \tag{10.6}$$

where $x_s = (x_{1_s}, \ldots, x_{n_s}) \in \mathbb{R}^{n_s}$, $x_m = (x_{1_m}, \ldots, x_{n_m}) \in \mathbb{R}^{n_m}$, $h_s : \mathbb{R}^{n_s} \to \mathbb{R}$, $h_m : \mathbb{R}^{n_m} \to \mathbb{R}$, $u_m = (u_{1m}, \ldots, u_{\bar{m}_n}) \in \mathbb{R}^{\bar{m}_n}$, $u_s : \mathbb{R}^{n_s} \times \mathbb{R} \to \mathbb{R}$, y_m, $y_s \in \mathbb{R}$, F_s, F_m, h_s, h_m are assumed to be polynomial in their arguments.

It should be noted that systems (10.5) and (10.6) are not necessarily affine nonlinear systems [12]. Indeed, the dynamics of the slave system does not need to be expressed as a linear part and a nonlinear part as in [14], where the nonlinear vector function is restricted to satisfy a Lipschitz condition.

Definition 10.2 (Generalized Synchronization (GS)) Slave and master systems are said to be in a state of GS if there exists a differential primitive element that generates a mapping $H_{ms} : \mathbb{R}^{n_s} \to \mathbb{R}^{n_m}$ with $H_{ms} = \phi_m^{-1} \circ \phi_s$ as well as an algebraic manifold $M = \{(x_s, x_m) \mid x_m = H_{ms}(x_s)\}$ and a compact set $B \subset \mathbb{R}^{n_m} \times \mathbb{R}^{n_s}$ with $M \subset B$ such that their trajectories with initial condition in B approach M as $t \to \infty$.

Definition 10.2 leads to the following criterion:

$$\lim_{t\to\infty} \| H_{ms}(x_s) - x_m \| = 0. \tag{10.7}$$

Remark 10.1 It should be noted that identical or complete synchronization is a particular case of GS, that is, the transformation H_{ms} is the identity.

The following remark is related to the general form in which one can choose the differential primitive element.

Remark 10.2 The differential primitive element is chosen as

$$y = \sum_i \alpha_i x_i + \sum_j \beta_j u_j \quad \alpha_i, \beta_j \in K\langle u \rangle, \tag{10.8}$$

where $K\langle u \rangle$ is a differential field generated by K, u, and their differential quantities.

Proposition 10.1 *Let systems (10.5) and (10.6) be transformable to a GOCF. Let us define $z_m = (z_{m_1}, \ldots, z_{m_n})'$ and $z_m = (z_{s_1}, \ldots, z_{s_n})'$ as the trajectories of master and slave systems in the coordinate transformation, respectively, with $z_{m_i} = y_m^{(i-1)}$ and $z_{s_i} = y_s^{(i-1)}$, for $1 \le i \le n$. Then*

$$\lim_{t\to\infty} \| z_m - z_s \| = 0, \tag{10.9}$$

which implies that[2]

$$\lim_{t\to\infty} \| H_{ms}(x_s) - x_m \| = 0, \tag{10.10}$$

[2] In other words, the complete synchronization in the coordinate transformation system is achieved, and consequently, GS is obtained in the original coordinates.

where y_m and y_s are the differential primitive elements for the master and slave systems, respectively.

Proof Without loss of generality, we can choose $u_m = 0 \in R^{\bar{m}_n}$. Then the differential primitive element for the master is taken as

$$y_m = \sum_i \alpha_{m_i} x_{m_i} \quad \alpha_{m_i} \in \mathbb{R}\langle u_m \rangle, \tag{10.11}$$

and for the slave system,

$$y_s = \sum_i \alpha_{s_i} x_{s_i} + \sum_j \beta_{s_j} u_{s_j} \quad \alpha_{s_i}, \beta_{s_j} \in \mathbb{R}\langle u_s \rangle, \tag{10.12}$$

which leads to

$$\begin{aligned} \dot{z}_{m_j} &= z_{m_{j+1}} \quad 1 \le j \le n-1, \\ \dot{z}_{m_n} &= -\mathscr{L}_m(z_{m_1}, \ldots, z_{m_n}), \end{aligned} \tag{10.13}$$

and

$$\begin{aligned} \dot{z}_{s_j} &= z_{s_{j+1}} \quad 1 \le j \le n-1, \\ \dot{z}_{s_n} &= -\mathscr{L}_s(z_{s_1}, \ldots, z_{s_n}, u_s, \dot{u}_s, \ldots, u_s^{(\gamma-1)}) + u_s^{(\gamma)}. \end{aligned} \tag{10.14}$$

Let us define the control signals as $u_1 = u$, $u_2 = \dot{u}_s$, $\ldots$, $u_\gamma = u_s^{(\gamma-1)}$. Then we propose the following dynamical system:

$$\begin{aligned} \dot{u}_j &= u_{j+1} \quad 1 \le j \le \gamma - 1, \\ \dot{u}_\gamma &= -\mathscr{L}_m(z_{m_1}, \ldots, z_{m_n}) + \mathscr{L}_s(z_{s_1}, \ldots, z_{s_n}, u_1, \ldots, u_\gamma) + \kappa(z_m - z_s), \end{aligned} \tag{10.15}$$

where $z_m = (z_{m_1}, \ldots, z_{m_n})'$, $z_s = (z_{s_1}, \ldots, z_{s_n})'$, and $\kappa = (\kappa_1, \ldots, \kappa_n)$.

Then the closed-loop dynamics of the synchronization error $e = z_m - z_s$ is given by the augmented system

$$\begin{aligned} \dot{e}_{z_j} &= e_{z_{j+1}} \quad 1 \le j \le n-1, \\ \dot{e}_{z_n} &= -\mathscr{L}_m(z_{m_1}, \ldots, z_{m_n}) + \mathscr{L}_s(z_{s_1}, \ldots, z_{s_n}, u_1, \ldots, u_\gamma) - \dot{u}_\gamma, \\ \dot{u}_j &= u_{j+1} \quad 1 \le j \le \gamma - 1, \\ \dot{u}_\gamma &= -\mathscr{L}_m(z_{m_1}, \ldots, z_{m_n}) + \mathscr{L}_s(z_{s_1}, \ldots, z_{s_n}, u_1, \ldots, u_\gamma) + \kappa e_z. \end{aligned} \tag{10.16}$$

Finally, we have that $\dot{e}_z = Ae_z$ with

$$A = \begin{bmatrix} 0 & 1 & 0 & 0 & \cdots & 0 \\ 0 & 0 & 1 & 0 & \cdots & 0 \\ \vdots & \vdots & \vdots & \ddots & \cdots & 0 \\ 0 & 0 & 0 & 0 & 1 & 0 \\ 0 & 0 & 0 & 0 & 0 & 1 \\ -\kappa_1 & -\kappa_2 & -\kappa_3 & -\kappa_4 & \cdots & -\kappa_n \end{bmatrix}, \tag{10.17}$$

where the control gains $(\kappa_1, \ldots, \kappa_n)$ are chosen such that the spectrum of $A \in \mathbb{R}^{n\times n}$ has only negative real parts. □

From Lemma 10.1 and Proposition 10.1, we establish the following important result.

Corollary 10.1 *A system is in a state of GS if and only if it is PV.*

Proof The proof is trivial and is omitted. □

10.3 Numerical Example

Consider the Lorenz chaotic system

$$\begin{aligned} \dot{x}_{1_L} &= a_L(x_{2_L} - x_{1_L}), \\ \dot{x}_{2_L} &= b_L x_{1_L} - x_{2_L} - x_{1_L} x_{3_L}, \\ \dot{x}_{3_L} &= -c_L x_{3_L} + x_{1_L} x_{2_L}, \end{aligned} \tag{10.18}$$

as the master, where a_L, b_L, and c_L are chosen such that (10.18) is chaotic. Let the differential primitive element be the output of system (10.18) as $y_L = x_{1_L}$.

Then we propose a coordinate transformation system

$$\begin{bmatrix} z_{1_L} \\ z_{2_L} \\ z_{3_L} \end{bmatrix} = \begin{bmatrix} y_L \\ \dot{y}_L \\ \ddot{y}_L \end{bmatrix} = \begin{bmatrix} x_{1_L} \\ a_L(x_{2_L} - x_{1_L}) \\ a_L(b_L x_{1_L} - x_{2_L} - x_{3_L} x_{1_L} - a_L(x_{2_L} - x_{1_L})) \end{bmatrix} = \Phi_L(x_L). \tag{10.19}$$

In the transformed coordinates (10.19), the Lorenz system (10.18) can be rewritten as

$$\begin{aligned} \dot{z}_{1_L} &= z_{2_L}, \\ \dot{z}_{2_L} &= z_{3_L}, \\ \dot{z}_{3_L} &= \Psi_L(x_L), \end{aligned} \tag{10.20}$$

where $\Psi_L(x_L) = (a_L^2 + a_L b_L - a_L x_{3_L})\dot{x}_{1_L} - (a_L^2 + a_L)\dot{x}_{2_L} - a_L x_{1_L} \dot{x}_{3_L}$.

Suppose Chua's chaotic system [15] is the controlled slave system,

$$\begin{aligned}\dot{x}_{1_c} &= a_c(x_{2_c} - x_{1_c} - \nu_x),\\ \dot{x}_{2_c} &= x_{1_c} - x_{2_c} + x_{3_c},\\ \dot{x}_{3_c} &= -b_c x_{2_c},\end{aligned} \tag{10.21}$$

where $\nu_x = m_o x_{1_c} + \frac{1}{2}(m_1 - m_o)(|x_{1_c} + 1| - |x_{1_c} - 1|) \in R$, and the parameters a_c, b_c, m_o, and m_1 are chosen such that (10.21) is chaotic.

In this case, we assume the differential primitive element as the output of system (10.21) along with the control input $y_c = x_{3_c} + u_1$.

Using Proposition 10.1, the controlled coordinate transformation system (10.21) can be rewritten as

$$\begin{bmatrix} z_{1_c} \\ z_{2_c} \\ z_{3_c} \end{bmatrix} = \begin{bmatrix} y_c \\ \dot{y}_c \\ \ddot{y}_c \end{bmatrix} = \begin{bmatrix} x_{3_c} + u_1 \\ -b_c x_{2_c} + u_2 \\ -b_c(x_{1_c} - x_{2_c} + x_{3_c}) + u_3 \end{bmatrix} = \Phi_c(x_c), \tag{10.22}$$

where $u_1 = u$, $u_2 = \dot{u}$, and $u_3 = \ddot{u}$ are control signals that need to be designed in order to achieve synchronization between trajectories of coordinate transformation systems (10.19) and (10.22). The augmented controlled system in the transformed coordinates (10.22) is represented as

$$\begin{aligned}\dot{z}_{1_c} &= z_{2_c},\\ \dot{z}_{2_c} &= z_{3_c},\\ \dot{z}_{3_c} &= \Psi(x_c) + \bar{u},\\ \dot{u}_1 &= u_2,\\ \dot{u}_2 &= u_3,\\ \dot{u}_3 &= \bar{u},\end{aligned} \tag{10.23}$$

where $\Psi_c(x_c) = -b(\dot{x}_{1_c} - \dot{x}_{2_c} + \dot{x}_{3_c})$.

Then the control objective is to find $\bar{u}$ such that the trajectories of slave system (10.23) follows the trajectories of master system (10.20). In other words, we need to find $\bar{u}$ of system (10.23) such that $(z_{1_c}, z_{2_c}, z_{3_c}) \to (z_{1_L}, z_{2_L}, z_{3_L})$ as $t \to \infty$.

Defining the synchronization error in the transformed coordinates as $e_z = z_L - z_c$, the error dynamics is given by

$$\begin{aligned}\dot{e}_1 &= e_2,\\ \dot{e}_2 &= e_3,\\ \dot{e}_3 &= \Psi_L(x_L) - \Psi_c(x_c) - \bar{u}_c(x_c, y_c).\end{aligned} \tag{10.24}$$

10.3.1 Stability Analysis

If the control input $\bar{u}$ is defined as

$$\bar{u}_c(x_c, y_L) = \dot{u}_3 = \Psi_L(x_L) - \Psi_c(x_c) + \kappa e_z,$$

then $\kappa = [\kappa_1, \kappa_2, \kappa_3]$ is the vector of gains. With the selected control input, the closed-loop dynamics is given by $\dot{e}_z = Ae_z$, where $A \in \mathbb{R}^{3\times 3}$:

$$A = \begin{bmatrix} 0 & 1 & 0 \\ 0 & 0 & 1 \\ -\kappa_1 & -\kappa_2 & -\kappa_3 \end{bmatrix}.$$

By means of the Routh–Hurwitz criterion, we conclude that $\|e_z\| \to 0$ as $t \to \infty$ if $\kappa_1 > 0$, $\kappa_3 > 0$, and $\kappa_2 > \dfrac{\kappa_1}{\kappa_3}$.

10.3.2 Simulation Results

Figure 10.1 shows the generalized synchronization of master and slave systems in the coordinate transformation, with $a_L = 10$, $b_L = 28$, $c_L = 8/3$, $a_c = 15$, $b_c = 25.58$, $m_o = -5/7$, $m_1 = -8/7$, $\kappa_1 = 130$, $\kappa_2 = 790$, and $\kappa_3 = 130$.

The inverse transformations leads to

$$\begin{bmatrix} x_{1_L} \\ x_{2_L} \\ x_{3_L} \end{bmatrix} = \begin{bmatrix} z_{1_L} \\ z_{1_L} + \dfrac{z_{2_L}}{a_L} \\ -\dfrac{z_{3_L}}{a_L z_{1_L}} - (1 + \dfrac{1}{a_L})\dfrac{z_{2_L}}{z_{1_L}} + b_L - 1 \end{bmatrix} = \Phi_L^{-1}(z_L) \tag{10.25}$$

and

$$\begin{bmatrix} x_{1_c} \\ x_{2_c} \\ x_{3_c} \end{bmatrix} = \begin{bmatrix} -\dfrac{1}{b_c}(z_{3_c} - u_3) - \dfrac{1}{b_c}(z_{2_c} - u_2) - (z_{1_c} - u_1) \\ -\dfrac{1}{b_c}(z_{2_c} - u_2) \\ z_{1_c} - u_1 \end{bmatrix} = \Phi_c^{-1}(z_c). \tag{10.26}$$

Figure 10.2 gives the corresponding synchronization errors in the transformed coordinates, illustrating the performance of the proposed approach. Finally, the

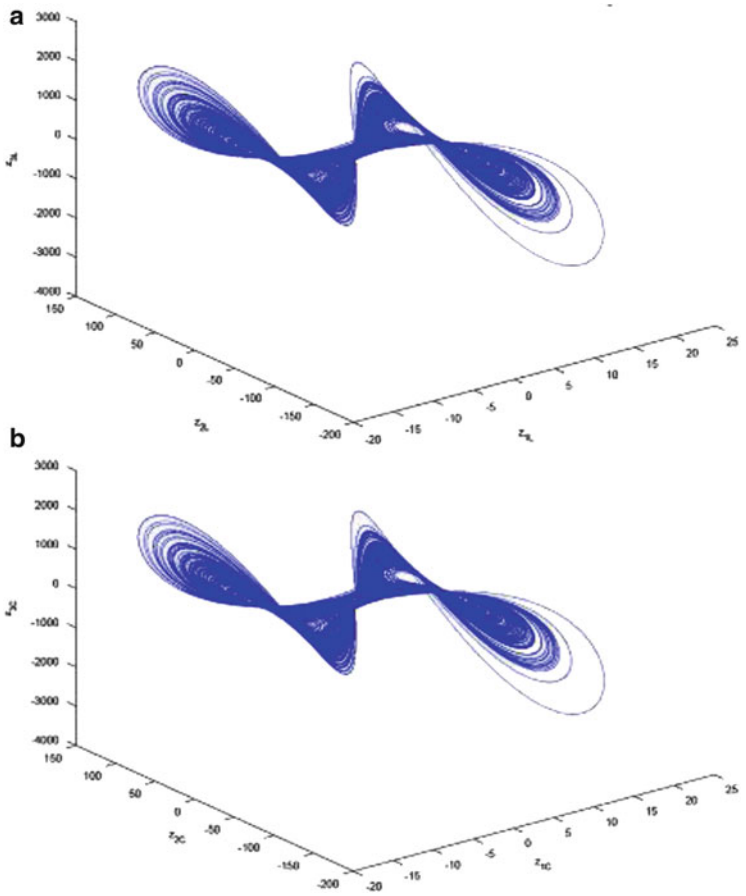

Fig. 10.1 Generalized synchronization in the transformed variables $(z_{1_L}, z_{2_L}, z_{3_L})$ and $(z_{1_c}, z_{2_c}, z_{3_c})$: (**a**) master system, (**b**) slave system

transformation that satisfies Definition 10.2 is given by

$$H_{Lc} = \Phi_L^{-1} \circ \Phi_c = \begin{bmatrix} -\frac{1}{b_c}[a_L \dot{x}_{2_L} - (a_L - 1)\dot{x}_{1_L}] - x_{1_L} + \frac{1}{b_c}(u_2 + u_3) + u_1 \\ -\frac{1}{b_c}(\dot{x}_{1_L} - u_2) \\ x_{1_L} - u_1 \end{bmatrix}.$$

Then GS is achieved, and Fig. 10.3 shows that $\|H_{cL}(x_c) - x_L\| \to 0$ as $t \to \infty$.

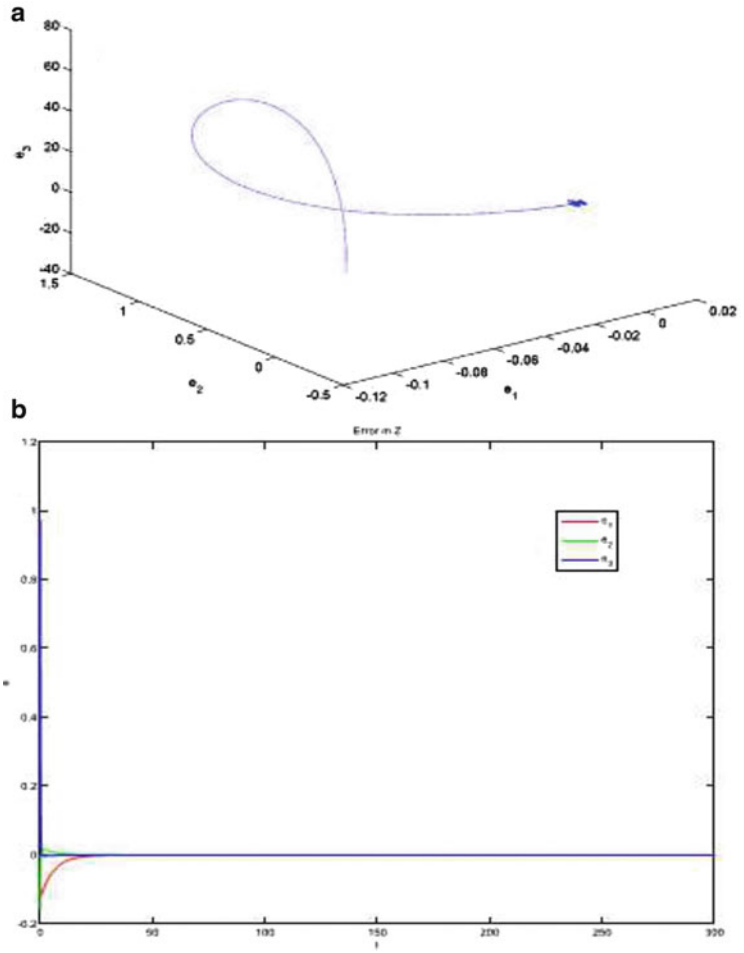

Fig. 10.2 Synchronization errors in the transformed coordinates: (**a**) phase portrait, (**b**) time scale

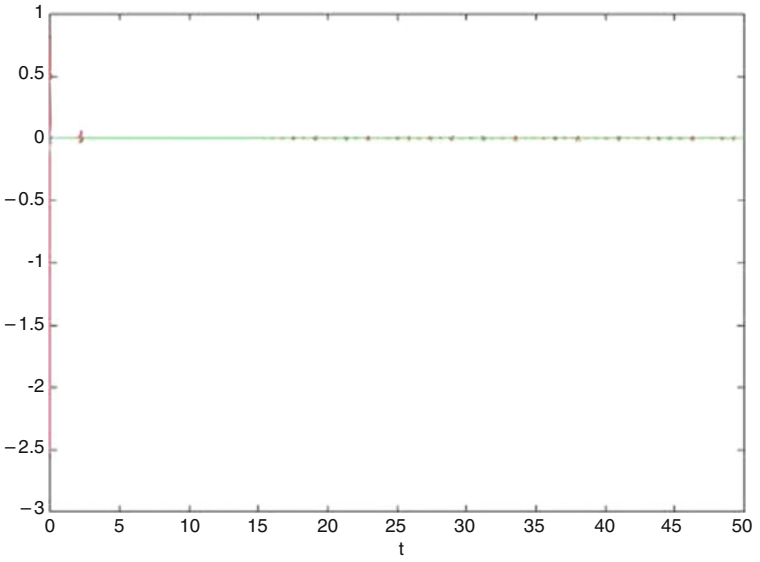

Fig. 10.3 Generalized synchronization errors in the original coordinates

10.4 Concluding Remarks

This chapter tackled the generalized synchronization problem in strictly different nonlinear systems by means of dynamical feedback control signals. To overcome this problem, we employed the differential primitive element given in general form as a linear combination of measurements and control inputs. We have also introduced a new definition using the concept of differential primitive element. Indeed, we have designed a dynamical feedback controller able to achieve identical synchronization in the coordinate transformation systems, and then GS in the original coordinates was obtained. Finally, some numerical results illustrated the effectiveness of the proposed methodology.

References

1. N.F. Rulkov, M.M. Sushchik, L.S. Tsimring, H.D.I. Abarbanel, Generalized synchronization of chaos in directionally coupled chaotic systems. Phys. Rev. E **51**, 980–994 (1995)
2. B.S. Dmitriev, A.E. Hramov, A.A. Koronovskii, A.V. Starodubov, D.I. Trubetskov, Y. Zharkov, First experimental observation of generalized synchronization phenomena in microwave oscillators. Phys. Rev. Lett. **102**, 74–101 (2009)
3. O.I. Moskalenko, A.A. Koronovskii, A.E. Hramov, Generalized synchronization of chaos for secure communication: remarkable stability to noise. Phys. Lett. A **374**, 2925–2931 (2010)
4. H. Liu, J. Chen, J. Lu, M. Cao, Generalized synchronization in complex dynamical networks via adaptive couplings. Physica A **389**, 1759–1770 (2010)

5. M. Sun, C. Zeng, L. Tian, Linear generalized synchronization between two complex networks. Commun. Nonlinear Sci. Numer. Simul. **15**, 2162–2167 (2010)
6. Y.-W. Wang, Z.-H. Guan, Generalized synchronization of continuous chaotic system. Chaos Solitons Fractals **27**, 97–101 (2006)
7. A. Kittel, J. Parisi, K. Pyragas, Generalized synchronization of chaos in electronic circuits experiments. Physica D **112**, 459–471 (1998)
8. Y.-W. Wen Wang, C. Yan, M. Xiao, J. Wen, Adaptive control and synchronization for chaotic systems with parametric uncertainties. Phys. Lett. A **372**(14), 2409–2414 (2008)
9. Y.H. Huang, Y.-W Wang, J.-W. Xiao, Generalized lag-synchronization of continuous chaotic system. Chaos Soliton Fractals **40**(2), 766–770 (2009)
10. W. Liu, X. Qiana, J. Yang, J. Xiao, Antisynchronization in coupled chaotic oscillators. Phys. Lett. A **354**, 119–125 (2006)
11. E.R. Kolchin, *Differential Algebra and Algebraic Groups* (Academic, New York, 1973)
12. R. Aguilar-López, J.L. Mata-Machuca, R. Martínez-Guerra, *Observability and Observers for Nonlinear Dynamical Systems: Nonlinear Systems Analysis* (Lambert Academic Publishing, Germany, 2011)
13. L. Kocarev, U. Parlitz, Generalized synchronization, predictability and equivalence of unidirectionally coupled dynamical systems. Phys. Rev. Lett. **76**, 1816–1819 (1996)
14. J. Meng, X. Wang, Generalized synchronization via nonlinear control. Chaos **18**, 023108 (2008)
15. R. Martínez-Guerra, D.M.G. Corona-Fortunio, J.L. Mata-Machuca, Synchronization of chaotic Liouvillian systems: an application to Chua's oscillator. Appl. Math. Comput. **219**, 10934–10944 (2013)

Chapter 11
Generalized Synchronization for a Class of Nondifferentially Flat and Liouvillian Chaotic Systems

Abstract In this chapter, we study the problem of generalized synchronization (GS) for a class of nondifferentially flat and Liouvillian systems. In nonlinear systems, the GS of a state exists if it is possible to define a mapping such that the states of one system are equal to those of another. From the point of view of differential algebra, we propose a very special transformation in order to achieve GS for this class of systems that have a nonflat output. The transformation is generated via the differential primitive element, which is a linear combination of states and inputs of the system with coefficients in a differential field. Finally, we construct a dynamical control obtained through a chain of integrators to reach the GS. This is illustrated by means of numerical simulations to show the effectiveness of the methodology proposed.

11.1 Introduction

The problem of synchronization between chaotic systems has been studied for many years. Among the pioneering works are those of Pecora–Carroll [8], who tackle the problem of complete or identical synchronization. In this case, the synchronization happens between two systems with the same dynamics but different initial conditions or parameters. Rulkov [9] studied the case of synchronization called generalized synchronization (GS), which considers systems with different dynamics, and [10] presents some possible applications of generalized synchronization of chaotic systems to communications.

The synchronization problem from a control theory point of view has been studied by various techniques, including differential geometry [1] and differential algebra [5]. The differential geometry approach employs Lie derivatives as tools, while differential algebra uses differential rings and fields as well as some elements of algebraic geometry. Using tools of differential algebra, the generalized synchronization problem can be solved if the system satisfies an alternative definition related to the algebraic observability condition (AOC) [7] for nondifferentially flat and Liouvillian systems, which is introduced in this chapter. If it is satisfied, we can construct a coordinate transformation using the differential primitive element theorem [5] to bring the system into so-called generalized observability canonical

R. Martínez-Guerra et al., *Synchronization of Integral and Fractional Order Chaotic Systems*, Understanding Complex Systems,
DOI 10.1007/978-3-319-15284-4_11

form (GOCF). And finally, generalized synchronization is achieved via a dynamical feedback controller obtained through a chain of integrators in the transformed space; as far as we know, the generalized synchronization problem has not previously been attacked from this standpoint.

Here we address the generalized synchronization problem to those systems that are nondifferentially flat and Liouvillian, that is, the output is nonflat, or in other words, there exist system variables that cannot be expressed as a differential algebraic function of the output (the algebraic defect is not zero [4, 6]) and can be obtained by an adjunction of integrals or exponential of an integral of elements of the flat field.

In this chapter, we attack the generalized synchronization problem by means of differential-algebra techniques for a class of nondifferentially flat and Liouvillian systems [3]. Later, we will show that it is possible to obtain a very special transformation whose the first component is the integral of the nonflat output system (differential primitive element). The rest of this chapter is organized as follows: In Sect. 11.2, we present some basic definitions. The problem statement and methodology for generalized synchronization are presented in Sect. 11.3, while numerical simulations are described in Sect. 11.4. Finally, Sect. 11.5 contains some concluding remarks.

11.2 Definitions

This section begins with some basic definitions of differential algebra, and we recall the Definitions given in Chap. 1. Here H can be considered a Hardy field [6].

Definition 11.1 A differential field extension H/k is given by the differential fields H and k such that:

(i) k is a subfield of H.
(ii) The usual rules of derivation of k are the restrictions of the rules of derivation of H.

Definition 11.2 An element $\alpha \in H$ is said to be differentially algebraic over k if it satisfies a differential equation defined by the polynomial over k in α and its time derivatives, $P(\alpha, \dot{\alpha}, \ldots, \alpha^{(n)}) = 0$.

Definition 11.3 An element $\alpha \in H$ is said to be differentially transcendental over k if it is not differentially algebraic over k.

In accordance with the theorem of the differential primitive element [5], there exists a differential primitive element $\delta \in H$ such that $H = k\langle\delta\rangle$, i.e., H is differentially generated by H and δ.

Definition 11.4 A dynamics is defined as a finitely generated differential algebraic extension $H/k\langle u\rangle$ of the differential field $k\langle u\rangle$, where $k\langle u\rangle$ denotes the differential field generated by k and a finite set of differential quantities $u = (u_1, u_2, \ldots, u_m)$.

Before giving the definition of a Liouvillian system that considers the concept of flat subsystem, we present the following nonlinear systems in order to motivate such a definition.

Example 11.1 We pick out the following nonlinear system (see Example 8.1):

$$\begin{aligned} \dot{x}_1 &= x_2 + x_3^2, \\ \dot{x}_2 &= x_3, \\ \dot{x}_3 &= u. \end{aligned} \tag{11.1}$$

Let the output be given by $y = x_2$. Then we have

$$\begin{aligned} x_2 &= y, \\ x_3 &= \dot{y}, \\ u &= \ddot{y}, \\ \dot{x}_1 &= y + \dot{y}^2. \end{aligned} \tag{11.2}$$

We can see that x_1 is the only variable of the system (11.1) that cannot be expressed as a differential algebraic function of the output y (see [7]).

Now we consider one more example.

Example 11.2 Consider the following chaotic system, which is the model of a Colpitts oscillator:

$$\begin{aligned} \dot{x}_1 &= -ae^{-x_2} + ax_3 + a, \\ \dot{x}_2 &= bx_3, \\ \dot{x}_3 &= -cx_1 - cx_2 - dx_3. \end{aligned} \tag{11.3}$$

Let $y = x_3$ be the system output of (11.3). Then the system's variables can be written as

$$\begin{aligned} x_3 &= y, \\ \dot{x}_2 &= by, \\ x_1 &= \frac{1}{c}[-\dot{y} - dy - cx_2]. \end{aligned} \tag{11.4}$$

It can be seen that x_1 and x_2 are not differentially algebraic, because neither state satisfies Definition 11.2, i.e., we cannot express them as a differential algebraic polynomial in y. By virtue of (11.2) and (11.4), we introduce the concept of Liouvillian system:

Definition 11.5 ([3, 6]) Let the system H/k and M be such that $k \subset M \subset H$. Moreover, we assume that M/k is the flat subsystem of H/k. Then we will say that H/k is Liouvillian if the elements of $H - M$ can be obtained by an adjunction of an integral or exponential of an integral of elements of the flat field M.

Definition 11.6 ([4, 6]) A system H/k is differentially flat if its algebraic defect is zero. If its algebraic defect is nonzero, then the system H/k is said nondifferentially flat.

An example that illustrates Definition 11.6 is the following:

Example 11.3 Let H/k be as in Example 11.1, but let the output be given by $y = x_1$, called a linearizing output. Then we obtain the following relationships:

$$\begin{aligned} x_1 &= y, \\ x_2 &= \dot{y} - y^2 \\ x_3 &= \ddot{y} - 2y\dot{y}, \\ u &= y^{(3)} - 2\dot{y}^2 - 2y\ddot{y}. \end{aligned} \tag{11.5}$$

It is clear that all variables of system (11.1) for the output $y = x_1$ can be expressed as a differential algebraic function of the output y.

We then say that the defect of the system is zero, because all variables of system (11.1) for $y = x_1$ can be written as a differential algebraic function of the output y (see Definition 11.2). Otherwise, the defect is different from zero, and its cardinality depends on the number of expressions that do not appear as differentially algebraic functions.

Taking Examples 11.1 and 11.2, we state that the defect for Example 11.1 is nonzero and equal to 1 and that the defect for Example 11.2 is equal to 2, that is, the systems of Examples 11.1 and 11.2 are nondifferentially flat.

Example 11.4 We continue with Examples 11.1 and 11.2, but now we consider Definition 11.5. For the system (11.1), x_1 can be obtained as

$$x_1 = \int (y + \dot{y}^2). \tag{11.6}$$

Now consider system (11.3). Then x_1 and x_2 can be obtained as

$$\begin{aligned} x_2 &= b \int y, \\ x_1 &= \frac{1}{c}\left[-\dot{y} - dy - cb \int y\right]. \end{aligned} \tag{11.7}$$

We conclude that the systems (11.1) and (11.3) with outputs $y = x_2$ and $y = x_3$ respectively are Liouvillian and that the state variables can be obtained by means of the output, its derivatives, and its integrals.

11.3 Problem Statement and Methodology to Generalized Synchronization (GS)

Under the master–slave configuration, we can solve the problem of GS if there exists a mapping H_{ms} from the master trajectories $x_m(t)$ in an algebraic manifold M to the slave trajectories $x_s(t)$ in the slave space, i.e., $H_{ms}(x_s) = x_m$. In order to find such mapping, we look for a transformation for both the master system and the slave system. Such transformations can be obtained via the differential primitive element, and they allow us to construct a dynamical feedback, which we propose as a tool for the generalized synchronization problem. The transformation will be dependent on the primitive element $\bar{y}$ and its derivatives such that $\bar{y}^{(n)}$ is dependent on $(\bar{y}, \ldots, \bar{y}^{(n-1)}) = (\int y, y, \dot{y}, \ldots, y^{(n-2)})$:

$$\bar{T}(\bar{y}, \ldots, \bar{y}^{(n-1)}, \bar{y}^{(n)}, u, u^{(1)}, \ldots, u^{(\gamma)}) = 0. \tag{11.8}$$

In a local way, the system (11.8) can be solved as

$$\bar{y}^{(n)} = -\mathscr{F}(\bar{y}, \ldots, \bar{y}^{(n-1)}, u, u^{(1)}, \ldots, u^{(\gamma-1)}) + u^{(\gamma)}, \tag{11.9}$$

and recalling $z_i = \bar{y}^{(i-1)},\ 1 \leq i \leq n$, we achieve a local form, which can be seen as a generalized observability canonical form (GOCF):

$$\begin{aligned}
\dot{z}_1 &= z_2, \\
\dot{z}_2 &= z_3, \\
&\vdots \\
\dot{z}_{n-1} &= z_n, \\
\dot{z}_n &= -\mathscr{F}(z_1, \ldots, z_n, u, u^{(1)}, \ldots, u^{(\gamma-1)}) + u^{(\gamma)}, \\
y_z &= z_2,
\end{aligned} \tag{11.10}$$

where $y = z_2$ is the output in new coordinates. Now we consider a nondifferentially flat and Liouvillian system class in general as

$$\begin{aligned}
\dot{x} &= F(x, u), \\
y &= Cx,
\end{aligned} \tag{11.11}$$

where $x \in \mathbb{R}^n$ is the state vector, $F(x,u)$ is a nonlinear vectorial function, u is the input, y is the output, and C is a real matrix of appropriate size.

The next lemma is an important result.

Lemma 11.1 *A nondifferentially flat and Liouvillian system class (11.11) is transformable to a GOCF if and only if it is PV.*

Proof Let the set $\{\zeta, \zeta^{(1)}, \ldots, \zeta^{(n-1)}\}$ be a finite differential transcendence basis with $\zeta = \int y$, $\zeta^{(i-1)} = y^{(i-2)}$, $2 \leq i \leq n$, where $n \geq 0$ is the minimum integer such that $y^{(n-1)}$ is dependent on $\int y, y, y^{(1)}, \ldots, y^{(n-2)}, u, \ldots$.

If we redefine $z_1 = \zeta = \int y$, then $z_i = \zeta^{(i-1)} = y^{(i-2)}$, $2 \leq i \leq n$ yields

$$\begin{aligned}
\dot{z}_j &= z_{j+1} \quad 1 \leq j \leq n-1,\\
\dot{z}_n &= -\mathscr{F}(z_1, \ldots, z_n, u, \dot{u}, \ldots, u^{(\gamma-1)}) + u^{(\gamma)},\\
y_z &= z_2.
\end{aligned}$$

□

Remark 11.1 PV systems are defined in Chap. 10.

We now study the problem of GS. First, we consider the master–slave configuration whereby both systems are nondifferentially flat and Liouvillian. Such a configuration is given as follows: The master system is given by

$$\begin{aligned}
\dot{x}_m &= F_m(x_m, u_m),\\
y_m &= h_m(x_m),
\end{aligned} \tag{11.12}$$

and we represent the slave system as

$$\begin{aligned}
\dot{x}_s &= F_s(x_s, u_s(x_s, y_m)),\\
y_s &= h_s(x_s),
\end{aligned} \tag{11.13}$$

where $x_s = (x_{1_s}, \ldots, x_{n_s}) \in \mathbb{R}^{n_s}$, $x_m = (x_{1_m}, \ldots, x_{n_m}) \in \mathbb{R}^{n_m}$, $h_s : \mathbb{R}^{n_s} \to \mathbb{R}$, $h_m : \mathbb{R}^{n_m} \to \mathbb{R}$, $u_m = (u_{1m}, \ldots, u_{\bar{m}_n}) \in \mathbb{R}^{\bar{m}_n}$, $u_s : \mathbb{R}^{n_s} \times \mathbb{R} \to \mathbb{R}$, $y_m, y_s \in \mathbb{R}$, $F_m(\cdot)$, $F_s(\cdot)$, $h_m(\cdot)$, $h_s(\cdot)$ are assumed to be polynomial in their arguments.

We establish the following important result.

Lemma 11.2 *A nondifferentially flat and Liouvillian system class that is a PV system is in a state of generalized synchronization.*

Proof The proof is followed immediately and is omitted (transitivity).

In what follows, we give an example of generalized synchronization of two systems that are nondifferentially flat and Liouvillian (Rössler and Chua).

11.4 Generalized Synchronization of Rössler and Chua Systems

In this section, we consider a Rössler's system [2] that is nondifferentially flat and Liouvilian when the output is chosen as $y_m = x_{m_1}$. The master system has the following dynamics:

$$\begin{aligned} \dot{x}_{m_1} &= -x_{m_2} - x_{m_3}, \\ \dot{x}_{m_2} &= x_{m_1}, \\ \dot{x}_{m_3} &= a_m(x_{m_2} - x_{m_2}^2) - b_m x_{m_3}, \\ y_m &= x_{m_1}. \end{aligned} \tag{11.14}$$

So by choosing the differential primitive element as $z_{m_1} = \bar{y}_m = \int y_m = x_{m_2}$, the coordinate transformation constructed is given by

$$\begin{bmatrix} z_{m_1} \\ z_{m_2} \\ z_{m_3} \end{bmatrix} = \begin{bmatrix} x_{m_2} \\ \dot{x}_{m_2} \\ \ddot{x}_{m_2} \end{bmatrix} = \begin{bmatrix} \int y_m \\ y_m \\ \dot{y}_m \end{bmatrix} = \begin{bmatrix} x_{m_2} \\ x_{m_1} \\ -x_{m_2} - x_{m_3} \end{bmatrix} = \Phi_m(x_m). \tag{11.15}$$

In the new coordinates, the system (11.14) is rewritten as

$$\begin{aligned} \dot{z}_{m_1} &= z_{m_2}, \\ \dot{z}_{m_2} &= z_{m_3}, \\ \dot{z}_{m_3} &= \Psi_m(x_m), \end{aligned} \tag{11.16}$$

where $\Psi_m(x_m) = -\dot{x}_{m_2} - \dot{x}_{m_3}$.

As slave system, we select the Chua chaotic system [7], which is nondifferentially flat and Liouvillian if its output is chosen as $y_s = x_{s_2}$, and its dynamics is given by the following relationship:

$$\begin{aligned} \dot{x}_{s_1} &= a_s(x_{s_2} - x_{s_1} - m_{0_s} x_{s_1} - m_{1_s} x_{s_1}^3), \\ \dot{x}_{s_2} &= x_{s_1} - x_{s_2} + x_{s_3}, \\ \dot{x}_{s_3} &= b_s x_{s_2}, \\ y_s &= x_{s_2}. \end{aligned} \tag{11.17}$$

We can choose $\bar{y}_s = b_s \int y_s + u_1 = x_{s_3} + u_1$. Then the controlled coordinate transformation is defined as

$$\begin{bmatrix} z_{s_1} \\ z_{s_2} \\ z_{s_3} \end{bmatrix} = \begin{bmatrix} x_{s_3} + u_1 \\ \dot{x}_{s_3} + u_2 \\ \ddot{x}_{s_3} + u_3 \end{bmatrix} = \begin{bmatrix} \int y_s + u_1 \\ y_s + u_2 \\ \dot{y}_s + u_3 \end{bmatrix} = \begin{bmatrix} x_{s_3} + u_1 \\ -b_s x_{s_2} + u_2 \\ -b_s(x_{s_1} - x_{s_2} + x_{s_3}) + u_3 \end{bmatrix} = \Phi_s(x_s), \tag{11.18}$$

where $u_1 = u_s$, $u_2 = \dot{u}_s$, and $u_3 = \ddot{u}_s$ are control signals, which will be used to achieve GS in the transformed space. The slave system with the control is given by the augmented controlled system

$$\begin{aligned} \dot{z}_{s_1} &= z_{s_2}, \\ \dot{z}_{s_2} &= z_{s_3}, \\ \dot{z}_{s_3} &= \Psi(x_s) + \bar{u}_s, \\ \dot{u}_1 &= u_2, \\ \dot{u}_2 &= u_3, \\ \dot{u}_3 &= \bar{u}_s, \end{aligned} \tag{11.19}$$

where $\Psi_s(x_s) = -b_m(\dot{x}_{s_1} - \dot{x}_{s_2} + \dot{x}_{s_3})$. Now we just need to define $\bar{u}_s$ in such a way that the trajectories of the slave system (11.19) follow the trajectories of the master system (11.16), i.e., $(z_{m_1}, z_{m_2}, z_{m_3}) \to (z_{s_1}, z_{s_2}, z_{s_3})$ as $t \to \infty$. To choose an appropriate control that satisfies the control objective, first we define the synchronization error in the transformed coordinates as $e_z = z_m - z_s$, and the error dynamics is given by

$$\begin{aligned} \dot{e}_1 &= e_2, \\ \dot{e}_2 &= e_3, \\ \dot{e}_3 &= \Psi_m(x_m) - \Psi_s(x_s) - \bar{u}_s(x_s, y_s), \end{aligned} \tag{11.20}$$

and the control signal is chosen as

$$\bar{u}_s(x_s, y_s) = \dot{u}_3 = \Psi_m(x_m) - \Psi_s(x_s) + \kappa e_z. \tag{11.21}$$

Here $\kappa = [\kappa_1, \kappa_2, \kappa_3]$ is the vector of gains. With the selected control input, the closed-loop dynamics is given by $\dot{e}_z = Ae_z$, where $A \in \mathbb{R}^{3\times 3}$:

$$A = \begin{bmatrix} 0 & 1 & 0 \\ 0 & 0 & 1 \\ -\kappa_1 & -\kappa_2 & -\kappa_3 \end{bmatrix}. \tag{11.22}$$

Finally, we choose $(\kappa_1, \kappa_2, \kappa_3)$ such that A is a Hurwitz matrix. Then we conclude that $\|e_z\| \to 0$ as $t \to \infty$.

The inverse transformations are given by the following relationships:

$$\begin{bmatrix} x_{m_1} \\ x_{m_2} \\ x_{m_3} \end{bmatrix} = \begin{bmatrix} z_{m_2} \\ z_{m_1} \\ -z_{m_1} - z_{m_3} \end{bmatrix} = \Phi_m^{-1}(z_m) \tag{11.23}$$

and

$$\begin{bmatrix} x_{s_1} \\ x_{s_2} \\ x_{s_3} \end{bmatrix} = \begin{bmatrix} -\frac{1}{b_s}(z_{s_3} - u_3) - \frac{1}{b_s}(z_{s_2} - u_2) - (z_{s_1} - u_1) \\ -\frac{1}{b_s}(z_{s_2} - u_2) \\ z_{s_1} - u_1 \end{bmatrix} = \Phi_s^{-1}(z_s). \tag{11.24}$$

To end this section, we verify the effectiveness of the proposed scheme by means of numerical simulations. The data for the simulations are $a_m = 0.386$, $b_m = 0.2$, $m_{0_s} = -8/7$, $m_{1_s} = 4/63$, $a_s = 9.5$ and $b_s = 100/7$, the gains vector is $\kappa = [15, 15, 15]$ and initial conditions are $x_{0_m} = [0.7, -0.6, 0.7]$ for the master and $x_{0_s} = [0.2, -0.1, -0.3]$ for the slave.

Figures 11.1 and 11.2 show the generalized synchronization in transformed coordinates, while Figs. 11.3 and 11.4 show the generalized synchronization obtained via inverse transformations [see (11.23) and (11.24)]. Finally, Fig. 11.5 describes the synchronization error in the transformed coordinates.

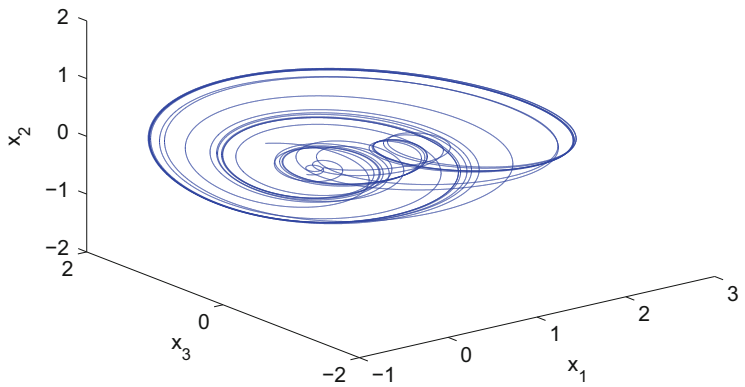

Fig. 11.1 Rössler system in transformed coordinates

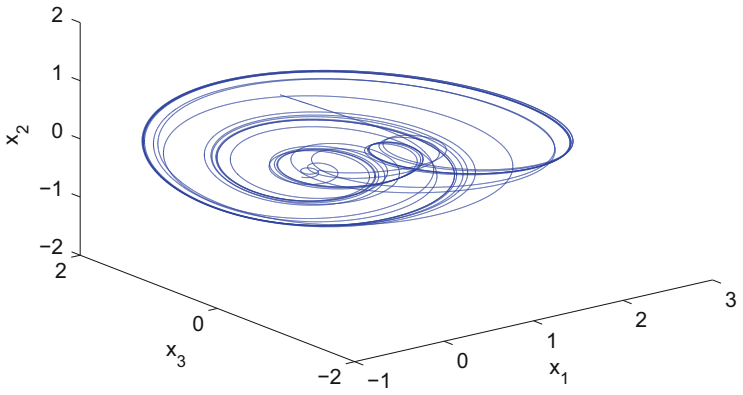

Fig. 11.2 Chua system in transformed coordinates, GS

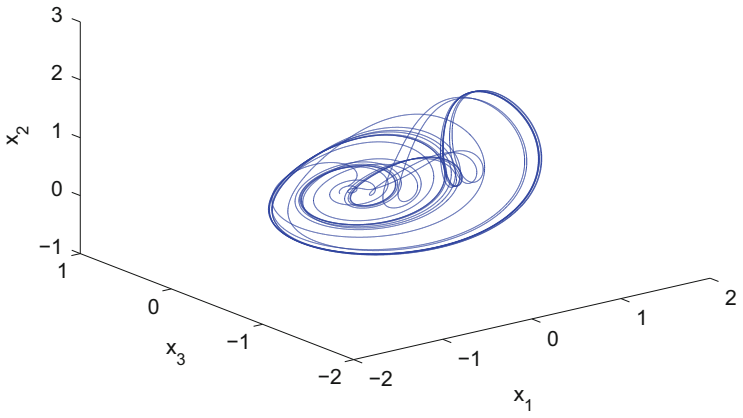

Fig. 11.3 Rössler system in original coordinates

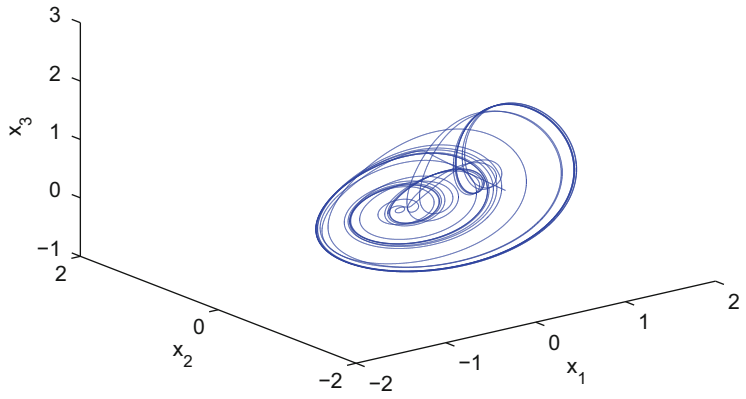

Fig. 11.4 Chua system in original coordinates, GS

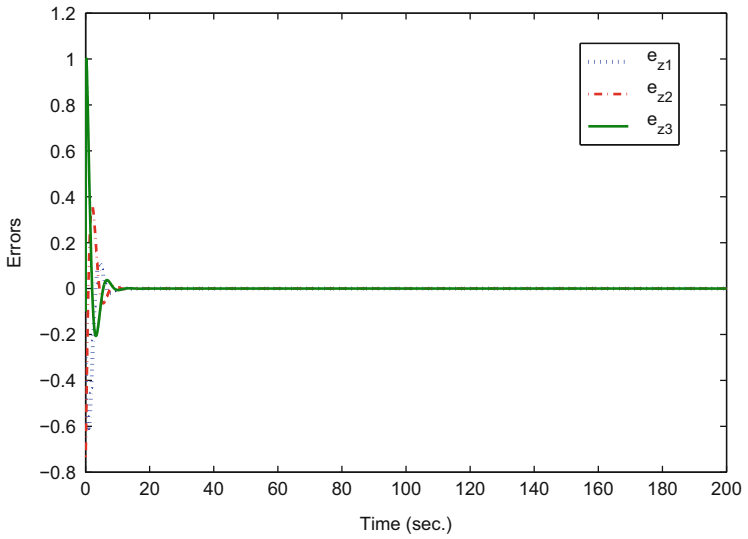

Fig. 11.5 Synchronization errors in transformed coordinates

11.5 Concluding Remarks

In this chapter, we have studied the problem of generalized synchronization between nondifferentially flat and Liouvillian systems. From the differential-algebraic point of view, this class of systems gave us a chance to extend the results in GS to a class of nondifferentially flat and Liouvillian systems. A dynamic control was constructed to achieve generalized synchronization, and it was generated by means of the differential primitive element, which is a linear combination of inputs and states of the system with coefficients in a differential field. In short, we have designed a

dynamical feedback controller as a chain of integrators, and we presented the GS between the Rössler and Chua systems. Finally the effectiveness of the proposed scheme was proven via numerical simulations.

References

1. R. Aguilar-Lopez, J.L. Mata-Machuca, R. Martínez-Guerra, *Observability and Observers for Nonlinear Dynamical Systems: Nonlinear Systems Analysis* (Lambert Academic Publishing, Germany, 2011)
2. J.-F. Chang, M.-L. Hung, Y.-S. Yang, T.-L. Liao, J.-J. Yan, Controlling chaos of the family of Rössler systems using sliding mode control. Chaos Solitons Fractals **37**(2), 609–622 (2008)
3. A. Chelouah, Extensions of differential flat fields and Liouvillian systems, in *36th Conference on Decision and Control* (IEEE, San Diego, 1997), pp. 4268–4273
4. M. Fliess, J. Lévine, P. Rouchon, Flatness and defect of nonlinear systems: introductory theory and examples. Int. J. Control **61**, 1327–1361 (1995)
5. E.R. Kolchin, *Differential Algebra and Algebraic Groups* (Academic, New York, 1973)
6. R. Martínez-Guerra, R. González-Galan, A. Luviano-Juárez, J. Cruz-Victoria, Diagnosis for a class of non-differentially flat and Liouvillian systems. IMA J. Math. Control Inform. **24**, 177–195 (2007)
7. R. Martínez-Guerra, D.M.G. Corona-Fortunio, J.L. Mata-Machuca, Synchronization of chaotic Liouvillian systems: an application to Chua's oscillator. Appl. Math. Comput. **219**(23), 10934–10944 (2013)
8. L.M. Pecora, T.L. Carroll, Synchronization in chaotic systems. Phys. Rev. Lett. **64**, 821–824 (1990)
9. N.F. Rulkov, M.M. Sushchik, L.S. Tsimring, H.D.I. Abarbanel, Generalized synchronization of chaos in directionally coupled chaotic systems. Phys. Rev. E **51**(2), 980–994 (1995)
10. S.S. Yang, K. Duan, Generalized synchronization in chaotic systems. Chaos Solitons Fractals **9**(10), 1703–1707 (1998)

Chapter 12
Generalized Multisynchronization by Means of a Family of Dynamical Feedbacks

Abstract In this chapter, we study the problem of generalized multisynchronization (GMS) of multiple decoupled chaotic systems under the master–slave configuration. From the viewpoint of differential algebra, we propose a family of transformations in order to achieve GMS for the whole slave family. The family of transformations is generated via the family of differential primitive elements, which are linear combinations of states and inputs of the families of master systems and slave systems with coefficients in a differential field. Finally, we construct multiple dynamical controls to reach the GMS. The effectiveness of the methodology proposed is illustrated by means of numerical simulations.

12.1 Introduction

A current challenge is to achieve and explain synchronization of strictly different chaotic systems. Synchronization was first initiated and recorded by Pecora and Carroll [1]. The generalized synchronization (GS) concept was introduced in [2], and a new definition is given in this chapter (Definition 12.2) for generalized multisynchronization (GMS) using concepts of differential algebra such as a family of differential primitive elements. GS is a fundamental phenomenon that has been widely studied recently, having both theoretical and applied significance [3].

In this chapter, we propose a method for synchronization of multiple decoupled chaotic nonlinear systems. It is sufficient to know the output of each system to generate a family of transformations that are represented by means of a differential transcendence basis. Such a family gives us the possibility to synchronize multiple chaotic systems. These transformations are obtained from a family of differential primitive elements given by $\bar{y}_j$ with $1 \leq j \leq p$ (p outputs), and we let $n_j \geq 0$ be the minimum integers such that $\bar{y}_j^{(n_j)}$ are analytically dependent on $(\bar{y}_j, \bar{y}_j^{(1)}, \ldots, \bar{y}_j^{(n_j-1)})$ such that

$$\bar{H}_j(\bar{y}_j, \bar{y}_j^{(1)}, \ldots, \bar{y}_j^{(n_j-1)}, \bar{y}_j^{(n_j)}, u_j, u_j^{(1)}, \ldots, u_j^{(\alpha_j)}) = 0. \tag{12.1}$$

R. Martínez-Guerra et al., *Synchronization of Integral and Fractional Order Chaotic Systems*, Understanding Complex Systems,
DOI 10.1007/978-3-319-15284-4_12

The main idea is to find a family of dynamical control signals through a chain of integrators such that it is possible to synchronize the coordinate transformation system; that is, the original system is carried out to a generalized observability canonical form multioutput (GOCFM) for multisystems through an adequate choice of a family of differential primitive elements given normally as a linear combination of the known states and the inputs of the system, where the coefficients belong to a differential field. The rest of this chapter is organized as follows: In Sect. 12.2, we present some basic definitions, the problem statement, and methodology for generalized synchronization of multiple decoupled systems. Numerical simulations are described in Sect. 12.3, and finally, Sect. 12.4 presents some concluding remarks.

12.2 Problem Formulation and Main Results

Before beginning the problem formulation, we consider an elementary definition.

Definition 12.1 A family of systems is Picard–Vessiot (PV) if the $k_j\langle u\rangle$-vector spaces generated by the derivatives of the family $\{\bar{y}_j^{(n_j)},\ n_j \geq 0,\ 1 \leq j \leq p\}$, have finite dimension.

The system (12.1) can be solved locally as

$$\bar{y}_j^{(n_j)} = -\mathscr{L}_j(\bar{y}_j, \bar{y}_j^{(1)}, \ldots, \bar{y}_j^{(n_j-1)}, u_j, u_j^{(1)}, \ldots, u_j^{(\alpha_j-1)}) + u_j^{(\alpha_j)}.$$

Let $\xi_i^{(n_j)} = \bar{y}_j^{(i-l)}$, $l = 1, n_1+1, n_1+n_2+1, \ldots, n_1+n_2+\cdots+n_{p-1}+1$; $1 \leq i \leq \sum_{1\leq j\leq p} n_j = n$, where the index j gives the jth system, and the n_j are the so-called indices of algebraic observability, whereby each index coincides with the system's dimension when it is flat [4]. Then it is possible to achieve a local representation for a set of p decoupled systems. That representation can be seen as a GOCFM:

$$\begin{aligned}
\dot{\xi}_1^{n_1} &= \xi_2^{n_1},\\
\dot{\xi}_2^{n_1} &= \xi_3^{n_1},\\
&\vdots\\
\dot{\xi}_{n_1-1}^{n_1} &= \xi_{n_1}^{n_1},\\
\dot{\xi}_{n_1}^{n_1} &= -\mathscr{L}_1(\xi_1^{n_1}, \xi_2^{n_1}, \ldots, \xi_{n_1}^{n_1}, u_1, u_1^{(1)}, \ldots, u_1^{(\alpha_1-1)}) + u_1^{\alpha_1},
\end{aligned}$$

$$
\begin{aligned}
\dot{\xi}^{n_2}_{n_1+1} &= \xi^{n_2}_{n_1+2},\\
\dot{\xi}^{n_2}_{n_1+2} &= \xi^{n_2}_{n_1+3},\\
&\vdots\\
\dot{\xi}^{n_2}_{n_1+n_2-1} &= \xi^{n_2}_{n_1+n_2},\\
\dot{\xi}^{n_2}_{n_1+n_2} &= -\mathscr{L}_2(\xi^{n_2}_{n_1+1}, \xi^{n_2}_{n_1+2}, \ldots, \xi^{n_2}_{n_1+n_2}, u_2, u_2^{(1)}, \ldots, u_2^{(\alpha_2-1)}) + u_2^{\alpha_2},\\
&\vdots\\
\dot{\xi}^{n_p}_{n_1+n_2+\cdots+n_{p-1}+1} &= \xi^{n_p}_{n_1+n_2+\cdots+n_{p-1}+2},\\
\dot{\xi}^{n_p}_{n_1+n_2+\cdots+n_{p-1}+2} &= \xi^{n_p}_{n_1+n_2+\cdots+n_{p-1}+3},\\
&\vdots\\
\dot{\xi}^{n_p}_{n_1+n_2+\cdots+n_{p-1}+n_p-1} &= \xi^{n_p}_{n_1+n_2+\cdots+n_{p-1}+n_p},\\
\dot{\xi}^{n_p}_{n_1+n_2+\cdots+n_{p-1}+n_p} &= -\mathscr{L}_p(\xi^{n_p}_{n_1+n_2+\cdots+n_{p-1}+1}, \xi^{n_p}_{n_1+n_2+\cdots+n_{p-1}+2}, \ldots,\\
&\qquad \xi^{n_p}_{n_1+n_2+\cdots+n_{p-1}+n_p}, u_p, u_p^{(1)}, \ldots, u_p^{(\alpha_p-1)}) + u_p^{\alpha_p},\\
y_j &= \xi^{n_j}_l.
\end{aligned}
\tag{12.2}
$$

In compact form, the new system (12.2) can be represented as

$$
\begin{aligned}
\dot{\xi} &= \mathscr{A}\xi - \Phi(\mathscr{L}_1, \ldots, \mathscr{L}_p) + \mathscr{U}(u_1^{(\alpha_1)}, \ldots, u_p^{(\alpha_p)}),\\
\mathscr{Y} &= \mathscr{C}\xi,
\end{aligned}
\tag{12.3}
$$

where $\xi, \Phi, \mathscr{U} \in \mathbb{R}^n$, $\mathscr{A} \in \mathbb{R}^{n\times n}$, $\mathscr{Y} \in \mathbb{R}^p$, and the matrices of (12.3) are defined as follows:

$$
\mathscr{A} = \begin{bmatrix} A_1 & & 0\\ & \ddots & \\ 0 & & A_p \end{bmatrix}
\tag{12.4}
$$

$$
A_j = \begin{bmatrix}
0 & 1 & 0 & 0 & \cdots & 0\\
0 & 0 & 1 & 0 & \cdots & 0\\
\vdots & \vdots & \vdots & \ddots & \cdots & 0\\
0 & 0 & 0 & 0 & 1 & 0\\
0 & 0 & 0 & 0 & 0 & 1\\
0 & 0 & 0 & 0 & 0 & 0
\end{bmatrix} \quad 1 \le j \le p
\tag{12.5}
$$

$$\Phi(\mathscr{L}_1,\ldots,\mathscr{L}_p)=\begin{bmatrix}\phi_1(\mathscr{L}_1)\\ \phi_2(\mathscr{L}_2)\\ \vdots\\ \phi_p(\mathscr{L}_p)\end{bmatrix};$$

$$\phi_j(\mathscr{L}_j)=\begin{bmatrix}0\\ 0\\ \vdots\\ 0\\ -\mathscr{L}_j(\xi^{n_j}_{n_1+n_2+\cdots+n_{j-1}+1},\ldots,\xi^{n_p}_{n_1+n_2+\cdots+n_j},u_j,u_j^{(1)},\ldots,u_j^{(\alpha_j-1)})\end{bmatrix} \tag{12.6}$$

$$\mathscr{U}(u_1^{(\alpha_1)},\ldots,u_p^{(\alpha_p)}))=\begin{bmatrix}\sqcap_1(u_1^{(\alpha_1)})\\ \sqcap_2(u_2^{(\alpha_2)})\\ \vdots\\ \sqcap_p(u_p^{(\alpha_p)})\end{bmatrix};\quad \sqcap_j(u_j^{(\alpha_j)})=\begin{bmatrix}0\\ 0\\ \vdots\\ 0\\ u_j^{(\alpha_j)}\end{bmatrix} \tag{12.7}$$

$$\mathscr{C}=\begin{bmatrix}C_1 & & 0\\ & \ddots & \\ 0 & & C_p\end{bmatrix};\quad C_j=\begin{bmatrix}1\,0\cdots 0\end{bmatrix}. \tag{12.8}$$

Let us now consider the following family of chaotic nonlinear systems:

$$\begin{aligned}\dot{x}_j&=F_j(x_j,u_j),\\ y_j&=C_jx_j,\end{aligned} \tag{12.9}$$

where $1\le j\le p$ denotes the jth system, $x_j\in\mathbb{R}^{n_j}$ is the state vector, $F_j(\cdot)$ is a nonlinear vector function, u_j is the input, y_j is the output, and C_j is a matrix of appropriate size.

We establish the following important result.

Lemma 12.1 *Consider the family of nonlinear systems (12.9). If the differential primitive element is chosen as*

$$y_j=\sum_{i=n-n_j+1}^{n}\gamma_ix_i+\sum_{k}^{m}\beta_ku_k,\quad \gamma_i,\beta_k\in K\langle u\rangle, \tag{12.10}$$

where $k\langle u\rangle$ is a differential field generated by k, u, and differential quantities, then the nonlinear system (12.9) is transformable to a GOCFM if and only if it is a PV family.

Proof Let the set $\{\zeta_j, \zeta_j^{(1)}, \ldots, \zeta_j^{(n_j-1)}\}$, $1 \leq j \leq p$ be a family of differential transcendence bases with $\zeta_j^{(i-l)} = y_j^{(i-l)}$, $1 \leq i \leq \sum_{j=1}^{p} n_j$, where $n_j \geq 0$ is the minimum integer such that $y_j^{(n_j)}$ is dependent on $y_j, y_j^{(1)}, \ldots, y_j^{(n_j-1)}, u_j, \ldots$. If we now redefine $\xi_i^{n_j} = \zeta_j^{(i-l)}$, $1 \leq i \leq \sum_{j=1}^{p} n_j$, we obtain

$$\begin{aligned}
\dot{\xi}_i^{n_1} &= \xi_{i+1}^{n_1}, \quad 1 \leq i \leq n_1 - 1, \\
\dot{\xi}_{n_1}^{n_1} &= -\mathscr{L}_1(\xi_1^{n_1}, \ldots, \xi_{n_1}^{n_1}, u_1, u_1^{(1)}, \ldots, u_1^{(\alpha_1-1)}) + u_1^{(\alpha_1)}, \\
\dot{\xi}_i^{n_2} &= \xi_{i+1}^{n_2}, \quad n_1 + 1 \leq i \leq n_1 + n_2 - 1, \\
\dot{\xi}_{n_1+n_2}^{n_2} &= -\mathscr{L}_2(\xi_{n_1+1}^{n_2}, \ldots, \xi_{n_1+n_2}^{n_2}, u_2, u_2^{(1)}, \ldots, u_2^{(\alpha_2-1)}) + u_2^{(\alpha_2)}, \\
&\vdots \\
\dot{\xi}_i^{n_p} &= \xi_{i+1}^{n_p}, \quad n_1 + \cdots + n_{p-1} + 1 \leq i \leq n_1 + \cdots + n_p - 1, \\
\dot{\xi}_{n_1+\cdots+n_p}^{n_p} &= -\mathscr{L}_p(\xi_{n_1+\cdots+n_{p-1}+1}^{n_p}, \ldots, \xi_{n_1+\cdots+n_p}^{n_p}, u_p, u_p^{(1)}, \ldots, u_p^{(\alpha_p-1)}) + u_p^{(\alpha_p)}.
\end{aligned} \tag{12.11}$$

□

We discuss the problem of generalized synchronization for a class of systems called flat systems. Within this class, we can find some chaotic systems. In this case, we consider the master–slave configuration. We define a master system family as

$$\begin{aligned}
\dot{x}_{m_\mu} &= F_{m_\mu}(x_{m_\mu}, u_{m_\mu}), \\
y_{m_\mu} &= h_{m_\mu}(x_{m_\mu}),
\end{aligned} \tag{12.12}$$

and the slave system family

$$\begin{aligned}
\dot{x}_{s_\nu} &= F_{s_\nu}(x_{s_\nu}, u_{s_\nu}), \\
y_{s_\nu} &= h_{s_\nu}(x_{s_\nu}),
\end{aligned} \tag{12.13}$$

where $x_{s_\nu} = (x_{1,s_\nu}, \ldots, x_{n_{s_\nu},s_\nu}) \in \mathbb{R}^{n_{s_\nu}}$, $x_{m_\mu} = (x_{1,m_\mu}, \ldots, x_{n_{m_\mu},m_\mu}) \in \mathbb{R}^{n_{m_\mu}}$, $h_{s_\nu} : \mathbb{R}^{n_{s_\nu}} \to \mathbb{R}$, $h_{m_\mu} : \mathbb{R}^{n_{m_\mu}} \to \mathbb{R}$, $u_{m_\mu} = (u_{1,m_\mu}, \ldots, u_{\alpha_{m_\mu},m_\mu}) \in \mathbb{R}^{\alpha_{m_\mu}}$, $u_{s_\nu} = (u_{1,s_\nu}, \ldots, u_{\alpha_{s_\nu},s_\nu}) \in \mathbb{R}^{\alpha_{s_\nu}}$, $1 \leq \nu \leq p-1$, $1 \leq \mu \leq p-\nu$. These conditions tell us that we can consider one or more slave systems associated with one master, but we cannot have a slave with more than one master. One slave is associated with one master when the number of slaves is equal to the number of masters, on the other hand it is possible to consider a case in which the number of slaves is greater than the number of masters, which means that a master system interacts with more than one slave system.

Definition 12.2 Let the vectors $X_m = (x_{m_1}, \ldots, x_{n_m}) \in \mathbb{R}^{n_m}$ and $X_s = (x_{s_1}, \ldots, x_{n_s}) \in \mathbb{R}^{n_s}$ be families of master and slave state vectors respectively. Then the family of slave systems is in a state of generalized multisynchronization (GMS) with their master systems family if there exist a family of differential primitive elements that generates a transformation $H_{ms} : \mathbb{R}^{n_s} \to \mathbb{R}^{n_m}$ with $H_{ms} = \Phi_m^{-1} \circ \Phi_s$, an algebraic manifold $M = \{(X_s, X_m) \mid X_m = H_{ms}(X_s)\}$, and a compact set $B \subset \mathbb{R}^{n_m} \times \mathbb{R}^{n_s}$ with $M \subset B$ such that the trajectories with initial condition in B tend to M as $t \to \infty$.

From Definition 12.2, we can say that GMS is achieved when $\lim_{t\to\infty} \| H_{ms}(X_s) - X_m \| = 0$.

Theorem 12.1 *Let a set of systems such as (12.12) and (12.13) be transformable to a GOCFM. Then* $\lim_{t\to\infty} \|\xi_m - \xi_s\| = 0$*, where* ξ_m *and* ξ_s *are respectively the trajectories in the transformed space of families of master and slave systems.*

Proof Without loss of generality, we consider that $u_{m_\mu} = 0$. The set of master systems has the following family of differential primitive elements:

$$y_{m_j} = \sum_{i=n-n_j+1}^{n} \gamma_i x_{i,m_j} = \xi_i^{n_{m_j}}, \ (i = l), \ \ \gamma_i \in \mathbb{R}\langle u_m \rangle, \tag{12.14}$$

and the family of differential primitive elements for the slave systems is

$$y_{s_j} = \sum_{i=n-n_j+1}^{n} \gamma_i x_{i,s_j} + \sum_k \beta_k u_{k,m_j} = \xi_i^{n_{s_j}}, \quad \gamma_i, \ (i = l), \ \beta_k \in \mathbb{R}\langle u_s \rangle, \tag{12.15}$$

which leads to

$$\begin{aligned}
\dot{\xi}_i^{n_{m_1}} &= \xi_{i+1}^{n_{m_1}}, \ \ 1 \le i \le n_{m_1} - 1 \\
\dot{\xi}_{n_{m_1}}^{n_{m_1}} &= -\mathscr{L}_{m_1}(\xi_1^{n_{m_1}}, \ldots, \xi_{n_{m_1}}^{n_{m_1}}), \\
\dot{\xi}_i^{n_{m_2}} &= \xi_{i+1}^{n_{m_2}}, \ \ n_{m_1} + 1 \le i \le n_{m_1} + n_{m_2} - 1, \\
\dot{\xi}_{n_{m_1}+n_{m_2}}^{n_{m_2}} &= -\mathscr{L}_{m_2}(\xi_{n_{m_1}+1}^{n_{m_2}}, \ldots, \xi_{n_{m_1}+n_{m_2}}^{n_{m_2}}), \\
&\vdots \\
\dot{\xi}_i^{n_{m_p}} &= \xi_{i+1}^{n_{m_p}}, \ \ n_{m_1} + \cdots + n_{m_p-1} + 1 \le i \le n_{m_1} + \cdots + n_{m_p} - 1, \\
\dot{\xi}_{n_{m_1}+\cdots+n_{m_p}}^{n_{m_p}} &= -\mathscr{L}_{m_p}(\xi_{n_{m_1}+\cdots+n_{m_{p-1}}+1}^{n_{m_p}}, \ldots, \xi_{n_{m_1}+\cdots+n_{m_p}}^{n_{m_p}}).
\end{aligned} \tag{12.16}$$

In compact form, (12.16) can be expressed as

$$\dot{\xi}_m = \mathscr{A}\xi_m - \Phi_m(\mathscr{L}_{m_1}, \ldots, \mathscr{L}_{m_p}). \tag{12.17}$$

Now let us define the following extended system, which represents the family of slave systems with its set of dynamical feedbacks:

$$\begin{aligned}
\dot{\xi}_i^{n_{s_1}} &= \xi_{i+1}^{n_{s_1}}, \quad 1 \le i \le n_{s_1} - 1 \\
\dot{\xi}_{n_{s_1}}^{n_{s_1}} &= -\mathscr{L}_{s_1}(\xi_1^{n_{s_1}}, \ldots, \xi_{n_{s_1}}^{n_{s_1}}, u_{s_1}, u_{s_1}^{(1)}, \ldots, u_{s_1}^{(\alpha_{s_1}-1)}) + u_{s_1}^{\alpha_{s_1}} \\
\dot{\xi}_i^{n_{s_2}} &= \xi_{i+1}^{n_{s_2}}, \quad n_{s_1} + 1 \le i \le n_{s_1} + n_{s_2} - 1 \\
\dot{\xi}_{n_{s_1}+n_{s_2}}^{n_{s_2}} &= -\mathscr{L}_{s_2}(\xi_{n_{s_1}+1}^{n_{s_2}}, \ldots, \xi_{n_{s_1}+n_{s_2}}^{n_{s_2}}, u_{s_2}, u_{s_2}^{(1)}, \ldots, u_{s_2}^{(\alpha_{s_2}-1)}) + u_{s_2}^{\alpha_{s_2}} \\
&\vdots \\
\dot{\xi}_i^{n_{s_p}} &= \xi_{i+1}^{n_{s_p}}, \quad n_{s_1} + \cdots + n_{s_{p-1}} + 1 \le i \le n_{s_1} + \cdots + n_{s_p} - 1 \\
\dot{\xi}_{n_{s_1}+\cdots+n_{s_p}}^{n_{s_p}} &= -\mathscr{L}_{s_p}(\xi_{n_{s_1}+\cdots+n_{s_{p-1}}+1}^{n_{s_p}}, \ldots, \xi_{n_{s_1}+\cdots+n_{s_p}}^{n_{s_p}}, u_{s_p}, u_{s_p}^{(1)}, \ldots, u_{s_p}^{(\alpha_{s_p}-1)}) + u_{s_p}^{\alpha_{s_p}} \\
\dot{u}_i^{n_{s_1}} &= u_{i+1}^{n_{s_1}}, \quad 1 \le i \le \alpha_{s_1} - 1 \\
\dot{u}_{\alpha_{s_1}}^{n_{s_1}} &= -\mathscr{L}_{m_1}(\xi_1^{n_{m_1}}, \ldots, \xi_{n_{m_1}}^{n_{m_1}}) + \mathscr{L}_{s_1}(\xi_1^{n_{s_1}}, \ldots, \xi_{n_{s_1}}^{n_{s_1}}, u_{s_1}, u_{s_1}^{(1)}, \ldots, u_{s_1}^{(\alpha_{s_1}-1)}) \\
&\quad + K_1(\xi^{n_{m_1}} - \xi^{n_{s_1}}) \\
\dot{u}_i^{n_{s_2}} &= u_{i+1}^{n_{s_2}}, \quad \alpha_{s_1} + 1 \le i \le \alpha_{s_1} + \alpha_{s_2} - 1 \\
\dot{u}_{\alpha_{s_1}+\alpha_{s_2}}^{n_{s_2}} &= -\mathscr{L}_{m_2}(\xi_{n_{m_1}+1}^{n_{m_2}}, \ldots, \xi_{n_{m_1}+n_{m_2}}^{n_{m_2}}) + \mathscr{L}_{s_2}(\xi_{n_{s_1}+1}^{n_{s_2}}, \ldots, \xi_{n_{s_1}+n_{s_2}}^{n_{s_2}}, u_{s_2}, \\
&\quad u_{s_2}^{(1)}, \ldots, u_{s_2}^{(\alpha_{s_2}-1)}) + K_2(\xi^{n_{m_2}} - \xi^{n_{s_2}}) \\
&\vdots \\
\dot{u}_i^{n_{s_p}} &= u_{i+1}^{n_{s_p}}, \quad \alpha_{s_1} + \cdots + \alpha_{s_{p-1}} + 1 \le i \le \alpha_{s_1} + \cdots + \alpha_{s_p} - 1 \\
\dot{u}_{\alpha_{s_1}+\cdots+\alpha_{s_p}}^{n_{s_p}} &= -\mathscr{L}_{m_p}(\xi^{n_{m_p}}) + \mathscr{L}_{s_p}(\xi^{n_{s_p}}, u_{s_p}, u_{s_p}^{(1)}, \ldots, u_{s_p}^{(\alpha_{s_p}-1)}) + K_p(\xi^{n_{m_p}} - \xi^{n_{s_p}})
\end{aligned} \tag{12.18}$$

$$\begin{aligned}
\dot{\xi}_s &= \mathscr{A}\xi_s - \Phi_s(\mathscr{L}_{s_1}, \ldots, \mathscr{L}_{s_p}) + \mathscr{U}(u_{s_1}^{(\alpha_{s_1})}, \ldots, u_{s_p}^{(\alpha_{s_p})}) \\
\dot{\bar{\mathscr{U}}} &= \mathscr{M}\bar{\mathscr{U}} + \mathscr{K}(\xi_m - \xi_s) - \Phi_m(\mathscr{L}_{m_1}, \ldots, \mathscr{L}_{m_p}) + \Phi_s(\mathscr{L}_{s_1}, \ldots, \mathscr{L}_{s_p}),
\end{aligned} \tag{12.19}$$

where the control signals are $u_1^{n_{s_j}} = u_{s_j}, u_2^{n_{s_j}} = \dot{u}_{s_j}, \ldots, u_{\alpha_{s_j}}^{n_{s_j}} = u_{s_j}^{\alpha_{s_j}-1}$, $\xi^{n_{s_j}} = [\xi_{n_{s_1}+\cdots+n_{s_{j-1}}+1}^{n_{s_j}}, \ldots, \xi_{n_{s_1}+\cdots+n_{s_j}}^{n_{s_j}}]^T$, $\xi^{n_{m_j}} = [\xi_{m_{s_1}+\cdots+n_{m_{j-1}}+1}^{n_{m_j}}, \ldots, \xi_{n_{m_1}+\cdots+n_{m_j}}^{n_{m_j}}]^T$ and $K_j = [k_{1,j}, \ldots, k_{n_j,j}]$, where the matrix $\mathscr{M}$ is defined as

$$\mathscr{M} = \begin{bmatrix} \bar{\mathscr{M}}_1 & & 0 \\ & \ddots & \\ 0 & & \bar{\mathscr{M}}_p \end{bmatrix} \tag{12.20}$$

$$\bar{\mathscr{M}}_j = \begin{bmatrix} 0 & 1 & 0 & 0 & \cdots & 0 \\ 0 & 0 & 1 & 0 & \cdots & 0 \\ \vdots & \vdots & \vdots & \ddots & \cdots & 0 \\ 0 & 0 & 0 & 0 & 1 & 0 \\ 0 & 0 & 0 & 0 & 0 & 1 \\ 0 & 0 & 0 & 0 & 0 & 0 \end{bmatrix}. \tag{12.21}$$

Finally, we consider the error of synchronization $e_\xi = \xi_m - \xi_s$, which has a dynamics given by

$$\begin{aligned} \dot{e}_\xi &= \mathscr{A}\xi_m - \Phi_m(\mathscr{L}_{m_1}, \ldots, \mathscr{L}_{m_p}) - \mathscr{A}\xi_s + \Phi_s(\mathscr{L}_{s_1}, \ldots, \mathscr{L}_{s_p}) - \mathscr{U} \\ \dot{\bar{\mathscr{U}}} &= \mathscr{M}\bar{\mathscr{U}} + \mathscr{K}(\xi_m - \xi_s) - \Phi_m(\mathscr{L}_{m_1}, \ldots, \mathscr{L}_{m_p}) + \Phi_s(\mathscr{L}_{s_1}, \ldots, \mathscr{L}_{s_p}), \end{aligned} \tag{12.22}$$

and after some algebraic operations, we have that

$$\dot{e}_\xi = (\mathscr{A} - \mathscr{K})e_\xi. \tag{12.23}$$

Then the synchronization error converges to zero if the matrix $\mathscr{A} - \mathscr{K} = \operatorname{diag}(\bar{\mathscr{A}_1}, \ldots, \bar{\mathscr{A}_p})$ is Hurwitz:

$$\bar{\mathscr{A}_j} = \begin{bmatrix} 0 & 1 & 0 & 0 & \cdots & 0 \\ 0 & 0 & 1 & 0 & \cdots & 0 \\ \vdots & \vdots & \vdots & \ddots & \cdots & 0 \\ 0 & 0 & 0 & 0 & 1 & 0 \\ 0 & 0 & 0 & 0 & 0 & 1 \\ -k_{1,j} & -k_{2,j} & -k_{3,j} & -k_{4,j} & \cdots & -k_{n_j,j} \end{bmatrix}. \tag{12.24}$$

□

Corollary 12.1 *All family of systems transformable to a GOCFM is in a state of GMS if and only if it is a PV family.*

Proof The result is immediate, and so the proof is omitted. □

12.3 Generalized Synchronization of Multiple Decoupled Systems

In this section, we consider a set of Colpitts oscillators as the family of slaves, while the master family consists of two systems: a Colpitts system and a Lorenz system. The first of these is chosen in order to show complete or identical synchronization, which is a special case of GS. The second system is chosen to show GS. Figure 12.1 shows the kind of interaction to be considered.

The dynamics of a family of master systems is given by

$$\begin{aligned}
\dot{x}_{1,m_1} &= -a_{m_1}\exp(-x_{2,m_1}) + a_{m_1}x_{3,m_1} + a_{m_1},\\
\dot{x}_{2,m_1} &= b_{m_1}x_3^{m_1},\\
\dot{x}_{3,m_1} &= -c_{m_1}x_{1,m_1} - c_{m_1}x_{2,m_1} - d_{m_1}x_{3,m_1},\\
\dot{x}_{4,m_2} &= a_{m_2}(x_{5,m_2} - x_{4,m_2}),\\
\dot{x}_{5,m_2} &= b_{m_2}x_{4,m_2} - x_{5,m_2} - x_{4,m_2}x_{6,m_2},\\
\dot{x}_{6,m_2} &= -c_{m_2}x_{6,m_2} + x_{4,m_2}x_{5,m_2}.
\end{aligned} \tag{12.25}$$

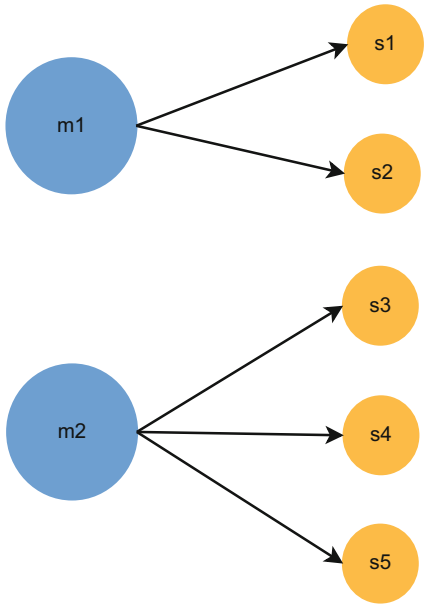

Fig. 12.1 Interaction between oscillators; m_1, m_2 are master systems, while s_j, $1 \leq j \leq 5$, are slave systems

For each slave system, we define the dynamics as follows:

$$\begin{aligned}\dot{x}_{1,s_j} &= -a_s \exp(-x_{2,s_j}) + a_s x_{3,s_j} + a_s,\\ \dot{x}_{2,s_j} &= b_s x_{3,s_j},\\ \dot{x}_{3,s_j} &= -c_s x_{1,s_j} - c_s x_{2,s_j} - d_s x_{3,s_j}.\end{aligned} \tag{12.26}$$

In this case, $1 \leq j \leq 5$. The transformed families of master and slave systems are given by (12.27) and (12.28) respectively:

$$\begin{aligned}\dot{\xi}_1^{m_1} &= \xi_2^{m_1},\\ \dot{\xi}_2^{m_1} &= \xi_3^{m_1},\\ \dot{\xi}_3^{m_1} &= \Psi_{m_1}(-b_m c_m \dot{x}_{1,m_1} - b_m c_m \dot{x}_{2,m_1} - b_m d_m \dot{x}_{3,m_1}),\\ \dot{\xi}_4^{m_2} &= \xi_5^{m_2},\\ \dot{\xi}_5^{m_2} &= \xi_6^{m_2},\\ \dot{\xi}_6^{m_2} &= \Psi_{m_2}([a_{m_2}^2 + a_{m_2} b_{m_2} - a_{m_2} x_6^{m_2}]\dot{x}_{4,m_2}\\ &\quad -[a_{m_2}^2 + a_{m_2}]\dot{x}_{5,m_2} - a_{m_2} x_4^{m_2} \dot{x}_{6,m_2})\end{aligned} \tag{12.27}$$

$$\begin{aligned}\dot{\xi}_1^{s_1} &= \xi_2^{s_1},\\ \dot{\xi}_2^{s_1} &= \xi_3^{s_1},\\ \dot{\xi}_3^{s_1} &= \Psi_{s_1}(-b_s c_s \dot{x}_{1,s_1} - b_s c_s \dot{x}_{2,s_1} - b_s d_s \dot{x}_{3,s_1}) + \dot{u}_3^{s_1},\\ \dot{\xi}_4^{s_2} &= \xi_5^{s_2},\\ \dot{\xi}_5^{s_2} &= \xi_6^{s_2},\\ \dot{\xi}_6^{s_2} &= \Psi_{s_2}(-b_s c_s \dot{x}_{1,s_2} - b_s c_s \dot{x}_{2,s_2} - b_s d_s \dot{x}_{3,s_2}) + \dot{u}_6^{s_2},\\ \dot{\xi}_7^{s_3} &= \xi_8^{s_3},\\ \dot{\xi}_8^{s_3} &= \xi_9^{s_3},\\ \dot{\xi}_9^{s_3} &= \Psi_{s_3}(-b_s c_s \dot{x}_{1,s_3} - b_s c_s \dot{x}_{2,s_3} - b_s d_s \dot{x}_{3,s_3}) + \dot{u}_9^{s_3},\\ \dot{\xi}_{10}^{s_4} &= \xi_{11}^{s_4},\\ \dot{\xi}_{11}^{s_4} &= \xi_{12}^{s_4},\\ \dot{\xi}_{12}^{s_4} &= \Psi_{s_4}(-b_s c_s \dot{x}_{1,s_4} - b_s c_s \dot{x}_{2,s_4} - b_s d_s \dot{x}_{3,s_4}) + \dot{u}_{12}^{s_4},\\ \dot{\xi}_{13}^{s_5} &= \xi_{14}^{s_5},\\ \dot{\xi}_{14}^{s_5} &= \xi_{15}^{s_5}\\ \dot{\xi}_{15}^{s_5} &= \Psi_{s_5}(-b_s c_s \dot{x}_{1,s_5} - b_s c_s \dot{x}_{2,s_5} - b_s d_s \dot{x}_{3,s_5}) + \dot{u}_{15}^{s_5},\end{aligned}$$

$$
\begin{aligned}
\dot{u}_1^{s_1} &= u_2^{s_1},\\
\dot{u}_2^{s_1} &= u_3^{s_1},\\
\dot{u}_3^{s_1} &= \bar{u}_{s_1},\\
\dot{u}_4^{s_2} &= u_5^{s_2},\\
\dot{u}_5^{s_2} &= u_6^{s_2},\\
\dot{u}_6^{s_2} &= \bar{u}_{s_2},\\
\dot{u}_7^{s_3} &= u_8^{s_3},\\
\dot{u}_8^{s_3} &= u_9^{s_3},\\
\dot{u}_9^{s_3} &= \bar{u}_{s_3},\\
\dot{u}_{10}^{s_4} &= u_{11}^{s_4},\\
\dot{u}_{11}^{s_4} &= u_{12}^{s_4},\\
\dot{u}_{12}^{s_4} &= \bar{u}_{s_4},\\
\dot{u}_{13}^{s_5} &= u_{14}^{s_5},\\
\dot{u}_{14}^{s_5} &= u_{15}^{s_5},\\
\dot{u}_{15}^{s_5} &= \bar{u}_{s_5}.
\end{aligned}
\tag{12.28}
$$

Remark 12.1 Since the number of master systems is less than the number of slave systems, to obtain the dynamical control feedbacks from the closed-loop dynamics of the synchronization error $e_\xi = \xi_m - \xi_s$, we extend the dimension of the master systems using virtual master systems, which will have the same dynamics as the original master system associated with the corresponding slave system. The closed-loop dynamics of the synchronization error $e_\xi = \xi_m - \xi_s$ is given by

$$
\begin{aligned}
\dot{e}_1^{s_1} =& e_2^{s_1},\\
\dot{e}_2^{s_1} =& e_3^{s_1},\\
\dot{e}_3^{s_1} =& \Psi_{m_1}(-b_m c_m \dot{x}_{1,m_1} - b_m c_m \dot{x}_{2,m_1} - b_m d_m \dot{x}_{3,m_1})\\
&- \Psi_{s_1}(-b_s c_s \dot{x}_{1,s_1} - b_s c_s \dot{x}_{2,s_1} - b_s d_s \dot{x}_{3,s_1}) - \dot{u}_3^{s_1},\\
\dot{e}_4^{s_2} =& e_5^{s_2},\\
\dot{e}_5^{s_2} =& e_6^{s_2},\\
\dot{e}_6^{s_2} =& \Psi_{m_1}(-b_m c_m \dot{x}_{1,m_1} - b_m c_m \dot{x}_{2,m_1} - b_m d_m \dot{x}_{3,m_1})\\
&- \Psi_{s_2}(-b_s c_s \dot{x}_{1,s_2} - b_s c_s \dot{x}_{2,s_2} - b_s d_s \dot{x}_{3,s_2}) - \dot{u}_6^{s_2},
\end{aligned}
$$

$$
\begin{aligned}
\dot{e}_7^{s_3} =& e_8^{s_3},\\
\dot{e}_8^{s_3} =& e_9^{s_3},\\
\dot{e}_9^{s_3} =& \Psi_{m_2}([a_{m_2}^2 + a_{m_2}b_{m_2} - a_{m_2}x_{6,m_2}]\dot{x}_{4,m_2},\\
& - [a_{m_2}^2 + a_{m_2}]\dot{x}_{5,m_2} - a_{m_2}x_{4,m_2}\dot{x}_{6,m_2})\\
& - \Psi_{s_3}(-b_s c_s \dot{x}_{1,s_3} - b_s c_s \dot{x}_{2,s_3} - b_s d_s \dot{x}_{3,s_3}) - \dot{u}_9^{s_3},\\
\dot{e}_{10}^{s_4} =& e_{11}^{s_4},\\
\dot{e}_{11}^{s_4} =& e_{12}^{s_4},\\
\dot{e}_{12}^{s_4} =& \Psi_{m_2}([a_{m_2}^2 + a_{m_2}b_{m_2} - a_{m_2}x_{6,m_2}]\dot{x}_{4,m_2},\\
& - [a_{m_2}^2 + a_{m_2}]\dot{x}_{5,m_2} - a_{m_2}x_{4,m_2}\dot{x}_{6,m_2})\\
& - \Psi_{s_4}(-b_s c_s \dot{x}_{1,s_4} - b_s c_s \dot{x}_{2,s_4} - b_s d_s \dot{x}_{3,s_4}) - \dot{u}_{12}^{s_4}\\
\dot{e}_{13}^{s_5} =& e_{14}^{s_5},\\
\dot{e}_{14}^{s_5} =& e_{15}^{s_5},\\
\dot{e}_{15}^{s_5} =& \Psi_{m_2}([a_{m_2}^2 + a_{m_2}b_{m_2} - a_{m_2}x_{6,m_2}]\dot{x}_{4,m_2},\\
& - [a_{m_2}^2 + a_{m_2}]\dot{x}_{5,m_2} - a_{m_2}x_{4,m_2}\dot{x}_{6,m_2})\\
& - \Psi_{s_5}(-b_s c_s \dot{x}_{1,s_5} - b_s c_s \dot{x}_{2,s_5} - b_s d_s \dot{x}_{3,s_5}) - \dot{u}_{15}^{s_5}\\
\dot{u}_1^{s_1} =& u_2^{s_1},\\
\dot{u}_2^{s_1} =& u_3^{s_1},\\
\dot{u}_3^{s_1} =& -\Psi_{m_1}(-b_m c_m \dot{x}_{1,m_1} - b_m c_m \dot{x}_{2,m_1} - b_m d_m \dot{x}_{3,m_1})\\
& + \Psi_{s_1}(-b_s c_s \dot{x}_{1,s_1} - b_s c_s \dot{x}_{2,s_1} - b_s d_s \dot{x}_{3,s_1}) + k_{s_1} e_\xi^{s_1},\\
\dot{u}_4^{s_2} =& u_5^{s_2},\\
\dot{u}_5^{s_2} =& u_6^{s_2},\\
\dot{u}_6^{s_2} =& -\Psi_{m_1}(-b_m c_m \dot{x}_{1,m_1} - b_m c_m \dot{x}_{2,m_1} - b_m d_m \dot{x}_{3,m_1})\\
& + \Psi_{s_2}(-b_s c_s \dot{x}_{1,s_2} - b_s c_s \dot{x}_{2,s_2} - b_s d_s \dot{x}_{3,s_2}) + k_{s_2} e_\xi^{s_2},\\
\dot{u}_7^{s_3} =& u_8^{s_3},\\
\dot{u}_8^{s_3} =& u_9^{s_3},\\
\dot{u}_9^{s_3} =& -\Psi_{m_2}([a_{m_2}^2 + a_{m_2}b_{m_2} - a_{m_2}x_{6,m_2}]\dot{x}_{4,m_2}\\
& - [a_{m_2}^2 + a_{m_2}]\dot{x}_{5,m_2} - a_{m_2}x_{4,m_2}\dot{x}_{6,m_2}),\\
& + \Psi_{s_3}(-b_s c_s \dot{x}_{1,s_3} - b_s c_s \dot{x}_{2,s_3} - b_s d_s \dot{x}_{3,s_3}) + k_{s_3} e_\xi^{s_3},
\end{aligned}
$$

$$
\begin{aligned}
\dot{u}_{10}^{s_4} =& u_{11}^{s_4},\\
\dot{u}_{11}^{s_4} =& u_{12}^{s_4},\\
\dot{u}_{12}^{s_4} =& -\Psi_{m_2}([a_{m_2}^2 + a_{m_2}b_{m_2} - a_{m_2}x_{6,m_2}]\dot{x}_{4,m_2}\\
&-[a_{m_2}^2 + a_{m_2}]\dot{x}_{5,m_2} - a_{m_2}x_{4,m_2}\dot{x}_{6,m_2})\\
&+\Psi_{s_4}(-b_s c_s \dot{x}_{1,s_4} - b_s c_s \dot{x}_{2,s_4} - b_s d_s \dot{x}_{3,s_4}) + k_{s_4} e_\xi^{s_4}\\
\dot{u}_{13}^{s_5} =& u_{14}^{s_5},\\
\dot{u}_{14}^{s_5} =& u_{15}^{s_5},\\
\dot{u}_{15}^{s_5} =& -\Psi_{m_2}([a_{m_2}^2 + a_{m_2}b_{m_2} - a_{m_2}x_{6,m_2}]\dot{x}_{4,m_2}\\
&-[a_{m_2}^2 + a_{m_2}]\dot{x}_{5,m_2} - a_{m_2}x_{4,m_2}\dot{x}_{6,m_2})\\
&+\Psi_{s_5}(-b_s c_s \dot{x}_{1,s_5} - b_s c_s \dot{x}_{2,s_5} - b_s d_s \dot{x}_{3,s_5}) + k_{s_5} e_\xi^{s_5},
\end{aligned}
\tag{12.29}
$$

and after some algebraic operations, we have that $\dot{e}_\xi = (\mathscr{A} - \mathscr{K})e_\xi$. Then the synchronization error converges to zero if the matrix $\mathscr{A} - \mathscr{K} = \text{diag}(\bar{\mathscr{A}_1}, \bar{\mathscr{A}_2}, \bar{\mathscr{A}_3}, \bar{\mathscr{A}_4}, \bar{\mathscr{A}_5})$ is Hurwitz:

$$
\bar{\mathscr{A}_j} = \begin{bmatrix} 0 & 1 & 0 \\ 0 & 0 & 1 \\ -k_{1,j} & -k_{2,j} & -k_{3,j} \end{bmatrix} \quad 1 \leq j \leq 5. \tag{12.30}
$$

The parameters for master and slave systems are $a_{m_1} = a_{s_j} = 6.2723$, $b_{m_1} = b_{s_j} = 6.2723$, $c_{m_1} = c_{s_j} = 0.0797$, $d_{m_1} = d_{s_j} = 0.6898$, $a_{m_2} = 10$, $b_{m_2} = 28$, $c_{m_2} = 8/3$, and $\kappa_{s_j} = (10, 10, 10)$ for $1 \leq j \leq 5$. Table 12.1 shows initial conditions for untransformed master and slave systems. The mapping $H_{ms}(X_s)$ is given in Eq. (12.31).

Table 12.1 Initial conditions for master and slave systems (original coordinates)

Initial conditions	
Master 1	$(0.2, -0.1, -0.3)^T$
Master 2	$(-1, -2, 0.8)^T$
Slave 1	$(-1.1, -1.3, -1.8)^T$
Slave 2	$(-1, -1, -1.5)^T$
Slave 3	$(0.05, -2.23, -2.89)^T$
Slave 4	$(1, -2, -0.5)^T$
Slave 5	$(0.2, -0.1, -0.3)^T$

$$
H_{ms} = \begin{bmatrix}
x_{1,s_1} - u_1^{s_1} - \dfrac{d_{s_1}}{c_{s_1} b_{s_1}} u_2^{s_1} - \dfrac{u_3^{s_1}}{c_{s_1} b_{s_1}} \\
x_{2,s_1} + u_1^{s_1} \\
x_{3,s_1} + u_2^{s_1} \\
x_{1,s_2} - u_4^{s_2} - \dfrac{d_{s_2}}{c_{s_2} b_{s_2}} u_5^{s_2} - \dfrac{u_6^{s_2}}{c_{s_2} b_{s_2}} \\
x_{2,s_2} + u_4^{s_2} \\
x_{3,s_2} + u_5^{s_2} \\
x_{2,s_3} + u_7^{s_3} \\
\dfrac{b_{s_3}}{a_{m_2}} x_{3,s_3} + \dfrac{u_8^{s_3}}{a_{m_2}} + x_{2,s_3} + u_7^{s_3} \\
b_{m_2} - 1 - (1 + 1/a_{m_2}) \dfrac{b_{s_3} x_{3,s_3} + u_8^{s_3}}{x_{2,s_3} + u_7^{s_3}} + \dfrac{b_{s_3} c_{s_3} x_{1,s_3} + b_{s_3} c_{s_3} x_{2,s_3} + b_{s_3} d_{s_3} x_{3,s_3} - u_9^{s_3}}{a_{m_2} (x_{2,s_3} + u_7^{s_3})} \\
x_{2,s_4} + u_{10}^{s_4} \\
\dfrac{b_{s_4}}{a_{m_2}} x_{3,s_4} + \dfrac{u_{11}^{s_4}}{a_{m_2}} + x_{2,s_4} + u_{10}^{s_4} \\
b_{m_2} - 1 - (1 + 1/a_{m_2}) \dfrac{b_{s_4} x_{3,s_4} + u_{11}^{s_4}}{x_{2,s_4} + u_{10}^{s_4}} + \dfrac{b_{s_4} c_{s_4} x_{1,s_4} + b_{s_4} c_{s_4} x_{2,s_4} + b_{s_4} d_{s_4} x_{3,s_4} - u_{12}^{s_4}}{a_{m_2} (x_{2,s_4} + u_{10}^{s_4})} \\
x_{2,s_5} + u_{13}^{s_5} \\
\dfrac{b_{s_5}}{a_{m_2}} x_{3,s_5} + \dfrac{u_{14}^{s_5}}{a_{m_2}} + x_{2,s_5} + u_{13}^{s_5} \\
b_{m_2} - 1 - (1 + 1/a_{m_2}) \dfrac{b_{s_5} x_{3,s_5} + u_{14}^{s_5}}{x_{2,s_5} + u_{13}^{s_5}} + \dfrac{b_{s_5} c_{s_5} x_{1,s_5} + b_{s_5} c_{s_5} x_{2,s_5} + b_{s_5} d_{s_5} x_{3,s_5} - u_{15}^{s_5}}{a_{m_2} (x_{2,s_5} + u_{13}^{s_5})}
\end{bmatrix}. \tag{12.31}
$$

Figure 12.2 shows states without synchronization, while Fig. 12.3 illustrates the synchronization-transformed coordinates. Finally, Fig. 12.4 shows the synchronization error in transformed space.

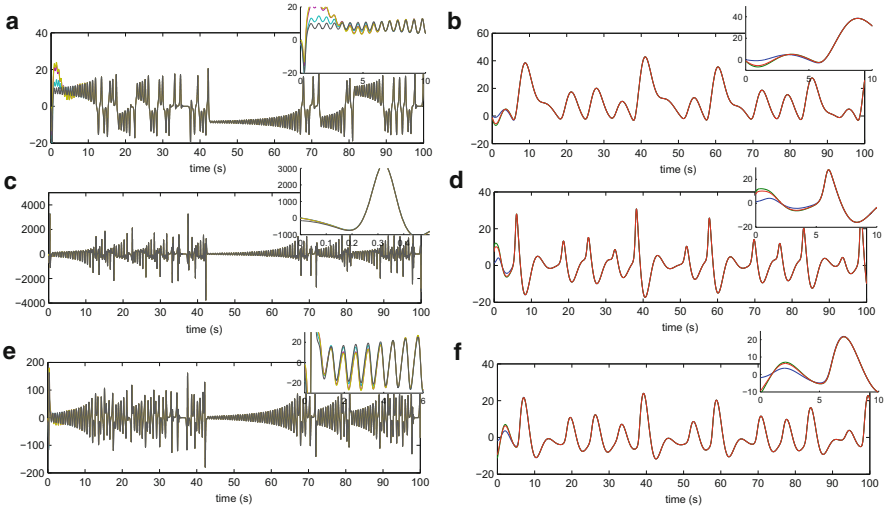

Fig. 12.2 Generalized synchronization in transformed coordinates: (**a**), (**c**), and (**e**) correspond to synchronization with a Lorenz system, while (**b**), (**d**), and (**f**) show the synchronization related to a Colpitts system

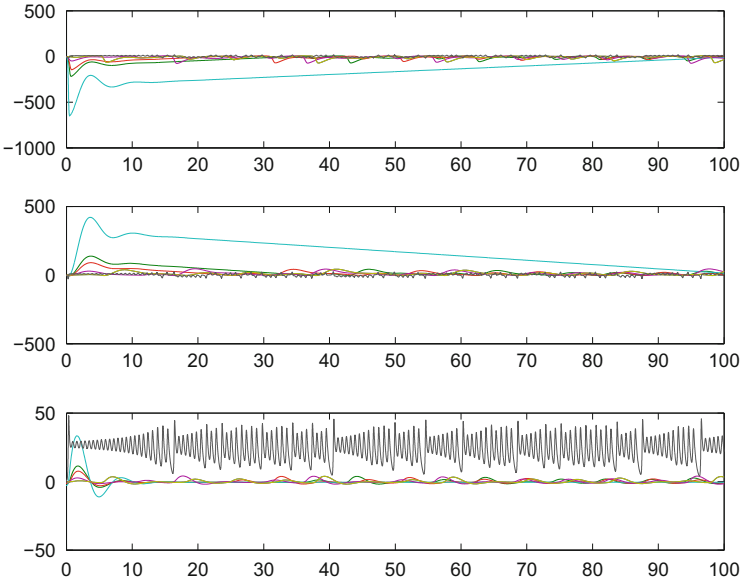

Fig. 12.3 Master and slave states out of synchronization

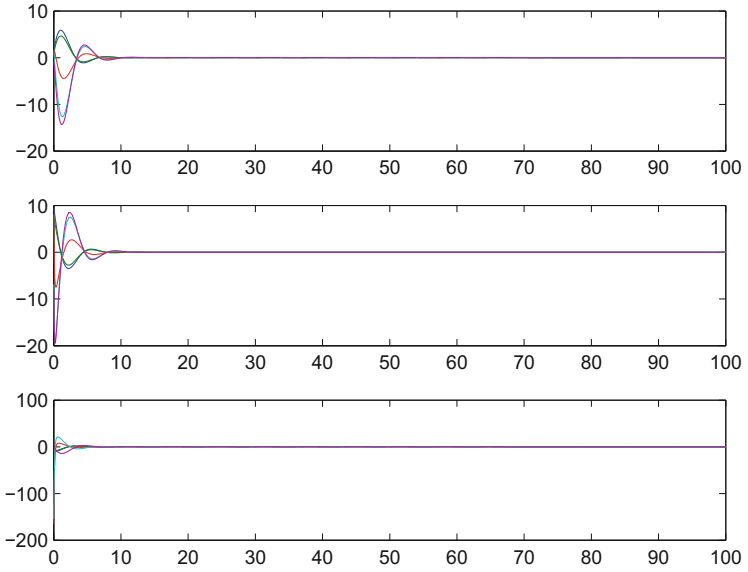

Fig. 12.4 Synchronization errors in transformed coordinates

12.4 Concluding Remarks

In this chapter, we have proposed a methodology for GMS via multiple dynamical feedbacks through a chain of integrators using differential-algebra techniques. We have designed a family of transformations by means of a family of differential primitive elements to carry out the master and slave families to a GOCFM. Then generalized synchronization is achieved for a family of decoupled systems. The effectiveness of this methodology was shown via numerical simulations.

References

1. L.M. Pecora, T.L. Carroll, Synchronization in chaotic systems. Phys. Rev. Lett. **64**, 821–824 (1990)
2. N.F. Rulkov, M.M. Sushchik, L.S. Tsimring, H.D.I. Abarbanel, Generalized synchronization of chaos in directionally coupled chaotic systems. Phys. Rev. E **51**(2), 980–994 (1995)
3. S.S. Yang, K. Duan, Generalized synchronization in chaotic systems. Chaos Solitons Fractals **9**(10), 1703–1707 (1998)
4. M. Fliess, J. Lévine, P. Rouchon, Flatness and defect of nonlinear systems: introductory theory and examples. Int. J. Control **61**, 1327–1361 (1995)

Chapter 13
Fractional Generalized Synchronization in Nonlinear Fractional-Order Systems via Dynamical Feedback

Abstract Generalized synchronization for nonlinear fractional-order systems occurs when the states of one system are identical to states of another by means of a functional mapping. This mapping can be obtained if there exists a fractional differential primitive element, whose elements are fractional derivatives that generate a differential transcendence basis. In this chapter, we investigate the fractional generalized synchronization (FGS) problem for strictly different nonlinear fractional-order systems, and we consider the master–slave synchronization scheme. Moreover, we construct in a natural manner a fractional generalized observability canonical form (FGOCF), and we introduce a fractional algebraic observability (FAO) property and we design a fractional dynamical controller able to achieve synchronization. These particular forms of FGS are illustrated with numerical results.

13.1 Introduction

The generalized synchronization (GS) concept was introduced in [15], and it is used to describe the onset of synchronization in directionally coupled chaotic systems. GS is a fundamental phenomenon, widely studied recently, having both theoretical and applied significance [2, 4, 7, 12, 16, 17]. GS occurs when the trajectories of one system are equal through a functional mapping to trajectories of another. In GS, two problems can be mentioned: determining whether there exists a functional mapping relating the slave with the master, and determining the form of that function.

In recent years, the applications of fractional calculus to physics, engineering, and control processing have become more interesting, and fractional dynamics is an attractive framework for understanding complex phenomena.

The synchronization problem is an interesting topic in fractional chaotic systems [18]. Synchronization of fractional-order chaotic systems was studied in [1], in which synchronization was carried out in the case of fractional Lü systems. In [6], it was shown by means of a control law that fractional-order chaotic systems can be synchronized using a similar scheme to that of their integer-order counterparts. In [9], a master–slave synchronization scheme for partially known

R. Martínez-Guerra et al., *Synchronization of Integral and Fractional Order Chaotic Systems*, Understanding Complex Systems,
DOI 10.1007/978-3-319-15284-4_13

nonlinear fractional-order systems was proposed, where the unknown dynamics is considered as the master system, and the slave system structure estimates the unknown state variables.

In this chapter, we propose a method for fractional generalized synchronization (FGS), In this case, we only need to know the output of the system to generate a mapping represented by a differential transcendence basis [8].

The main goal is to find a fractional dynamical synchronization control signal such that it is possible to synchronize the coordinate transformation system, that is, the original system is transformed into a so-called fractional generalized observability canonical form (FGOCF). This is achieved with an adequate choice of the fractional differential primitive element, given naturally as a linear combination of the states and the inputs of the system, where the coefficients belong to the differential field generated by the field K and the control input u.

The rest of this chapter is organized as follows. Section 13.2 includes some basic concepts about fractional-order systems as well as a description of the FGS problem and its solution. In Sect. 13.3, the proposed methodology is applied to an FGS between a fractional-order Chua system and a Rössler system. Finally, we give some concluding remarks in Sect. 13.4.

13.2 Main Result

There are several definitions of a fractional derivative of order α [11, 13, 14]. We will use the Caputo fractional operator in the definition of fractional-order systems (see Chap. 9), because the meaning of the initial conditions for systems described using this operator is the same as that for integer-order systems.

We take the initial condition problem for a fractional-order nonlinear system, with $0 < \alpha < 1$:

$$\begin{aligned} x^{(\alpha)} &= f(x,u), \quad x(0) = x_0, \\ y &= h(x), \end{aligned} \tag{13.1}$$

where $x \in \Omega \subset \mathbb{R}^n$ is the state vector, $f : \mathbb{R}^n \times \mathbb{R}^m \to \mathbb{R}^n$ is a Lipschitz continuous function with $x_0 \in \Omega \subset \mathbb{R}^n$. In this case, $y \in \mathbb{R}^p$ denotes the available output of the system, $h : \mathbb{R}^n \to \mathbb{R}^p$ is a continuous function, and $u \in \mathbb{R}^m$ is the vector input.

We extend the definition about the fractional algebraic observability property of system (13.1) given in Chap. 9.

Definition 13.1 (FAO) A state variable $x_i \in \mathbb{R}$ satisfies the fractional algebraic observability (FAO) property if it is a function of the first $r_1, r_2 \in \mathbb{N}$ sequential derivatives of the available output y and the input u, i.e.,

$$x_i = \phi_i \left(y,\ y^{(\alpha)}, \mathscr{D}^{(2\alpha)} y, \ldots, \mathscr{D}^{(r_1\alpha)} y, u,\ u^{(\alpha)}, \mathscr{D}^{(2\alpha)} u, \ldots, \mathscr{D}^{(r_2\alpha)} u \right), \tag{13.2}$$

where $\phi_i : \mathbb{R}^{(r_1+1)p} \times \mathbb{R}^{(r_2+1)m} \to \mathbb{R}$.

We introduce a new definition about fractional differential primitive element, which states that there exists a single element $\delta \in L$, which is a differential primitive element, such that $L = K\langle\delta\rangle$, that is, L is differentially generated by K and δ, where K is a differential field.

Definition 13.2 A dynamics is defined as a finitely generated differentially algebraic extension $L/K\langle u\rangle$ of the differential field $K\langle u\rangle$, where $K\langle u\rangle$ denotes the differential field generated by K and the elements of a finite set $u = (u_1, u_2, \ldots, u_m)$ of differential quantities.

Definition 13.3 The fractional-order system (13.1) is Picard–Vessiot (PV) if the $k\langle u\rangle$-vector space generated by the derivatives of the set $\{\mathscr{D}^{(\mu\alpha)}\bar{y},\ \mu \in \mathbb{N} \cup \{0\}\}$ has finite dimension, where $\bar{y}$ is the fractional differential primitive element.

That is, there exists an element $\bar{y} \in \mathbb{R}$, and let $n \in \mathbb{N} \cup \{0\}$ be the minimum integer such that $\mathscr{D}^{(n\alpha)}\bar{y}$ is analytically dependent on

$$\left\{\bar{y}, \bar{y}^{(\alpha)}, \mathscr{D}^{(2\alpha)}\bar{y}, \ldots, \mathscr{D}^{([n-1]\alpha)}\bar{y}\right\}.$$

Then

$$\mathscr{D}^{(n\alpha)}\bar{y} = -\mathscr{L}\left(\bar{y}, \bar{y}^{(\alpha)}, \mathscr{D}^{(2\alpha)}\bar{y}, \ldots, \mathscr{D}^{([n-1]\alpha)}\bar{y}, u, u^{(\alpha)}, \mathscr{D}^{(2\alpha)}u, \ldots, \mathscr{D}^{([\gamma-1]\alpha)}u\right) + \mathscr{D}^{(\gamma\alpha)}u,$$

with $n, \gamma \in \mathbb{N} \cup \{0\}$.

Defining

$$\xi_i = \mathscr{D}^{((i-1)\alpha)}\bar{y}, \qquad 1 \le i \le n,$$

we obtain the FGOCF of system (13.1):

$$\begin{aligned}
\xi_1^{(\alpha)} &= \xi_2,\\
\xi_2^{(\alpha)} &= \xi_3,\\
&\vdots\\
\xi_{n-1}^{(\alpha)} &= \xi_n,\\
\xi_n^{(\alpha)} &= -\mathscr{L}\left(\xi_1, \ldots, \xi_n, u, u^{(\alpha)}, \mathscr{D}^{(2\alpha)}u, \ldots, \mathscr{D}^{([\gamma-1]\alpha)}u\right) + \mathscr{D}^{(\gamma\alpha)}u,\\
\bar{y} &= \xi_1.
\end{aligned} \tag{13.3}$$

This enables us to establish the following lemma, which is proved as above.

Lemma 13.1 *A nonlinear fractional-order system (13.1) is transformable to an FGOCF if and only if it is PV.* □

Let us consider two fractional-order nonlinear systems in a master–slave configuration, where the master system is given by

$$\begin{aligned} x_m^{(\alpha)} &= F_m(x_m, u_m), \\ y_m &= h_m(x_m), \end{aligned} \tag{13.4}$$

and the slave by

$$\begin{aligned} x_s^{(\alpha)} &= F_s(x_s, u_s(x_s, y_m)), \\ y_s &= h_s(x_s), \end{aligned} \tag{13.5}$$

where $x_s \in \Omega \subset \mathbb{R}^n$, $F_s \in \Omega \subset \mathbb{R}^n$, $F_m \in \Omega \subset \mathbb{R}^n$, $x_m \in \Omega \subset \mathbb{R}^n$, $h_s : \Omega \to \mathbb{R}$, $h_m : \Omega \to \mathbb{R}$, $u_m \in \mathbb{R}^{\bar{m}_m}$, $u_s \in \mathbb{R}^{\bar{m}_s}$, $y_m, y_s \in \mathbb{R}$, F_s, F_m, h_s, h_m are assumed to be polynomial in their arguments, with initial conditions $x_{m_0} = x_m(0)$ and $x_{s_0} = x_s(0)$.

Definition 13.4 (Fractional Generalized Synchronization (FGS)) Slave and master systems are said to be in a state of fractional generalized synchronization (FGS) if there exists a fractional differential primitive element that generates a transformation $H_{ms} : \mathbb{R}^{n_s} \to \mathbb{R}^{n_m}$ with $H_{ms} = \Phi_s^{-1} \circ \Phi_m$ as well as an algebraic manifold $M = \{(x_s, x_m) | x_m = H_{ms}(x_s)\}$ and a compact set $B \subset \mathbb{R}^{n_s} \times \mathbb{R}^{n_m}$ with $M \subset B$ such that their trajectories with initial conditions in B approach M as $t \to \infty$.

From Definition 13.4, we obtain the following result.

Corollary 13.1 *Every fractional-order system is in a state of FGS if and only if is PV.*

Proof The proof is trivial and is omitted. □

FGS is taken to occur if there exists a fractional differential primitive element that generates a mapping H_{ms} from the trajectories $x_m(t)$ of the attractor in the master algebraic manifold M to the trajectories $x_s(t)$ in the slave space $\mathbb{R}^{n_s}$, i.e., $H_{ms}(x_s(t)) = x_m(t)$ (see Definition 13.4). For identical systems, the functional mapping corresponds to the identity [5]. For nonidentical master and slave systems, the map differs from the identity, which complicates detection of FGS. In fact, the attractors in the variables x_m and x_s seem to be unsynchronized.

Definition 13.4 leads to the following criterion:

$$\lim_{t \to \infty} \| H_{ms}(x_s) - x_m \| = 0.$$

Remark 13.1 It should be noted that identical or complete synchronization is a particular case of FGS, that is, the transformation H_{ms} is the identity.

The following remark is related to the general form in which one can choose the fractional differential primitive element.

Remark 13.2 The fractional differential primitive element is chosen as

$$y = \sum_i \alpha_i x_i + \sum_j \beta_j u_j \ , \qquad \alpha_i, \beta_j \in K\langle u \rangle,$$

where $K\langle u \rangle$ is a differential field generated by K, u, and their differential quantities.

Theorem 13.1 *Let systems (13.4) and (13.5) be transformable to an FGOCF. Let us define* $z_m = (z_{m_1}, z_{m_2} \ldots, z_{m_n})'$ *and* $z_s = (z_{s_1}, z_{s_2} \ldots, z_{s_n})'$ *as the trajectories of the master and slave systems in the coordinate transformation, respectively, with* $z_{m_i} = \mathscr{D}^{((i-1)\alpha)} \bar{y}_m$ *and* $z_{s_i} = \mathscr{D}^{((i-1)\alpha)} \bar{y}_s$, *for* $1 \leq i \leq n$. *Then*

$$\lim_{t \to \infty} \| z_m - z_s \| = 0.$$

In other words, complete synchronization in the coordinate transformation system is achieved, and consequently, FGS is obtained in the original coordinates, that is,

$$\lim_{t \to \infty} \| H_{ms}(x_s) - x_m \| = 0,$$

where $\bar{y}_m$ *and* $\bar{y}_s$ *are the fractional differential primitive elements for the master and slave systems, respectively.*

Proof Without loss of generality, we can choose $u_m = 0 \in \mathbb{R}^{\bar{m}_m}$. Then the fractional differential primitive element for the master is taken as

$$\bar{y}_m = \sum_i \alpha_{m_i} x_{m_i} = z_{m_1} \ , \qquad \alpha_{m_i} \in \mathbb{R},$$

and for the slave,

$$\bar{y}_s = \sum_i \alpha_{s_i} x_{s_i} + \sum_j \beta_{s_j} u_{s_j} = z_{s_1} \ , \qquad \alpha_{s_i}, \beta_{s_j} \in \mathbb{R},$$

which leads to the following FGOCF of system (13.4),

$$\begin{aligned} z_{m_j}^{(\alpha)} &= z_{m_{j+1}}, \\ z_{m_n}^{(\alpha)} &= -\mathscr{L}_m(z_{m_1}, \ldots, z_{m_n}), \end{aligned}$$

and the FGOCF of system (13.5),

$$\begin{aligned} z_{s_j}^{(\alpha)} &= z_{s_{j+1}}, \qquad 1 \leq j \leq n-1, \\ z_{s_n}^{(\alpha)} &= -\mathscr{L}_s\left(z_{s_1}, \ldots, z_{s_n}, u_1, u_2, \ldots, u_\gamma\right) + u_\gamma^{(\alpha)}, \end{aligned}$$

where

$$\begin{aligned} u_1 &= u_s, \\ u_2 &= u_s^{(\alpha)}, \\ &\vdots \\ u_\gamma &= \mathscr{D}^{((\gamma-1)\alpha)} u_s. \end{aligned}$$

Then we propose the following dynamical system:

$$\begin{aligned} u_j^{(\alpha)} &= u_{j+1}, \qquad 1 \le j \le \gamma - 1, \\ u_\gamma^{(\alpha)} &= -\mathscr{L}_m(z_{m_1}, \ldots, z_{m_n}) + \mathscr{L}_s(z_{s_1}, \ldots, z_{s_n}, u_1, u_2, \ldots, u_\gamma) + \kappa(z_m - z_s), \end{aligned}$$

where $z_m = (z_{m_1}, z_{m_2} \ldots, z_{m_n})'$, $z_s = (z_{s_1}, z_{s_2} \ldots, z_{s_n})'$ and $\kappa = (k_1, k_2, \ldots, k_n)$.

Then the dynamics of the synchronization error $e_z = z_m - z_s$ is given by the augmented system

$$\begin{aligned} e_{z_j}^{(\alpha)} &= e_{z_{j+1}}, \qquad 1 \le j \le n - 1, \\ e_{z_n}^{(\alpha)} &= -\mathscr{L}_m(z_{m_1}, \ldots, z_{m_n}) + \mathscr{L}_s(z_{s_1}, \ldots, z_{s_n}, u_1, u_2, \ldots, u_\gamma) - u_\gamma^{(\alpha)}, \\ u_i^{(\alpha)} &= u_{i+1}, \qquad 1 \le i \le \gamma - 1, \\ u_\gamma^{(\alpha)} &= -\mathscr{L}_m(z_{m_1}, \ldots, z_{m_n}) + \mathscr{L}_s(z_{s_1}, \ldots, z_{s_n}, u_1, u_2, \ldots, u_\gamma) + \kappa\, e_z. \end{aligned}$$

Then we have that

$$e_z^{(\alpha)} = A\, e_z \tag{13.6}$$

with

$$A = \begin{bmatrix} 0 & 1 & 0 & \cdots & & 0 \\ 0 & 0 & 1 & 0 & \cdots & 0 \\ \vdots & & & \ddots & & \vdots \\ 0 & 0 & \cdots & 0 & 1 & 0 \\ 0 & 0 & \cdots & & 0 & 1 \\ -k_1 & -k_2 & \cdots & & -k_{n-1} & -k_n \end{bmatrix}.$$

The stability of Eq. (13.6) is determined from the following result for linear fractional-order systems.

Theorem 13.2 (Matignon [10]) *Let $\alpha < 2$ and $\overline{A} \in \mathbb{C}^{n\times n}$. The autonomous system*

$$x^{(\alpha)} = \overline{A}x \qquad \textit{with} \quad x(0) = x_0$$

is asymptotically stable if and only if $|\arg(\lambda_i(\overline{A}))| > \alpha\pi/2$, *where* $\lambda_i(\overline{A})$ *is the* i*th eigenvalue of matrix* $\overline{A}$. □

Then, applying Theorem 13.2, we have that Eq. (13.6) is asymptotically stable if the gains $\kappa = (k_1, k_2, \ldots, k_n)$ are chosen such that

$$|\arg(\lambda_i(A))| > \frac{\alpha\pi}{2}.$$

□

Remark 13.3 As a particular case of Theorem 13.2, for $0 < \alpha < 1$, every Hurwitz matrix satisfies the condition

$$|\arg(\lambda_i(A))| > \frac{\pi}{2} > \frac{\alpha\pi}{2}.$$

13.3 Fractional Generalized Synchronization Between Chua and Rössler Systems

Consider the fractional-order Chua system [3]

$$\begin{aligned} x_{1_c}^{(\alpha)} &= a\left(x_{2_c} + \frac{x_{1_c} - 2x_{1_c}^3}{7}\right), \\ x_{2_c}^{(\alpha)} &= x_{1_c} - x_{2_c} + x_{3_c}, \\ x_{3_c}^{(\alpha)} &= -\beta x_{2_c}. \\ y_c &= x_{3_c} \end{aligned} \tag{13.7}$$

With $a = 12.75$, $\beta = 100/7$, and $\alpha = 0.9$, the system (13.7) presents chaotic behavior (see Fig. 13.1).

In this case, system (13.7) is considered the master system. The fractional differential primitive element is chosen as the output of system (13.7),

$$y_c = x_{3_c}.$$

We propose the coordinate transformation

$$\begin{aligned} \begin{pmatrix} z_{1_c} \\ z_{2_c} \\ z_{3_c} \end{pmatrix} &= \begin{pmatrix} y_c \\ y_c^{(\alpha)} \\ \mathscr{D}^{(2\alpha)} y_c \end{pmatrix} = \begin{pmatrix} x_{3_c} \\ -\beta x_{2_c} \\ -\beta(x_{1_c} - x_{2_c} + x_{3_c}) \end{pmatrix} \\ &= \Phi_c(x_c). \end{aligned} \tag{13.8}$$

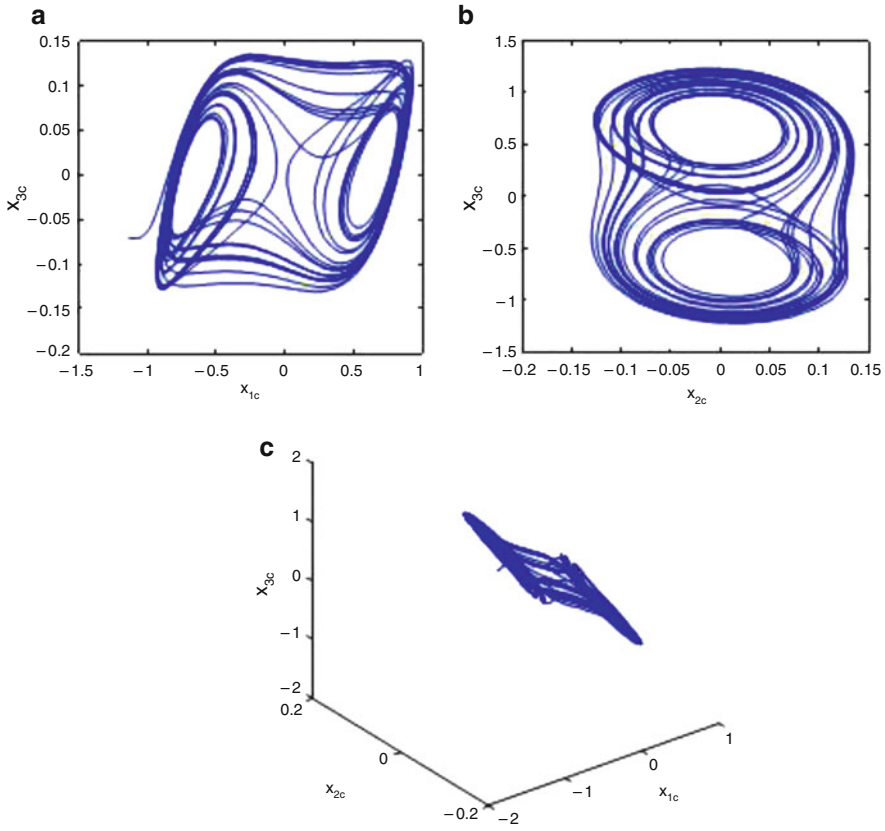

Fig. 13.1 Chua chaotic system of fractional order. (**a**) Variables x_{1_c} and x_{2_c}, (**b**) variables x_{2_c} and x_{3_c}, (**c**) variables x_{1_c}, x_{2_c}, and x_{3_c}

With the coordinate transformation (13.8), the Chua system (13.7) is expressed in terms of the FGOCF

$$\begin{pmatrix} z_{1_c}^{(\alpha)} \\ z_{2_c}^{(\alpha)} \\ z_{3_c}^{(\alpha)} \end{pmatrix} = \begin{pmatrix} z_{2_c} \\ z_{3_c} \\ \Psi_c(x_c) \end{pmatrix}, \tag{13.9}$$

where $\Psi_c(x_c) = -\beta(x_{1_c}^* - x_{2_c}^* + x_{3_c}^*)$, $x_{1_c}^* = a\left(x_{2_c} + \dfrac{x_{1_c} - 2x_{1_c}^3}{7}\right)$, $x_{2_c}^* = x_{1_c} - x_{2_c} + x_{3_c}$, $x_{3_c}^* = -\beta x_{2_c}$, $x_{1_c} = -\frac{1}{\beta} z_{3_c} - \dfrac{z_{2_c}}{\beta} - z_{1_c}$, $x_{2_c} = -\dfrac{z_{2_c}}{\beta}$ y $x_{3_c} = z_{1_c}$. Figure 13.2 shows the behavior of the transformed system (13.9).

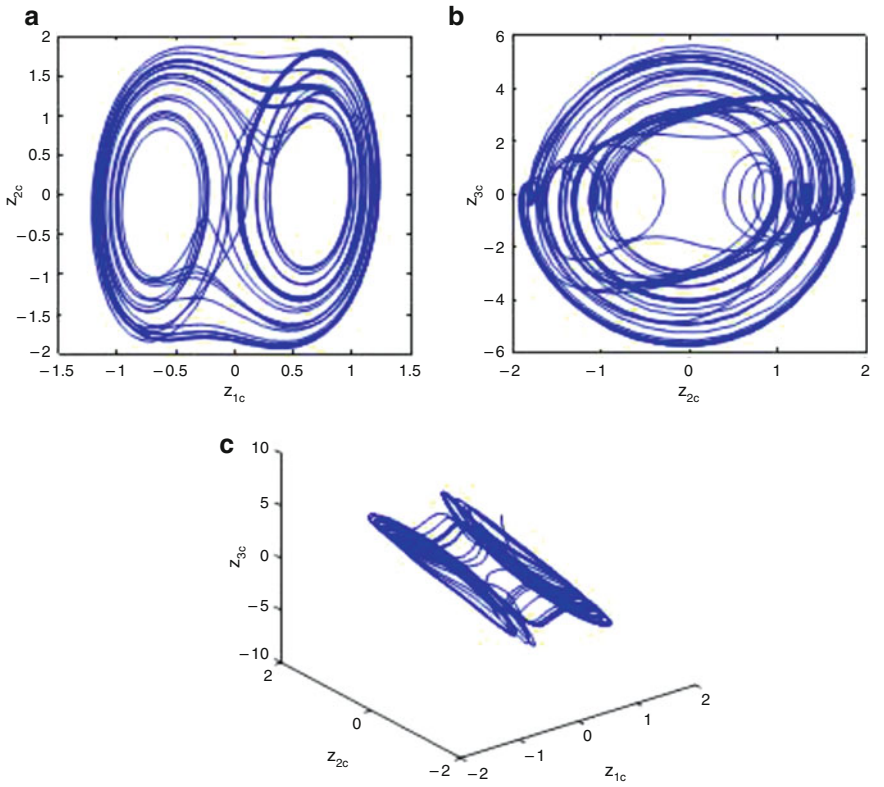

Fig. 13.2 Chua chaotic system of fractional order in the FGOCF. (**a**) Variables z_{1_c} and z_{2_c}, (**b**) variables z_{2_c} and z_{3_c}, (**c**) variables z_{1_c}, z_{2_c}, and z_{3_c}

As slave system, we consider the fractional order Rössler system given by

$$\begin{aligned} x_{1_r}^{(\alpha)} &= -(x_{2_r} + x_{3_r}), \\ x_{2_r}^{(\alpha)} &= x_{1_r} + a x_{2_r}, \\ x_{3_r}^{(\alpha)} &= 0.2 + x_{3_r}(x_{1_r} - 10), \\ y_r &= x_{2_r}. \end{aligned} \tag{13.10}$$

For $a = 0.4$ and $\alpha = 0.9$, system (13.10) exhibits chaotic behavior (see Fig. 13.3).

Consider the change of variables

$$\begin{aligned} \begin{pmatrix} z_{1_r} \\ z_{2_r} \\ z_{3_r} \end{pmatrix} &= \begin{pmatrix} y_r \\ y_r^{(\alpha)} \\ \mathscr{D}^{(2\alpha)} y_r \end{pmatrix} = \begin{pmatrix} x_{2_r} + u_1 \\ x_{1_r} + a x_{2_r} + u_2 \\ x_{1_r}^{(\alpha)} + a x_{2_r}^{(\alpha)} + u_3 \end{pmatrix} \\ &= \Phi_r(x_r), \end{aligned} \tag{13.11}$$

where $u_2 = u_1^{(\alpha)}$ and $u_3 = u_2^{(\alpha)}$.

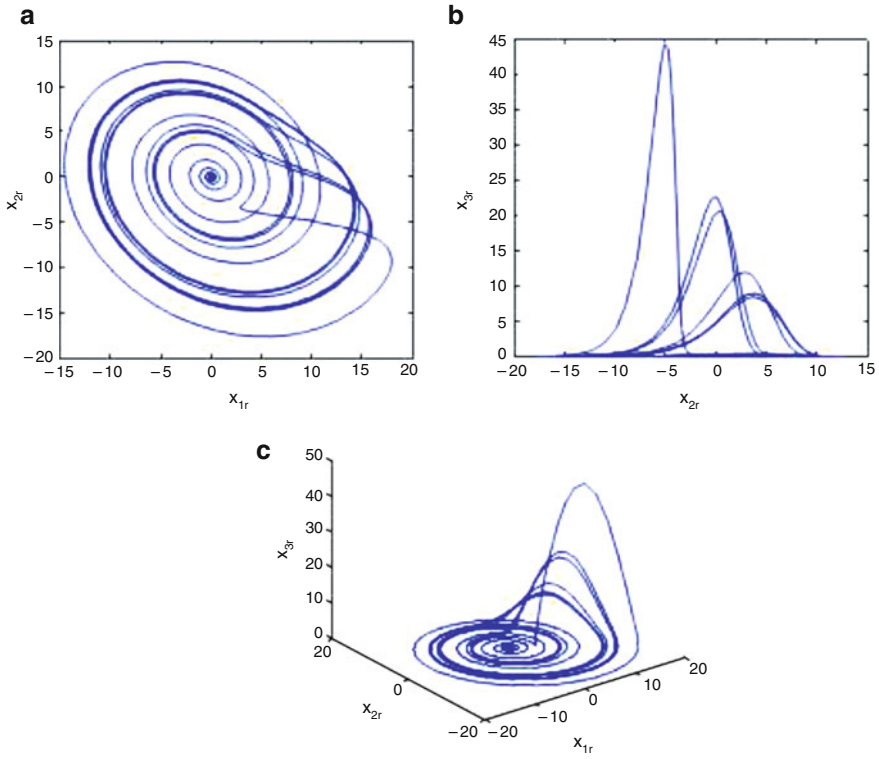

Fig. 13.3 Rössler chaotic system of fractional order. (**a**) Variables x_{1_r} and x_{2_r}, (**b**) variables x_{2_r} and x_{3_r}, (**c**) variables x_{1_r}, x_{2_r}, and x_{3_r}

Then the FGOCF of system (13.10) is

$$\begin{pmatrix} z_{1_r}^{(\alpha)} \\ z_{2_r}^{(\alpha)} \\ z_{3_r}^{(\alpha)} \end{pmatrix} = \begin{pmatrix} z_{2_r} \\ z_{3_r} \\ \Psi_r(x_r) \end{pmatrix}, \tag{13.12}$$

where $\Psi_r(x_r) = (a^2-1)x_{2_r}^* - x_{3_r}^* + ax_{1_r}^* + u_3^{(\alpha)}$, $x_{1_r}^* = -(x_{2_r} + x_{3_r})$, $x_{2_r}^* = x_{1_r} + ax_{2_r}$, $x_{3_r}^* = 0.2 + x_{3_r}(x_{1_r} - 10)$, $x_{1_r} = z_{2_r} - az_{1_r} + au_1 - u_2$, $x_{2_r} = z_{1_r} - u_1$ and $x_{3_r} = -z_{3_r} + az_{2_r} - z_{1_r} + u_1 + u_3 - a(u_2 + au_1)$.

The idea is that by means of the control signals, the trajectories of the transformed Rössler system $z_{1_r}, z_{2_r}, z_{3_r}$ follow the trajectories of the transformed Chua system $z_{1_c}, z_{2_c}, z_{3_c}$, respectively. It should be noted from Figs. 13.2 and 13.4 (autonomous Rössler system) that the chaotic attractors of the systems to be synchronized are totally different (Fig. 13.5).

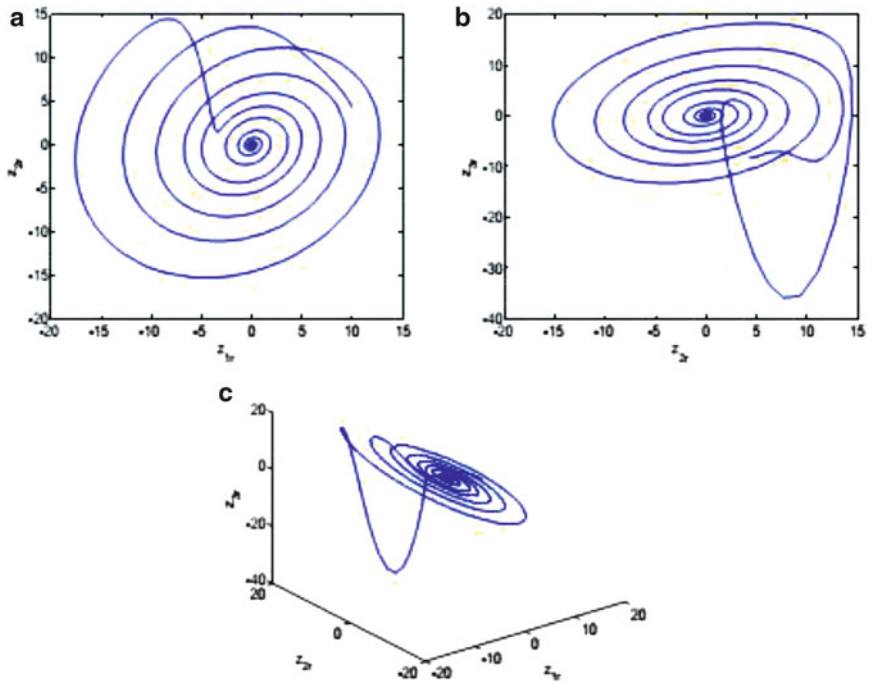

Fig. 13.4 Autonomous Rössler chaotic system of fractional order in FGOCF. (**a**) Variables z_{1_r} and z_{2_r}, (**b**) variables z_{2_r} and z_{3_r}, (**c**) variables z_{1_r}, z_{2_r}, and z_{3_r}

From Theorem 13.1, we propose the following controlled slave system:

$$\begin{pmatrix} z_{1_r}^{(\alpha)} \\ z_{2_r}^{(\alpha)} \\ z_{3_r}^{(\alpha)} \\ u_1^{(\alpha)} \\ u_2^{(\alpha)} \\ u_3^{(\alpha)} \end{pmatrix} = \begin{pmatrix} z_{2_r} \\ z_{3_r} \\ \Psi_r(x_r) \\ u_2 \\ u_3 \\ \Psi_c - \Psi_r + ke_z \end{pmatrix}, \tag{13.13}$$

where $k = (k_1, k_2, k_3)$ y $e_z = (z_{1_c} - z_{1_r}, z_{2_c} - z_{2_r}, z_{3_c} - z_{3_r})^T$.

The synchronization between Chua and Rössler systems expressed in the FGOCF is presented in Fig. 13.6. The synchronization errors are shown in Fig. 13.5, with $k_1 = 1$, $k_2 = 2$, and $k_3 = 1$.

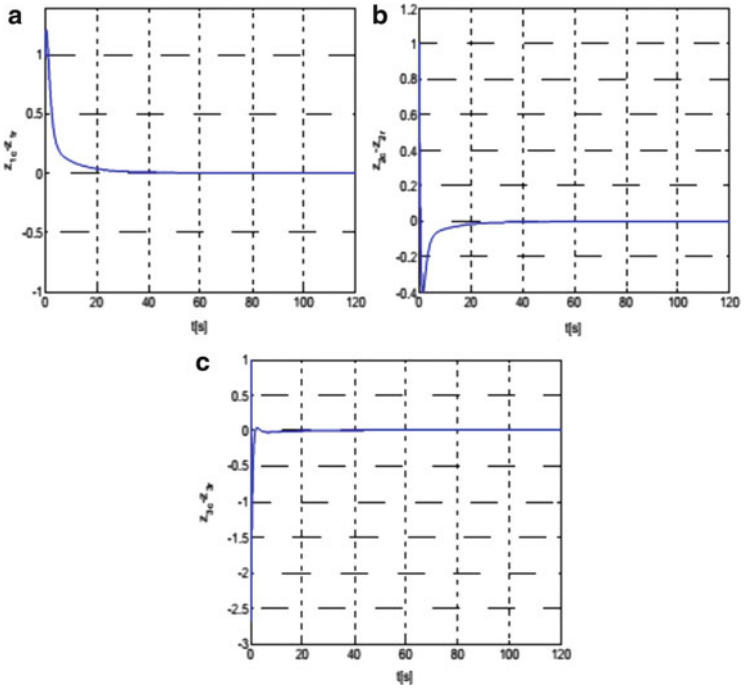

Fig. 13.5 Synchronization errors: (**a**) $z_{1_c} - z_{1_r}$, (**b**) $z_{2_c} - z_{2_r}$, (**c**) $z_{3_c} - z_{3_r}$

The original variables can be obtained with the response of the transformed systems, since they satisfy the FAO condition. That is,

$$\begin{cases} x_{1_c} = -\frac{1}{\beta} z_{3_c} - \dfrac{z_{2_c}}{\beta} - z_{1_c}, \\ x_{2_c} = -\dfrac{z_{2_c}}{\beta}, \\ x_{3_c} = z_{1_c}, \end{cases}$$

$$\begin{cases} x_{1_r} = z_{2_r} - a z_{1_r} + a u_1 - u_2, \\ x_{2_r} = z_{1_r} - u_1, \\ x_{3_r} = -z_{3_r} + a z_{2_r} - z_{1_r} + u_1 + u_3 - a(u_2 + a u_1). \end{cases}$$

Figure 13.7 shows the original reconstructed trajectories of the Chua and Rössler systems.

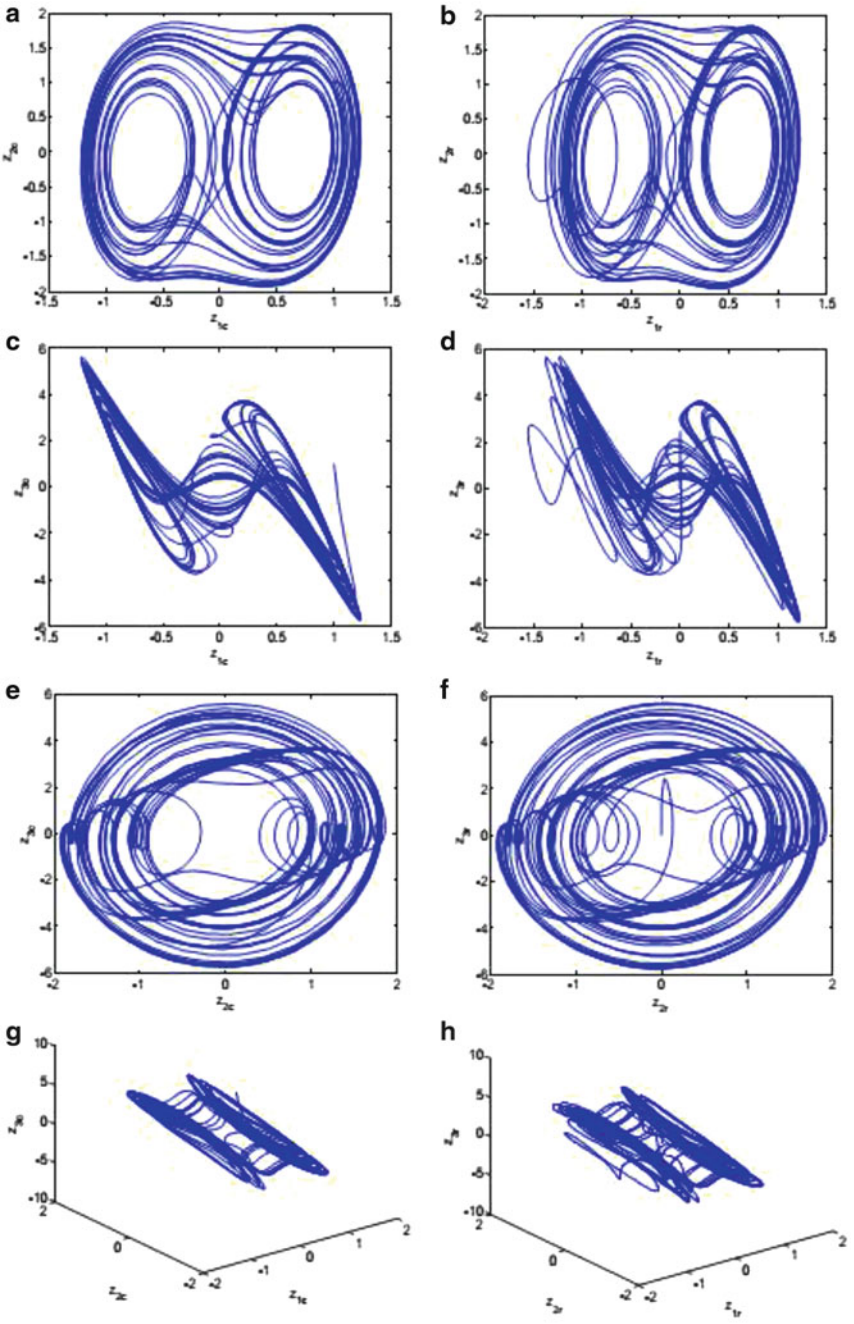

Fig. 13.6 Synchronization between Chua and Rössler systems expressed in the FGOCF. (**a**) Variables z_{1_c} and z_{2_c}, (**b**) variables z_{1_r} and z_{2_r}, (**c**) variables z_{1_c} and z_{3_c}, (**d**) variables z_{1_r} and z_{3_r}, (**e**) variables z_{2_c} and z_{3_c}, (**f**) variables z_{2_r} and z_{3_r}, (**g**) variables z_{1_c}, z_{2_c}, and z_{3_c}, (**h**) variables z_{1_r}, z_{2_r}, and z_{3_r}

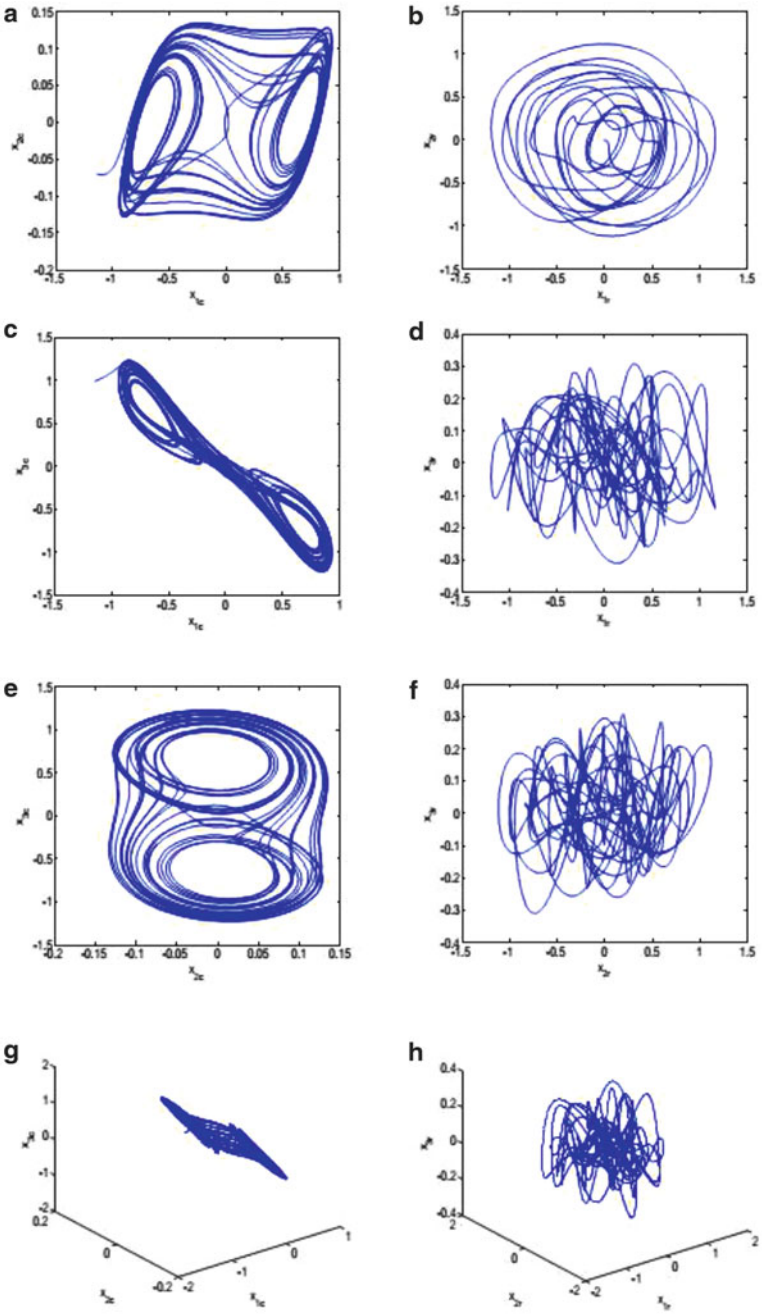

Fig. 13.7 Original coordinates. (**a**) Variables x_{1_c} and x_{2_c}, (**b**) variables x_{1_r} and x_{2_r}, (**c**) variables x_{1_c} and x_{3_c}, (**d**) variables x_{1_r} and x_{3_r}, (**e**) variables x_{2_c} and x_{3_c}, (**f**) variables x_{2_r} and x_{3_r}, (**g**) variables x_{1_c}, x_{2_c}, and x_{3_c}, (**h**) variables x_{1_r}, x_{2_r}, and x_{3_r}

13.4 Concluding Remarks

This chapter tackled the fractional generalized synchronization problem in strictly different nonlinear systems by means of fractional dynamical feedback control signals. To solve this problem, we employed the fractional differential primitive element given in general form as a linear combination of measurements and control inputs. We introduced some new concepts such as the fractional differential primitive element, the FAO, the FGOCF, and the FGS. Indeed, we designed a fractional dynamical feedback controller able to achieve identical synchronization in the coordinate transformation systems, and then FGS in the original coordinates was obtained. Finally, some numerical results illustrated the effectiveness of the proposed methodology.

References

1. W.H. Deng, C.P. Li, Chaos synchronization of the fractional Lü system. Physica A **353**, 61–72 (2005)
2. B.S. Dmitriev, A.E. Hramov, A.A. Koronovskii, A.V. Starodubov, D.I. Trubetskov, Y. Zharkov, First experimental observation of generalized synchronization phenomena in microwave oscillators. Phys. Rev. Lett. **102**, 74–101 (2009)
3. T.T. Hartley, C.F. Lorenzo, H.K. Qammer, Chaos in a fractional order Chua's system. IEEE Trans. Circuits Syst. I Fundam. Theory Appl. **42**, 485–490 (1995)
4. A. Kittel, J. Parisi, K. Pyragas, Generalized synchronization of chaos in electronic circuits experiments. Physica D **112**, 459–471 (1998)
5. L. Kocarev, U. Parlitz, Generalized synchronization, predictability and equivalence of unidirectionally coupled dynamical systems. Phys. Rev. Lett. **76**, 1816–1819 (1996)
6. C. Li, X. Liao, J. Yu, Synchronization of fractional order chaotic systems. Phys. Rev. E **68**, 067203-1–067203-3 (2003)
7. H. Liu, J. Chen, J.-A. Lu, M. Cao, Generalized synchronization in complex dynamical networks via adaptive couplings. Physica A **389**, 1759–1770 (2010)
8. R. Martínez-Guerra, J.L. Mata-Machuca, *Fault Detection and Diagnosis for Nonlinear Systems: A differential and algebraic viewpoint. Springer Understanding Complex Systems* (Springer international publishing Switzerland, 2014)
9. R. Martínez-Martínez, J.L. Mata-Machuc, R. Martínez-Guerra, J.A León, G. Fernández-Anaya, Synchronization of nonlinear fractional order systems. Appl. Math. Comput. **218**, 3338–3347 (2011)
10. D. Matignon, Stability results for fractional differential equations with applications to control processing, in *Proceedings of IMACS-SMC*, Lille (1996), pp. 963–968
11. K.S. Miller, B. Ross, *An Introduction to the Fractional Calculus and Fractional Differential Equations* (Wiley, New York, 1993)
12. O.I. Moskalenko, A.A. Koronovskii, A.E. Hramov, Generalized synchronization of chaos for secure communication: remarkable stability to noise. Phys. Lett. A **374**, 2925–2931 (2010)
13. I. Podlubny, *Fractional Differential Equations*, 9th edn. (Academic, San Diego, 1999)
14. I. Podlubny, Geometric and physical interpretation of fractional integration and fractional differentiation. Fract. Calc. Appl. Anal. **5**, 367–386 (2002)
15. N.F. Rulkov, M.M. Sushchik, L.S. Tsimring, H.D.I. Abarbanel, Generalized synchronization of chaos in directionally coupled chaotic systems. Phys. Rev. E **51**, 980–994 (1995)

16. M. Sun, C. Zeng, L. Tian, Linear generalized synchronization between two complex networks. Commun. Nonlinear Sci. Numer. Simul. **15**, 2162–2167 (2010)
17. Y.-W. Wang, Z-H. Guan, Generalized synchronization of continuous chaotic system. Chaos Solitons Fractals **27**, 97–101 (2006)
18. T. Zhou, C. Li, Synchronization of fractional-order differential systems. Physica D **212**, 2733–2740 (2005)

Chapter 14
An Observer for a Class of Incommensurate Fractional-Order Systems

Abstract In this chapter, we present a new observer-model-free type of synchronization for a certain class of incommensurate fractional-order systems. We apply our proposals to the master–slave synchronization scheme, where the unknown dynamics are considered the master system, and we propose an observer structure as a slave system that estimates the unknown state variables. For solving this problem, we introduce a new incommensurate fractional algebraic observability (IFAO) property, which is used as the main ingredient in the design of the slave system. Some numerical results show the effectiveness of the suggested approach.

14.1 Introduction

The synchronization problem is an interesting topic in fractional chaotic systems [1]. The synchronization of integer-order chaotic systems has been a subject of investigation since its introduction by Pecora and Caroll [2].

Some techniques related to chaos synchronization in fractional systems have been reported. For instance, we mention the works [3], in which the authors propose the employment of a feedback controller, which allows one to achieve synchronization between two identical fractional-order chaotic systems; in [4], a classical Luenberger observer design is presented for the synchronization of fractional-order chaotic systems, i.e., the observer structure requires a copy of the system, and the application is restricted to incommensurate fractional-order systems.

The main contribution of this chapter is to present a new observer for the synchronization problem in partially known nonlinear incommensurate fractional-order systems. We propose a novel technique using the master–slave synchronization scheme for estimating the unknown state variables based on a new incommensurate fractional algebraic observability (IFAO) property. As far as we know, this class of estimation scheme has not appeared in the literature in relation to incommensurate fractional-order systems.

The remainder of this chapter is organized as follows: In Sect. 14.2, we establish the basic concepts needed to tackle the synchronization problem for incommensurate fractional-order systems. In Sect. 14.3, we introduce a new concept

R. Martínez-Guerra et al., *Synchronization of Integral and Fractional Order Chaotic Systems*, Understanding Complex Systems,
DOI 10.1007/978-3-319-15284-4_14

given by Definition 14.2 (IFAO), and we propose a new system to estimate the unknown dynamics (slave system), called an incommensurate fractional reduced-order observer (IFROO). In Sect. 14.4, we apply our methodology to incommensurate fractional-order Rössler, Chua–Hartley, and financial systems. The reason we have chosen these systems is to clarify the proposed methodology and to highlight the simplicity and flexibility of the suggested approach. Also, we present some numerical results to confirm the effectiveness of the suggested approach. Finally, we close this chapter with some concluding remarks.

14.2 Basic Concepts

There are several definitions of a fractional derivative of order α [5–7]. We will use the Caputo fractional operator in the definition of fractional-order systems (as in Chap. 9).

Definition 14.1 (Caputo Fractional Derivative [8]) The Caputo fractional derivative of order $\alpha \in \mathbb{R}^+$ of a function x is defined as

$$\begin{aligned} x^{(\alpha)} &= {}_{t_0}D_t^{\alpha} x(t) \\ &= \frac{1}{\Gamma(m-\alpha)} \int_0^t \frac{d^m x(\tau)}{d\tau^m} (t-\tau)^{m-\alpha-1} d\tau, \end{aligned} \tag{14.1}$$

where $m-1 \leqslant \alpha < m$, $\dfrac{d^m x(\tau)}{d\tau^m}$ is the mth derivative of x in the usual sense, $m \in \mathbb{N}$, and Γ is the gamma function.

Now we define a sequential operator, see [5], as follows:

$$D^{r\alpha} x(t) = \underbrace{{}_{t_0}D_t^{\alpha}\, {}_{t_0}D_t^{\alpha} \ldots {}_{t_0}D_t^{\alpha}}_{r\text{-times}} x(t), \tag{14.2}$$

i.e., it is the Caputo fractional derivative of order α applied $r \in \mathbb{N}$ times sequentially, with $D^0 x(t) = x(t)$. We note that if $r = 1$, then $D^{\alpha} x(t) = x^{(\alpha)}$.

14.2.1 Mittag-Leffler-Type Functions

The Mittag-Leffler function with two parameters is defined as [11]

$$E_{\alpha,\beta}(z) = \sum_{i=0}^{\infty} \frac{z^i}{\Gamma(\alpha i + \beta)}, z, \beta \in \mathbb{C}, \mathbb{R}e(\alpha) > 0. \tag{14.3}$$

This function is used to solve fractional differential equations in analogy to the exponential function in integer-order systems. In the particular case $\alpha = \beta = 1$, we have that $E_{1,1}(z) = e^z$. Now if we have particular values of α, the function (14.3) has asymptotic behavior at infinity.

Theorem 14.1 ([7]) *If $\alpha \in (0, 2)$, β is an arbitrary complex number and μ is an arbitrary real number such that*

$$\frac{\pi\alpha}{2} < \mu < \min\{\pi, \pi\alpha\}, \tag{14.4}$$

then for an arbitrary integer $k \geqslant 1$, the following expansion holds:

$$E_{\alpha,\beta}(z) = -\sum_{i=1}^{k} \frac{1}{\Gamma(\beta - \alpha i) z^i} + O\frac{1}{|\ z\ |^{k+1}} \tag{14.5}$$

with $|\ z\ | \to \infty,\ \mu \leqslant |\arg(z)| \leqslant \pi$. □

The Mittag-Leffler function has the following properties:

Property 14.1 ([7])

$$\int_0^t \tau^{\beta-1} E_{\alpha,\beta}(-k\tau^\alpha) d\tau = t^\beta E_{\alpha,\beta+1}(-kt^\alpha), \beta > 0.$$

Property 14.2 ([9]) $E_{\alpha,\beta}(-x)$ is completely monotonic, i.e., $(-1)^n E^{(n)}_{\alpha,\beta}(-x) \geqslant 0$ for $0 < \alpha \leqslant 2$ and $\beta \geqslant \alpha$, for all $x \in (0, \infty)$ and $n \in \mathbb{N} \cup \{0\}$.

We will use these facts in the following problem.

14.3 Problem Statement and Main Result

Consider the following class of incommensurate fractional-order systems:

$$\frac{d^{\alpha_i}}{dt^{\alpha_i}} x_i = f_i(x_1, \ldots, x_n), 1 \leq i \leq n, i \in \mathbb{Z}^+, \tag{14.6}$$

where the α_i are rational numbers between 0 and 1.

Consider the system given by (14.6). We will separate it into two dynamical systems with states $\bar{x} \in \mathbb{R}^p$ and $\eta \in \mathbb{R}^{n-p}$, respectively, with $x_i^T = (\bar{x}_i^T, \eta_i^T)$. The first system describes the known states, and the second system represents unknown

states. Then the systems (14.6) can be written as

$$\begin{aligned} \bar{x}^{(\alpha_i)} &= \bar{f}(\bar{x}, \eta), \\ \eta^{(\alpha_j)} &= \Delta(\bar{x}, \eta), \\ y_{\bar{x}} &= h_{\bar{x}}(\bar{x}), \end{aligned} \tag{14.7}$$

where $\bar{x} \in \mathbb{R}^p$, $h : \mathbb{R}^p \to \mathbb{R}^q$ is a continuous function, $1 \leq p \leq n$, and $f^T(x) = (\bar{f}^T(\bar{x}, \eta), \Delta^T(\bar{x}, \eta))$, $\bar{f} \in \mathbb{R}^p$, $\Delta \in \mathbb{R}^{n-p}$.

How can we estimate the states of the various values of η? This question arises, because if we know the η's states, we can use these signals to generate measurements depending on them. In order to solve this observation problem, let us introduce the following observability property.

Definition 14.2 (IFAO) A state variable $\eta_i \in \mathbb{R}$ satisfies the IFAO property if it is a function of derivatives of the available output $y_{\bar{x}}$, i.e.,

$$\eta_i = \phi_i(y_{\bar{x}}, y_{\bar{x}}^{(\alpha_1)}, y_{\bar{x}}^{(\alpha_1+\alpha_2)}, \ldots, y_{\bar{x}}^{(\alpha_1+,\ldots,+\alpha_n)}), 0 \leq \sum_{i=1}^{n} \alpha_i \leq 2, \tag{14.8}$$

where $\phi_i : \mathbb{R}^{(n+1)q} \to \mathbb{R}$. If we assume that the components of the unknown state vector η are IFAO, then we can describe our problem in terms of the master–slave synchronization scheme, which is defined in the following way.

Let us consider the master system

$$\eta^{(\alpha_i)} = \Delta_i(\bar{x}, \eta), \tag{14.9}$$

$$y_{\eta_i} = \eta_i = \phi_i(y_{\bar{x}}, y_{\bar{x}}^{(\alpha_1)}, y_{\bar{x}}^{(\alpha_1+\alpha_2)}, \ldots, y_{\bar{x}}^{(\alpha_1+,\ldots,+\alpha_n)}), \tag{14.10}$$

and consider an unknown dynamic

$$\eta^{(\bar{\alpha}_i)} = \bar{\Delta}_i(\bar{x}, \eta), \tag{14.11}$$

where $0 < \bar{\alpha}_i < 2$ is a rational number, and $\bar{\Delta}_i(\bar{x}, \eta)$ is an unknown dynamics that contains $\Delta_i(\bar{x}, \eta)$. Now let us propose an IFROO with order $\bar{\alpha}_i$, so the slave system is given by

$$\hat{\eta}^{(\bar{\alpha}_i)} = k_{\hat{\eta}_i}(\eta_i - \hat{\eta}_i), \tag{14.12}$$

$$y_{\hat{\eta}_i} = \hat{\eta}_i. \tag{14.13}$$

In the master–slave synchronization scheme, the output of the master system represents the target signal, while the slave's output is the response signal. Therefore, given a master system and our slave system, some conditions should be determined

for synchronizing the output of the slave system with the output of the master system.

Let us define the synchronization error as

$$e_i = y_{\eta_i} - y_{\hat{\eta}_i} = \eta_i - \hat{\eta}_i. \tag{14.14}$$

We establish the following assumptions:

H1: η_i satisfies the IFAO property for $i \in (p+1, \ldots, n)$.
H2: $\bar{\Delta}_{p+1}$ is bounded, i.e., $\exists\ M \in \mathbb{R}^+$ such that $\|\bar{\Delta}(X)\| \leq M, \forall\ x$ in a compact set Ω, where $\bar{\Delta}(X) = (\bar{\Delta}_1, \ldots, \bar{\Delta}_n)^T$.
H3: $k_{\hat{\eta}_i} \in \mathbb{R}^+$.

Now we are in position to propose the following proposition.

Proposition 14.1 *Let the system (14.6) be expressed as (14.7), where the above conditions are fulfilled. Then (14.14) converges asymptotically to an open set $B_r(0)$, with $r = \dfrac{M}{k_{\hat{\eta}_i}}$, i.e., synchronization is achieved.*

Proof From H1, we can write Eqs. (14.11)–(14.14). Taking the fractional derivative of Eq. (14.14), we have

$$e_i^{(\bar{\alpha}_i)} = \eta_i^{(\bar{\alpha}_i)} - \hat{\eta}_i^{(\bar{\alpha}_i)}. \tag{14.15}$$

Substituting the fractional dynamics (14.11) and (14.12) into (14.14), we obtain

$$e_i^{(\bar{\alpha}_i)} + k_{\hat{\eta}_i} e_i = \Delta_i\ (x). \tag{14.16}$$

There exists a unique solution to the system (14.16), due to the fact that $\Delta_i\ (x(t)) - k_{\hat{\eta}_i} e_i(t)$ is a Lipschitz continuous function on e.[1] Solving the above equation, we have

$$\begin{aligned} e_i(t) = {} & e_{i_0} E_{\bar{\alpha}_i,1}(-k_{\hat{\eta}_i} t^{(\bar{\alpha}_i)}) \\ & + \int_0^t (t-\tau)^{\bar{\alpha}_i - 1} E_{\bar{\alpha}_i,\bar{\alpha}_i}(k_{\hat{\eta}_i}(t-\tau)^{\bar{\alpha}_i})\ \Delta_i\ (\tau) d\tau, \end{aligned} \tag{14.17}$$

where $e_i(0) = e_{i_0}$. Using the triangle and Cauchy–Schwarz inequalities and H2 yields

$$\begin{aligned} |\ e_i(t)\ | \leqslant {} & |\ e_{i_0} E_{\bar{\alpha}_i,1}(-k_{\hat{\eta}_i} t^{\bar{\alpha}_i})\ | \\ & + M \int_0^t |\ (t-\tau)^{\bar{\alpha}_i - 1} E_{\bar{\alpha}_i,\bar{\alpha}_i}(-k_{\hat{\eta}_i}(t-\tau)^{\bar{\alpha}_i})\ |\ d\tau. \end{aligned} \tag{14.18}$$

[1] Equation (14.16) is nonautonomous, but the Lipschitz condition ensures a unique solution [10].

The functions $(t-\tau)^{\bar{\alpha}_i-1}E_{\bar{\alpha}_i,\bar{\alpha}_i}(-k_{\hat{\eta}_i}(t-\tau)^{\bar{\alpha}_i})$ and $E_{\bar{\alpha}_i}(-k_{\hat{\eta}_i}t^{\bar{\alpha}_i})$ are nonnegative, due to Property 14.2 of the Mittag-Leffler function and H3:

$$\begin{aligned} \mid e_i(t) \mid \leqslant \mid e_{i_0} \mid E_{\bar{\alpha}_i,1}(-k_{\hat{\eta}_i}t^{\bar{\alpha}_i}) \\ +M\int_0^t (t-\tau)^{\bar{\alpha}_i-1}E_{\bar{\alpha}_i,\bar{\alpha}_i}(-k_{\hat{\eta}_i}(t-\tau)^{\bar{\alpha}_i})d\tau. \end{aligned} \tag{14.19}$$

Using Property 14.1 of the Mittag-Leffler function gives us

$$\mid e_i(t) \mid \leqslant \mid e_{i_0} \mid E_{\bar{\alpha}_i,1}(-k_{\hat{\eta}_i}t^{\bar{\alpha}_i}) + Mt^{(\bar{\alpha}_i)}E_{\bar{\alpha}_i,\bar{\alpha}_i+1}(-k_{\hat{\eta}_i}t^{\bar{\alpha}_i}). \tag{14.20}$$

If $t \to \infty$, we use Eq. (14.5) with $\mu = 3\pi\dfrac{\bar{\alpha}_i}{4}$ due to H3:

$$\begin{aligned} \lim_{t\to\infty} \mid e_i(t) \mid \leq \mid e_{i_0} \mid \lim_{t\to\infty} E_{\bar{\alpha}_i,1}(-k_{\hat{\eta}_i}t^{\bar{\alpha}_i}) \\ +M\lim_{t\to\infty} t^{\bar{\alpha}_i}E_{\bar{\alpha}_i,\bar{\alpha}_i+1}(-k_{\hat{\eta}_i}t^{\bar{\alpha}_i}) = \frac{M}{k_{\hat{\eta}_i}}. \end{aligned} \tag{14.21}$$

□

14.4 Numerical Results

In this section, we study the problem of synchronization of incommensurate fractional dynamical systems by means of numerical simulations. Consider the fractional-order Rössler system [11] as follows:

$$\begin{aligned} x_1^{(\alpha_1)} &= -x_1 - x_3, \\ x_2^{(\alpha_2)} &= x_1 + 0.63x_2, \\ x_3^{(\alpha_3)} &= 0.2 + x_3(x_1 - 10), \end{aligned} \tag{14.22}$$

where $x = (x_1, x_2, x_3)^T$ is the state vector, $\alpha_1 = 0.9$, $\alpha_2 = 0.8$, and $\alpha_3 = 0.7$, and we take the system output as $y = x_2$. The system (14.7) can be rewritten as (14.7):

$$\begin{aligned} \bar{x}_2^{(\alpha_2)} &= \eta_1 + 0.63\bar{x}_2, \\ \eta_1^{(\alpha_1)} &= -\bar{x}_2 - \eta_3, \\ \eta_3^{(\alpha_3)} &= 0.2 + \eta_3(\eta_1 - 10), \end{aligned} \tag{14.23}$$

where $x_2 = \bar{x}_2$, $x_1 = \eta_1$, $x_3 = \eta_3$, and $y = \bar{x}_2$. From (14.23), the following relationships are achieved:

$$\eta_1 = y^{(\alpha_2)} - 0.63y, \tag{14.24}$$

$$\eta_3 = -y + 0.63y^{(\alpha_1)} - y^{(\alpha_1+\alpha_2)}, \tag{14.25}$$

and from (14.24) and (14.25), we can see that $\eta_3 = x_3$ and $\eta_1 = x_1$ are IFAO. The master systems are given by

$$\eta_1^{(\alpha_1)} = -\bar{x}_2 - \eta_3, \tag{14.26}$$

$$y_{\eta_1} = \eta_1 = y^{(\alpha_2)} - 0.63y, \tag{14.27}$$

$$\eta_3^{(\alpha_3)} = 0.2 + \eta_3(\eta_1 - 10), \tag{14.28}$$

$$y_{\eta_3} = \eta_3 = -y + 0.63y^{(\alpha_1)} - y^{(\alpha_1+\alpha_2)}. \tag{14.29}$$

Remark 14.1 To design the slave system, the derivative order for each $\hat{\eta}_i$ is chosen such that $\bar{\alpha}_i$ is equal to the largest fractional derivative order of the output y.

We now design the slave system for (14.27), where in this case, $\bar{\alpha}_i = \alpha_2 = 0.8$. Then we have

$$\hat{\eta}_1^{(\alpha_2)} = k_1(\eta_1 - \hat{\eta}_1), \tag{14.30}$$

and substituting (14.24) into (14.30), we obtain

$$\hat{\eta}_1^{(\alpha_2)} = k_1(y^{(\alpha_2)} - 0.63y - \hat{\eta}_1). \tag{14.31}$$

In order to avoid fractional-order derivatives, we propose a change of variable $\hat{\eta}_1 = \gamma_1 + k_1 y$, and from Eq. (14.31), after some manipulations, we obtain

$$\gamma_1^{(\alpha_2)} = k_1(-0.63y - \gamma_1 - k_1 y). \tag{14.32}$$

It is now time to estimate x_3, but in this case, we consider x_1 unknown, and we use

$$x_1^{(\alpha_1)} = x_2^{(\alpha_1+\alpha_2)} - 0.63x_2^{(\alpha_1)}. \tag{14.33}$$

Since the system is incommensurate, the previous equation contains a derivative that depends on different fractional orders; however, it is possible to obtain a reduced-order observer after additional manipulations, as we show. From the first equation of (14.22) and Eq. (14.33), the following expression is obtained:

$$x_3 = \eta_3 = -y + 0.63y^{(\alpha_1)} - y^{(\alpha_1+\alpha_2)}. \tag{14.34}$$

In this case, $\bar{\alpha}_i = \alpha_1 + \alpha_2 = 1.7$, which is smaller than 2. At the outset, the slave system for (14.28) has the following representation:

$$\hat{\eta}_3^{(\alpha_1+\alpha_2)} = k_2(-y - y^{(\alpha_1+\alpha_2)} + 0.63y^{(\alpha_1)} - \hat{\eta}_3). \tag{14.35}$$

We introduce in (14.35) the change of variable $\hat{\eta}_3 = \beta_1 - k_2 y$ in order to avoid the term $y^{(\alpha_1+\alpha_2)}$. Then we have

$$\beta_1^{(\alpha_1+\alpha_2)} = k_2(-y + 0.63y^{(\alpha_1)} - \beta_1 + k_2 y). \tag{14.36}$$

Finally, we need to avoid one more term, namely $y^{(\alpha_1)}$. To achieve this goal, we propose a change of variable as follows: first consider a new variable β_2 and substitute the change of variable $\beta_1 = \beta_2^{(-\alpha_2)} + 0.63k_2 y^{(-\alpha_2)}$ into (14.36); then after some algebraic manipulations, it is possible to achieve the following relationship:

$$\beta_2^{(\alpha_1)} = k_2(-y - \beta_2^{(-\alpha_2)} - 0.63k_2 y^{(-\alpha_2)} + k_2 y). \tag{14.37}$$

We select the observer's constant parameters as $k_1 = 120$ and $k_2 = 7{,}000$.

Figures 14.1 and 14.2 show the original system states and the slave system synchronized with the master system respectively. To end this example, we see in Figs. 14.3 and 14.4 the convergence of the estimates to the original states. Now consider the following fractional-order Chua system [12]:

$$\begin{aligned} x_1^{(\alpha_1)} &= ax_2 + \frac{ax_1}{7} - \frac{2ax_1^3}{7}, \\ x_2^{(\alpha_2)} &= x_1 - x_2 + x_3, \\ x_3^{(\alpha_3)} &= -\beta x_2, \end{aligned} \tag{14.38}$$

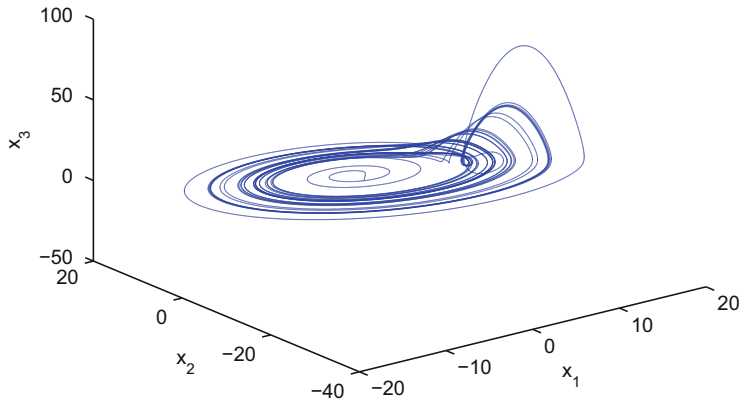

Fig. 14.1 Phase plot of the incommensurate fractional-order system with initial conditions $x_1(0) = 1$, $x_2(0) = 0$ and $x_3(0) = -5$

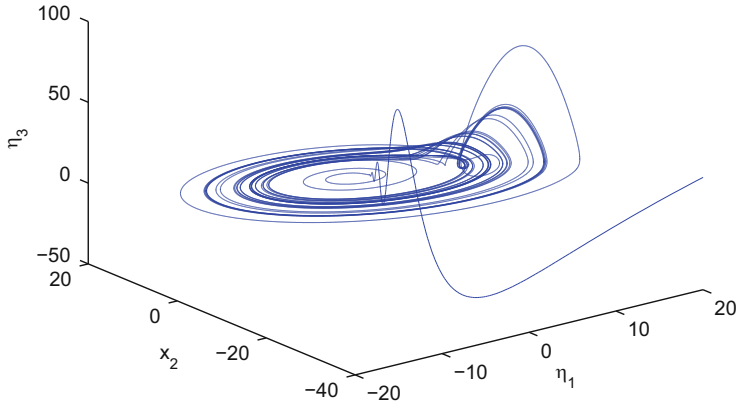

Fig. 14.2 Phase plot of the slave incommensurate fractional-order system with initial conditions $\hat{\eta}_1(0) = 100$ and $\hat{\eta}_3(0) = 200$

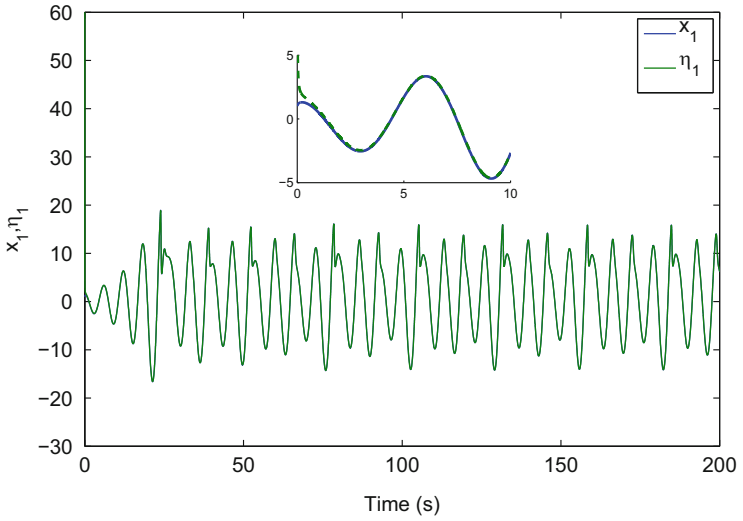

Fig. 14.3 Synchronization of the incommensurate fractional-order system, state x_1, vs. estimate η_1

where $a = 12.75$, $\beta = \dfrac{100}{7}$, $x = (x_1, x_2, x_3)^T$ is the state vector, $\alpha_1 = 0.99$, $\alpha_2 = 0.91$, and $\alpha_3 = 0.95$, and we take the system output as $y = x_1$. The system (14.38) can be rewritten as

$$\begin{aligned} \bar{x}_1^{(\alpha_1)} &= a\eta_2 + \frac{a\bar{x}_1}{7} - \frac{2a\bar{x}_1^3}{7}, \\ \eta_2^{(\alpha_2)} &= \bar{x}_1 - \eta_2 + \eta_3, \\ \eta_3^{(\alpha_3)} &= -\beta\eta_2, \end{aligned} \tag{14.39}$$

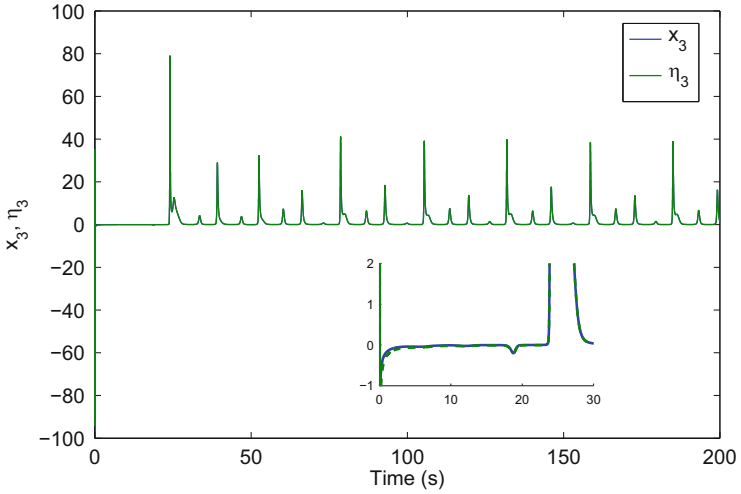

Fig. 14.4 Synchronization of the incommensurate fractional-order system, state x_3, vs. estimate η_3

where $x_1 = \bar{x}_2$, $x_2 = \eta_2$, $x_3 = \eta_3$, and $y = \bar{x}_1$. From (14.39), the following relationships are obtained:

$$\eta_2 = \frac{y^{(\alpha_1)}}{a} - \frac{y}{7} + \frac{2y^3}{7}, \tag{14.40}$$

$$\eta_3 = \frac{y^{(\alpha_1+\alpha_2)}}{a} - \frac{y^{(\alpha_2)}}{7} + \frac{2y^{3(\alpha_2)}}{7} - y + \frac{y^{(\alpha_1)}}{a} - \frac{y}{7} + \frac{2y^3}{7}, \tag{14.41}$$

and from (14.40) and (14.41), we can see that $\eta_2 = x_2$ and $\eta_3 = x_3$ are IFAO:

$$\eta_2^{(\alpha_2)} = \bar{x}_1 - \eta_2 + \eta_3, \tag{14.42}$$

$$y_{\eta_2} = \eta_2 = \frac{y^{(\alpha_1)}}{a} - \frac{y}{7} + \frac{2y^3}{7}, \tag{14.43}$$

$$\eta_3^{(\alpha_3)} = -\beta\eta_2, \tag{14.44}$$

$$y_{\eta_3} = \eta_3 = \frac{y^{(\alpha_1+\alpha_2)}}{a} - \frac{y^{(\alpha_2)}}{7} + \frac{2y^{3(\alpha_2)}}{7} - y + \frac{y^{(\alpha_1)}}{a} - \frac{y}{7} + \frac{2y^3}{7}. \tag{14.45}$$

Now we design the slave system for (14.27) in the case $\bar{\alpha}_i = \alpha_1 = 0.99$. Then we have

$$\hat{\eta}_2^{(\alpha_1)} = k_1(\eta_2 - \hat{\eta}_2), \tag{14.46}$$

and substituting (14.40) into (14.46), we obtain

$$\hat{\eta}_2^{(\alpha_1)} = k_1 \left(\frac{y^{(\alpha_1)}}{a} - \frac{y}{7} + \frac{2y^3}{7} - \hat{\eta}_2 \right). \tag{14.47}$$

In order to avoid fractional-order derivatives, we propose a change of variable $\hat{\eta}_2 = \gamma_1 + \dfrac{k_1 y}{a}$, and from Eq. (14.47), after some algebraic manipulations, we obtain

$$\gamma_1^{(\alpha_1)} = k_1 \left(-\frac{y}{7} + \frac{2y^3}{7} - \gamma_1 - \frac{k_1 y}{a} \right). \tag{14.48}$$

We now estimate x_3, but in this case, we consider x_2 unknown, and we use

$$x_2^{(\alpha_2)} = \bar{x}_1 - \eta_2 + \eta_3. \tag{14.49}$$

Since the system is incommensurate, the previous equation contains a derivative that depends on different fractional orders; however, it is possible to obtain a reduced-order observer after some manipulation, as we show. From the first equation of (14.38) and Eq. (14.49), the following expression is obtained:

$$\begin{aligned} x_3 = \eta_3 &= \eta_2^{(\alpha_2)} - y - \eta_2, \\ \eta_3 &= \frac{y^{(\alpha_1+\alpha_2)}}{a} - \frac{y^{(\alpha_2)}}{7} + \frac{2y^{3(\alpha_2)}}{7} - y + \frac{y^{(\alpha_1)}}{a} - \frac{y}{7} + \frac{2y^3}{7}. \end{aligned} \tag{14.50}$$

In this case, $\bar{\alpha}_i = \alpha_1 + \alpha_2 = 1.9$, which is smaller than 2. At the outset, the slave system for (14.44) has the following representation:

$$\hat{\eta}_3^{(\alpha_1+\alpha 2)} = k_2(\eta_3 - \hat{\eta}_3), \tag{14.51}$$

$$\begin{aligned} \hat{\eta}_3^{(\alpha_1+\alpha_2)} = k_2 \Bigg(&\frac{y^{(\alpha_1+\alpha_2)}}{a} - \frac{y^{(\alpha_2)}}{7} + \frac{2y^{3(\alpha_2)}}{7} \\ &-y + \frac{y^{(\alpha_1)}}{a} - \frac{y}{7} + \frac{2y^3}{7} - \hat{\eta}_3 \Bigg). \end{aligned} \tag{14.52}$$

We introduce in (14.52) the change of variable $\hat{\eta}_3 = \beta_1 + \dfrac{k_2 y}{a}$ in order to avoid the term $y^{(\alpha_1+\alpha_2)}$. Then we have

$$\begin{aligned} \beta_1^{(\alpha_1+\alpha_2)} = k_2 \Bigg(&-\frac{y^{(\alpha_2)}}{7} + \frac{2y^{3(\alpha_2)}}{7} - y + \frac{y^{(\alpha_1)}}{a} \\ &-\frac{y}{7} + \frac{2y^3}{7} - \beta_1 - \frac{k_2 y}{a} \Bigg). \end{aligned} \tag{14.53}$$

Finally, we need to avoid derivatives $y^{(\alpha_1)}$ and $y^{(\alpha_2)}$. To achieve this goal, we propose a change of variable as follows:

$$\beta_1 = \beta_2^{(-\alpha_2)} - \frac{k_2 y^{(-\alpha_1)}}{7} + \frac{2k_2 y^{3(-\alpha_1)}}{7} + \frac{k_2 y^{(-\alpha_2)}}{a}. \tag{14.54}$$

Substituting the change (14.54) into (14.36), we finally, after some algebraic manipulations, we arrive at

$$\beta_2^{(\alpha_1)} = k_2 \left(-y \frac{-y}{7} + \frac{2y^3}{7} - \frac{k_2 y}{a} - \beta_1 \right). \tag{14.55}$$

We select the observer's constant parameters as $k_1 = 100$ and $k_2 = 1{,}000$.

In Fig. 14.5, we can observe the original systems, while Fig. 14.6 shows the slave system synchronized with the master system. Finally, the convergence of estimates to the original states is shown in Figs. 14.7 and 14.8 .

To conclude, we study the problem of a fractional financial system, [13]

$$\begin{aligned} x_1^{(\alpha_1)} &= x_3 + (x_2 - 3)x_1, \\ x_2^{(\alpha_2)} &= 1 - 0.1x_2 - x_1^2, \\ x_3^{(\alpha_3)} &= -x_1 - x_3, \end{aligned} \tag{14.56}$$

where the interest rate, investment demand, and price index are given by x_1, x_2, x_3 respectively, $x = (x_1, x_2, x_3)^T$ is the state vector, $\alpha_1 = 0.95$, $\alpha_2 = 0.98$, and

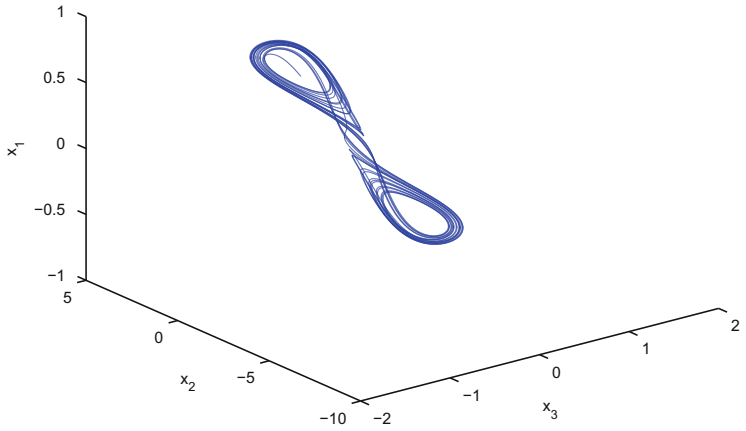

Fig. 14.5 The incommensurate fractional-order system with initial conditions $x_1(0) = 1, x_2(0) = 2$ and $x_3(0) = -1$

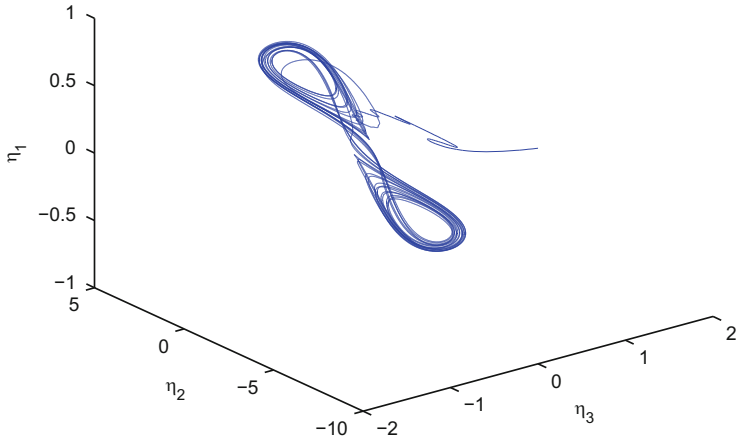

Fig. 14.6 The slave incommensurate fractional-order system with initial conditions $\hat{\eta}_1(0) = -10$ and $\hat{\eta}_2(0) = 0$

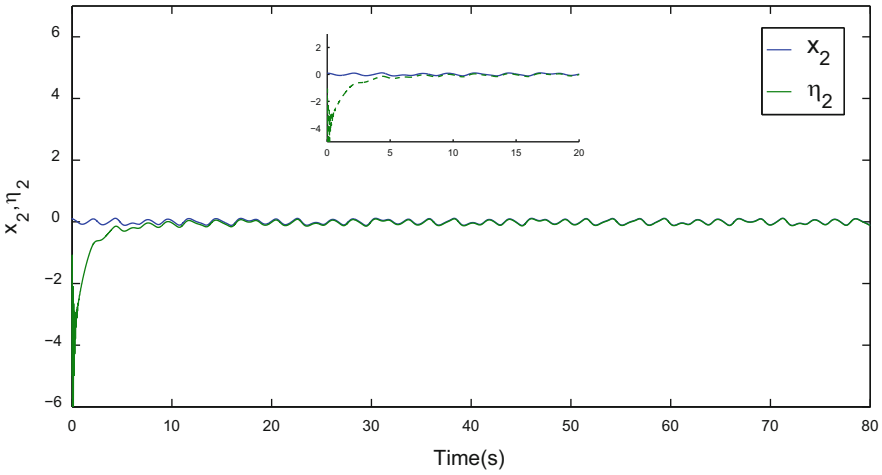

Fig. 14.7 Synchronization of the incommensurate fractional-order system, state x_2, vs. estimate η_2

$\alpha_3 = 0.99$, and we take the system output as $y = x_3$. The system (14.56) can be rewritten as (14.7):

$$\begin{aligned} \bar{x}_3^{(\alpha_3)} &= -\eta_1 - \bar{x}_3, \\ \eta_1^{(\alpha_1)} &= \bar{x}_3 + (\eta_2 - 3)\eta_1, \\ \eta_2^{(\alpha_2)} &= 1 - 0.1\eta_2 - \eta_1^2, \end{aligned} \tag{14.57}$$

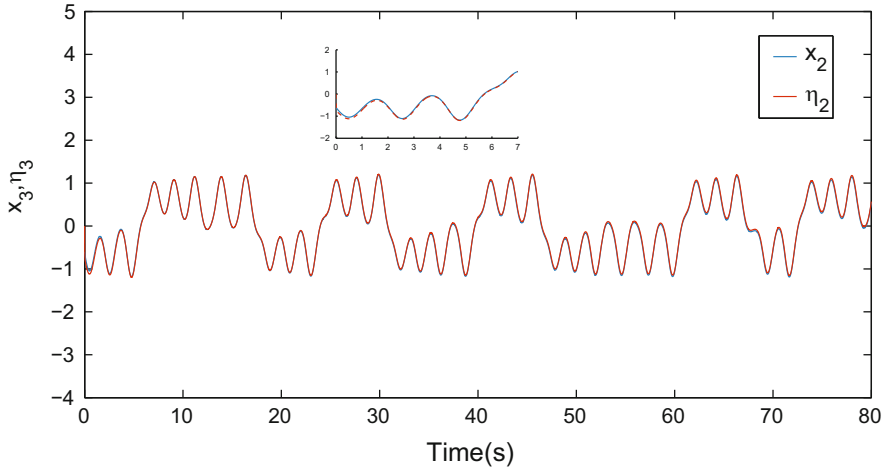

Fig. 14.8 Synchronization of the incommensurate fractional-order system, state x_3, vs. estimate η_3

where $x_3 = \bar{x}_3$, $x_1 = \eta_1$, $x_2 = \eta_2$, and $y = \bar{x}_3$. From (14.57), the following relations are achieved:

$$\eta_1 = -y^{(\alpha_3)} - y, \tag{14.58}$$

$$\eta_2 = \frac{1}{-y^{(\alpha_3)} - y}[y^{(\alpha_1+\alpha_3)} - y^{(\alpha_1)} - y + 3(-y^{(\alpha_3)} - y)], \tag{14.59}$$

and from (14.58) and (14.59), we can see that $\eta_1 = x_1$ and $\eta_2 = x_2$ are IFAO:

$$\eta_1^{(\alpha_1)} = \bar{x}_3 + (\eta_2 - 3)\eta_1, \tag{14.60}$$

$$y_{\eta_1} = \eta_1 = -y^{(\alpha_3)} - y, \tag{14.61}$$

$$\eta_2^{(\alpha_2)} = 1 - 0.1\eta_2 - \eta_1^2, \tag{14.62}$$

$$y_{\eta_2} = \frac{1}{-y^{(\alpha_3)} - y}[y^{(\alpha_1+\alpha_3)} - y^{(\alpha_1)} - y + 3(-y^{(\alpha_3)} - y)]. \tag{14.63}$$

Now we design the slave system for (14.60), and we have

$$\hat{\eta}_1^{(\alpha_3)} = k_1(\eta_1 - \hat{\eta}_1). \tag{14.64}$$

Substituting (14.58) into (14.64) yields

$$\hat{\eta}_1^{(\alpha_3)} = k_1(-y^{(\alpha_3)} - y - \hat{\eta}_1). \tag{14.65}$$

In order to avoid fractional-order derivatives, we propose a change of variable $\hat{\eta}_1 = \gamma_1 - k_1 y$, and from Eq. (14.65), after some manipulations we obtain

$$\gamma^{(\alpha_3)} = k_1(k_1 y - y - \gamma_1). \tag{14.66}$$

To estimate x_2, there is a problem when $-y^{(\alpha_3)} - y = 0$. At this moment, the IFAO property is lost, so in order to overcome this drawback, from (14.57) we use as an estimate:

$$\eta_2 = 10 - 10\hat{\eta}_2^{(\alpha_2)} - 10\hat{\eta}_1^2. \tag{14.67}$$

Then the slave system for (14.62) is given by

$$\hat{\eta}_2^{(\alpha_2)} = k_2(\eta_2 - \hat{\eta}_2). \tag{14.68}$$

Substituting (14.67) into (14.68), after some algebraic manipulations we achieve the following observer:

$$\hat{\eta}_2^{(\alpha_2)} = \frac{1}{1 + 10k_2}(10k_2 - 10k_2\hat{\eta}_1^2 - k_2\hat{\eta}_2). \tag{14.69}$$

The simulation shows the effectiveness of the proposed observer; in the simulations, the gains are $k_1 = 100$ and $k_2 = 100$.

Figure 14.9 shows the original systems, while Fig. 14.10 shows the slave system synchronized with the master system. To end this section, we mention that Figs. 14.11 and 14.12 show the convergence of the estimates to the original states.

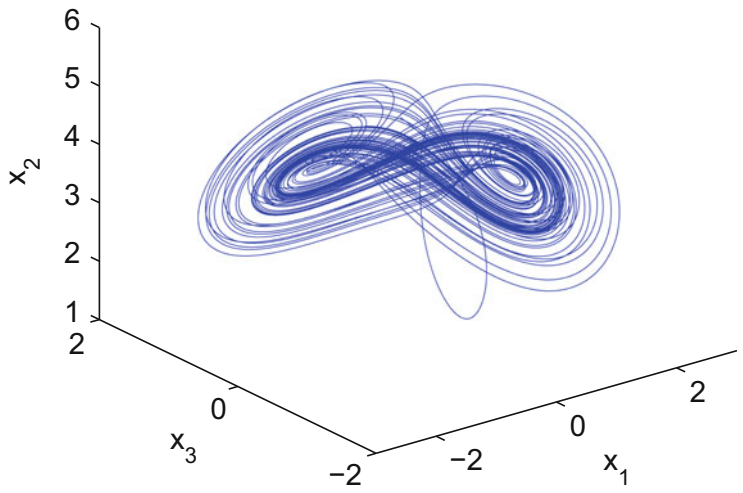

Fig. 14.9 Original system initial conditions $x_0 = (2, 3, 2)$

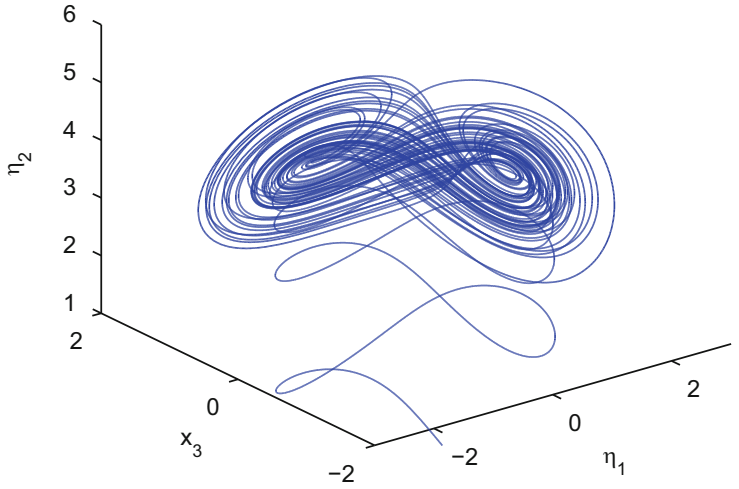

Fig. 14.10 Slave system initial conditions $\eta_1 = 20$, $\eta_2 = 30$

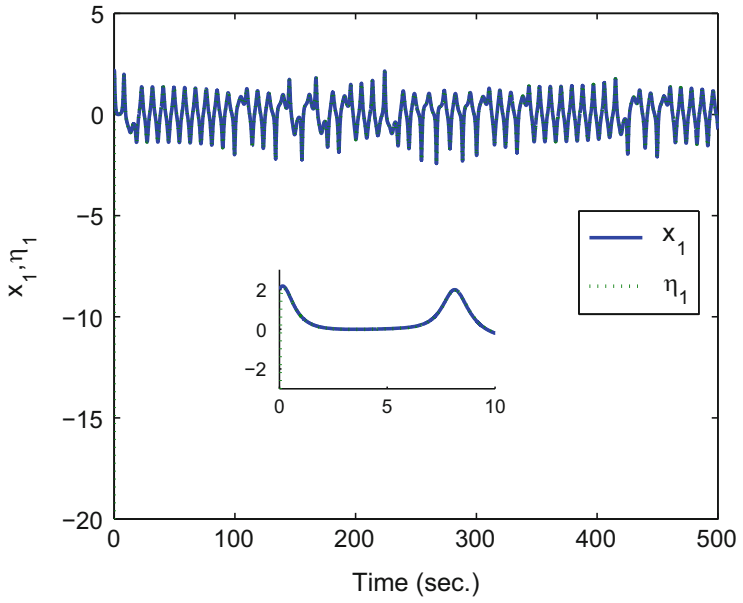

Fig. 14.11 State x_1 vs. estimate η_1

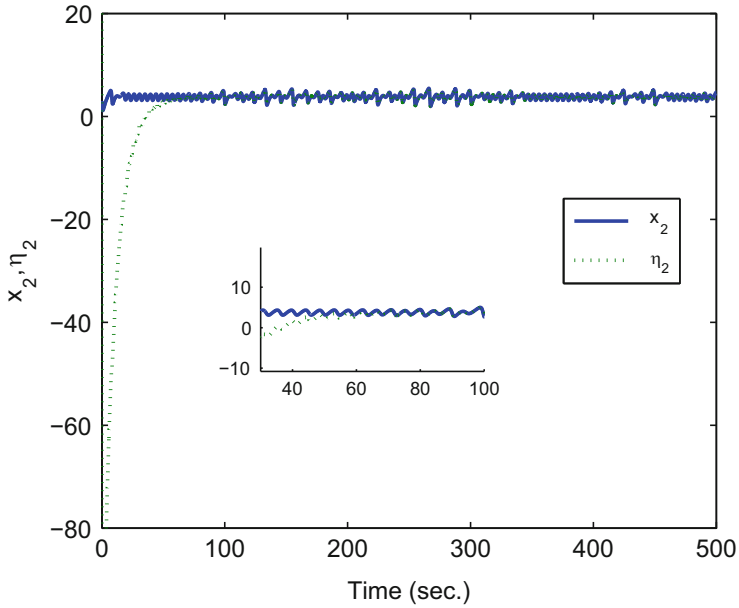

Fig. 14.12 State x_2 vs. estimate η_2

14.5 Conclusions

In this chapter, we introduced a new concept, IFAO and a new observer (IFROO) to solve the synchronization problem for incommensurate fractional dynamical systems. The scheme was applied to incommensurate fractional chaotic systems; however, it could be applied to other classes of systems that satisfy the conditions of Proposition 14.1. Finally, numerical simulations showed the effectiveness of the suggested approach.

References

1. T. Zhou, C. Li, Synchronization of fractional-order differential systems. Physica D **212**, 111–125 (2005)
2. L. Pecora, T. Carrol, Synchronization in chaotic systems. Phys. Rev. Lett. **64**, 821–824 (1990)
3. C. Li, J. Yan, The synchronization of three fractional differential systems. Chaos Solitons Fractals **32**, 751–757 (2007)
4. J.G. Lu, Synchronization of a class of fractional-order chaotic systems via a scalar transmitted signal. Chaos Solitons Fractals **27**, 519–525 (2006)
5. I. Podlubny, Geometric and physical interpretation of fractional integration and fractional differentiation. Fract. Calc. Appl. Anal. **5**, 367–386 (2002)

6. K.B. Oldham, J. Spanier, *The Fractional Calculus: Theory and Applications of Differentiation and Integration of Arbitrary Order*. Dover Books on Mathematics (Dover Publications, New York, 2006)
7. I. Podlubny, *Fractional Differential Equations*, 9th edn. (Academic, San Diego, 1999)
8. J.J. de Espindola, J. Neto, E. Lopes, A generalized fractional derivative approach to viscoelastic material properties measurement. Appl. Math. Comput. **164**, 493–506 (2005)
9. K.S. Miller, S.G. Samko, Completely monotonic functions. Integr. Transforms Spec. Funct. **12** (4), 389–402 (2001)
10. A.A. Kilbas, H.M. Srivastava, J.J. Trujillo, *Theory and Applications of Fractional Differential Equations* (Elsevier, Amsterdam, 2006)
11. M.S. Tavazoei, M. Haeri, Chaotic attractors in incommensurate fractional-order systems. Physica D **237**, 2628–2637 (2008)
12. R. Caponetto, G. Dongola, L. Fortuna, I. Petrás, *Fractional Order Systems*. World Scientific Series on Nonlinear Science, Series A, vol. 72 (World Scientific Publishing, Singapore, 2010), pp. 53–75
13. W.C. Chen, Nonlinear dynamics and chaos in a fractional-order financial system. Chaos Solitons Fractals **36**(5), 1305–1314 (2008)

Appendix

Estimation Error Convergence to the Zone $\tilde{\mu}$ Asymptotically (Ultimately Bounded)

Consider the Lyapunov function $V(e)$ satisfying the equality

$$\dot{V} = -\alpha V - \vartheta\sqrt{V} + \beta.$$

The equilibrium point V^* of this equation, satisfying

$$-\alpha V^* - \vartheta\sqrt{V^*} + \beta = 0,$$

is as follows:

$$V^* = \left(\sqrt{(\vartheta/2\alpha)^2 + \beta/\alpha} - \vartheta/2\alpha\right)^2$$
$$= \frac{(\beta/\alpha)^2}{\left(\sqrt{(\vartheta/2\alpha)^2 + \beta/\alpha} + \vartheta/2\alpha\right)^2}.$$

Proof of (3.22)
Defining $\Delta := (V - V^*)^2$, we derive

$$\dot{\Delta} = 2\left(V - V^*\right)\dot{V} \leq 2\left(V - V^*\right)\left[-\alpha V - \vartheta\sqrt{V} + \beta\right]$$
$$= 2\left(V - V^*\right)\left[-\alpha V - \vartheta\sqrt{V} + \beta + \left(\alpha V^* + \vartheta\sqrt{V^*} - \beta\right)\right]$$
$$2\left(V - V^*\right)\left[-\alpha\left(V - V^*\right) - \vartheta\left(\sqrt{V} - \sqrt{V^*}\right)\right]$$
$$= -2\alpha\left(V - V^*\right)^2 - 2\vartheta\left(\sqrt{V} + \sqrt{V^*}\right)\left(\sqrt{V} - \sqrt{V^*}\right)^2 < 0$$

for all $V \neq V^*$, which implies $V \underset{t\to\infty}{\to} V^*$. For

$$G := [V - \tilde{\mu}]_+^2 = V^2\left[1 - \frac{\tilde{\mu}}{V}\right]_+^2,$$

R. Martínez-Guerra et al., *Synchronization of Integral and Fractional Order Chaotic Systems*, Understanding Complex Systems,
DOI 10.1007/978-3-319-15284-4

we obtain

$$\begin{aligned}\dot{G} :&= 2\left[V-\tilde{\mu}\right]_+ \dot{V} = 2V\left[1-\frac{\tilde{\mu}}{V}\right]_+ \dot{V}_t \\ &\leq 2V\left[1-\frac{\tilde{\mu}}{V}\right]_+ \left(-\alpha V - \vartheta\sqrt{V}+\beta\right) \\ &= -2V\left[1-\frac{\tilde{\mu}}{V}\right]_+ \left[\alpha\left(V-V^*\right)+\vartheta\left(\sqrt{V}-\sqrt{V^*}\right)\right] \leq 0.\end{aligned}$$

The last inequality implies that G_t converges, that is,

$$G_t \to G_t^* < \infty.$$

Integration of the last inequality from 0 to T yields

$$\begin{gathered}G_T - G_0 \leq \\ -2\int_0^T V_t\left[1-\tfrac{\tilde{\mu}}{V}\right]_+ \left[\alpha\left(V_t-V_t^*\right)+\vartheta\left(\sqrt{V_t}-\sqrt{V_t^*}\right)\right]dt,\end{gathered}$$

which leads to the following inequality:

$$\begin{gathered}2\int_0^T V_t\left[1-\tfrac{\tilde{\mu}}{V}\right]_+ \left[\alpha\left(V_t-V_t^*\right)+\vartheta\left(\sqrt{V_t}-\sqrt{V_t^*}\right)\right]dt \\ \leq G_0 - G_T \leq G_0.\end{gathered}$$

Dividing by T and taking the upper limits of both sides, we obtain

$$\limsup_{T\to\infty}\frac{1}{T}\int_0^T V_t\left[1-\frac{\tilde{\mu}}{V}\right]_+ \left[\alpha\left(V_t-V_t^*\right)+\vartheta\left(\sqrt{V_t}-\sqrt{V_t^*}\right)\right]dt \leq 0,$$

and hence there exists a subsequence t_k such that

$$V_{t_k}\left[1-\tfrac{\tilde{\mu}}{V}\right]_+ \left[\alpha\left(V_{t_k}-V_t^*\right)+\vartheta\left(\sqrt{V_{t_k}}-\sqrt{V_t^*}\right)\right] \to 0,$$

or

$$G_{t_k} \underset{k\to\infty}{\to} 0.$$

So it follows that $G = 0$, which is equivalent to the fact that

$$\left[1-\frac{\tilde{\mu}}{V}\right]_+ \to 0.$$

□

Index

R. Martínez-Guerra et al., *Synchronization of Integral and Fractional Order Chaotic Systems*, Understanding Complex Systems,
DOI 10.1007/978-3-319-15284-4